January 2000

Theoretical and Applied Karstology, Volume 13-14, 2000-2001

Silviu Constantin

Romanian Academy
" Emil Racoviţă "
Institute of Speleology

Theoretical and Applied Karstology

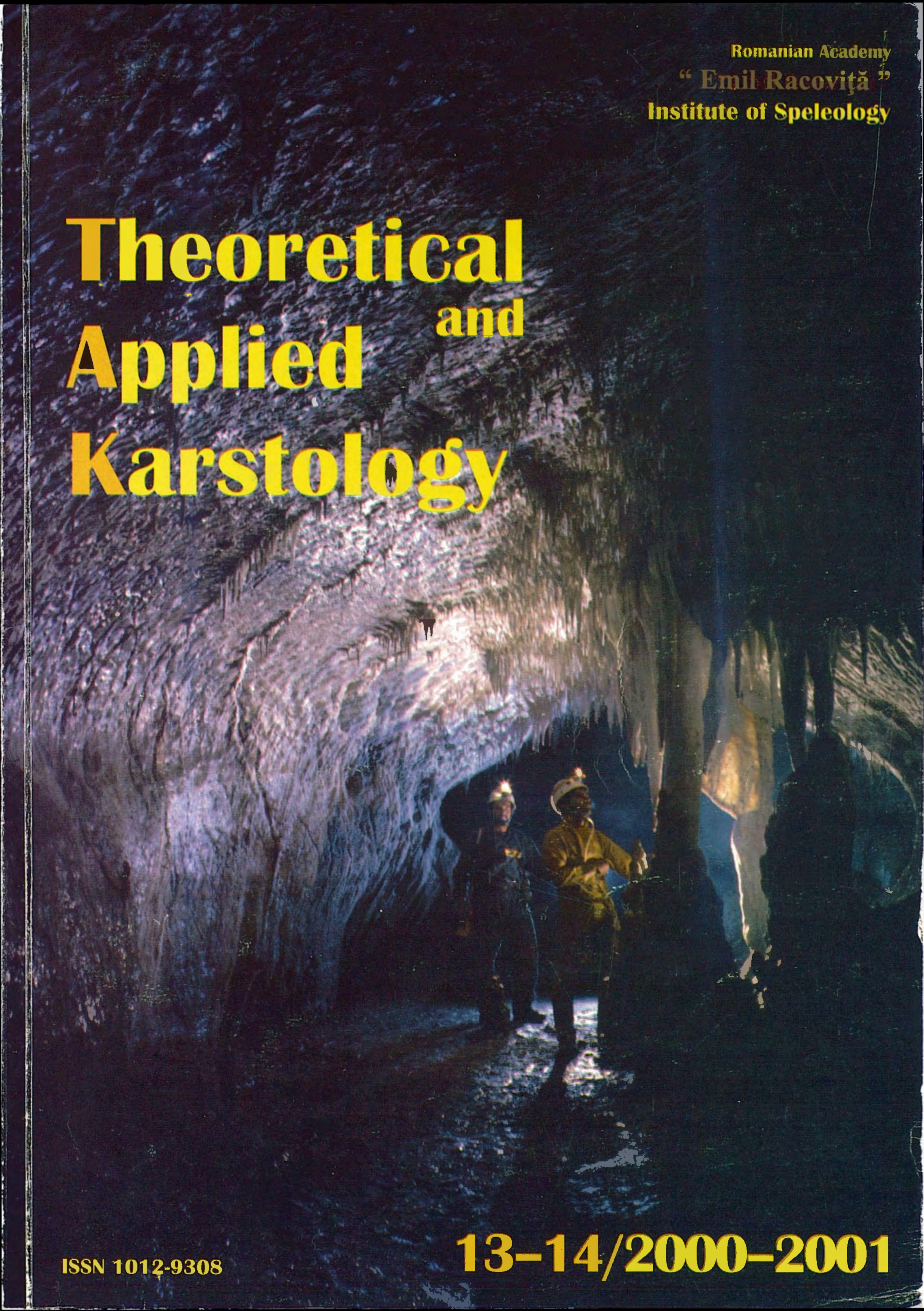

ISSN 1012-9308

13–14/2000–2001

Theoretical and Applied Karstology

Volumes 13–14

Theoretical and Applied Karstology

vol. 13-14/2000-2001

ISSN: 1012-9308

Indexation: Georef

EDITURA ACADEMIEI ROMÂNE

Calea 13 Septembrie 13, P.O. Box 5-42, 76117 Bucureşti, România. tel:+40-1-4119008

Theoretical and Applied Karstology (TAK) is an annual journal dedicated to the karst and caves sciences. The first four issues were published by the "Emil Racovita" Institute of Speleology, as a series, between 1983 and 1991. Since 1992, TAK has been edited by the Institute and published by the Romanian Academy's Publishing House.

TAK publishes original contributions (review articles, research papers, short notes and book reviews) covering the whole range of karstology and physical speleology: karst geology and mineralogy, chemistry and physics of karst processes, karst geomorphology, karst hydrology and hydrogeology, speleo-chronology and landscape evolution, speleogenesis, climate and subterranean environment, speleo-paleontology, engineering and environmental problems in karst, karst managment, etc. The Editors welcome the submission of contributions from all over the world.

The "Emil Racovita" Speleological Institute encourages the exchange between TAK and specialized journals. Past TAK issues are also available to the Institute. Please address any inquiries concerning publication exchanges, subscriptions, and any article submission to:

Theoretical & Applied Karstology Editorial Board
Institutul de Speologie "Emil Racovita"
str. Frumoasa 11, C.P. 220-12, R-78114 Bucuresti, Romania.
tel: +40-1-6503465; tel/fax: +40-2113874
email: karstology@yahoo.com
http:// www.geocities.com/karstology

Cover photographs by Cristian Lascu:

Front cover: A passage of epiphreatic origin with an elliptical cross-section in the Epuran Cave (Topolnita–Epuran Cave System, see paper page 67).

Back cover: Ice stalagmites in "The Church" Chamber, Scarisoara Ice-Cave (Bihor Mountains, see paper page 33).

Language revisions: Rodica Florescu

DTP Editor: Silviu Constantin

This volume was supported by the Romanian Federation of Speleology.

Orders may be sent to:

Editura Academiei Române, Calea 13 Septembrie, nr. 13, P.O.Box 5-42, Bucharest, Romania. tel:+40-1-4119008.

Rodipet S.A.: Piata Presei Libere 1, P.O.Box 35-57, Bucharest, Romania. fax:+40-1-2226407; tel: +40-1-2224126.

Orion Press Impex 2000: P.O.Box 77-19, Bucharest 3, Romania.

Romanian Academy
"Emil Racoviță" Institute of Speleology

Editura Academiei Române
București, 2001

Theoretical and Applied Karstology

Volumes 13–14/2000–2001

Contents

Editorial

To the usual TAK readers this double-issue may look familiar, in spite of some obvious changes to its layout. For us, editors, as seen from 'the inside' the journal has changed from many other viewpoints. The following lines will attempt to reveal some of those changes.

Traditionally, TAK articles were selected from those papers presented to the annual "Symposiums of Theoretical and Applied Karstology". Unfortunately, for several reasons, among which the economic challenges that Romania in general and research institutions in particular have to face, the organizers of this symposium (the "Emil Racoviță" Institute of Speleology and the "Prospecțiuni" Company for Geological Research) were forced to disrupt its annual organization. The last 'independent' TAK Symposium was held in the spring of 1998, in Băile Herculane; the next one was held in 2000, in Cluj, in conjunction with the 15th "Friends of Karst" Meeting and the first workshop of the IGCP 448 Committee.

As a first, predictable, consequence of this decrease in periodicity, the number and the frequency of contributions submitted to our journal strongly diminished. In an inertial attempt to 'keep the pace' with the TAK-Symposium, the journal appeared in 1999 for the first time as a double-issue (11–12). However, we were well aware that this 'solution' was unacceptable: there are very few authors (if any!) that would submit their contributions to TAK knowing that the publishing time will exceed one year. In order to 'keep alive' the journal, its dependence on the TAK Symposiums should come to an end.

This, again, double-issue has a 'transitional' structure. Some of its articles were submitted at the above-mentioned joint meeting in Cluj 2000, while other were independently received during the year 2001. It is the first time when TAK does not (almost) exclusively rely on symposium contributions.

Independent submission, however, demands an increased exigency. Symposium presentations often benefit by helpful criticism; in most cases the result of this was a noticeable improvement of the quality of the 'final form' of the contributions. As a newly direct-submission journal, TAK had to boost its peer-review system in order to ensure a high scientific standard.

In May 2001, the Editorial Board was renewed and the Board of Reviewers was substantially enlarged. The peer-review system was fully enforced and we benefit now of the expertise and the support of 36 established specialists in almost all fields of caves and karst sciences. At the same time, we decided to make our way on the Internet: the first TAK homepage has been created at http://www.geocities.com/karstology. Of course, for the time being this page is still in its infancy and could be improved in many ways. Still, the contents and abstracts of all TAK issues are there and we have also offered a temporary access to the full text of the articles in the latest issue. This and our future efforts will aim to increase the accessibility and scientific circulation of the journal for the benefit of all our contributors.

This issue features articles belonging to various domains, from cave mineralogy, to paleoclimate reconstructions, speleogenesis, karst modeling and karst hydrogeology. The common points of its eclectic content are caves and karst and this is something that we would like to inherit from the 'old TAK'. After all, there are not so many scientific journals where one can publish the results of researches carried on in karst and, at the same time, feel "in the family". Since many of the articles were presented at the joint TAK–"Friends of Karst" meeting in Cluj, we considered that a brief presentation of the latter would be appropriate. This was done right in the next pages by professor White, one of the FOK's 'inventors'. As a novelty, we have also introduced a new section, of "Book reviews", which was thought to be useful.

Volume 13–14 of TAK is the result of a collective, enthusiastic work, carried out not only by the editorial staff but also by our friends all over the world that have made valuable suggestions and, sometimes have assumed some 'less scientific' tasks such as suggesting language corrections or ways of layout improvement. We thank them all and assure everybody that we'll continue our work to make TAK a better journal.

Silviu Constantin

TAK Meetings

The Friends of Karst

Because the Friends of Karst is a very low profile organization (or non-organization) some explanation and a short history is given here.

The Friends of Karst has operated quite effectively for more than 30 years with no officers, nor organizational structure, no dues, and no membership. Its primary function is to host occasional meetings, some with field trips, when regular professional meetings are deemed insufficient. These meetings are intended for open discussion of work in progress. In practice some of the meeting have been highly informal with little or nothing in the way of printed records. Other have been more formal with published abstracts and in several cases, published proceedings. Decisions about the level of formality are the responsibility of the organizers.

Field trips have been an important part of the meetings. The idea is to have the participants get a first hand look at the host's favorite field areas. Open discussion of karst problems in the field promotes understanding at a very fundamental level.

Those karst researchers present at the annual meeting of the Geological Society of America have traditionally met in Will and Bet White's hotel room where they talk, drink some beer, and devote not more than five minutes to an annual business meeting. In recent years, others have volunteered their hotel room but thus far no more formal arrangement has been necessary. Meetings are organized when someone expresses an interest in hosting a meeting. The host then makes the necessary arrangements and organizes the program and field trips.

The meeting of the Friends of Karst in Cluj was number 15 in the series and the first such meeting held in Europe. The complete list of meetings is given below.

1. **Hamilton, Ontario, September, 1968**. Hosted by Derek Ford at his farmhouse outside of Hamilton. About 25 in attendance including Marjorie Sweeting and Paul Williams. This meeting set the format of informal discussions of on-going work; not professional meeting summaries of completed work.

Participants to the Friends of Karst Meeting in Cluj, July 2000, in front of the "Emil Racoviţă" Institute, just before the start of the field-trip (Photo: Bogdan Onac).

2. **Penn State University, May, 1970**. Hosted by W. B. White, R. R. Parizek, and D. Langmuir as a special conference for members of the karst working group of the International Hydrologic Decade. A field trip was organized for this conference.

3. **McMaster University, October, 1971**. Joint meeting with the Cave Research Associates. Abstracts published in *Cave Notes* **13**, 37–44, 8–51 (1971).

4. **West Virginia University, Morgantown, 1974**. Hosted by Henry Rauch. A more formal meeting with a published proceedings: *Fourth Conference on Karst Geology and Hydrology Proceedings*, H.W. Rauch and E. Werner, Eds., West Virginia Geological Survey, Morgantown, 187 p. (1974).

5. **Mammoth Cave, Kentucky, April, 1978**. Hosted by James F. Quinlan. Intensive technical sessions and surface and underground field trips. This was the first meeting to formally call itself the "Friends of Karst". The first version of the Central Kentucky Karst drainage basin map by J.F. Quinlan and J.A. Ray was called *Special Publication No. 1 of the Friends of Karst*. Abstracts published in *Geo*, 5, 22–28 (1978).

6. **Ely, Nevada, September, 1979**. Hosted by Jack Hess and Roger Jacobson. Abstracts published in *Geo* **7**, 27–30 (1980).

7. **McMaster University, April, 1982**. Hosted by Derek Ford. Although listed as a meeting of the Friends of Karst, this meeting was (more or less) by invitation only and had 22 people in attendance.

8. **University of Puerto Rico, Mayaguez, February, 1984**. Hosted by Joseph W. Troester. First "off shore" meeting. Good field trip though the cone and tower karst. Abstracts published in *Geo*, **11**, 44–49 (1984).

9. **State University College, Oneonta, New York, March, 1987**. Hosted by Arthur and Margaret Palmer. Informal meeting with no published abstract. 37 people in attendance.

10. **San Salvador Island, Bahamas, February 1988**. Hosted by John Mylroie. 42 people in attendance. Abstracts published in *Geo*, **15**, 29–34 (1988).

11. **Decorah, Iowa, April, 1990**. Hosted by George Huppert. Abstracts published in *Geo*, **17**, 59–87 (1990).

12. **Radford University, Radford, Virginia, March 1991**. Hosted by Ernst and Karen Kastning. Part of special symposium on Appalachian Karst. 72 people in attendance. Proceedings volume: *Appalachian Karst*, E.H. Kastning and K.M. Kastning, Eds., National Speleological Society, Huntsville, AL, 239 p. (1991).

13. **Tennessee Technological University, Cookeville, Tennessee, April, 1992**. Hosted by Albert Ogden. 122 people in attendance. Abstracts and a guidebook for two days of field trips were distributed at the meeting but not otherwise published.

14. **Bowling Green, Kentucky, September, 1998**. Hosted by Chris Groves and Joe Meiman. Joint meeting with IGCP Project 379. At this meeting there were a large number of attendees from overseas.

15. **Cluj, Romania, July, 2000**. Hosted by Bogdan Onac and the Babeş-Bolyai University, Speological Institute "Emil Racoviţă" and Romanian Speleological Federation. 131 people in attendance from 17 countries. First European meeting of the Friends of Karst. Proceeding volume: *Karst Studies and Problems: 2000 and Beyond* (Onac, B.P. and Tamas, T., Eds.), Presa Universitara Clujeana, Cluj, 196 p. (2000). Both proceedings and a guidebook were distributed at the beginning of the meeting.

At the time of the early meetings of the Friends of Karst, there were few karst papers at professional meetings. During the 30 years that the Friends of Karst has been functioning, the number of papers at meetings such as the Geological Society of America has grown and has the number of karst scientists attending the meeting. Other specialist conferences such as those organized by the Karst Waters Institute, the International Association of Hydrogeologists, the National Association of Water Scientists and Engineers and the Sinkhole Conferences have appeared in increasing numbers. Scientific communication between the US and Europe has continued to grow. However, it seems likely that future meetings of the Friends of Karst will continue to be scheduled, if for no other reason than that karst researchers appreciate the opportunity to display their favorite karst areas to their friends and colleagues.

William B. White

Department of Geosciences, The Pennsylvania State University, University Park, PA 16802 USA

TAK Anniversary

Iosif Viehmann — a lifetime for karst

On the first of September 2000, our colleague **Dr. Iosif (Pepi) Viehmann** celebrated his 75th birthday anniversary. Pepi Viehmann's activity identifies with the post-war beginnings of scientific speleology in our country. His interest for karst research appeared since he was still a student, and at the very beginning he was coordinated by Emil Racoviţă, the founder of the first Speleological Institute in the world. Pepi Viehmann dedicated more than 50 years to the exploration and study of several karst regions of Romania, Apuseni and Rodnei Mountains being the closest to his heart.

His activity, longer than half a century, has been highlighted by many achievements in both exploration and publication fields. He was member of the teams that during the '50s and '60s considerably increased the inventory of Romanian caves through their exceptional discoveries and explorations. Together with Mihai Şerban, Marcian Bleahu, Emilian Cristea, Dan Coman, Vali Crăciun, Theo Rusu and Gheorghe Racoviţă, he surveyed caves such as *Pojarul Poliţei, Cetăţile Ponorului, Avenul din Şesuri, Căput, Peştera Neagră, Avenul Gemănata, Tăuşoare, Jgheabul lui Zalion, Peştera Urşilor*, to remind only a few of them. A brief survey of the four books released with the same title: *Peşteri din România (Caves of Romania)*, reveals the name of Pepi Viehmann on numerous cave maps, suggesting an intensive field activity.

From a scientific point of view, our colleague Pepi Viehmann published more than a hundred papers in Romanian and foreign journals. Among these, there are to be remarked the monographs concerning karren and stream potholes (whirlpools), as well as the series of studies on the genesis and morphology of cave pearls. He is the main author of the picture book of Gheţarul de la Scărişoara, also co-authoring two other books illustrating and describing the caves of Romania. Added to these is the release, in this anniversary year, of his *General Speleology* textbook for students.

A particular place in Pepi Viehmann's scientific activities was occupied by the field trips to the *Gheţarul de la Scărişoara*, where, each month over 40 years, he gathered climatic and glaciologic data which were used in several papers published in collaboration or as a single author. His biospeleological observations were fructuously used by his biologist colleagues.

Gifted with a special capacity of observation, knowing how to value each detail, master in designing original methods to explain various genetic processes, Pepi Viehmann surprised the scientific community by some very ingenious experiments. He marked with paint numerous cave pearls and cave rafts to examine their evolution, he ringed eccentric speleothems with a chemical pencil to prove the antigravitational crystallogenesis process and he revealed the presence of the permanent drop on top of crystallictites.

Pepi Viehmann's name is linked to the sensational discoveries of the prehistoric human footprints in the clay of *Ciur-Izbuc* Cave or in the moonmilk of the *Vârtop* Glacier (Casa de Piatră). Added to these are his thorough observations on the cave bears traces and their cohabitation with the prehistoric humans.

Excellent pedagogue and good mate in the field campaigns, he led with professionalism several series of students in the fascinating world of caves. He attracted them and made them love speleology with the help of his charming slide shows and his unforgettable caving camps. He helps anyone looking for advice and knows how to be loved and appreciated by all. His major merit, as Cristian Lascu pointed out, was not only that he discovered some of the outstanding Romanian caves, but mostly that he has continuously *discovered people who, in their turn, discover and studied new caves.*

The boundless love and passion for the magnificent world of karst is the secret of his youth and power of work. All these characteristics make Pepi Viehmann to be a living stimulus for the young generation in the Speleological Institute. For all above-mentioned reasons we all wish to have him near us as long as possible.

Bogdan P. Onac

Theoretical and Applied Karstology, **13–14** (2000–2001), pp. 9–23

Conduit fragmentation, cave patterns, and the localization of karst ground water basins: the Appalachians as a test case

William B. White[1] * & Elizabeth L. White[2]

[1] *Materials Research Laboratory and Dept. of Geosciences, The Pennsylvania State University, University Park, PA 16802, USA.*

[2] *Environmental Resources Research Institute, The Pennsylvania State University, University Park, PA 16802, USA.*

Abstract

Because conduit systems in maturely developed karst aquifers have a low hydraulic resistance, aquifers drain easily and karst aquifers are subdivided into well-defined ground water basins. Ground water elevations are highest at basin boundaries; lowest at the spring where the ground water is discharged. Parameters that control the type of conduit development are (1) the effective hydraulic gradient, (2) the focus of the drainage basin, and (3) the karstifiability of the bedrock. Moderate to highly effective hydraulic gradients permit the runaway process that leads to single conduit caves and well ordered branchwork systems. Low hydraulic gradients allow many alternate flow paths and thus a large degree of fuzziness in the basin boundaries. Low gradient ground water basins also tend to merge due to rising water tables during periods of high discharge. Focus is provided by geological constraints that optimize discharge at specific locations that can evolve into karst springs. Karstifiability is a measure of the bulk rate at which aquifer rocks will dissolve. Fine grained, pure limestones and shaley dolomites mark the opposite ends of the range. The cave surveys of the Appalachian Highlands provide a data base that can be used to classify the lateral arrangements of conduit systems and thus determine the relative importance of the factors defined above.

Keywords:conduits, triple permeability, karst parameters, karstifiability, lithologic controls, structural controls.

Fragmentation des conduits, modèles des réseaux souterraines et localisation des bassins hydro-karstiques: étude de cas sur les Monts Appalaches

Résumé

A cause de la faible résistance hydraulique des systèmes de conduits des aquifères karstiques matures ceux-ci sont facilement drainés et peuvent être subdivisés dans des bassins hydrogéologiques distincts. Les altitudes des nappes karstiques sont maxima au bords des bassins et plus basses vers les sources. Les paramètres qui contrôlent le type de développement des conduits sont: (1) le gradient hydraulique effectif, (2) la concentration du bassin de drainage et (3) la «karstifiabilité» de la roche. Des gradients hydrauliques modérés ou élevés permettent le drainage rapide qui, à son tour, favorise la formation des grottes à galerie unique et des systèmes dendritiques bien ordonnés. Les gradients hydrauliques bas permettent la formation de plusieurs voies d'écoulement et, par conséquente, les limites des bassins karstiques sont moins nettes. En plus, les bassins à gradients bas ont la tendance de fusionner l'un à l'autre en suivant la remontée du niveau des nappes phréatiques pendant les crues. La concentration est donnée par les contraintes géologiques qui optimisent le drainage vers des points bien définis, pouvant devenir des sources karstiques. La «karstifiabilité» est une mesure de la vitesse globale de dissolution des roches qui constituent l'aquifère. Les calcaires fines, pures, et les dolomies marneux se situent aux extrêmes du domaine de karstifiabilité. La topographie des grottes des Monts Appalaches constitue une base de données qui peut être utilisée pour la classification des modèles des systèmes de conduits et, par conséquente, pour déterminer l'importance relative des facteurs définis ci-dessus.

Mots-clés: conduits, triple perméabilité, paramètres karstiques, karstifiabilité, contrôle lithologique, contrôle structural.

* corresponding author. *E-mail address*: wbw2@psu.edu.

Introduction

Karst aquifers have (among others) two characteristics that distinguish them from most other aquifers. One is an extreme permeability distribution generally described by the "triple porosity" model, one component of which is a system of pipes (known as "conduits"). The second is an intimate connection between ground water and surface water. Any functional model of karst aquifers must take account of the conduit system. In general, this is difficult because the complete conduit system can only rarely be directly observed and there are no really reliable techniques for mapping the conduit system from the land surface. The only data usually available are the results of tracer experiments which give overall connections and transit times, measurements of hydrographs and chemographs at the springs, and such segments as may be accessible to cave explorers. This leaves an immense amount of uncertainty in the proper placing of conduits and the internal functioning of ground water basins.

The most direct information on conduit patterns is obtained from the maps of caves that occur within the drainage basin. Caves consist of those fragments of active and abandoned portions of the conduit system large enough to permit human exploration. However, cave maps require interpretation. Cave explorers regard all accessible passages as part of the same cave. Thus, a large cave can be composed of a sampling of conduit system fragments that may be separated in both time and space. Higher (and generally dryer) parts of the cave are portions of conduits that were formed under earlier conditions sometimes extending far back into the Pleistocene and may not be related to contemporary drainage basins. A single accessible cave may also represent portions of the conduit system of more than one drainage basin. The most serious limitation is that almost all caves represent only small fractions of the complete conduit system.

A great deal of effort has gone into modeling the evolution of karst aquifers along the time axis. Recent papers, e.g. PALMER (1991), DREYBRODT (1992; 1996), GROVES & HOWARD (1994), HOWARD & GROVES (1995), SIEMERS & DREYBRODT (1998), KAUFMANN & BRAUN (1999, 2000), have shown that it is possible to describe the evolution from an initial fracture to a fully developed conduit and place the proeesses on a reasonable time scale. Although a tremendous number of caves systems have been examined in many parts of the world (KLIMCHOUK *et al.*, 2000), the geological constraints that limit ground water basin development have not been as well systematized. In this paper we return to issues of the development of karst ground water basins that were first raised long ago (WHITE, 1969; 1977). Using examples from the Appalachian Highlands to illustrate points, we attempt to understand the geological factors that control development of karst drainage basins and their associated conduit systems.

The Appalachian Mountains of eastern United States have extensive regions of karst development including the complexly folded and faulted Cambrian, Ordovician, and Devonian carbonate rocks of the Valley and Ridge Province and the dissected Appalachian Plateaus with low dip Mississippian limestones overlain by caprocks of shale and quartzite (DAVIES & LEGRAND, 1972; DAVIES *et al.*, 1984). The varying geologic settings in the Appalachian Mountains provide examples of many combinations of geologic constraints on karst drainage basin development.

Aquifers, Karst Aquifers, and Surface Water Basins

As a point of reference, we briefly describe what may be called a "textbook aquifer" ("textbook" means such standard references as FREEZE & CHERRY (1979), DOMENICO & SCHWARTZ (1990), or FETTER (1994)). A 'textbook' aquifer consists of these parts, arranged vertically: (1) The land surface where recharge is provided by precipitation. (2) The soil with its vegetative cover where precipitation is distributed between stored soil moisture, water that is infiltrated downward into the aquifer, and water that is returned to the atmosphere through evaporation and transpiration. (3) The vadose zone, a region of bedrock and regolith with air-filled pore spaces, that serves as a pathway for water in excess of soil moisture to move downward into the aquifer. (4) The water table, the surface that delineates the boundary between saturated and unsaturated portions of the aquifer. (5) The phreatic (or saturated) zone where all void spaces are water filled.

The "textbook aquifer" is characterized by the aquifer thickness (the total thickness of the rock unit for a confined aquifer and the thickness of the saturated zone for an unconfined aquifer), and the hydraulic conductivity of the medium. There are, in addition, hydraulic boundaries set in place by impermeable beds and structural constraints such as folding, and faulting. However, the width of the aquifer is usually unspecified — the aquifer is limited only by the limits of the rock unit. Flow fields are set by highs and lows in the water table which in turn are controlled largely by surface topography. Surface streams act as zones of ground water discharge.

Karst aquifers are rather more complicated. The essential components have been discussed at length in several textbooks (WHITE, 1988; FORD & WILLIAMS, 1989) and in recent papers (WHITE, 1998; 1999) and are sketched in Figure 1. As with the "textbook" aquifer, there is a diffuse component of recharge infiltrating through the soil and moving downward through fractures into the aquifer. As an additional factor, there may be some storage in the epikarst. Closed depressions on the land surface act as catchments for storm runoff which enters the aquifer through drains in the bottoms of the closed depressions. The third source is from sinking surface streams that provide what is known as allogenic recharge. The fraction of the ground water basin occupied by the catchment areas for sinking surface streams is one of the important parameters characterizing karst ground water basins.

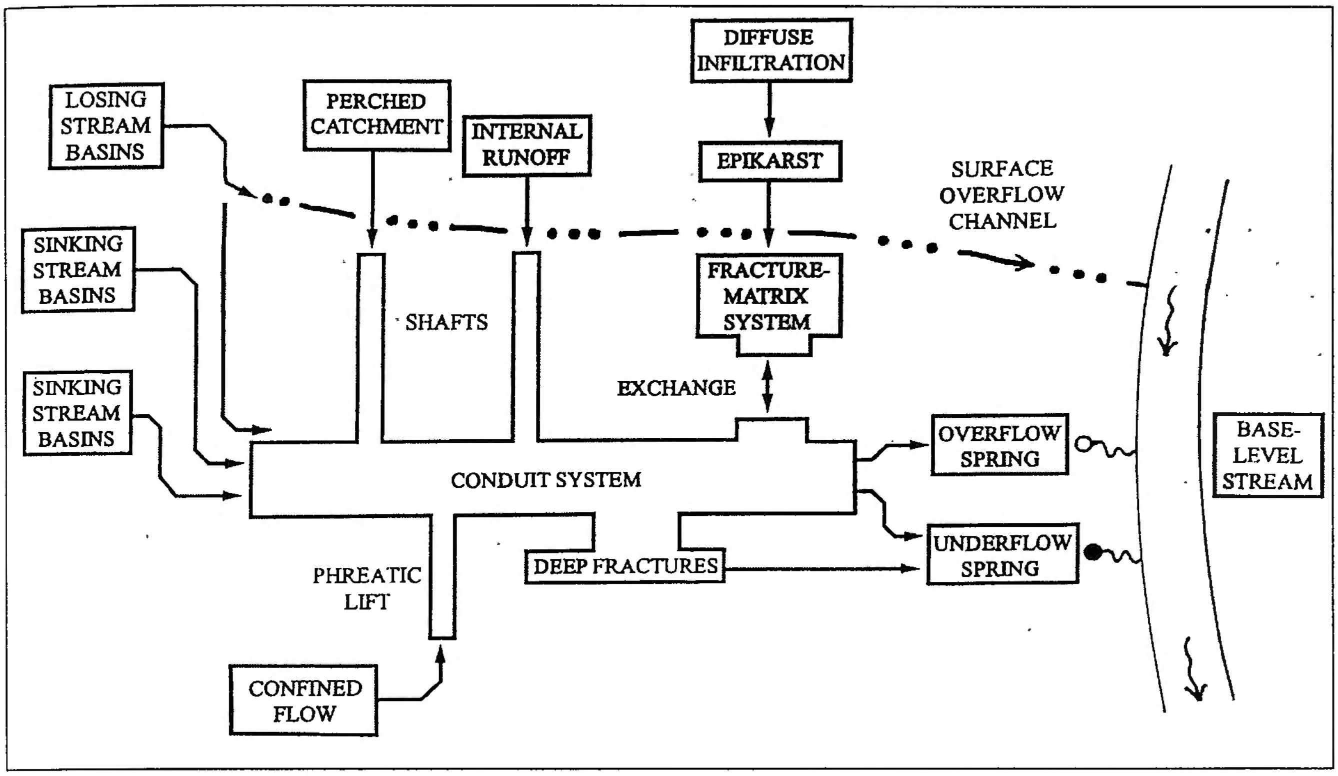

Fig. 1. Conceptual model for a karstic aquifer. From White (1999) with modification by J. A. Ray.
Modèle d'un aquifère karstique. D'après White (1999), modifié par J. A. Ray.

Sinking surface streams and the drains from closed depressions feed directly into the conduits which act as master drains transmitting water at high velocities to their discharge points at karst springs. Well developed conduits have low hydraulic resistance and often create troughs in the water table. Hydraulic gradients within the surrounding bedrock thus point toward the conduits rather than toward the springs (Ewers & Quinlan, 1981). Because of the arrangements of hydraulic gradients, each conduit system with its up-gradient infeeders and its set of sinking surface streams defines a ground water basin. The better the development of the conduit system, the better defined is the ground water basin. Hydraulic heads are low along the conduit and high between adjacent conduit collection systems. Thus the shallow part of the aquifer becomes segregated into cells, each functioning as a separate ground water basin. The downstream ends of the basins are located at springs where the drainage returns to surface routes. The boundaries of the ground water basins are defined by the total recharge areas including all surface stream catchments that drain into the conduit system. Ground water basins evolve with time as the base level surface streams continue to downcut their channels. The evolutionary pattern has been interpreted in the Mammoth Cave area (Quinlan & Ewers, 1989).

Some karst ground water basins are truly isolated so that all precipitation that falls within the basin ultimately appears at the spring. The boundaries of these basins often show a good degree of correlation with the boundaries of overlying surface water basins. Others, however, are linked by either piracy routes or spillover routes. Conduits may develop across surface water divides and thereby transmit water to or from other nearby surface water basins. Piracy routes are common and result in ground water basins seriously out of register with overlying surface water basins. The term "spillover route" is used for abandoned conduits that lie just above the active conduit system. These transmit water only during high flow conditions. Thus a ground water basin may have one set of flow paths active during base flow conditions and a quite different set of flow paths during flood flow conditions. The boundaries of the ground water basins also depend on ground water stages and flow conditions. The greater the internal relief of the basin – that is the head difference between the spring and the basin divides, the more localized the basin and the more stable the basin boundaries.

Karst aquifers in the Appalachian Highlands of eastern United States are restricted because of the limited thickness of the carbonate rock units. The Mississippian limestones that underlie the Cumberland and Allegheny Plateaus have thicknesses of only a few hundred meters. The Ordovician carbonate rocks of the folded Appalachians range in thickness up to several thousand meters but consist of mixed limestone and dolomite sequences. As a result, most ground water basins span the entire saturated thickness of the aquifer. The entire aquifer must be interconnected by diffuse flow through the matrix and fracture permeability but the transmission of water

through the conduit system is so much more efficient that the ground water basins account for nearly all of the water budget.

The active conduit systems in the Appalachian ground water basins are generally shallow. Some can be explored under base flow conditions as open cave passages with free-surface streams. Often the conduit is an alternating sequence of open stream passage and sections that are completely flooded. Explorations by cave divers are revealing some of the characteristics of the flooded sections. Typically, these extend to depths on the order of tens of meters below base level. Much greater depths have been reached in other areas and much remains unknown concerning the extent of conduit development below local base levels. Evidence from diving exploration and from the vertical development of some dry caves shows that these depths can reach hundreds of meters.

Conduit and Permeability Patterns

The *triple permeability model* (or triple porosity model) contains three components: *matrix permeability*, *fracture permeability*, and *conduit permeability*. Matrix permeability is the permeability of the bedrock itself – the interconnected pores, vugs, and other void spaces on the scale of individual mineral grains. Unconsolidated sand or gravel is an example of a medium with only matrix permeability. Fracture permeability is the result of mechanical rupturing of the rock, either joints, joint swarms, faults, or bedding plane partings. Brittle rocks are usually fractured. In some rocks, such as fractured granites, fracture permeability is the only significant permeability. Other rocks, such as massive sandstones, may contain both fracture and matrix permeability. Conduit permeability is provided by pipe-like openings created in such rocks as limestone, dolomite, and gypsum by the solvent action of circulating ground water. Although conduit permeability is usually confined to karstic rocks, it also occurs in some volcanic rock aquifers.

There is a great diversity of karstic aquifers depending on the relative contributions of the three permeability types as illustrated schematically in Figure 2. Many of the karst aquifers in eastern United States have formed in Paleozoic limestones with a negligible matrix permeability and are dominated by conduit systems and by allogenic recharge from surface catchments. Fracture flow plays an important role in transmitting water from diffuse recharge on the land surface to the conduits and in transmitting water to wells drilled in these aquifers. Aquifers in dolomite tend to have more poorly developed conduit systems so that the ground water movement is dominated by fracture flow. Fractured dolomites tend to be more useful for water supplies because the water can be more readily accessed by properly located wells and because the supply is less threatened by surface contaminants derived from sinkholes and sinking streams. In contrast, young limestones such as those making up the Floridan aquifer are highly permeable so that much of the ground water is transported through the matrix. Concentrated flows produce large conduits within the permeable rock mass. Fractures are relatively less important. The *Edwards Aquifer* in Texas is an intermediate case involving all three types of permeability.

Ground water velocity increases in a nonlinear fashion with the effective aperture of fractures and conduits, resulting in a concentration of flow along a few preferred pathways. Flow velocities in conduits are often sufficient to drive the system into a turbulent regime. The contrast in velocity between the least permeable and most permeable parts of the same aquifer is often six to ten orders of magnitude. It is a common fallacy to assume that if one scales over a sufficient volume of the aquifer, then the fractures and conduits will average out and the aquifer as a whole can again be characterized by a single hydraulic conductivity. This does not work. The contrast in velocity and flow is too extreme. WORTHINGTON (1999) has calculated that more than 90% of the flow in a selection of karst aquifers is through what he calls the "channel" system.

The karstic characteristics of an aquifer can be evaluated in terms of the degree of development of the conduit system, the degree of coupling between the conduit permeability and the matrix and fracture permeability, and on the relative contribution of surface water. The arrangements of the conduit system are reflected in resulting cave patterns. Some of the possibilities are sketched in Figure 3 in a manner similar to patterns proposed by PALMER (1991).

The pattern in 3(A) shows a *single conduit cave* with the stream from a surface catchment entering one end and the discharging through the other end. The cave segment itself

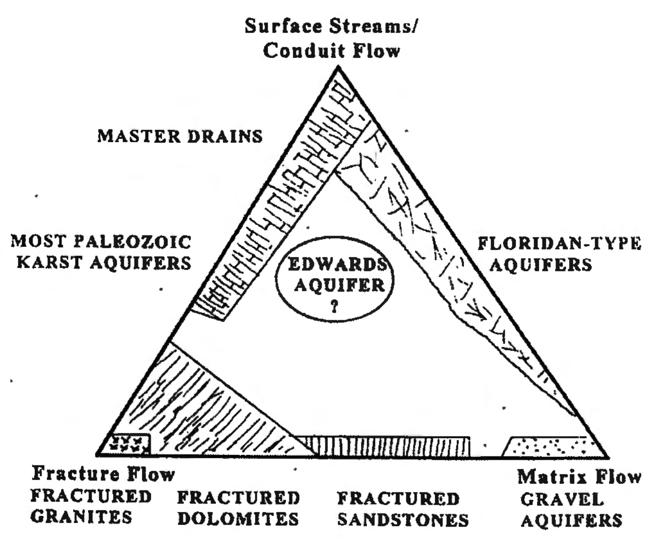

Fig. 2. Contributions of the three components of the triple permeability model to various aquifers.
Contributions des trois composantes du modèle de la triple perméabilité pour différents aquifères.

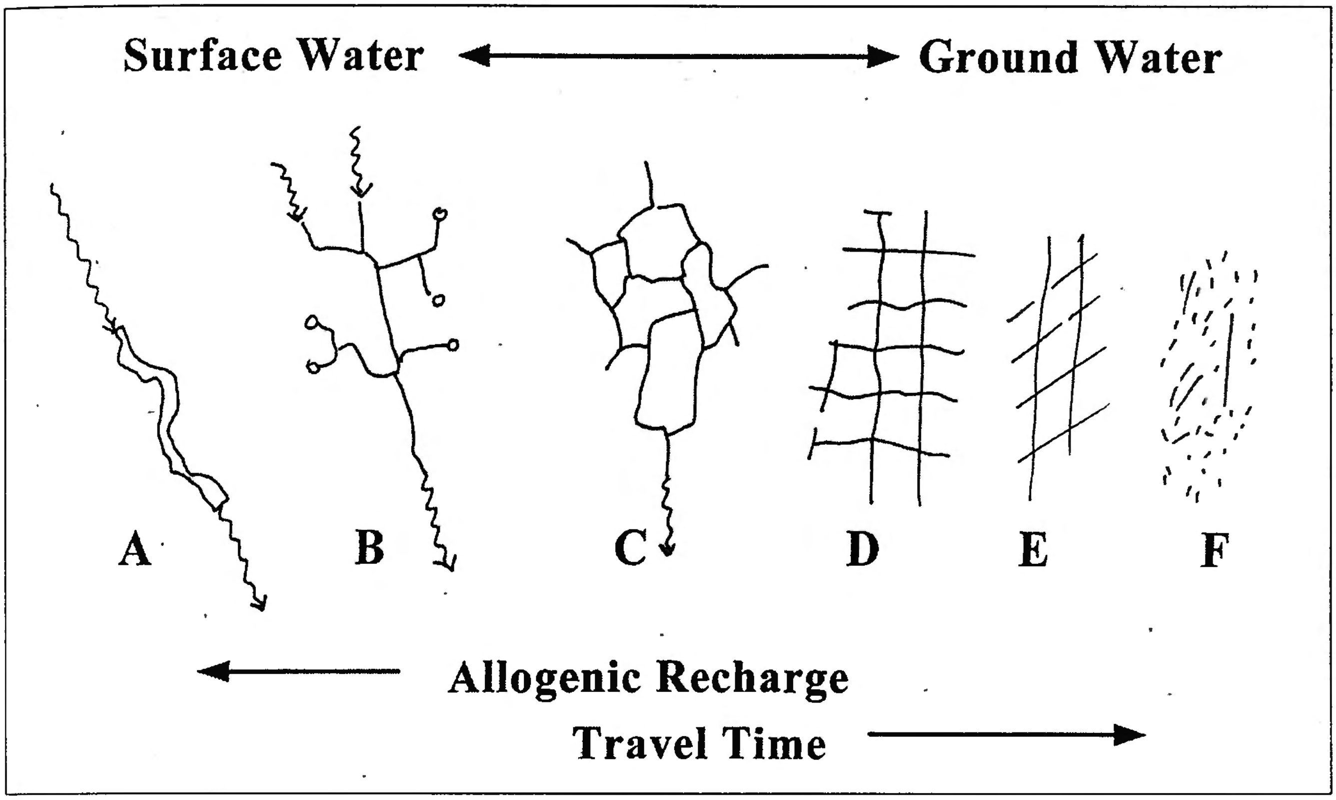

Fig. 3. Sequences along the continuum from a single conduit cave acting as an underground route for a surface stream to non-karstic fracture and porous media aquifers.
Séquences le long d'une cavité qui fonctionne comme voie souterraine d'un cours de surface vers des aquifères fracturés et poreux non-karstiques.

may either contain a free-surface stream or be located completely in the phreatic zone. There is little hydraulic coupling between the water stored in the surrounding bedrock and the surface water draining through the cave. The limit, as the length of the cave segment is made shorter and shorter, is the natural bridge. Many caves are found in many parts of the world that are essentially underground reaches of surface streams. The best known such cave in the Appalachians is the Sinks of Gandy (Fig. 4). Whether or not the water in such conduit segments should be considered ground water is a matter of semantics. The main catchment is a surface water basin with a well-defined divide.

The pattern in 3(B) is that of a *branchwork cave*. There are multiple surface inputs both from sinking steams and from the drains of closed depressions. The underground pattern has many features in common with the headwaters regions of surface streams. The branchwork drains into a master trunk that ultimately leads to the spring. A cave fragment of the downstream trunk, of course, is not distinguishable from a trunk of type 3(A) except that its catchment is underground rather than on the surface. The branchwork pattern is typical of many Appalachian ground water basins. What is usually observed are inlet caves at stream sinks or at sinkhole collapses, outlet caves accessed through springs or paleosprings, and other bits of the collector system accessed in various ways through shafts, collapses, and valley intersections. In many drainage basins, various caves can be spliced together along with locations of stream sinks and rise points to construct a moderately accurate description of the conduit system. Figure 5 shows a particularly nice reconstruction of conduit system for the Buffalo Spring Basin in Mammoth Cave National Park, Kentucky (MEIMAN & RYAN, 1999).

Patterns 3(C) and 3(D) are both characteristic of low gradient aquifers. Circulation of water primarily along bedding plane partings produces an anastomotic maze pattern; circulation of water primarily along joints produces a *network maze* pattern (PALMER, 1975). Flow velocities are lower both because of lower gradients and because of the larger effective cross-section since the flow is distributed over a large number of individual cave passages. The catchment boundaries for patterns (C) and (D) are less well defined. Exploration into the perimeters of such cave systems is often limited by passages simply too small for human penetration. The limit of pattern 3(D) is pattern 3(E). The solutional enlargement of joints and bedding plane partings becomes less and less until the passage becomes impenetrable by humans and at the limit becomes fracture permeability. Fewer and fewer fractures and all that remains is the matrix permeability, 3(F). With patterns 3(E) and 3(F) the basin boundaries have essentially disappeared and in the limit, the karstic ground water basins have blurred into fracture or porous media aquifers.

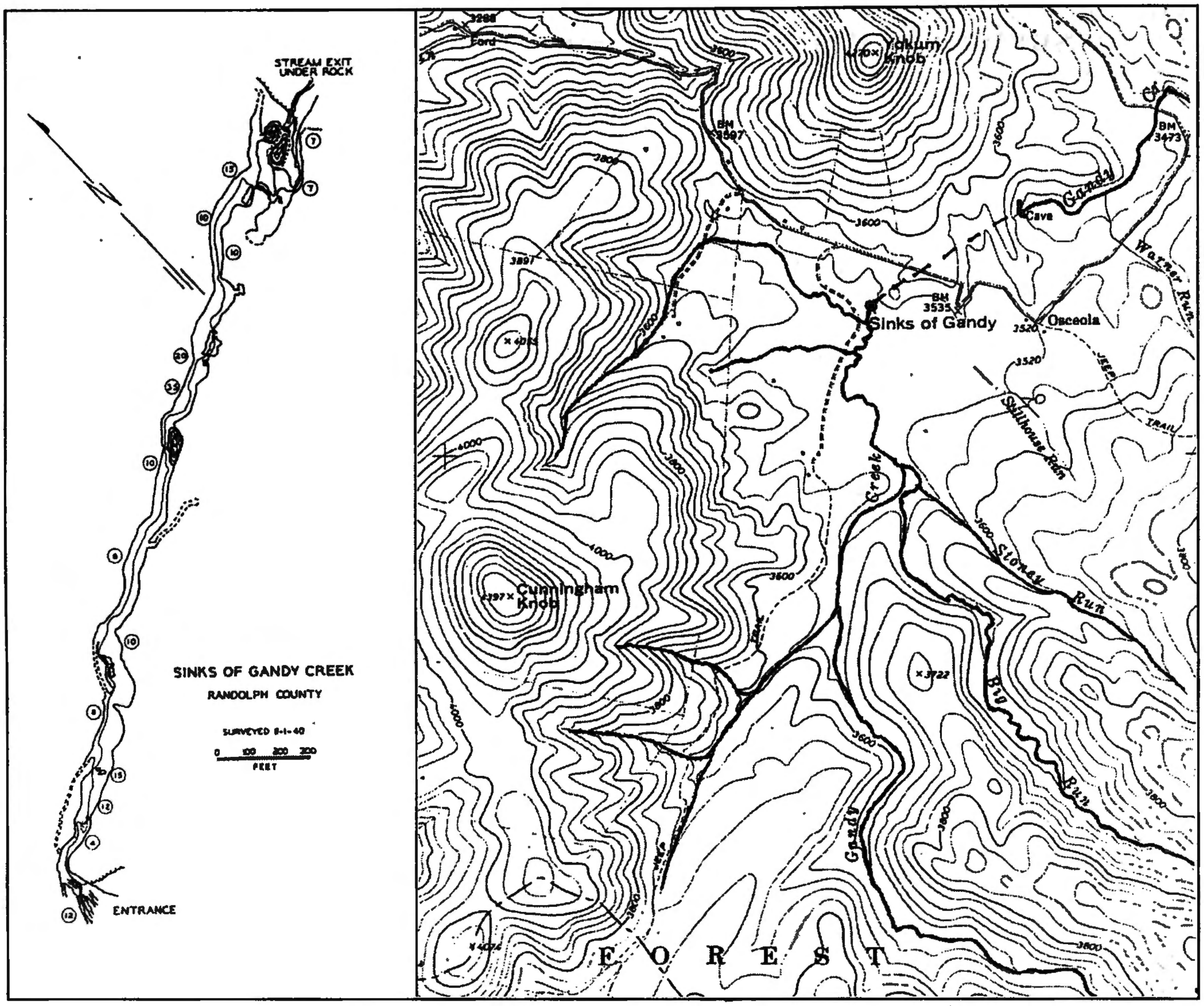

Fig. 4. Map of the Sinks of Gandy, Randolph County, West Virginia. Topography from US Geological Survey Sinks of Gandy 7.5 minute Quadrangle. Cave map from Davies (1958). A more detailed map appears in Dasher (2000).
Carte de Sinks of Gandy, Randolph County, West Virginia. Topographie d'après l'US Geological Survey Sinks of Gandy, rectangle de 7,5 minutes. Carte de la grotte d'après Davies (1958). Une carte plus détaillée a été publiée par Dasher (2000).

In the sequence of conduit permeabilities sketched in Figure 3, those on the left are dominated by surface water; those on the right by ground water. The fraction of allogenic recharge decreases from left to right. Travel times increase from left to right. The concept of a ground water basin is well defined for conduit systems of the left. Basin boundaries and indeed the very concept of a ground water basin becomes increasingly fuzzy and finally fades away completely from left to right.

Parameters controlling the development of karst ground water basins

There have been three broad approaches to the study of karst aquifers: (1) Calculations of the flow mechanisms in the conduits. (2) Geochemical/hydrodynamic modeling of the evolution of fracture systems to maturely developed conduits. (3) Interpretation of cave patterns and drainage basin patterns based on the geologic setting in which the cave or basins are located. Calculations of type (1) have assumed various geologic frameworks but generally take the geologic framework as a given condition. Early speleogenetic research was largely intuitive and depended strongly on the geologic framework. As analysis of karst aquifers became more mathematically and geochemically sophisticated, the emphasis shifted to approaches (1) and (2). Recent work has been returning to the geologic framework.

Our concern here is with the geologic boundary conditions that provide the limitations on how the ground water basins can develop. If we think – in a rather idealistic sense – of the process of conduit system development being guided by a

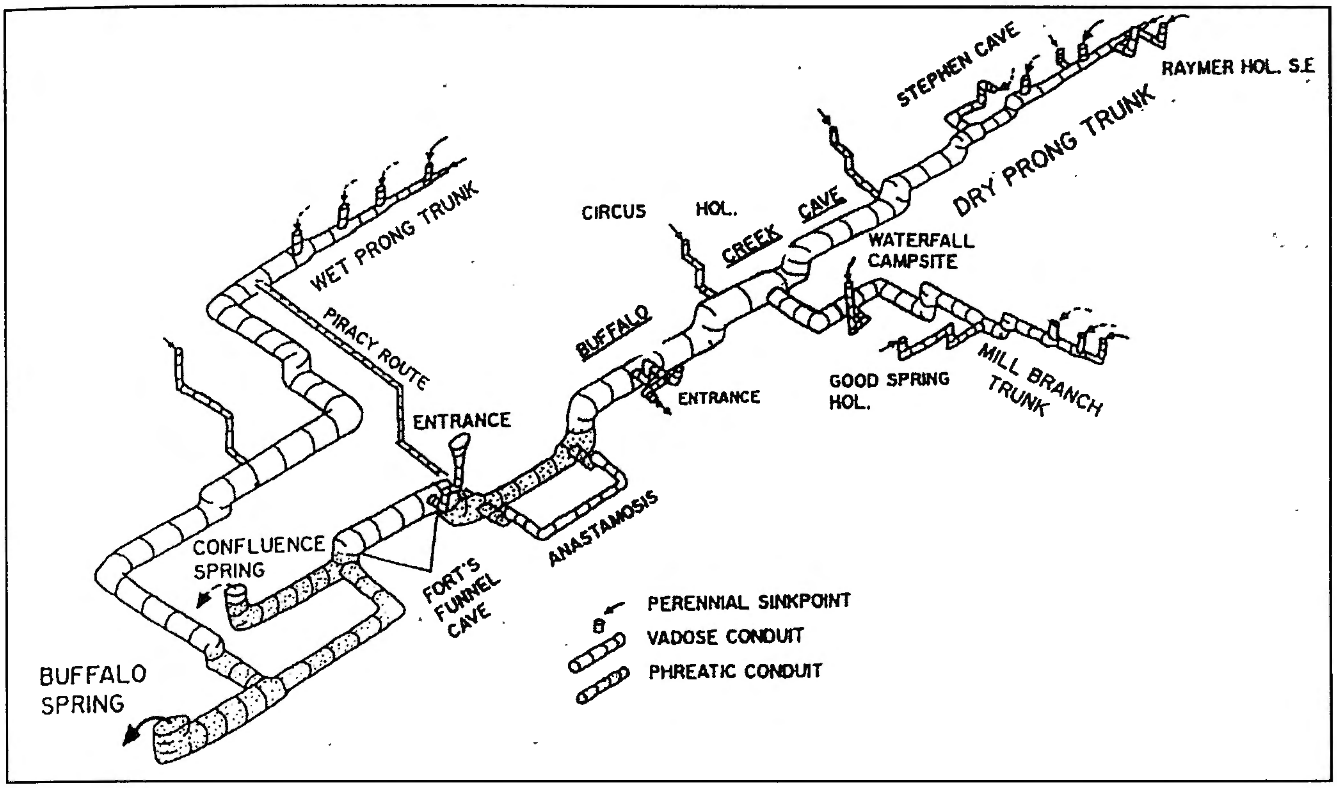

Fig. 5. Conduit system for Buffalo Spring drainage basin, Mammoth Cave National Park, Kentucky. Reconstruction from surveyed caves and known sink and spring locations by MEIMAN & RYAN (1999).
Système souterrain du bassin de drainage de Buffalo Spring, Parc National de Mammoth Cave, Kentucky. Reconstruction par MEIMAN & RYAN (1999) d'après la topographie des grottes et la situation des pertes et des sources connues.

differential equation, there must be parameters that provide the boundary conditions for the differential equation. Parameters that describe the boundary conditions for the development of the aquifer can be broadly classified into: (1) the effective hydraulic gradient, (2) the focus of the drainage basin, and (3) the karstifiability of the bedrock.

Effective Hydraulic Gradient

Localization of ground water flow into a relatively small number of relatively large conduits is a runaway process driven by local hydraulic gradients. Steep gradients such as those in the tributary valleys of the dissected Cumberland Plateau which range from 0.01 to 0.03 are more than adequate. Cave profiles in these settings tend to be stair-step with vertical segments interspersed with reaches of low gradient passage. The gradients in the Mammoth Cave area of Kentucky are in the range of 0.001. Gradients in the Valley and Ridge Province and in the Great Valley Province where the carbonate rocks occur on the valley floor, are in the range of 0.01 to 0.001. All of these are entirely adequate for the development of conduits and distinct ground water basins. If other factors are favorable, conduits and thus localization of flow into ground water basins will occur with extremely low gradients. As other factors become less favorable, higher gradients are needed to overdrive the system.

The overall hydraulic gradient of a drainage basin is given by H/L where H represents the maximum internal relief between the highest input point and the discharging spring. L represents the length of the basin. Larger basins require higher relief to maintain the same gradient. The internal relief of Appalachian karst drainage basins is generally less than 300 meters. The lengths of Appalachian basins are generally in the range of a few kilometers to a few tens of kilometers so in this setting hydraulic gradients are rarely controlling factors. In low relief karst areas and and in very large karst drainage basins hydraulic gradient becomes more important.

Focus

"Focus" is a term introduced to describe the role of the physiographic and geologic setting in forcing the underground drainage into localized regimes. Development of contemporary karst drainage systems has taken place on time scales of hundreds of thousands of years although earlier stages may extend back to several million years. In general, and certainly in the Appalachians, these time scales are short compared with the age of most structural and stratigraphic features. The geologic setting can be taken as a fixed framework within which the ground water system must develop. Factors that serve to focus conduit drainage systems into particular patterns are summarized in Table 1 and discussed below.

In the Appalachian Plateaus, the most important of the focusing agents is the precursor surface drainage. Base level streams determine the down-gradient end of the drainage system. Preexisting tributary valleys on the clastic rocks overlying the carbonate units determine the pattern of surface drainage. When these tributary streams downcut into the underlying carbonate rocks, the gradient along the surface stream channel is sufficient to drive the development of a conduit system. The surface streams are eventually pirated underground and become the master conduits for a ground water basin. Underground drainage in a very large number of the tributary valleys of the dissected Cumberland Plateau of Tennessee and Alabama roughly parallel the surface drainage. The conduits are often offset from the valley thalweg and occur under the valley walls. The ground water basins with their allogenic surface catchments are well defined and are often almost coincident with the surface divides.

An example is Sinking Cove located in the dissected southern margin of the Cumberland Plateau in Tennessee (Fig. 6). Ancestral Little Crow Creek drained from the clastic rocks of the Cumberland Plateau to the ancestral Tennessee River. The river breached the sandstone caprock along a northeast-southwest trending anticline to form the Sequatchie Valley and rapidly downcut through the underlying carbonate rocks. Crow Creek and its tributary Little Crow Creek cut headward to the northwest gradually exposing carbonate rock along the tributary valley. Disruption of the surface drainage by underground piracies eventually produced large closed depressions along the valley floor known sequentially as Cave Cove, Farmers Cove and Wolf Cove and a 2 km-long dry valley at the bottom known as Sinking Cove. The surface stream from the Cumberland Plateau first sinks in the floor of Cave Cove, follows underground routes through Farmers Cove and Wolf Cove to appear at a spring at Sinking Cove Cave. The floor of Sinking Cove is supported by the 5 – 7 m thick Hartselle Sandstone. The sandstone is breached and the drainage goes underground again to finally reappear at the head of the Little Crow Creek Valley. The master conduit system has been fragmented but almost the entire conduit is accessible through Cave Cove Cave, Farmers Cove Cave and Sinking Cove Cave. In this example, the ground water basin is in close alignment with the surface water basin and the entire pattern of the conduit system, except for the deflecting influence of the Hartselle Sandstone, was dictated by the precursor surface drainage.

Table 1. Factors serving to focus the development of conduit systems.
Facteurs qui contrôlent la concentration dans le développement des systèmes de conduits.

Precursor drainage

Structural factors

- Large scale structures
- Small scale structures
    - Fracture frequency
    - Fracture homogeneity

Stratigraphic factors

- Overall thickness of carbonate rocks above and below base level
- Hydrologic barriers
- Stratigraphic homogeneity

Large scale structural features such as folds and faults have a major controlling influence on both surface and ground water basins. This is most evident in the Valley and Ridge and Great Valley Provinces of the Folded Appalachians. Here major northeast-southwest trending folds bring up Ordovician and Cambrian carbonate rocks along anticlinal valleys. Faulting is common and is mostly parallel to the regional northeast-southwest structural trend. Here structural components completely dominate the development of ground water basins. The carbonate rocks are mixed sequences of limestones and dolomites. Because the carbonate rocks are in the lower part of the stratigraphic sequence, they tend to be exposed in the valley floors of breached anticlines. Allogenic recharge is collected from small basins on the synclinal ridges composed mainly of clastic rocks. The surface streams draining these catchments sink at the contact with the carbonate rocks. The underground drainage, however, tends to be parallel to the strike so the flow paths make a right angle turn and discharge at springs located where secondary valleys have cut across the regional structure. The surface catchments are defined by precursor drainage but the underground component is controlled largely by structure. Caves in steeply dipping rocks tend to extend primarily along strike as documented in central Pennsylvania by Deike (1969) and in many other examples in Virginia, West Virginia, and east Tennessee. Maze caves can form where dips are low on the crests of anticlines (White, 1960; Palmer, 1975). Caves as conduit fragments are particularly helpful in identifying dominant structural controls on ground water flow systems.

Small structures are mainly fractures: joints, joint swarms, and bedding plane partings. The important parameters are the density of fracturing, the initial apertures of the fractures, and the homogeneity of fracture apertures. The importance of fracture density was recognized by Ford & Ewers (1978) and used as the basis for their "four states" hypothesis for cave development. The higher the fracture density, the more readily the ground water flow can follow paths dictated by hydraulic gradients alone and thus reflect the overlying surface water basin. Because flow through fractures increases with the cube of the fracture aperture, the heterogeneity of the fracture sets is very important. Master fractures dominate the flow

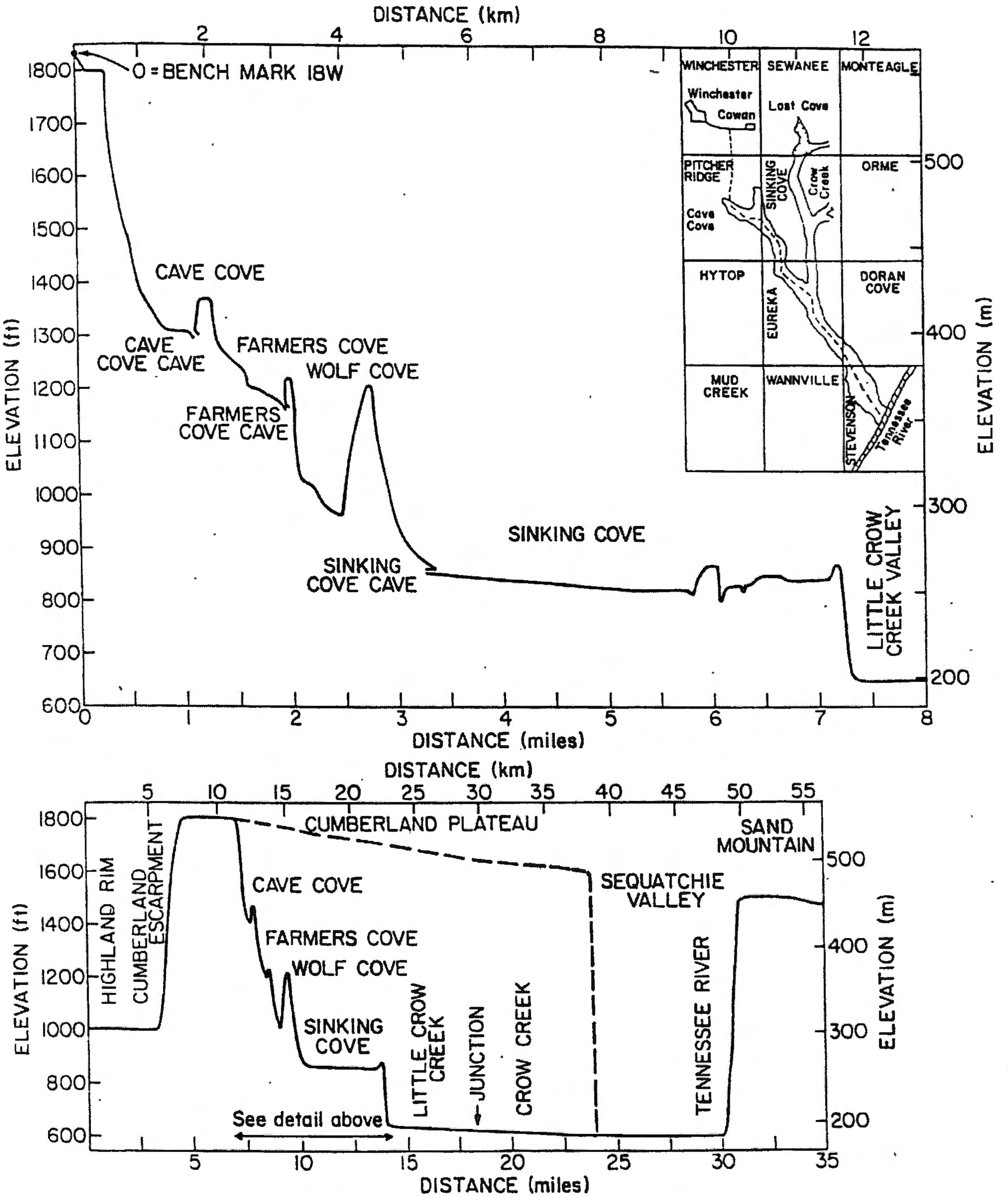

Fig. 6. Longitudinal profile of Sinking Cove, southern Tennessee. The upper figure gives the detailed profile along the valley thalweg constructed from US Geological Survey 7.5 minute topographic quadrangle maps. The maps used are given in the insert. The lower figure shows a larger scale profile across the Cumberland Plateau.

Profil longitudinal du Sinking Cove, Tennessee du Sud. En haut, profil détaillé le long du thalweg d'après la carte de l'US Geological Survey, rectangle de 7,5 minutes. En vignette, les cartes utilisées. En bas, profil à une échelle plus générale le long du plateau de Cumberland.

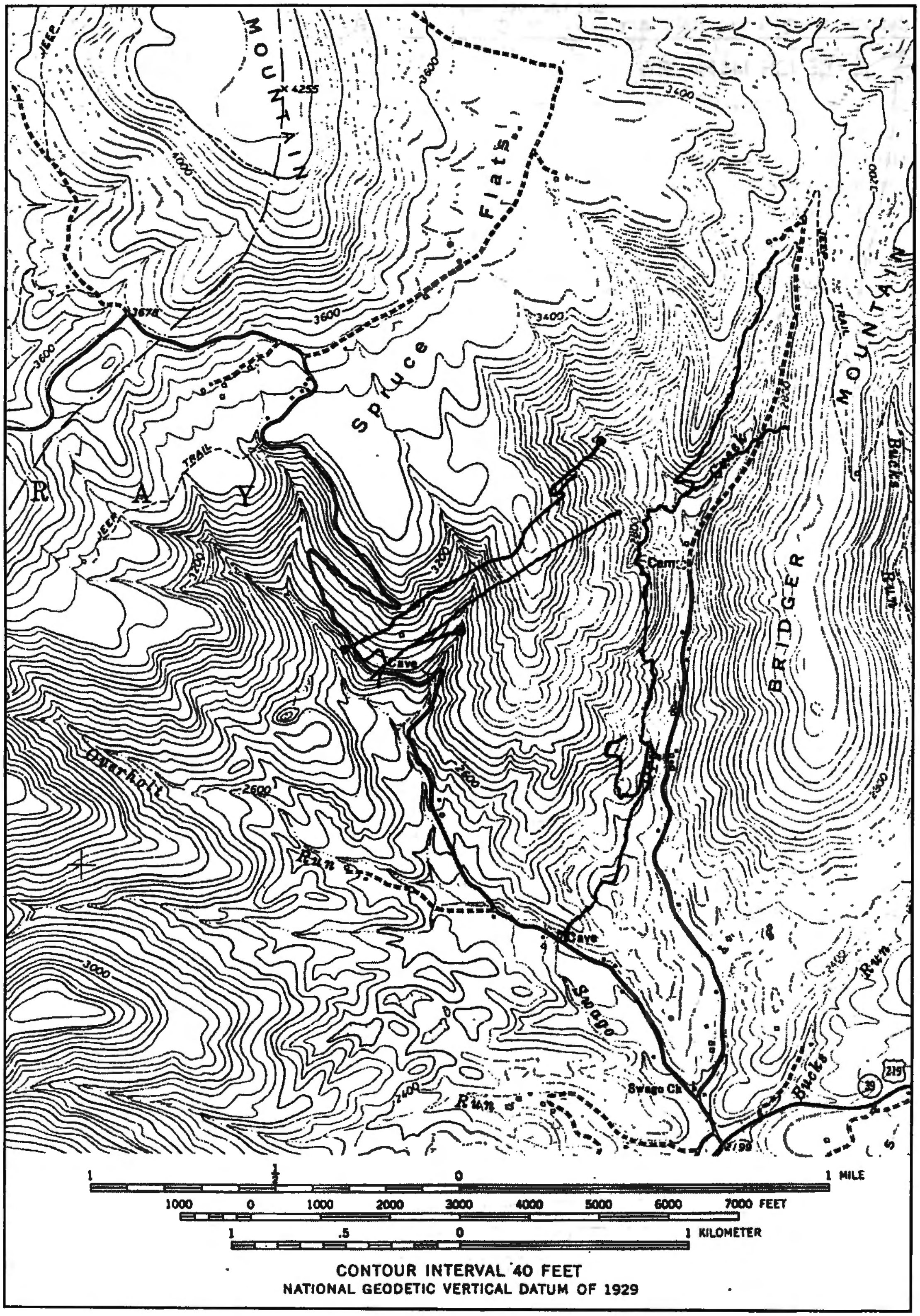

Fig. 7. The Swago Creek Basin, Pocahontas County,West Virginia. Base map from US Geological Survey Hillsboro 7.5 minute quadrangle. Superimposed cave maps adapted from Storrick (1992). Overholt Blowing Cave follows the surface route of Dry Creek. The Swago-Carpenters Cave System is guided by N60°E master fractures.

Le Bassin du Swago Creek, en Pocahontas County, West Virginia. Carte de base d'après l'US Geological Survey Hillsboro, rectangle de 7,5 minutes. Cartes des grottes superimposées, adaptées d'après Storrick (1992). La grotte d'Overholt Blowing suit le trajet de surface du ruisseau de Dry Creek. Le système de Swago-Carpenters est contrôlé par des fractures majeures orientées N60°E.

system The eventual development of a conduit system will trend along the path provided by the widest fractures even if such pathway is not along the maximum hydraulic gradient. Tension fractures parallel to anticlines may assist in controlling the strike-oriented drainage in folded rocks. Stress release fractures are young geological features with wide apertures and so are important in guiding conduit systems along tributary valley walls rather than down the thalweg as is observed in many Appalachian basins (SASOWSKY & WHITE, 1994). If fracture apertures are strongly heterogeneous, the large aperture master fractures can completely dominate the pattern of the conduit system.

The ability of master fractures to override the inherited surface drainage can be seen in the Swago-Carpenters Cave System in the Swago Creek Basin, Pocahontas County, West Virginia (Fig. 7). There are two active drainage lines in this dendritic valley each fed by surface catchments on overlying clastic rocks. Multiple small surface streams sink into the nearly flat-lying Mississippian Greenbrier Limestone. The Dry Creek sub-basin is underdrained by Overholt Blowing Cave which is parallel to the surface channel although offset from it under the valley wall. The Swago-Carpenters Cave System is one of the tributaries of the second sub-basin, with a more complicated drainage that ultimately discharges in Cave Creek Spring. The Swago-Carpenters System is developed along a N60°E master fracture set which is oblique to the surface drainage. The master fracture has allowed drainage to be diverted from the Dry Creek sub-basin to the Cave Creek sub-basin.

Lineaments are lines of structural weakness on a scale somewhat larger than that of master fractures. Lineaments often cross-cut local structures. The best West Virginia example of the influence of lineaments on drainage basin development is the Simmons-Mingo Cave System in Randolph County. The cave is developed along a major lineament and diverts drainage beneath a major topographic divide along a path oblique to the surface drainage lines (MEDVILLE, 1977). The presence of a lineament is apparently responsible for the exceptional depth development in Fern Cave, Alabama (WILSON, 1977) and for other cavern development is the southern Cumberland Plateau.

Stratigraphic factors that guide the evolution of karst ground water include the overall thickness of carbonate rocks, interbedded shales, sandstones and other rocks that can act as hydrologic barriers, and the homogeneity of the carbonate rock units.

Thickness of carbonate rocks is a self-evident factor, long recognized. Conduit drainage systems require a certain volume of rock in which to develop. The great karst regions of the world such as the Adriatic karst and the south China karst are developed on thousands of meters of carbonate rock. Fluvial drainage systems have been lost long ago to predominantly karstic drainage systems. In moderate relief terrains such as the Appalachians, a few hundred meters of good limestone is sufficient for the development of large and complex karst ground water basins. Fifteen to 20 meters of Alderson Limestone in West Virginia allows the development of significant caves. The 6–7 meter thickness of the Vanport Limestone in western Pennsylvania hosts large and complex maze caves such as Porters Cave, Brady's Bend Cave, and Harlensburg Cave (WHITE, 1976).

An interesting question is whether there is a minimum thickness for carbonate rock. It appears from observations on thin, but good quality limestones in western Pennsylvania that there is a minimum thickness and it is on the order of one to two meters. In the thin limestone units that occur in the Pennsylvanian and Mississippian sequences of mainly clastic rocks, there are solutionally modified fractures, some of which would qualify as conduits in the sense that they exceed the 10 mm aperture required for the onset of karstic flow dynamics but they have not evolved into caves. There are, of course, other factors. Thin limestones sandwiched between impermeable shales may have no source of recharge. Hydraulic gradients are important and may be too low along the flat-lying thin limestone to initiate cave development.

Hydrologic barriers are beds of shales, sandstones, and cherts that impede ground water flow. Such barriers are particularly important in the early stages of conduit development when the choice of flow path is very sensitive to the characteristics of the bedrock. (PALMER, 1991; SIEMERS & DREYBRODT, 1998). The role of hydrologic barriers has been examined in considerable detail by LOWE & GUNN (1997), LOWE (2000) & OSBORNE (1999) as part of the concept of "inception horizons". Thin layers of shale or shaly limestone can guide the initiation phase of cave development but these barriers are usually breached as the conduit enlarges. Thicker beds can function as hydrologic barriers guiding the overall development of the drainage basin.

In the Mississippian Greenbrier Limestone of West Virginia are two such units: the Greenville Shale, 15 – 20 meters thick which separates the Alderson Limestone from the remainder of the carbonate units, and the Taggard Shale, a 7 m thick limey shale that occurs in about the middle of the carbonate section (Fig. 8A) (WHITE & WHITE, 1983). The Greenville Shale is sufficiently thick that the Alderson Limestone is hydrologically isolated from the other carbonates. Caves developed in the Alderson are not connected with caves in the remainder of the carbonate section. The Taggard sometimes limits vertical circulation in the limestones and sometimes is breached so that cave development crosses the Taggard. Underground crossings of the Taggard Shale occur mainly along major fractures. Passages take a canyon form indicating that erosive underground streams may have been necessary to cut through the shale. In the southern Appalachians, the Hartselle sandstone, a 5–7 meter-thick unit separates the Mississippian Monteagle and Bangor Limestones (Fig. 8B). Again, this unit serves to block vertical flow so that caves tend to develop either immediately above or immediately

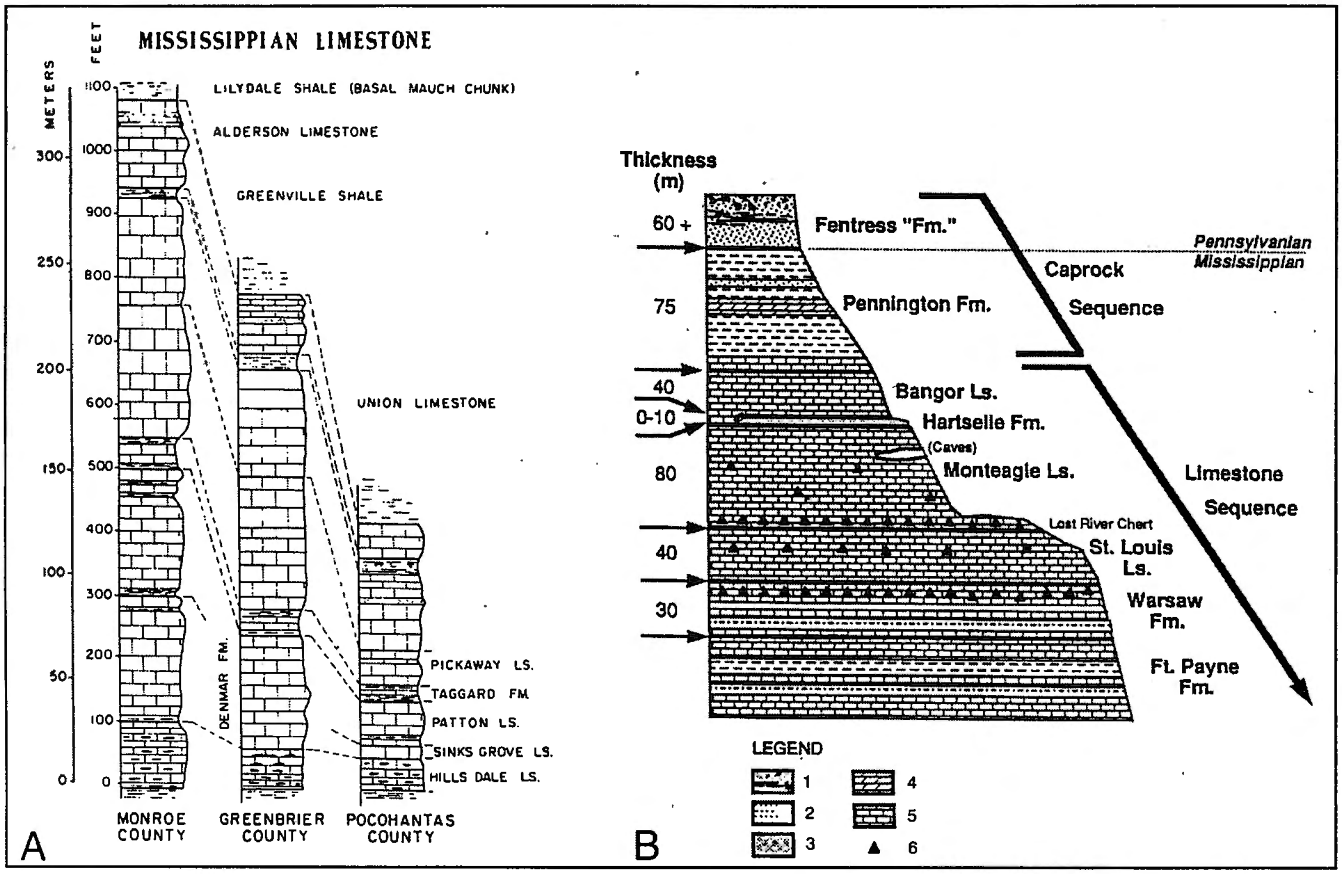

Fig. 8. Stratigraphic sections for (A) the Mississippian Greenbrier limestone of eastern West Virginia and (B) the Mississippian limestone sequence of the southern Cumberland Plateau showing the location of hydrologic barriers.
Sections stratigraphiques par: (A) les calcaires du Mississippien de Greenbrier (est de la West Virginia) et (B) séquence des calcaires mississippiens du sud du Plateau de Cumberland avec la situation des barrières hydrologiques.

below the Hartselle Sandstone. Both Taggard shale and Hartselle sandstone act as inception horizons. In some cases caves are formed directly above these units because they perch the ground water flow. In other cases, the caves form directly below the shaley units which can also act as confining beds. Interbedded chert horizons can also interrupt ground water flow and can act as perching or confining horizons.

Stratigraphic homogeneity is the variability in lithologic character along the stratigraphic sequence from one bed to another. In a perfectly homogeneous carbonate sequence all beds would have the same chemical composition and all would consist of the same carbonate lithology. Such sequences are rare. Highly cavernous rock units often vary in lithologic character, e.g. micrites, sparites, oolitic limestones and others, without disrupting cave-forming processes. Alternating beds of pure limestone and shaley limestone or alternating beds of pure limestone and dolomite inhibit the cave-forming process. Much depends on the scale of the interbedding. Alternating sequences of thin beds are most effective at inhibiting cave-forming processes.

Karstifiability

"Karstifiability" is introduced as a term that describes the ease with which a particular rock unit yields to karst-forming processes. Karstifiability is related to the kinetics of carbonate rock dissolution but is more inclusive in that it also includes the pacifying effects of other components and the role of insoluble residues in blocking further dissolution of the primary bedrock. The main components of sedimentary rocks are sketched in Fig. 9. Within the Appalachians, the best developed conduit systems occur within the Mississippian Greenbrier, Bangor, Monteagle, and St. Louis Limestones all of which are relatively pure limestones. Conduits do occur in the dolomites of the Valley are Ridge but are generally less well developed. Fracture aquifers are common in the dolomites. High concentrations of quartz sand do not seem to inhibit conduit development. The cavernous

Loyalhanna Limestone in western Pennsylvania contains about 50 percent quartz sand. In contrast, shaley limestones are rarely cavernous. These rocks, in fact often act as aquicludes. Their presence disrupts the normal development of ground water basins.

Although the role of lithology in determining the karstifiability is well understood in qualitative terms, quantitative analysis is much more difficult. A detailed comparison of cave volume with chemical, petrologic and mineralogic characteristics of the carbonate rocks (RAUCH & WHITE, 1970) revealed subtle distinctions such as an inverse relationship between cave development and the aluminum content of the bedrock. A more important question is whether there is a threshold in the impurity content that would distinguish between karstifiable and non-karstifiable rock units. The existence of such a threshold would be important in assessing land use hazards in carbonate terrains.

As a proposal for quantitative assessment of karstifiability we can consider the bulk chemical composition of the rocks. The petrologic complexity of karstic rocks can be reduced to a set of chemical components [CaO], [MgO], [SiO_2], and [Al_2O_3], leaving aside the carbonate, [CO_2] component and also any other minor elements that may be present. The quantities in square brackets are in units of moles, derived from chemical analyses of the rock. These can be normalized as mole fractions. The mole fraction of CaO, for example is defined as:

$$N(\mathrm{CaO}) = \frac{[\mathrm{CaO}]}{[\mathrm{CaO}] + [\mathrm{MgO}] + [\mathrm{SiO_2}] + [\mathrm{Al_2O_3}]}$$

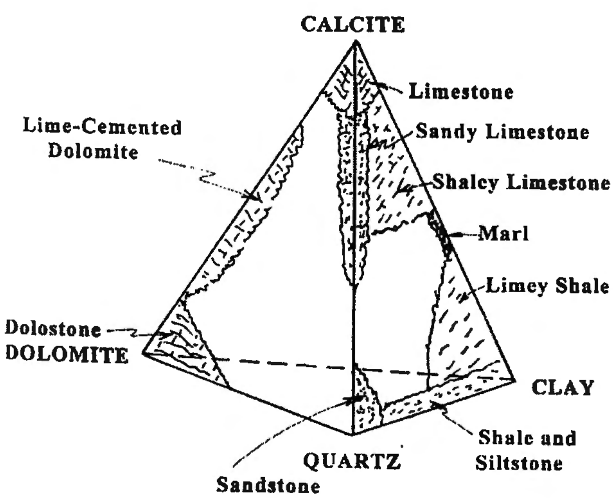

Fig. 9. Composition tetrahedron for sedimentary rocks.
Le tétraèdre des composantes des roches sédimentaires.

The mole fractions of MgO, Al_2O_3 and SiO_2 are defined in the same manner as *N*(CaO).
The sum of *N*(CaO) + *N*(MgO) can be used as a measure of total carbonate minerals. The dolomitic character of the rock can be represented by:

$$N(\mathrm{dol}) = \frac{[\mathrm{MgO}]}{[\mathrm{CaO}] + [\mathrm{MgO}]}$$

The composition of the rock can be represented as total carbonates, clay minerals and free silica. Clay and related layer silicate minerals can be represented by kaolinite, $Al_4Si_4O_{10}(OH)_8$. Because Al and Si occur in a 1:1 ratio in kaolinite (or in a 1:2 ratio as the oxides, Al_2O_3 and SiO_2), we can deduct the silica needed to produce clay minerals and then use the remaining silica as a plotting variable. The three plotting variables, which must be re-normalized to 100 percent, are {*N*(CaO) + *N*(MgO)} representing carbonates, {*N*(Al_2O_3)} representing total clay minerals, and {*N*(SiO_2) – 2*N*(Al_2O_3)} representing free silica (quartz grains, silicified fossil fragments, or chert). These quantities can be used to plot the chemical compositions of the rock on a triangular diagram in a way that relates composition to mineralogy.

Attempts to use published rock analyses to map karstifiability are suggestive but inconclusive (Fig. 10). Three relatively pure limestones, the Pennsylvanian Vanport of western Pennsylvania, the Mississippian Monteagle of central Tennessee, and the Ordovician Stones River of eastern West Virginia are all highly cavernous. The Devonian Tonoloway of Pennsylvania and West Virginia is marginally cavernous. The Mississippian Warsaw of Tennessee is a shaley limestone that usually acts as an aquiclude. The problem is that published analyses are often from samples of unknown stratigraphic positions within a given formation. Further, most published analyses are for samples taken from rock quarries and thus represent the better quality limestone. Analyses on impure limestones with limited cave development are sparse. Although carbonate formations with limited cave development are known in the Appalachians, there are, at present, insufficient data on their chemical compositions to actually contour karstifiability on a diagram such as Figure 10.

Conclusions

Conduit systems provide high efficiency pathways for the movement of ground water through carbonate aquifers. Because conduits act as drains of low hydraulic resistance, ground water flow becomes localized in ground water basins with well-defined drainage divides. Although entire conduit systems are only rarely accessible to human inspection, many conduits can be reconstructed from survey and mapping of existing caves within the drainage basin. Factors that determine the pattern of the conduit system and the localization of

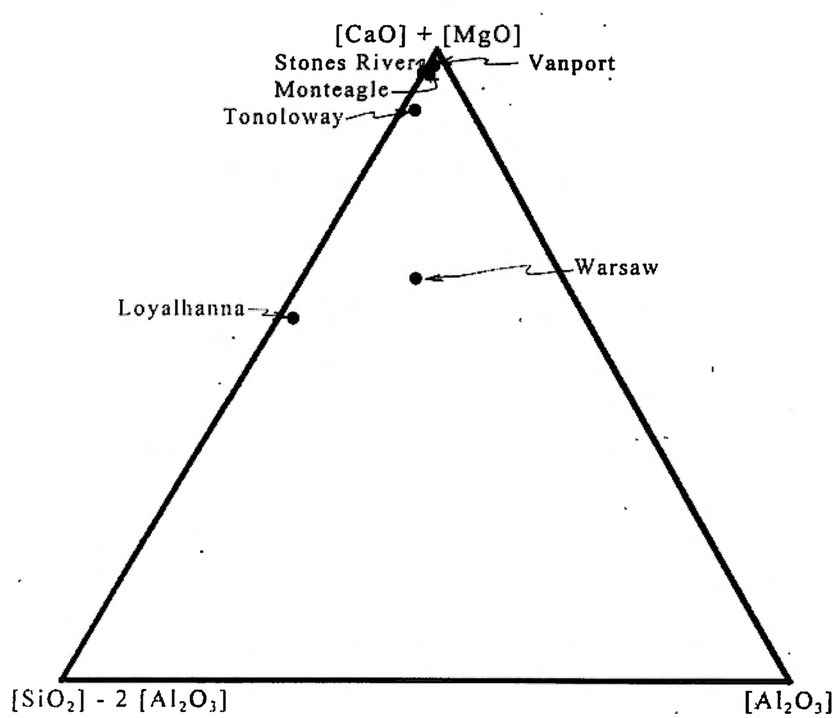

Fig. 10. Triangular plot of carbonate rock composition in terms of the three components that represent carbonates, clays, and silica. Compositions are calculated from published rock analyses. Pennsylvania data (Vanport and Loyalhanna Limestones) from O'NEILL (1964). West Virginia data (Stones River and Tonoloway Limestones) from McCUE *et al.* (1939). Tennessee data (Monteagle and Warsaw Formations) from HERSHEY & MAHER (1985).

Diagramme triangulaire de la composition des roches carbonatées en fonction de trois composantes représentant les carbonates, l'argile et la silice. Compositions calculées à partir des analyses publiées. Pour la Pennsylvania (Calcaires de Vanport et de Loyalhanna) les données d'après O'NEILL (1964). Les données de West Virginia (Calcaires de Stones River et de Tonoloway) d'après McCUE et al.(1939). Les données du Tennessee (Formations de Monteagle et de Warsaw) d'après HERSHEY & MAHER (1985).

the associated ground water basin are the hydraulic gradient, geologic factors that provide focus for the basin, and the karstifiability of the carbonate bedrock.

Caves provide useful fragments of the conduit system. Inspection of cave patterns provides a useful assessment of the geologic parameters that have guided the development of the ground water basin. In particular, the competition between superimposed drainage and local hydraulic gradients and structural controls is often well displayed in the cave systems.

Acknowledgements

The work described in this paper draws on many earlier investigations and the graduate students who conducted them. The support of the Environmental Resources Research Institute is acknowledged.

References

DASHER, G. R. (2000) The caves of East Central West Virginia. *West Virginia Speleological Survey Bulletin*, **14**, 296 p.

DAVIES, W. E. (1958) Caverns of West Virginia., *West Virginia Geologic and Economic Survey*, **XIX**, *A*, 330 p.

DAVIES, W. E., & LEGRAND, H. E. (1972) Karst of the United States. Chap. 15. In *Karst: Important Karst Regions of the Northern Hemisphere* (HERAK, M., & STRINGFIELD V. T., *Eds*.), Elsevier, Amsterdam, pp. 467–505.

DAVIES, W. E., SIMPSON, J. S., OHLMACHER, G. C., KIRK, W. S., & NEWTON E. G. (1984) Engineering Aspects of Karst. *US Geological Survey National Atlas of the United States of America*, one sheet.

DEIKE, R. G. (1969) Relations of jointing to orientation of solution cavities in limestones of central Pennsylvania. *Am. J. of Science*, **267**, pp. 1230–1248.

DOMENICO, P. A., & SCHWARTZ, F. W. (1990) *Physical and Chemical Hydrogeology*. Second Edition, John Wiley, New York, 506 p.

DREYBRODT, W. (1992) Dynamics of karstification: A model applied to hydraulic structure in karst terranes. *Applied Hydrogeology*, **3**, pp. 20–32.

DREYBRODT, W. (1996) Principles of early development of karst conduits under natural and man-made conditions revealed by mathematical analysis of numerical models. *Water Resources Research*, **32**, pp. 2923–2935.

EWERS, R. O., & QUINLAN, J. F. (1981) Cavern porosity development in limestone: A low dip model from Mammoth Cave, Kentucky. *Proc. of the Eighth International Congress of Speleology, Bowling Green*, KY, pp. 727–731.

FETTER, C. W. (1994) *Applied Hydrogeology*. Third Edition, Macmillan, New York, 691 p.

FORD, D. C., & EWERS, R. O. (1978) The development of limestone cave systems in the dimensions of length and depth. *Canadian J. of Earth Sciences*, **15**, pp. 1783–1798.

FORD, D. C., & WILLIAMS, P. W. (1989) *Karst geomorphology and hydrology*. Unwin Hyman, London, 602 p.

FREEZE, R. A., & CHERRY, J. A. (1979) *Groundwater*. Prentice-Hall, Englewood Cliffs, NJ, 604 p.

GROVES, C. G., & HOWARD, A. D. (1994) Early development of karst systems. 1. Preferential flow path enlargement under laminar flow. *Water Resources Research*, **30**, pp. 2837–2846.

HERSHEY, R. E., & MAHER, S. W. (1985) Limestone and dolomite resources of Tennessee. *Tennessee Division of Geology Bulletin* **65**, 252 p.

HOWARD, A. D., & GROVES, C. G. (1995) Early development of karst systems. 2. Turbulent flow. *Water Resources Research*, **31**, pp. 19–26.

KAUFMANN, G., & BRAUN, J. (1999) Karst aquifer evolution in fractured rocks. *Water Resources Research*, **35**, pp. 3223–3228.

KAUFMANN, G., & BRAUN, J. (2000) Karst aquifer evolution in fractured porous rocks. *Water Resources Research*, **36**, pp. 1381–1391.

KLIMCHOUK, A. B., FORD, D. C., PALMER, A. N., & DREYBRODT, W. *Eds*. (2000) *Speleogenesis: Evolution of Karst Aquifers*. National Speleological Society, Huntsville, AL, 527 p.

LOWE, D. J., & GUNN, J. (1997) Carbonate speleogenesis: an inception horizon hypothesis. *Acta Carsologica*, **26**, pp. 457–488.

LOWE, D. J. (2000) Role of stratigraphic elements in speleogenesis: The speleoinception concept. In *Speleogenesis: Evolution of Karst Aquifers* (KLIMCHOUK, A., FORD, D. C., PALMER, A. N., & DREYBRODT, W., *Eds*.), NSS, Huntsville, pp. 65–76.

McCUE, J. B., LUCKE, J. B., & WOODWARD, H. P. (1939) Limestones of West Virginia. *West Virginia Geological Survey*, **12**, 560 p.

MEDVILLE, D. M. (1977) Karst hydrology in the upper Elk River Basin, West Virginia. *NSS Bulletin*, **39**, pp. 19–26.

MEIMAN, J., & RYAN, M. T. (1999) The development of basin-scale conceptual models of the active-flow conduit system. In *Proceedings of the Karst Modeling Symposium*, (PALMER, A. N., PALMER, M. V., & SASOWSKY, I. D., *Eds*.), Karst Waters Institute Special Publication, **5**, pp. 203–212.

O'NEILL, B. J. Jr. (1964) *Atlas of Pennsylvania's mineral resources. Part 1. Limestones and dolomites of Pennsylvania*. Pennsylvania Geologic Survey Mineral Resources Report M50, 40 folio pages + 9 maps.

OSBORNE, R. A. (1999) The inception horizon hypothesis in vertical to steeply dipping limestone: applications in New South Wales, Australia. *Cave and Karst Science*, **26**, pp. 5–12.

PALMER, A. N. (1975) The origin of maze caves. *NSS Bulletin*, **37**, pp. 57–76.

PALMER, A. N. (1991) Origin and morphology of limestone caves. *Geological Society of America Bulletin*, **103**, pp. 1–21.

QUINLAN, J. F., & EWERS, R. O. (1989) Subsurface drainage in the Mammoth Cave area. In *Karst Hydrology: Concepts from the Mammoth Cave Area* (WHITE, W. B., & WHITE, E. L. *Eds*.), Van Nostrand Reinhold, NY, pp. 65–103.

RAUCH, H. W., & WHITE, W. B. (1970) Lithologic controls on the development of solution porosity in carbonate aquifers. *Water Resources Research*, **6**, pp. 1175–1192.

SASOWSKY, I. D., & WHITE, W. B. (1994) The role of stress release fracturing in the development of cavernous porosity in carbonate aquifers. *Water Resources Research*, **30**, pp. 3523–3530.

SIEMERS, J., & DREYBRODT, W. (1998) Early development of karst aquifers on percolation networks of fractures in limestone. *Water Resources Research*, **34**, pp. 409–419.

STORRICK, G. D. (1992) The caves and karst hydrology of southern Pocahontas County and the upper Spring Creek Valley. *West Virginia Speleological Survey Bulletin*, **10**, 215 p.

WHITE, W. B. (1960) Terminations of passages in Appalachian caves as evidence for a shallow phreatic origin. *NSS Bulletin*, **22**, pp. 43–53.

WHITE, W. B. (1969) Conceptual models for limestone aquifers. *Groundwater*, **7**, *3*, pp. 15–21.

WHITE, W. B. (1976) The caves of western Pennsylvania. *Pennsylvania Geological Survey General Geology Report*, **67**, 97 p.

WHITE, W. B. (1977) Conceptual models for carbonate aquifers: Revisited. In *Hydrologic Problems in Karst Terrains*. (DILAMARTER, R. R., & CSALLANY, S. C., *Eds*.), Western Kentucky University, Bowling Green, KY, pp. 176–187.

WHITE, W. B. (1988) *Geomorphology and hydrology of karst terrains*., Oxford University Press, New York, 464 p.

WHITE, W. B. (1998) Groundwater flow in karstic aquifers. In: *The Handbook of Groundwater Engineering*, (DELLEUR, J. W. *Ed*.), CRC Press, Boca Raton, pp. 18-1–18-36.

WHITE, W. B. (1999) Karst hydrology: Recent developments and open questions. In: *Hydrogeology and Engineering Geology of Sinkholes and Karst*, (BECK, B., F. PETTIT, A., J. & HERRING, J., G. *Eds*.), A.A.Balkema, Rotterdam, pp. 3–21.

WHITE, W. B., & WHITE, E. L. (1983) Patterns of cave development and speleogenesis in West Virginia. In *1983 NSS Convention Guidebook*, (MEDVILLE, D. M., DASHER, G. R., & WERNER, E., *Eds*.), NSS, Huntsville, pp. 7–24.

WILSON, J. R. (1977) Lineaments and the origin of caves in the Cumberland Plateau of Alabama. *NSS Bulletin*, **39**, pp. 9–12.

WORTHINGTON, S. R. H. (1999) A comprehensive strategy for understanding flow in carbonate aquifers. In: *Proc. of Karst Modeling Symposium*, (PALMER, A. N., PALMER, M. V., & SASOWSKY, I. D., *Eds*.), KarstWaters Institute Special Publication, **5**, pp. 30–37.

Theoretical and Applied Karstology, 13–14 (2000–2001), pp. 25–32

U–Th TIMS chronology of two stalagmites from V11 Cave (Bihor Mountains, Romania)

Tudor Tămaş[1*] & Christiane Causse[2]

[1] *Quaternary Research Group, Dept. of Mineralogy, Babes-Bolyai University, Kogălniceanu 1, and "Emil Racoviță" Institute of Speleology, Clinicilor 5, 3400 Cluj-Napoca, Romania.*
[2] *LSCE – Laboratoire des Sciences du Climat et de l'Environnement, 12, Av. de la Terrasse, 91198 Gif sur Yvette, France.*

Abstract

Two stalagmites (S22, S117) from V11 Cave (Bihor Mountains, Romania) were dated by thermal ionisation mass-spectrometry (TIMS). The 40 subsamples dated had uranium contents between 0.229 and 0.676 ppm, a $^{234}U/^{238}U_{actual} \leq 1$ and generally low detrital contamination. Ages obtained range between 138.3 ± 1.6 ka and 5.6 ± 0.1 ka and are distributed in six growth periods separated by hiatuses. Growth rates calculated show that calcite deposition was slow in both stalagmites for most of the depositional periods recorded during oxygen isotope (OI) stage 5 (1.3–3 mm/ka), with the exception of the OI substage 5e, when S117 experienced fast growth (50 mm/ka). After an interruption of 22 ka, calcite deposition in S22 resumed during OI stage 3 (2.5 mm/ka). The age of 23.4 ± 0.12 ka recorded in S117 confirms previous evidence for a short depositional period during OI stage 2. Termination I was determined in S117 at 16.08 ka. The last growth interval during OI stage 1 is marked by a strong increase in growth rates of both stalagmites, determined by warming and by a significant increase in precipitation. The presented dataset frames the main climatic events that occurred in the last 140 ka and brings a precise chronology in this time span, in good agreement with previous studies from Europe and NW Romania.

Key words: U-Th TIMS dating, stalagmites, growth rates, climate, Bihor Mountains, Romania.

Chronologie U–Th TIMS de deux stalagmites de la Grotte V11 (Monts de Bihor, Roumanie)

Résumé

Deux stalagmites (S22, S117) provenant de la Grotte V11 (Monts de Bihor, Roumanie) ont été datées par spectrométrie de masse à ionisation thermique (TIMS). Les 40 échantillons datés ont eu des concentrations d'uranium comprises entre 0,229 et 0,676 ppm, un rapport $^{234}U/^{238}U_{actuel} \leq 1$ et une faible contamination détritique. Les âges obtenus varient entre 138,3 ± 1,6 ka et 5,6 ± 0,1 ka et sont distribués en six intervalles de croissance, séparés par plusieurs hiatus. Les taux de croissance calculés montrent une précipitation lente dans les deux stalagmites durant le stade isotopique 5 (1,3–3 mm/ka), à l'exception du substade 5e, quand la stalagmite S117 a marqué une croissance rapide (50 mm/ka). Dans le cas de la stalagmite S22, après une interruption de 22 ka, la précipitation de la calcite à été reprise pendant le stade isotopique 3 (2,5 mm/ka). L'âge de 23,4 ± 0,12 ka déterminé pour S117 confirme les données obtenues par d'autres auteurs concernant l'existence d'une courte période de dépôt au cours du stade isotopique 2. La terminaison I a été datée dans la S117 à 16,08 ka. Le dernier intervalle de croissance enregistré couvre la plus grande partie du stade isotopique 1; il se caractérise pour les deux stalagmites par une forte hausse des taux de croissance, due à l'échauffement général du climat et à l'augmentation significative des précipitations atmosphériques. L'ensemble des données place les principaux événements climatiques produits au cours des derniers 140 ka et offrent une chronologie précise de cet intervalle de temps, en accord avec les études antérieures portant sur l'Europe et le Nord-Ouest de la Roumanie.

***Mots-clés:** datations U-Th par TIMS, stalagmites, taux de croissance, climat, Monts de Bihor, Roumanie.*

* corresponding author. *E-mail address:* tudort@bioge.ubbcluj.ro

Introduction

Calcium carbonate deposits from caves, such as stalagmites or flowstones, can provide information on the nature of the past environments. Changes of climatic conditions were proven to influence speleothem deposition (Hendy & Wilson, 1968; Schwarcz, 1986; Ayliffe *et al.*, 1998). Speleothem calcium carbonate is suitable for U-Th dating, thus making speleothems good repositories of palaeoenvironmental information. U-Th dating of carbonates, such as coral or speleothem, by thermal ionisation mass-spectrometry (TIMS) provides an enhanced precision of results in terms of radiometric ages as well as sample stratigraphy (Edwards *et al.*, 1986; Li *et al.*, 1989; Cheng *et al.*, 2000). Dating of speleothem by TIMS proves a good absolute timescale and gives valuable information when correlated with other proxies such as $\delta^{18}O$ and $\delta^{13}C$ records (Dorale *et al.*, 1998; Frumkin *et al.*, 1999; McDermott *et al.*, 1999; Desmarchelier *et al.*, 2000).

In Romania, U-Th ages obtained on speleothem, as well as $\delta^{18}O$ and $\delta^{13}C$ analyses and correlations with other palaeoclimatic proxies have been reported by Lauritzen & Onac (1995; 1999), Onac & Lauritzen (1996), Constantin & Lauritzen (1999), Onac *et al.* (1999), Onac (2000).

Site description

V11 Cave (The Cave from Vărăşoaia Glade) was discovered in 1990 in the southeastern part of Vărăşoaia Glade (Bihor Mountains) (Fig. 1), at an elevation of 1254 m. It is situated in an area with alpine climate, with a mean annual temperature of 4 °C, precipitation reaching 1400 mm/year and an average of 6 months of snow. V11 Cave is carved in Anisian carbonate rocks: black limestones (*Guttenstein* facies) and grey dolostones. It has 1166 m of passages, and a maximum depth of 67 m (–37 m; +30 m) (Fig. 2a). It is a dendritic maze developed on four main karstification levels (Damm, 1993).

Two stalagmites (S22, S117) were collected from a passage, 200 m away from the cave entrance and some 60 m below the surface. The passage has no noticeable airflow and the humidity is close to 100 %.

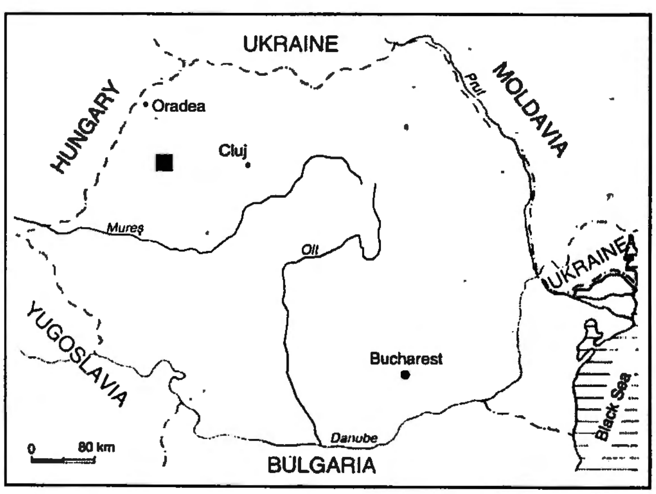

Fig. 1. Map of Romania with location of the V11 Cave (black square). *Localisation de la Grotte V11 sur la carte de la Roumanie (rectangle noir).*

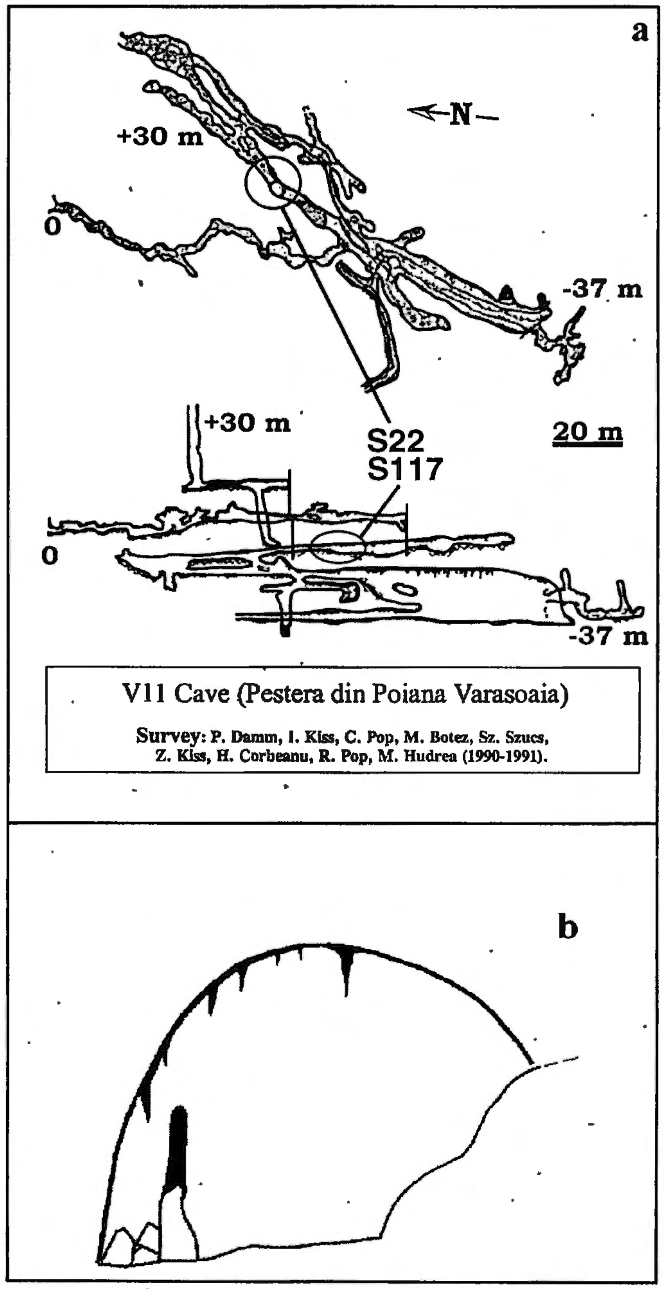

Fig. 2. a: Map and cross section of V11 Cave with location of stalagmites S22 and S117; b: Cross section of passage with sampling point of S22.
a: Plan et profil de la Grotte V11 indiquant la localisation des stalagmites S22 et S117; b: Coupe transversale de la galerie, avec le point d'échantillonnage de S22.

Sample morphology

S22 (Fig. 3a) is a 34 cm-tall stalagmite formed on a limestone block fallen from the ceiling of the cave passage. The sample consists of low-Mg calcite and shows numerous growth levels, with colour variations from white to yellow – light brown (richer in organic substance). Calcite crystals are large prismatic, continuous from one growth level to another and oriented oblique to the outer surface. On the first 8 cm from the base one can observe an alternance of thin transparent and opaque levels, which ends with a well-marked hiatus. Growth seems continuous on the following 26 cm to the top. In the interval 10.5 to 5.8 cm from the top, there is an opaque level made up by calcite microcrystals with high porosity.

S117 (Fig. 3b) has a total length of 48 cm (measured along the growth axes), and formed on the floor of the same passage, some 5 m away from S22. Its composition is similar to the sample previously described, but S117 has a more complicated stratigraphy due to its repeated movement with respect to the feeding point. This displacement was probably produced by sliding over the clayey substratum. On the basis of macroscopic observations, we divided the sample in 4 zones:

I. 0–9 cm: from the base to a fracture line covered by subsequent deposition (growth axes A10–A8); thin growth levels, dark brown calcite with a slight porosity.

II. 9–29.5 cm (A7–A5). Light brown to white compact calcite; at 25 cm there is a small hiatus, marked by a thin film of clay. This sequence ended when the stalagmite broke (not shown in Fig. 3b).

III. 29.6–36.4 cm (A4–A2); deposition resumed and new growth layers covered the fracture separating zones I and II. Yellowish white, transparent, non-porous calcite, alternating with porous growth layers. At the base there appear two hiatuses, separating a thin growth layer.

IV. 32.5–48 cm (A1). The stalagmite slipped once more over the substratum and the younger growth layers partly covered zone III.

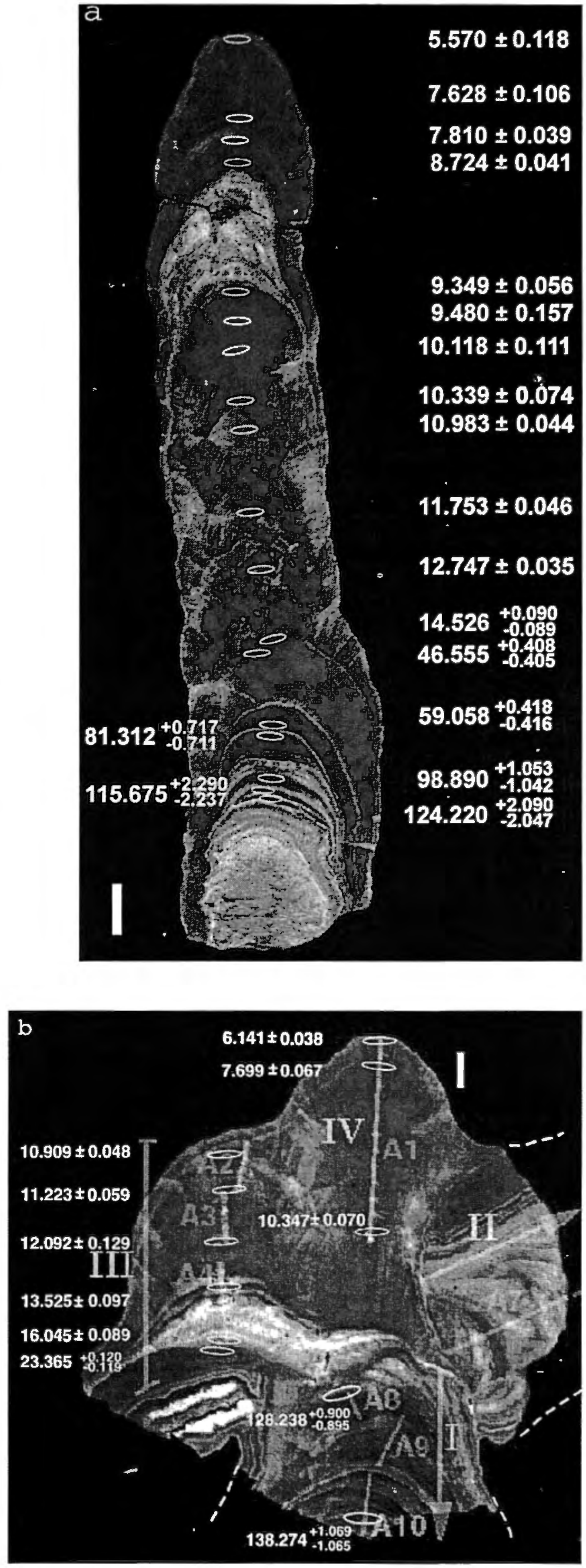

Fig. 3. (a) Cross – sections through stalagmites S22 (scale bar = 2 cm) and (b) S117 (scale bar = 1 cm) showing the positions and the ages of the subsamples dated. S117: I-IV: growth zones; A1-A10: growth axes. The upper part of zone II of S117 is not shown in the picture.

Sections longitudinales des stalagmites S22 (a) (échelle = 2 cm) et S117 (b) (échelle = 1cm) indiquant les positions et les âges des sous-échantillons datés. S117: I-IV: zones de croissance; A1-A10: axes de croissance. La partie supérieure de la zone II de S117 n'est pas comprise dans la figure.

Chemical procedure

We selected for TIMS dating 40 subsamples (23 from S22 and 17 from S117), 3 to 4 mm thick and weighing 1-2 grams. Chemical separations generally followed the procedure presented by Turney *et al.* (2001). Subsamples were cut out of stratigraphically distinct layers using a steel dental disk. All visible impurities were mechanically removed. Further, subsample surfaces were cleaned in alternating acetone/distilled water ultrasonic baths, and then dissolved in HNO_3. Organics were destroyed using hydrogen peroxide, then a ^{229}Th–^{233}U–^{236}U spike ($^{233}U/^{236}U$ ~0.98) was added. Th/U ratio in the spike was calibrated with respect to the HU-1 standard uraninite, considered in secular equilibrium (Ludwig *et al.* 1992). U and Th were precipitated by $Fe(OH)_3$ at pH 7.0, purified by anion exchange in 7M HNO_3 and then extracted with 8M HCl and H_2O respectively. Radionuclide purified fractions were dried, re-dissolved in 1M HNO_3 and then loaded in a graphite sandwich on single outgassed Re filaments.

$^{234}U/^{235}U$, $^{235}U/^{236}U$, $^{233}U/^{236}U$, $^{229}Th/^{230}Th$ and $^{229}Th/^{232}Th$ ratios were measured in peak jumping, ion counting mode on a Finnigan-MAT262 solid source mass spectrometer. The half-lives used were from Steiger *et al.* (1977) for ^{238}U, respectively 75.381 ka for ^{230}Th and 244.600 ka for ^{234}U (Ludwig *et al.*, 1992).

Results

The uranium contents of the samples were between 0.229 and 0.676 ppm. As most subsamples showed a relatively high $^{230}Th/^{232}Th$ ratio, we did not apply corrections for detrital contaminations. Most subsamples dated have shown a $^{234}U/^{238}U_{actual} \leq 1$, characteristic for both speleothems. Such ratios

Table 1. U-Th ages and isotope ratios obtained on the S22 stalagmite. *Ages U-Th et rapports isotopiques obtenus pour la stalagmite S22.*

Sample	d*(cm)	U(ppm)	$^{234}U/^{238}U_a$	$^{234}U/^{238}U_i$	$^{230}Th/^{234}U$	$^{230}Th/^{232}Th$	Age (ka BP)
22top	33.7	0.407±0.002	0.993±0.021	0.992±0.018	0.050±0.001	27.5	**5.570 ± 0.118**
22A	30.2	0.446±0.000	0.970±0.003	0.969±0.003	0.068±0.001	189	**7.628 ± 0.106**
22B	29.4	0.417±0.000	0.981±0.003	0.980±0.002	0.069±0.001	505	**7.810 ± 0.039**
22C	28.5	0.371±0.000	1.001±0.002	1.000±0.002	0.077±0.001	282	**8.724 ± 0.041**
22D	23.0	0.450±0.000	0.927±0.003	0.925±0.002	0.082±0.001	851	**9.349 ± 0.056**
22E	21.8	0.440±0.000	0.927±0.003	0.925±0.002	0.083±0.002	371	**9.480 ± 0.157**
22F	20.8	0.411±0.001	0.929±0.005	0.927±0.004	0.089±0.001	283	**10.118 ± 0.111**
22G	19.8	0.344±0.000	0.930±0.002	0.928±0.002	0.092±0.001	779	**10.536 ± 0.141**
22H	18.9	0.403±0.000	0.921±0.002	0.918±0.002	0.091±0.001	775	**10.339 ± 0.074**
22I	15.9	0.493±0.000	0.921±0.003	0.918±0.002	0.096±0.001	193	**10.983 ± 0.044**
22J	12.0	0.549±0.000	0.905±0.002	0.901±0.002	0.102±0.001	263	**11.753 ± 0.046**
22K	10.0	0.520±0.001	0.919±0.003	0.916±0.002	0.110±0.001	137	**12.747 ± 0.035**
22L	8.4	0.609±0.000	0.885±0.002	0.880±0.001	0.125±0.001	100	**14.526 ± 0.090**
22M	8.0	0.363±0.000	0.933±0.002	0.924±0.002	0.347±0.003	355	**46.555 +0.408;–0.405**
22N	6.0	0.356±0.000	0.953±0.003	0.946±0.002	0.382±0.003	172	**52.602 +0.476;–0.473**
22O	5.3	0.492±0.000	0.901±0.002	0.884±0.002	0.404±0.003	71	**56.953 +0.495;–0.492**
22P	4.8	0.539±0.000	0.903±0.002	0.886±0.002	0.415±0.003	140	**59.058 +0.418;–0.416**
22Rt	4.4	0.321±0.000	0.998±0.002	0.998±0.002	0.526±0.004	419	**81.312 +0.717;–0.711**
22R	4.2	0.296±0.001	1.006±0.008	1.008±0.008	0.532±0.006	284	**82.396 +1.119;–1.116**
22Rb	3.9	0.276±0.000	1.030±0.002	1.037±0.002	0.528±0.004	2675	**81.336 +0.839;–0.832**
22S	3.5	0.229±0.000	1.022±0.002	1.030±0.002	0.599±0.005	56	**98.890 +1.053;–1.042**
22T	2.7	0.274±0.000	0.983±0.002	0.976±0.003	0.653±0.008	28	**115.675 +2.290;–2.237**
22U	1.8	0.296±0.000	0.976±0.002	0.966±0.003	0.678±0.007	119	**124.220 +2.090;–2.047**

*d=distance from base

are quite unusual in speleothems, and when occuring they generally indicate a preferential leaching of ^{234}U from the sample, thus resulting in calculating ages greater then the real ones. Our samples show a relative constancy of the uranium content and of the $^{234}U/^{238}U_{actual}$ along the growth intervals, sustaining that after deposition the stalagmites acted as a closed system with respect to uranium isotopes. The unusual $^{234}U/^{238}U_{actual}$ ratios recorded in the speleothems might have their origin in the host rock above the cave.

The ages obtained generally show a progressive decrease from 124 ± 2 ka to 5.6 ± 0.1 ka (Table 1), and 138 ± 1.6 ka to 6.1 ± 0.04 ka, respectively (Table 2). One age (subsample 22G) was not concordant with the rest of the values obtained due to analytical errors and was rejected.

The evolution of S22 and S117 stalagmites from V11 Cave is shown in Figure 4. Stalagmite S22 begins with two growth episodes of short duration, at 124.2 ± 2.0 ka and 115.7 ± 2.2 ka, on which the growth rates could not be determined because of the thinness of the deposits. The next growth episode, between 98.9 ± 1.0 ka and 81.3 ± 0.7 ka, has an average growth rate of 1.3 mm/ka. After an interruption of some 22 ka, four ages (59.1 ± 0.4 ka – 46.5 ± 0.4 ka) indicate another growth period with an average rate of 2.5 mm/ka. The next interruption was determined at about 32 ka, but its precise duration was probably shorter. The hiatus line marking the interruption has an irregular shape and crosses over several growth layers, probably due to the setting of conditions unfavourable for calcite deposition in S22 when drip water alimentation resumed (corrosive water which removed part of the material previously deposited) (Fig. 3). The last depositional episode recorded took place between 14.5 ± 0.09 ka and 5.6 ± 0.1 ka, the average growth rate being 30.5 mm/ka (Fig. 4).

S117 started growing before 138.3 ± 1.6 ka B.P. Between 138.3 ± 1.6 ka and 128.2 ± 0.9 ka (zone I), calcite deposition was slow (circa 2 mm/ka), after which follows a period marked by fast growth (50 mm/ka) until 123 ± 0.7 ka. After an interruption of 26.5 ka (upper part of zone II), deposition resumes at around 96 ka B.P. (average growth rate 3 mm/ka), until 86.4 ± 0.8 ka. The next hiatus recorded in S117 is very long (86.4 ± 0.84 to 23.4 ± 0.12 ka B.P.), but its extension is not controlled by climate oscillations, but by local causes (the break and displacement of zone II of the stalagmite). This assumption is supported both by our other dates in V11 Cave and by studies on speleothems from other caves in the Apuseni Mountains (Onac & Lauritzen, 1996; Onac, 2000). Zone III in S117 starts with a short growth period (3 mm-thick), with an age of 23.4 ± 0.12 ka, followed by another hiatus. Growth resumed at 16.0 ± 0.09 ka and continued without interruption until 6.1 ± 0.04 ka, at an average growth rate of 13.5 mm/ka.

Table 2. U-Th ages and isotope ratios obtained on S117 stalagmite. *Ages U-Th et rapports isotopiques obtenus pour la stalagmite S117.*

Sample	d*(cm)	U(ppm)	$^{234}U/^{238}Ua$	$^{234}U/^{238}Ui$	$^{230}Th/^{234}U$	$^{230}Th/^{232}Th$	Age (ka BP)
117A1-1	47.8	0.283±0.000	0.953±0.003	0.952±0.002	0.055±0.001	86	6.141 ± 0.038
117A1-3	47.1	0.447±0.001	0.923±0.008	0.922±0.006	0.068±0.001	311	7.699 ± 0.067
117A1-6	44.5	0.446±0.000	0.904±0.002	0.901±0.002	0.082±0.001	429	9.268 ± 0.069
117A1-4	41.4	0.333±0.000	0.930±0.003	0.928±0.003	0.091±0.001	838	10.347 ± 0.070
117A2-1	40.8	0.345±0.000	0.881±0.002	0.877±0.002	0.095±0.001	490	10.909 ± 0.048
117A2-2	39.3	0.378±0.000	0.870±0.002	0.866±0.002	0.098±0.001	943	11.223 ± 0.059
117A2-3	38.0	0.655±0.001	0.882±0.002	0.878±0.002	0.105±0.001	1376	12.092 ± 0.129
117A3-2	35.9	0.519±0.001	0.863±0.003	0.858±0.002	0.114±0.001	874	13.198 ± 0.135
117A4-1	35.5	0.467±0.000	0.867±0.002	0.862±0.002	0.117±0.001	650	13.525 ± 0.097
117A4-2	34.6	0.513±0.000	0.819±0.002	0.810±0.001	0.137±0.001	29	16.045 ± 0.089
117A4-3	34.3	0.522±0.001	0.838±0.002	0.827±0.002	0.192±0.001	49	23.365 ± 0.120
117TR	33.8	0.355±0.000	0.954±0.003	0.942±0.003	0.545±0.004	458	86.447 +0.841;−0.834
117A6-1	30.9	0.651±0.001	0.949±0.002	0.933±0.002	0.571±0.004	171	92.961 +0.847;−0.840
117A6-2	32.8	0.406±0.001	0.910±0.003	0.882±0.004	0.581±0.003	770	96.513 ± 0.645
117A6-4	31.5	0.676±0.001	0.918±0.003	0.883±0.003	0.668±0.003	2515	123.020 +0.790;−0.784
117A9-1	4.0	0.286±0.000	0.968±0.002	0.954±0.003	0.689±0.003	366	128.238 +0.900;−0.895
117A9-2	0.2	0.654±0.001	0.923±0.003	0.886±0.004	0.709±0.005	38	138.274 +1.609;−1.605

*d=distance from base

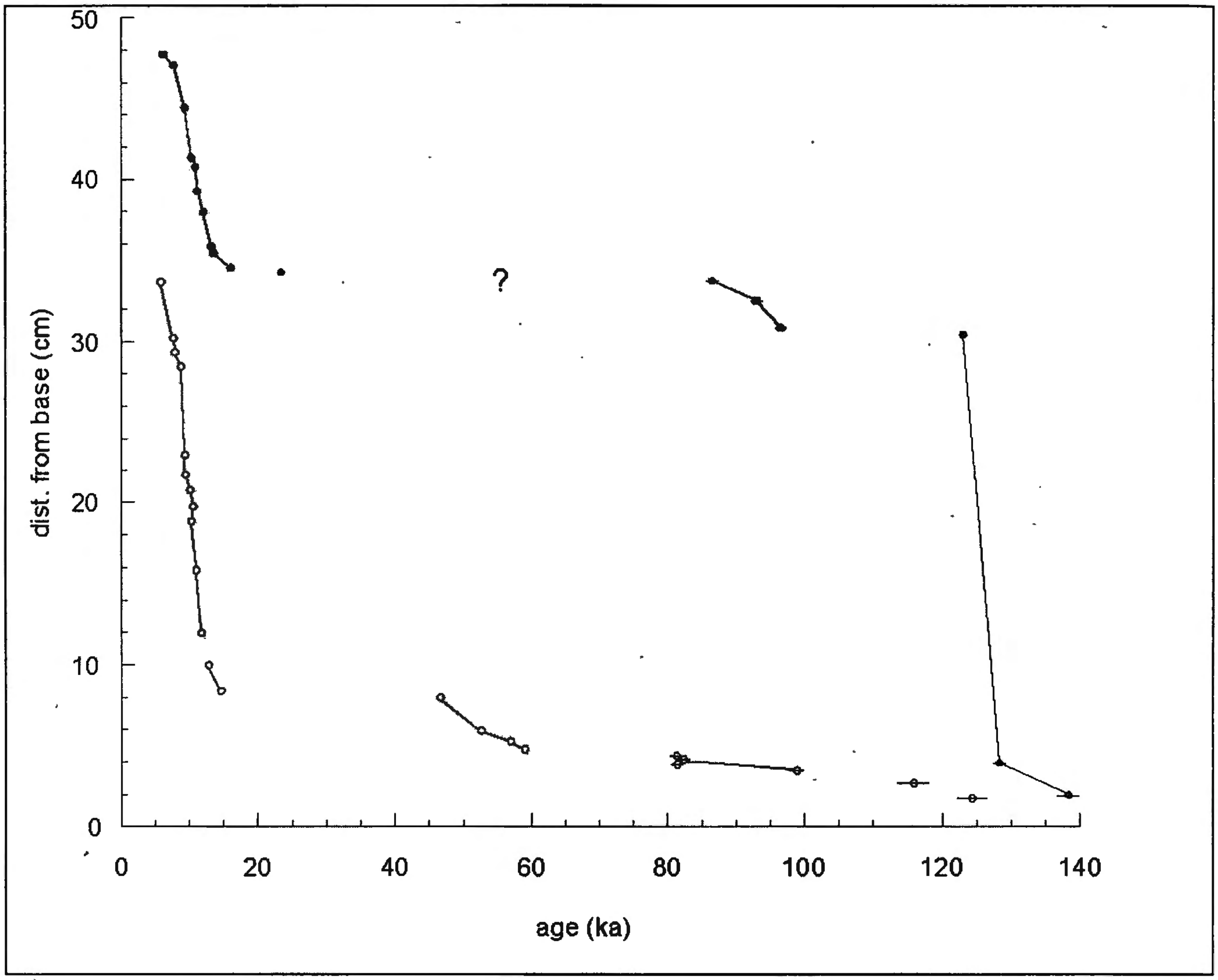

Fig. 4. Graph of S22 (open circles) and S117 (solid circles) stalagmite ages vs. distance from base. Growth intervals are marked with continuous lines. Error bars shown are 2_σ counting errors of age determinations (most age error bars are smaller than data symbols).
Diagramme des âges de S22 (cercles vides) et S117 (cercles pleins) par rapport à la distance vers la base. Les barres d'erreur représentent 2_σ des déterminations des âges (la plupart sont plus petites que les symboles).

Discussion and conclusions

The 40 samples dated from stalagmites S22 and S117 in V11 Cave cover a time span of nearly 140 ka (marine OI stages 5 to 1), and are distributed in six growth periods (Fig. 5d). Calculated growth rates show that calcite deposition was slow in both stalagmites during most of the OI stage 5. The first two short growth intervals in S22 correspond to OI substadial 5e and with peak J3 and an unmarked intermediary peak of the NW European speleothem record (Baker *et al.*, 1993). S117 starts growing at the end of OI stage 6 (slow growth), then follows a fast-growth period marking OI substadial 5e after Termination II. Isotope substage 5d was colder/dryer and calcite deposition stopped in both stalagmites.

The next depositional interval of S22 covers part of OI substadial 5c, all of 5b and part of 5a. The upper growth limit in S22 for this interval is 81.3 ka, confirming the increased severity of climate at the transition 5a – 4 and during OI stage 4.

Deposition in S22 during OI substadial 5b is sustained by the growth interval in S117, whose upper limit is determined by the sliding of the stalagmite over the clayey substratum and not by climate control.

The growth period determined on S22 between 59 ka and 46 ka corresponds to an amelioration of climatic conditions during isotope stage 3 (substadials 3.31 and 3.3, respectively the F2 and F1 peaks of the NW Europe speleothem record), documented in Romanian speleothems from Scărişoara Glacier

Cave and Humpleu Cave System, Bihor Mountains (Onac & Lauritzen, 1996) and certifies the presence of a warm/wet event, followed by a cool/dry one. Calcite deposition in V11 speleothems was not resumed during substadial 3.13, marked by well-defined peaks on both NW Europe and Romanian speleothem record. The difference from the Romanian speleothem record may be linked to an altitude effect, as the U-Th dates covering that period come from caves situated nearly 600 m lower than our study area (Onac & Lauritzen, 1996). The situation may be similar for the peak at 76 ka on the Romanian speleothem record.

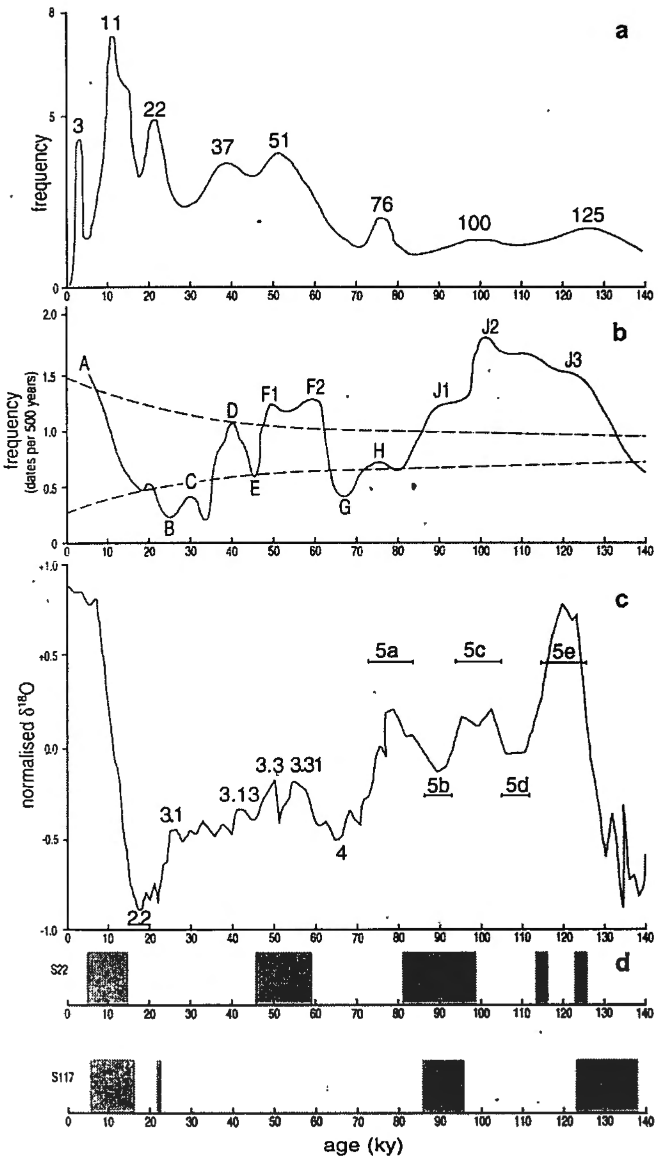

Fig. 5. Growth intervals of S22 and S117 (gray squares, 5d) compared with the Romanian speleothem record (Onac & Lauritzen, 1996 — 5a), NW Europe speleothem record (Baker *et al.*, 1993 —5b) and oxygen isotope chronology (Martinson *et al.*, 1987, events from Pisias *et al.*, 1984 — 5c).
Intervalles de croissance de S22 et S117 (rectangles gris, 5d) comparés avec les données obtenues sur les spéléothèmes de Roumanie (Onac & Lauritzen, 1996 — 5a), les données de Baker et al. (1993) pour les spéléothèmes de l'Europe de NO (5b) et la chronologie des isotopes de l'oxygène (Martinson et al., 1987, événements de Pisias et al., 1984 — 5c).

The growth level at 23.4 ± 0.12 ka recorded in S117 points to a short depositional period during OI stage 2. This uncorrelates both with the oxygen isotope record of Martinson *et al.* (1987) and with the NW speleothem record, where it is somewhat close to through B; it correlates however with U-Th dates recorded on speleothems from Scărişoara Glacier Cave, Bihor Mountains (Onac & Lauritzen, 1996; Onac, 2000) and might indicate a short climate improvement (wetter conditions?) occuring in this particular area. This depositional interval is missing from S22, however there is morphological evidence for the removal of a part of the calcite deposited prior to water alimentation.

Termination I was determined in S117 at 16.08 ka and in S22 at 14.5 ka. The disagreement of these two values is due to the setting of conditions unfavourable for calcite deposition in S22. The last growth interval, during OI stage 1 is marked in both stalagmites by a strong increase in growth rates determined by warming and by a significant increase in precipitation.

Acknowledgements

We thank Emil Silvestru and Antoniu Bodnariuc for help in collecting the samples and Linda Ayliffe for invaluable help in laboratory analyses. We extend special thanks to our referees, Dr. Derek Ford and Dr. Stein-Erik Lauritzen, and to the editorial staff of *Theoretical and Applied Karstology* who gave helpful comments on an earlier draft of this manuscript. U-Th datings were done at the Laboratoire des Sciences du Climat et de l'Environnement (LSCE), Gif-sur-Yvette, France. This work was supported by the Ministère Français de l'Education Nationale, de la Recherche et de la Technologie "Réseau Formation Recherche Pays Europe Centrale et Orientale – Réseau Franco - Roumain" (Contract 4778836 A), Coordinator Dr. Ch. Causse, and partly by the IGCP-379 to Dr. Yuan Daoxian and by the ANSTI B37/2000 project of the Romanian Agency for Science and Technology to Tudor Tămaş. This is the 7th contribution to the SPEP III program in Romania.

References

Ayliffe, L. K., Marianelli, P., Moriarty, K. C., Wells, R. T., McCulloch, M. T., Mortimer, G. E., & Hellstrom, J. C. (1995) 500 ka precipitation record from southeastern Australia: Evidence for interglacial relative aridity. *Geology*, **26**, 2, pp. 147–150.

BAKER, A., SMART, P. L., & FORD, D. C. (1993) Northwest European paleoclimate as indicated by growth frequency variations of secondary calcite deposits. *Palaeogeography, Palaeoclimatology, Palaeoecology*, **100**, pp. 291–301.

BAKER, A., SMART, P. L. & EDWARDS, R. L. (1995) Paleoclimate implications of mass spectrometric dating of a British flowstone. *Geology*, **23**, *4*, pp. 309–312.

CHENG, H., ADKINS, J., EDWARDS, R. L., & BOYLE, E. A. (2000) U-Th dating of deep-sea corals. *Geochimica et Cosmochimica Acta*, **64**, *14*, pp. 2401–2416.

CONSTANTIN, S., & LAURITZEN, S.-E. (1999) Speleothem datings in Romania, 1: Evidence for a continuous speleothem growth in Peştera Cloşani during Oxygen Isotope stages 5-3 and its paleoclimatic significance. *Theor. Appl. Karstology*, **11-12**, pp. 35–46.

DAMM, P. (1993) Consideraţii asupra sistemului carstic Vărăşoaia-Boga (Munţii Bihor). *An. Şt. al Societăţii Ardelene de Speologie*, pp. 30–49.

DESMARCHELIER, J. M., GOEDE, A., AYLIFFE, L. K., MCCULLOCH, M. C., & MORIARTY, K. (2000) Stable isotope record and its palaeoenvironmental interpretation for a late Middle Pleistocene speleothem from Victoria Fossil Cave, Naracoorte, South Australia. *Quaternary Science Reviews*, **19**, pp. 763–774.

DORALE, J. A., EDWARDS, R. L., ITO, E., & GONZÁLEZ, L. A. (1998) Climate and Vegetation History of the Midcontinent from 75 to 25 ka: A Speleothem Record from Crevice Cave, Missouri, USA. *Science*, **282**, pp. 1871–1874.

EDWARDS, R. L., CHEN, J. H., & WASSERBURG, G. J. (1986) ^{238}U–^{234}U–^{230}Th–^{232}Th systematics and the precise measurement of time over the past 500,000 years. *Earth and Planetary Science Letters*, **81**, pp. 175–192.

FRUMKIN, A., FORD, D. C., & SCHWARCZ, H. P. (1999) Continental Oxygen Isotopic Record of the Last 170,000 Years in Jerusalem. *Quaternary Research*, **51**, pp. 317–327.

HENDY, C. H., & WILSON, A. T. (1968) Palaeoclimatic Data from Speleothems. *Nature*, **219**, pp. 48–51.

LAURITZEN, S.-E. (1995) High-resolution palaeotemperature proxy record for the last interglaciar based on Norwegian speleothems. *Quaternary Research*, **43**, pp. 133–146.

LAURITZEN, S.-E., & ONAC, B. P. (1995) Uranium series dating of some speleothems from Romania. *Theor. Appl. Karstology*, **8**, pp. 25–36.

LAURITZEN, S.-E., & ONAC, B. P. (1999) Isotopic stratigraphy of a Last Interglacial stalagmite from north-western Romania: correlation with the deep-sea record. *J. of Cave and Karst Studies*, **61**, *1*, pp. 22–30.

LI, W.-X., LUNDBERG, J., DICKIN, A. P., FORD, D. C., SCHWARCZ, H. P., MCNUTT, R., & WILLIAMS, D. (1989) High-precision mass-spectrometric uranium-series dating of cave deposits and implications for palaeoclimate studies. *Nature*, **339**, pp. 534–536.

LUDWIG, K. R., SIMMONS, K. R., SZABO, B. J., WINOGRAD, I. J., LANDWEHR, J. M., RIGGS, A. C., & HOFFMAN, R. J. (1992) Mass-spectrometric ^{230}Th–^{234}U–^{238}U dating of the Devils Hole calcite vein. *Science*, **258**, pp. 284–287.

MARTINSON, D. G., PISIAS, N. G., HAYS, J. D., IMBRIE, J., MOORE, T. C., & SHACKLETON, N. J. (1987) Age dating and the orbital theory of the ice age: Development of a high-resolution 0 to 300,000-years chronostratigraphy. *Quaternary Research*, **27**, pp. 1–29.

MCDERMOTT, F., FRISIA, S., HUANG, Y., LONGINELLI, A., SPIRO, B., HEATON, T. H. E., HAWKESWORTH, C. J., BORSATO, A., KEPPENS, E., FAIRCHILD, I. J., V. D. BORG, K., VERHEYDEN, S., & SELMO, E. (1999) Holocene climate variability in Europe: Evidence from dd^{18}O, textural and extension-rate variations in three speleothems. *Quaternary Science Reviews*, **18**, pp. 1021–1038.

ONAC, B. P. (2000) Mineralogical and Uranium Series Dating Studies in Scărişoara Glacier Cave (Bihor Mountains, Romania). *Theor. Appl. Karstology*, **13**, pp. 33–38.

ONAC, B. P., & LAURITZEN, S.-E. (1996) The Climate of the Last 150,000 Years Recorded in Speleothems: Preliminary Results from North-Western Romania. *Theor. Appl. Karstology*, **9**, pp. 9–21.

ONAC, B. P., CONSTANTIN, S., & LAURITZEN, S.-E. (1999) The palaeoclimate recorded in a Late Glacial to Holocene stalagmite from Ursilor Cave (Romania): preliminary results. *Lucr. Simp. "Realizări şi perspective în studiul Cuaternarului din România" April, 2000, Cluj-Napoca, Romania*, pp. 13–16.

PISIAS, N. G., MARTINSON, D. G., MOORE, J. T. C., SHACKLETON, N. J., PRELL, W., HAYS, J., & BODEN, G. (1984) High resolution stratigraphic correlation of benthic oxygen isotopic records spanning the last 300,000 years. *Marine Geology*, **56**, pp. 119–136.

SCHWARCZ, H. P. (1986) Geochronology and Isotopic Geochemistry of Speleothems. In: *Handbook of Environmental Isotope Geochemistry* (FRITZ, P., & FONTES, J-Ch., *Eds*), **2B**, pp. 271–303.

SHACKLETON, N. J., & OPDYKE, N. D. (1973) Oxygen isotope and palaeomagnetic stratigraphy of Equatorial Pacific Core V28-238: oxygen isotope temperature and ice volumes on a 105 year and 106 year scale. *Quaternary Research*, **3**, pp. 39–55.

STEIGER, R. H., & JÄGER, E. (1977) Subcomission on Geochronology: Convention on the use of the decay constants in geo- and cosmochronology. *Earth and Planetary Science Letters*, **36**, pp. 359–362.

TURNEY, C. S. M., BIRD, M. I., FIFIELD, L. K., ROBERTS, R. G., SMITH, M., DORTCH, C. E., GRÜN, R., LAWSON, E., AYLIFFE, L. K., MILLER, G. H., DORTCH, J., & CRESSWELL, R. G. (2001) Early Human Occupation at Devil's Lair, Southwestern Australia 50,000 Years Ago. *Quaternary Research*, **55**, pp. 3–13.

Theoretical and Applied Karstology, **13–14** (2000–2001), pp. 33–38

Mineralogical studies and Uranium-series dating of speleothems from Scărişoara Glacier Cave (Bihor Mountains, Romania)

Bogdan P. Onac*

Quaternary Research Group, Dept. of Mineralogy, "Babeş-Bolyai" University, Kogalniceanu 1, and "Emil Racoviţă". Institute of Speleology, Cluj Department, Clinicilor 5, 3400 Cluj, Romania.

Abstract

Recent mineralogical investigations carried out in Scarisoara Glacier Cave pointed out the presence of speleothems made up of monohydrocalcite and hydromagnesite. Although both minerals were documented earlier from other Romanian caves this is for the first time when a speleothem is described as being entirely composed of monohydrocalcite. Crocoite, a rare mineral was also identified; however, this is not a real cave mineral being transported into the cave by the percolating waters. U-Th dating of some speleothems from Scarisoara Glacier Cave enabled us to draw some considerations concerning the palaeoclimate changes and the age of the cave.

Key words: speleothems, cave mineralogy, U-Th dating, Scarisoara Glacier Cave, Bihor Mountains, Romania.

Études minéralogiques et datations U-Th des spéléothèmes de la Grotte-Glacière de Scărişoara (Monts du Bihor, Roumanie)

Résumé

Les recherches minéralogiques récentes effectuées dans la Glacière de Scărişoara ont mis en évidence la présence des spéléothèmes composés de monohydrocalcite et d'hydromagnésite. Bien que ces deux dernières aient été déjà décrites aussi d'autres grottes, c'est pour la première fois que la monohydrocalcite constitue ici des spéléothèmes bien distincts. La crocoïte, un minéral rare, a été également identifiée, mais sa présence est très probablement due à un transport depuis la surface par l'eau de percolation. Les datations par la méthode U-Th de certains spéléothèmes de la Glacière de Scărişoara nous ont permis également de faire quelques considérations concernant les changements paléoclimatiques et l'âge de la grotte.

Mots-clés: spéléothèmes, minéralogie des grottes, datation par la série d'Uranium, Grotte Glacière de Scărişoara, Monts du Bihor, Roumanie.

Introduction

Scărişoara Glacier Cave is located on the left bank of the Gârda Seacă Valley, 5 km upstream from its confluence with Ordâncuşa Valley, within the Ocoale-Scărişoara karst depression (Rusu *et al.*, 1970).

The cave develops on thick-layered limestones of the Upper Jurassic (Bucur & Onac, 2000). The carbonate deposit forms a monocline dipping about 20° towards SW.

Further informations concerning Scărişoara Glacier Cave can be found in Racoviţă & Onac (2000).

Morphology and mineralogy of speleothems

In Scărişoara Glacier Cave, the carbonate minerals *calcite*, *aragonite*, *monohydrocalcite*, and *hydromagnesite* are deposited as various speleothems from dripping, seeping, and pooling water. Calcite composes the majority of the speleothems. The other three carbonate minerals occurred only in one or a maximum of two types of speleothems. Tămas (*pers. comm.*)

* corresponding author. *Email*: bonac@bioge.ubbcluj.ro

also identified a few phosphates, which will be presented in a forthcoming note.

Scărişoara Glacier Cave contains a variety of calcite speleothems. Many of these decorate the passages and chambers located within the warm meroclimate zone of the cave. These include calcite clusterites, cave pearls corraloids, rimstone dams (*gours*), draperies (with or without odontolithes), rafts, stalactites, stalagmites, columns, boxwork, and impressive flowstones.

Among these, cave pearls are the more outstanding, due to their unusual mechanism of formation (Viehmann, 1963; 1967). Viehmann postulated that freezing of percolating water has caused the separation of dissolved substances (calcite) in a cryptocrystalline form (*lublinite*). As the process continues, these cryptocrystals develop into micropearls.

Aragonite is the second most common carbonate cave mineral after calcite. However, in Scărişoara Cave it is not well represented; it is only found in some stalactites, clusterites, and cave pearls (Bădău, 1984; Bodolea, 1992). In all of these occurrences, aragonite was identified by thin section examination using a polarizing microscope.

Aragonite and calcite coexist as alternating layers in most of the speleothems analyzed. All these samples exhibit pseudomorphism of calcite after aragonite (the initial internal structure was changed while the external form was preserved).

Patches of micron or millimeter-thick coatings, composed of white, finely crystalline material, were found covering the walls in a few of the sectors within the *Rezervaţia Mică* (=Little Reserve) (Fig. 1). X-ray diffraction and thin section examination showed these crusts to be composed of **monohydrocalcite**. Under a polarizing microscope, monohydrocalcite exhibits second to third order interference colors and moderate birefringence. In addition, when the crusts were stained with alizarid red-S (Friedman, 1959), the dark red color (a darker shade than that obtained when staining calcite or aragonite) confirmed the presence of monohydrocalcite. *To our knowledge this is for the first time when monohydrocalcite is found to be the only mineral component of a speleothem in a Romanian cave.*

Crusts composed of monohydrocalcite can only be found in a particular area of the periglacial sector of the cave where the temperature ranges from 0.3 to 3°C. In this area, monohydrocalcite occurs in a zone where small water droplets hit the ice stalagmite heads, ejecting onto the walls, forming a fine mist (aerosol) environment. Although no water chemistry data is available for this cave passage, the appearance of hydromagnesite and monohydrocalcite speleothems deposited in the same area indicates the likely presence of magnesium-rich solutions.

Worldwide, monohydrocalcite has been documented in relatively few caves (Hill & Forti, 1997). In Romania, it has been reported in only two caves (*Humpleu* and *Lucia Mică*), being identified in the composition of moonmilk (Onac & Ghergari, 1993).

The only explanation we have found for the presence of monohydrocalcite in Scărişoara Cave is the one proposed by Fischbeck (1976) and Fischbeck & Müller (1971). They assumed the following conditions for precipitation of monohydrocalcite: Mg/Ca ratio in solution higher then 1, solution temperature to be lower than 20 °C, and the presence of aerosols. All these conditions are met in Scărişoara Cave.

In "*Palatul Sânzienelor*" (upper part of the 'Little Reserve'), patches of white mats of an earthy pasty mass (moonmilk-

Fig. 1. Long profile through Scărişoara Glacier Cave with the location of anlysed samples. *Profil longitudinal parmi la Grotte-Glacère de Scărişoara et la localisation des échantillons analysées.*

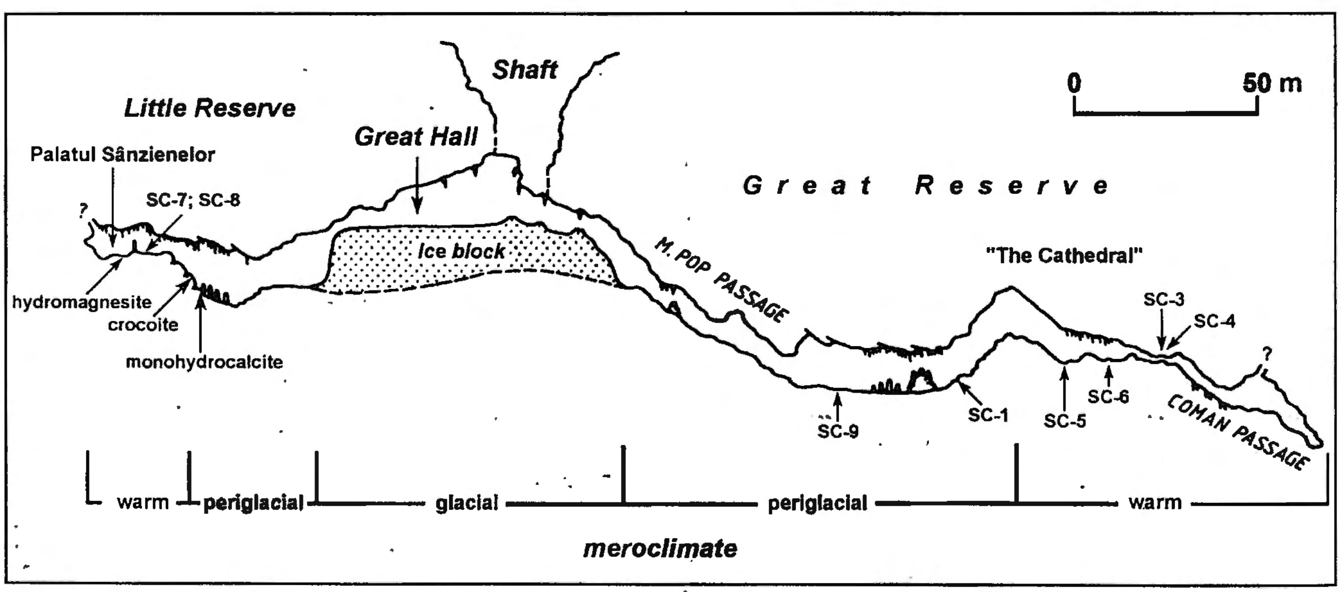

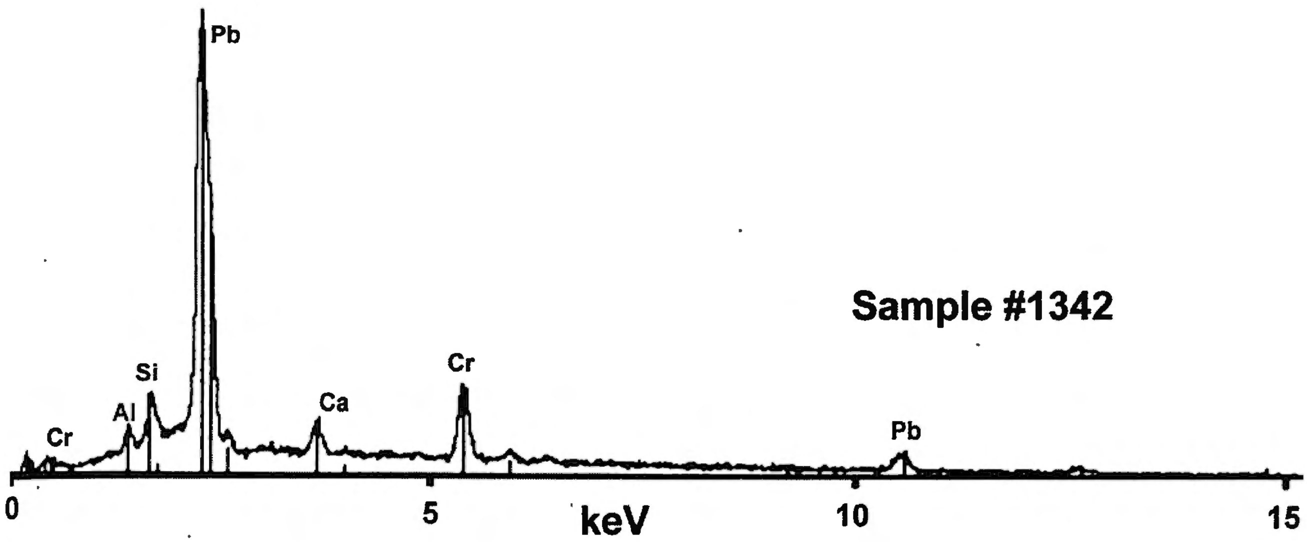

Fig. 2. Energy dispersive X-ray spectra of crocoite. *Spectre énergétique en RX de la crocoïte.*

Table 1. X-ray data for crocoite.
Données de l'analyse RX pour la crocoïte.

d(Å)	Intensity	hkl
5.38	6	101
5.01	8	110
4.89	18	011
4.32	30	111
3.71	8	111
3.67	8	020
3.44	48	200
3.24	100	120
3.20	8	021
3.11	8	210
3.00	48	012
2.97	18	112
2.68	10	202
2.57	10	112
2.52	10	212
2.23	24	103
2.22	10	111
2.13	2	131
2.07	16	212
1.98	8	231
1.95	16	132
1.94	10	320
1.82	18	322
1.79	4	232
1.77	6	140
1.68	4	141

like speleothems) were collected from a side passage (Fig. 1). The average size of these patches is about 1.5 cm. X-ray diffraction analysis of the samples revealed the presence of **hydromagnesite**.

Hydromagnesite is a common carbonate cave mineral, and its presence is not a surprise. However, currently it is the only magnesium carbonate mineral found in Scărişoara. We believe that hydromagnesite was precipitated from magnesium-rich percolating solutions due to the degassing of carbon dioxide in passages located above the periglacial meroclimate zone.

Scattered within the same area where monohydrocalcite speleothems were identified, bright yellow-greenish minerals occurred as scaly crusts (*see* Fig. 1). Under binocular the crystals were translucent and showed adamantine luster. Chemical analysis of the mineral by energy dispersive secondary X-ray (EDX) shows its composition to be dominated by the elements Pb and Cr, and the remaining being a mixture of Ca, Si and Al (Fig. 2).

The powder diffraction data were collected using a Scintag Pad V diffractometer operated at 45 kV and 40 mA. The instrument employs Cu-Ka radiation. The X-ray diffraction (XRD) pattern is sharp and well resolved, indicating a well-crystallized material. The peak search revealed a good match for most of 2-theta values for the **crocoite** ($PbCrO_4$) pattern, whereas some of the peaks were assigned to calcite. Table 1 displays the results. These values are almost identical to those reported in the JCDD file of crocoite (08-209). Small systematic shifts in the pattern may reflect either a slightly different composition or an uncorrected calibration of the instrument.

Table 2. U-series dating results of speleothems from Scărişoara Cave.
Résultats des datations des spéléothèmes de la Grotte de Scărişoara.

Sample	U (ppm)	$^{230}Th/^{234}U$	$^{234}U/^{238}U$	$^{230}Th/^{232}Th$	Age (ka)	Corrected age (ka)
SC-1a	0.023	0.358±0.042	2.382±0.216	18	46.01 (6.72/-6.4)	43.00(7.11/-6.8)
SC-1c	0.044	0.384±0.036	2.02±0.146	72	50.41(6.06/-5.79)	
SC-3 (a)	0.035	0.214±0.021	1.758±0.152	22	25.77(2.93/-2.87)	
SC-3 (b)	0.029	0.216±0.019	1.749±0.147	57	24.82(1.12/-1.08)	
SC-4 base	0.039	0.129±0.015	2.404±0.13	>1000	14.83(1.87/-1.85)	
SC-4 top	0.033	0.094±0.018	2.958±0.235	>1000	10.69(2.17/-2.13)	
SC-5 base	0.102	0.672±0.007	0.976±0.002	215	126.3(0.89/-0.91)	
SC-5 top	0.108	0.65±0.006	1.001±0.001	850	105.2(0.67/-0.63)	
SC-6 base	0.133	0.677±0.007	0.977±0.002	725	124.9(0.78/-0.781)	
SC-6 top	0.109	0.579±0.003	0.91±0.003	749	96.4(0.56/-0.055)	
SC-7	0.055	1.164±0.079	1.78±0.095	217	>350	
SC-8	0.085	1.032±0.049	1.299±0.072	>1000	>350	
SC-9	0.037	1.075±0.041	1.387±0.051	>1000	>350	

Refinement of the XRD data using POWDER 2.0 program produced the following monoclin unit-cell parameters: a = 7.02 Å ; b = 7.32 Å ; c = 6.71 Å , and β = 102.32 Å .

Scanning electron microscope images of crocoite show slender prismatic crystals.

Crocoite is a rare mineral even for the surface environment. Its presence in Scărişoara Glacier Cave is enigmatic. In the natural environment, the mobile specie of chromium is the Cr^{6+} ion. Under oxidizing conditions, Cr^{3+} is the stable valence state in equilibrium with the atmosphere, occurring either as the $HCrO_4$ or CrO_4^{2-} anion (Drever, 1997). Because, within the cave environment, the pH is typically in the range of 7 to 8, and the redox potential in the range of +0.4 to 0.6 volts, the Cr^{3+} can not oxidizes to form Cr^{6+} (chromate).

The precipitation of crocoite in Scărişoara Glacier Cave as a secondary mineral is hard to accept. Considering the remote location of the cave, and the fact that Pb and Cr ions are rare in the environment, a natural origin for this mineral is excluded. In addition , there are no ore deposits containing lead and chromium within at least 250 km from Scărişoara. Hence, it cannot be considered a true cave mineral.

The presence of crocoite raises the question of lead and chromium origin. The only explanation we can put forward is that the occurrence of crocoite in Scărişoara Glacier Cave has a human-induced origin. It is known that various chromates are used for artificial dye preparation. Such dye could have been dumped in the close vicinity of the cave and then crocoite formed from its components was transported into the cave by the percolating waters. If so, crocoite would be the first mineral that can actually be considered a pollutant of the cave environment.

Uranium-series dating of speleothems

Speleothems provide a sensitive tool for studying past climatic changes. Their growth (deposition of calcite) coincides with relatively warm and humid episodes, while breaks in calcite deposition correspond to cool or dry phases. To study this process, eight speleothems (four stalagmites and four fragments of flowstone) were collected from 'The Cathedral', 'Great Reserve', and 'Little Reserve' in Scărişoara Cave (Fig. 1). These samples were cut into thirteen sub-samples and dated by means of uranium-series dating ($^{230}Th/^{234}U$) using both alpha-particle[1] (Onac & Lauritzen, 1996) and thermal ionization mass-spectrometry (TIMS) techniques[2].

---

[1] The U-series alpha dating was done at the Departement of Geology, Bergen University, Norway.

[2] TIMS dating was performed at the Geological Institute, University of Copenhagen, Denmark.

The sample age can be determined by the activity ratio of ^{234}U to its decay product ^{230}Th, providing the speleothems contain no clay or other insoluble detritus. Clay and insoluble material are known to be carriers of detrital thorium. This ratio can be calculated using standard algorithms (IVANOVICH & HARMON, 1992).

A sample (SC) was taken from a 15-cm thick layer of flowstone found under some breakdown blocks located at the edge of the ice stalagmite field. Sample SC consists of yellowish-brown,. porous, micro-crystalline calcite. Both sub-samples extracted off the speleothem (SC-1a and SC-1c) gave dates of ca. 43 ka[3] (top) and 50 ka (base) but with large standard errors (Table 2).

Sample SC-3 is a 77 cm-tall stalagmite, collected close to the entrance in the 'Galeria Coman'. The stalagmite consists of dense, medium to large crystalline, milky white, banded calcite laminae. The sample was located on top of some collapse breakdown blocks and was actively growing at the time of sampling. For dating, two sub-samples were taken from its bottom. The resultant dates for both samples are reliable and reasonably precise at ca. 26 ka.

Stalagmite SC-4 (25 cm in height) was collected from approximately the same position and under the same settings as sample SC-3. The speleothem showed a pattern of thin gray opaque horizons separated by thick white opaque layers. Signs of corrosion (small pores) are evident in its central part. The base and top of the stalagmite gave reliable ages of ~14.8 ka and ~10.7 ka, respectively.

Within the same area of 'The Cathedral' two other small stalagmites (up to 15 cm each) were sampled and analyzed by means of TIMS. These two samples, SC-5 and SC-6, produced dates of high precision, showing that they grew entirely during the oxygen isotope (OI) stage 5 (Riss-Würm or Eemian interglacial).

Growth of SC-5 commenced prior to 126.3 ka and halted after 105.2 ka. The age of the base of SC-6 was 124.9 ka, while the top of this stalagmite gave an age of 96.4 ka. Based on these ages the growth periods of the two speleothems can be placed within the sub-stages 5e and 5c, respectively.

Two fragments of flowstone (SC-7, 8) were detached from the upper part of the Little Reserve, and another (SC-9) from a small side passage within the Great Reserve. The ages of all three samples were beyond the limit of the alpha-particle counting method (350 ka).

The results of the thirteen dates performed are shown in Table 2. Without exception all samples were low in uranium content, which was in part compensated for by using larger samples and prolonged counting times (when using the alpha-spectrometry method). The levels of detrital ^{230}Th contamination were acceptable, and only one date was corrected using $B_0 = 1.5$ in SCHWARCZ's (1980) equation[4]. With all these precautions, some of the dates still have large analytical errors.

The most prominent paleoclimatic results obtained when analyzing the collective properties of the dates are:

- an active speleothem growth period took place at sometime beyond 350 ka;
- there is an evidence for a gradual shift towards cooler or/and drier climate during sub-stages 5d and 5b when stalagmites SC-5 and SC-6 ceased their growth;
- the continuous growth of speleothems through the isotope stages 2 (Würm III or Late Weichselian) when the ice sheet was only 500 km away from Apuseni Mountains (LOWE & WALKER, 1997). This confirms that this area of the Bihor Mountains was neither covered by alpine glaciers nor experienced enough severe permafrost conditions to suppress water percolation and hence speleothem growth.

The two stalagmites found on top of the limestone breakdown and the flowstone fragments were dated to more than 350 ka. From these dates, we may estimate that Scărişoara Glacier Cave was formed during the Middle- or even Lower Pleistocene period.

Acknowledgements

I am deeply indebted to Joe Kearns for crocoite analysis. Many thanks go to Dr. Lucreţia Ghergari and Dr. William B. White for helpful comments on crocoite geochemistry. The fieldwork for this study was financially supported through the CNCSIS grant No. 11/50 to Bogdan Onac. This is the 6th contribution to the SPEP III Program in Romania.

References

BĂDĂU, A. (1984) Remarques sur la structure microscopique de certaines perles de caverne. *Theor. Appl. Karstology*, 1, pp. 51-57.

BODOLEA, A. (1992) Mineralogia speleothemelor în peşteri din Munţii Bihor. *Lucrare de licenţă*, Facultatea de Biologie-Geologie, Universitatea Babes-Bolyai, Cluj, 105 p.

BUCUR, I., & ONAC, B. P. (2000) New data concerning the age of Mesozoic limestone from Scărişoara (Bihor Mountains, Romania). *Studia Univ. Babes-Bolyai, Geologia*, XLV, 2, pp. 13-20.

DREVER, J. I. (1997) *The geochemistry of natural waters.* (3rd ed.), Prentice Hall, New Jersey, 436 p.

[3] 1 ka = 1000 years.

[4] B_0 represents the $^{230}Th/^{232}Th$ ratio in the detritus.

FISCHBECK, R. (1976) Mineralogie und Geochimie Carbonatischer Ablagerungen in Europäischen Höhlen, - ein Beitrag zur Bildung und Diagenese von Speleothemen. *Neues Jahrbuch. Miner. Abh.*, **126**, pp. 269–291.

FISCHBECK, R., & MÜLLER, G. (1976) Monohydrocalcite, hydromagnesite, nesquehonite, dolomite, aragonite and calcite in speleothems of the Fränkische Schweiz, Western Germany. *Contr. Miner. and Petrol.* **33**, pp. 87–92.

FRIEDMAN, G. M. (1959) Identification of carbonate minerals by staining methods. *Jour. Sed. Petrology.* **29**, *1*, pp. 87–97.

HILL, C. A., & FORTI, P. *Eds.* (1997) *Cave minerals of the world.* 2nd ed., NSS, Huntsville, Alabama, 464 p.

IVANOVICH, M. & HARMON, R. S. (1992) *Uranium-series disequilibrium. Applications to Earth, Marine, and Environmental Sciences.* 2nd ed., Oxford University Press, 910 p.

LOWE, J. J., & WALKER, M. J. C. (1997) *Reconstructing Quaternary Environments.* 2nd ed., Longman, 466 p.

ONAC, B. P., & GHERGARI, L. (1993) Moonmilk mineralogy in some Romanian and Norwegian caves. *Cave Science*, **20**, *3*, pp. 107–111.

ONAC, B. P., & LAURITZEN, S.-E. (1996) The climate of the last 150,000 years recorded in speleothems: preliminary results from north-western Romania. *Theor. Appl. Karstology*, **9**, pp. 9–21.

RACOVIȚĂ, G., & ONAC, B. P. (2000) *Scărişoara Glacier Cave. Monographic Study.* Carpatica, Cluj, 140 p.

RUSU, T., RACOVIȚĂ, G., & COMAN, D. (1970) Contributions à l'étude du complexe karstique de Scarisoara. *Ann. Spéléol.*, **25**, *2*, pp. 383–408.

SCHWARCZ, H. P. (1980) Absolute age determination of archaeological sites by uranium dating of travertines. *Archaeometry*, **22**, *1*, pp. 3–24.

VIEHMANN, I. (1963) Un nou proces de geneză a perlelor de cavernă. *Lucr. Inst. Speol. "E. Racoviță"*, **I-II**, pp. 295–303.

VIEHMANN, I. (1967) Noi contribuţii la geneza perlelor de cavernă din peşterile cu gheaţă. *Lucr. Inst. Speol. "E. Racovita"*, **VI**, pp. 141–147.

Theoretical and Applied Karstology, 13–14 (2000–2001), pp. 39–50

Karst evolution in the Danube Gorge from U-series dating of a cave-bear skull and calcite speleothems from Peştera de la Gura Ponicovei (Romania)

Silviu Constantin[1*], Stein-Erik Lauritzen[2], Emanoil Ştiucă[1] & Alexandru Petculescu[1]

[1] *"Emil Racoviţă" Institute of Speleology, str. Frumoasă 11, 78114 Bucureşti, Romania.*
[2] *Bergen University, Department of Geology, Allegaten 41, 5009 Bergen, Norway.*

Abstract

Two bone samples taken from a cave-bear skull discovered in Pestera de la Gura Ponicovei (Danube Gorge, Romania) have been dated by U-series liquid-liquid extraction procedure. They allowed the determination of a minimum age of the cave as well as the minimum age of Danube's fourth terrace at c. 277 ka. This age has been also used to ascertain the paleontologic determination of the bear species as *Ursus deningeri* v. Reichenau. Datings on speleothem calcite indicate that the minimum age of the active level of the cave is ~30 ka and enabled rough estimations of the incision rate of the underground river and of the fluvial erosion rate of the Danube at 0.05 m/ka and 0.67 m/ka, respectively.

Keywords: karst evolution, speleogenesis, paleogeography, cave bears, *Ursus deningeri*, Danube Gorge, Romania.

Evolution du karst dans le Défilé du Danube d'après quelques datations par la série de l'Uranium d'un crâne d'ours de caverne et des quelques spéléothèmes de calcite de la Peştera de la Gura Ponicovei (Roumanie)

Résumé

*Deux échantillons d'os prélevés d'un crâne d'ours de caverne découvert dans la Peştera de la Gura Ponicovei (Défilé du Danube, Roumanie) ont été datés par la méthode de la série de l'Uranium, en appliquant la procédure d'extraction liquide-liquide. Les résultats ont permis de déterminer l'âge minimum de la grotte ainsi que de la quatrième terrasse du Danube, qui est d'environ 277 ka. Cet âge a servi à l'élimination des incertitudes de l'analyse paléontologique classique, de même que pour établir qu'il s'agit d'un individu d'*Ursus deningeri *v. Reichenau. Les datations des quelques spéléothèmes de calcite ont indiqué que l'âge minimum de la galerie active de la grotte est d'environ 30 ka. En outre, elles ont permis d'établir le taux d'approfondissement de la rivière souterraine à 0,05 m/ka et celui d'érosion fluviale du Danube tout au plus à 0,67 m/ka.*

Mots clés: évolution du karst, spéléogenèse, paléogéographie, ours de caverne, Ursus deningeri, *Défilé du Danube, Roumanie.*

Introduction

Cave deposits are well known as preserving important paleoclimatic and paleogeographic information. Speleothems are now largely used for paleoclimatic reconstructions, mainly based on their isotopic record — which can be accurately dated by means of U-series methods (see, for example, Ford, 1997 and references therein). Other cave deposits, such as the fossil remains of micromammals, may also bear important paleoclimatic significances (e.g. Mein, 1976 or Lowe & Walker, 1997 and references), but they usually yield only a relative chronology being not suitable for absolute dating.

The use of large mammal fossils (such as cave-bear bones) for speleogenetic purposes is scarce. First, such remains cannot usually be associated with key-episodes within the lifespan of a cave; in general, their only significance is that they postdate the formation of the passage where found. Second, absolute

* corresponding author. *E-mail address*: Silviu.Constantin@geol.uib.no

dating of such remains is often impossible by means of the radiocarbon method (due to its low time-range) and it has been problematic by the U-series method due to the high phosphate content of the bones which impede both the extraction and the chemical separation of U and Th and usually cause low chemical yields.

The new liquid-liquid separation method developed by LAURITZEN *et al.* (1997) at the U-series laboratory – University of Bergen allowed us to perform two successful dates of a cave-bear skull from "Peştera de la Gura Ponicovei" (Romania). Moreover, since the recovered bone remains were not sufficient for a unique paleontological diagnosis, the absolute dating has actually eliminated some alternatives and finally led to the species determination. The significance of the dating of the fossil remains, together with several conventional alpha-spectrometric dates of speleothem calcite are further used to pinpoint some of the erosion phases of the evolution of the Danube Gorge during the Upper Quaternary.

Fig. 1. Location of Ponicova Cave and the remnants of the VIIIth terrace within the Cazane sector of the Danube Gorge. a. General location of the Danube Gorge; b. Cross-section through the gorge in the sector of Ponicova Cave showing the positions of different surface and cave levels. Note the asymmetry of the Danube sides. Vertical scale is 4x exaggerated. Base map and profile after SENCU (1979) with modifications. 1. The limit of the Danube Valley at the end of the Pliocene; 2. Remnant surfaces of the VIIIth terrace; 3. Saddle; 4. Elevation; 5. Limestone cliff; 6. Gorge; 7. Cave entrance; 8. Direction of the Ponicova Cave main passages; 9. Ponicova Valley before the underground piracy. →

Situation de la grotte de Ponicova et des surfaces de la VIII-ème terrasse dans le secteur de Cazane du Défilé du Danube. a. Situation générale du Défilé du Danube; b. Coupe transversale du défilé dans le secteur de la grotte, avec les positions des différents niveaux de surface et souterrains. A noter l'asymétrie des deux versants du Danube. Carte de base et coupe d'après SENCU *(1979) modifiées.*

1. Limite de la vallée du Danube à la fin du Pliocène; 2. Surfaces de la VIII-ème terrasse du Danube; 3. Ensellement; 4. Cote; 5. Abrupt calcaire; 6. Gorge; 7. Entrée de la grotte; 8. Direction des principales galeries de la grotte; 9. Direction de la vallée de Ponicova avant la capture souterraine.

Material and methods

The Danube Gorge

The "Danube Gorge" is Europe's longest defile stretching along some 135 km at the border between Romania and Yugoslavia (*see* Fig. 1a). It includes four sectors of limestone gorges (SENCU, 1979) among which, the most spectacular and narrow is the so-called '*Cazanele* (=Giants' Pots) *Dunării*', in Romanian and *Djerdap* (= rocky rims) — in Serbian. Within this sector, the river flows between steep limestone cliffs for some 10 km; the gorge is interrupted for only 1 km (and only on the Romanian side) at Dubova where a small Miocene sedimentation basin may be found. All along the gorge, the cross-profile of the riversides is asymmetrical: on the left (Romanian) side, the cliffs top at *c.* 320 m asl., while on the right side they reach an average altitude of ~700 m (Fig. 1).

The genesis of the Danube Gorge has made the subject of many theories since the beginning of the 20th Century. The principal hypotheses are those assuming either the "antecedence" of the river that has cut the uplifting Carpathian range, or the stream piracy between tributaries of the Getic and Pannonian Basins, respectively. Regardless of any genetic theory, it seems quite clear that the genesis of the Danube Gorge extends back in time until at least the Pliocene, since this is the age of the gravels covering the karst plateaus on the Romanian side (based on paleontological evidence, *see* VÂLSAN, 1918). These karst plateaus seem to correspond to the oldest terrace (the VIII-th) of the Danube ('*der Pontischer Talboden*' of CVIJIC, 1908) with an absolute elevation of 310–320 m. The remaining seven terraces of the river are mostly preserved in the Romanian Plain (POSEA *et al.*, 1969); within the Danube Gorge sector their distribution is limited to very small surfaces and little is known about the Quaternary history of river's entrenchment. The most clearly recognizable terraces along the Danube Gorge are the terraces no. VII (250–300 m), VI (170–200 m) and V (150–160 m); the later may be continuously followed downstream towards the Romanian Plain. Following the construction of the "Iron Gates" Dam, the last two terraces, with relative altitudes of 10–20 m (80–90 m asl.) and 6–8 m (~55 m asl.), respectively, were totally inundated by the water within the entire Danube Gorge sector (POSEA *et al.*, 1976)

Geological background

The "Cazane" Gorge was formed at the northern end of the karst plateau of Miroć, being mainly carved in massive reef limestones, Upper Jurassic to Lower Cretaceous in age. On the Romanian side these limestones have a spatial extension of less then one kilometer and are overlied westwards by Cretaceous flysch sediments. The gorge is divided into two sectors by a small basin filled by Miocene sediments at Dubova. Detailed accounts of the geological structure of the 'Cazane' and Danube Gorge region, may be found, e.g. in MUTIHAC (1990), GRUBIC (1994), GRUBIC & BERZA (1997). The karst plateau of Ciucarul Mare displays a large number of sinkholes, accounting for almost 39% of its total surface (SENCU, 1979).

[1] Following the construction of the "Iron Gates" Dam, in the late '60s the Danube's level rose with ~30-40 m within the "Cazane" sector. Since this paper is concerned with Danube's Quaternary evolution, all **relative** altitudes are quoted with respect to the **former** Danube level. All **absolute** (asl.) elevations are quoted with respect to the Black Sea level.

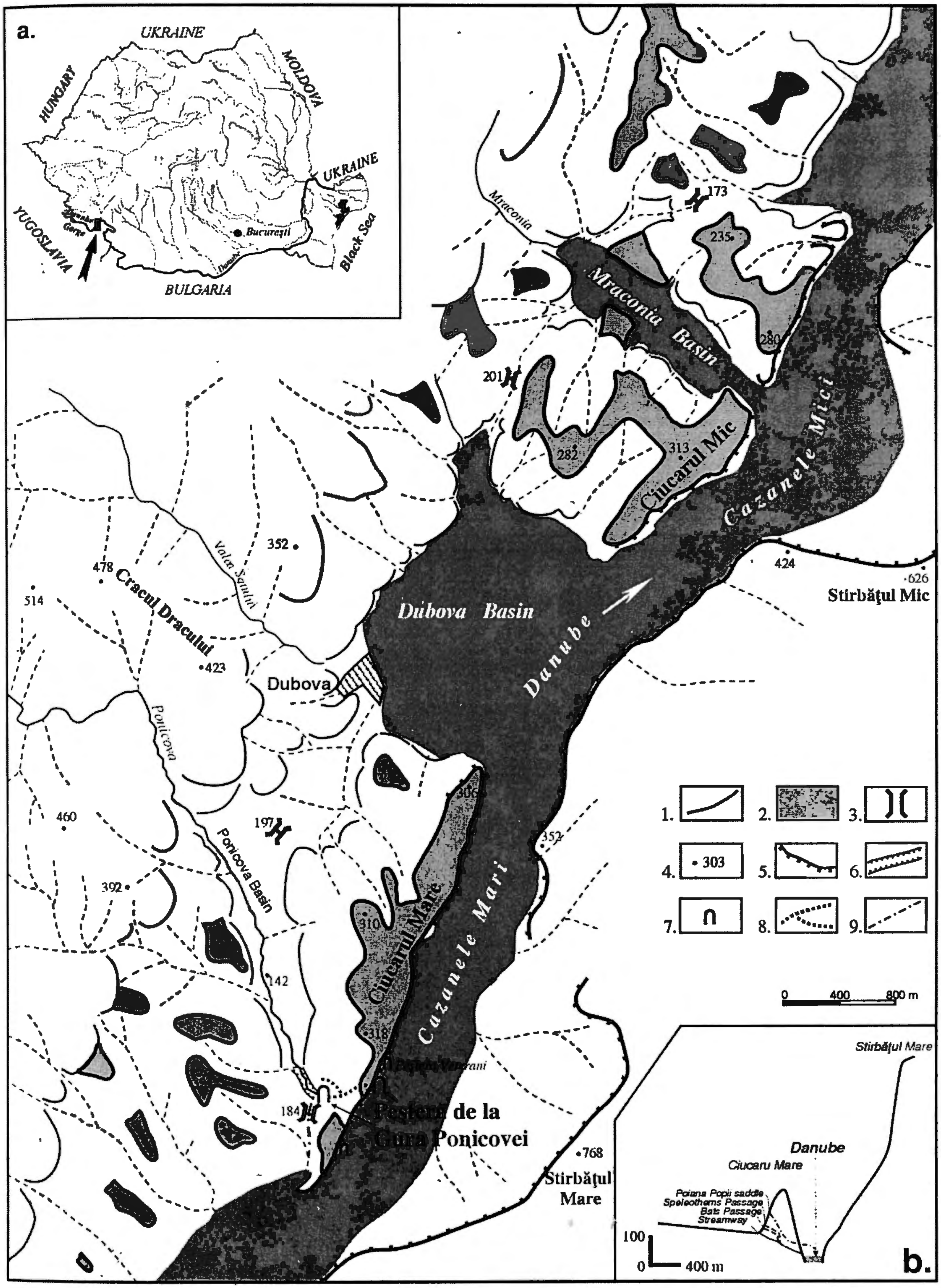

a.
UKRAINE
HUNGARY
MOLDOVA
UKRAINE
YUGOSLAVIA
Danube Gorge
Bucureşti
Black Sea
BULGARIA
Mraconia
Mraconia Basin
Ciucarul Mic
Cazanele Mici
Dubova Basin
Danube
Dubova
Craciul Dracului
Valea Satului
Ponicova
Ponicova Basin
Ciucarul Mare
Cazanele Mari
Peştera de la Gura Ponicovei
Stirbăţul Mic
Stirbăţul Mare
173
235
280
201
282
313
352
478
514
423
424
626
306
197
460
392
352
310
142
318
184
768
1.
2.
3.
4.
303
5.
6.
7.
8.
9.
0
400
800 m
Stirbăţul Mare
Danube
Ciucaru Mare
Poiana Popii saddle
Speleothems Passage
Bats Passage
Streamway
100
0
400 m
b.

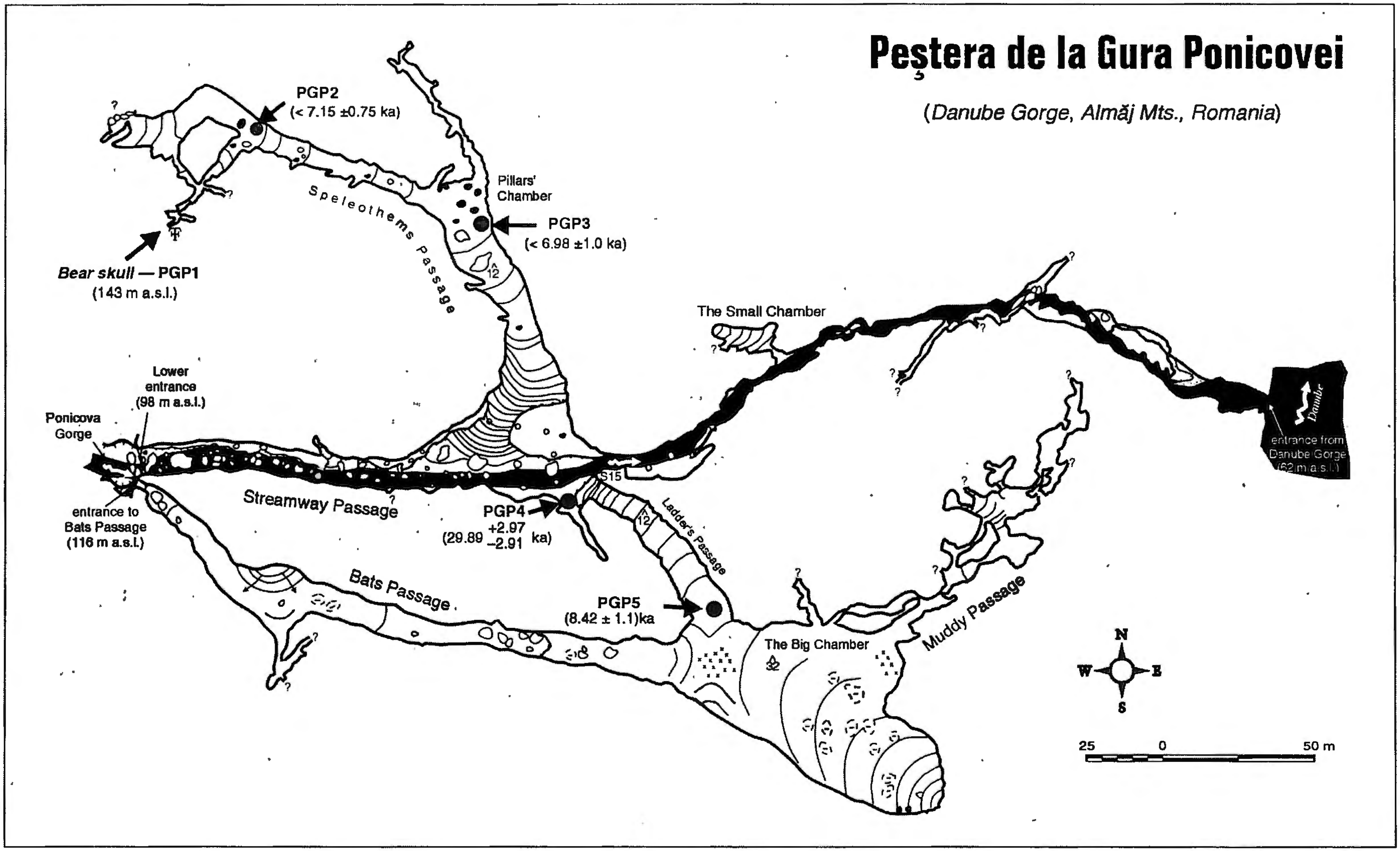

Fig. 2. Plan of Ponicova Cave with the location of the analyzed samples. Base map after Negrea & Negrea (1979), simplified.

Plan de la grotte de Ponicova avec la localisation des échantillons analysés. Relevé de base d'après Negrea & Negrea (1979) simplifié.

Peştera de la Gura Ponicovei

Peştera de la Gura Ponicovei (hereafter named **Ponicova Cave** for simplicity) is the most important cave in the Cazane Gorge. It is a tiered, through-cave, centered along the small Ponicova Brook. This river collects its waters from the crystalline schists of the basement and the impervious flysch deposits then, shortly after reaching the Jurassic limestones enters into the cave through a majestic porch, over 25 m-high (98 m asl.). In the underground, the stream flows through a 400 m-long passage with heights of more than 25 m and a canyon-shape; eventually it reaches the "Iron-Gates" dam lake through another, smaller, porch (Fig. 2).

Two other systems of passages are worth-noticing: on the southern side of the Streamway Passage, at a height of 15–20 m, the *Bats Passage* has its distinct entrance suspended above the main one (altitude: 116 m). This is an inactive passage that includes a large collapse chamber (*The Big Chamber*) and a secondary system of narrow, muddy, ascending passages on its eastern end. Bats Passage communicates with the Streamway Passage through a descending gallery (*Ladders' Passage*) which ends with a 20 m drop above the underground river.

From this intersection, a third large, ascending, passage may be followed towards the NW. This is known as *Speleothems Passage*, although only the most massive speleothems are still preserved, such as large stalagmites and pillars, a thick flowstone pavement and large-size anemolites. This sector includes several small side passages and finally comes to a dead-end at an altitude of 143 m (81 m above the lowest entrance). Gravel elements of metamorphic rocks may be noticed on the floor and, in some sectors, also on the ceiling of this passage; together with the presence of the anemolites, they indicate that this passage has acted as a former paleo-Ponicova subterranean drain (NEGREA & NEGREA, 1979).

Ponicova Cave has been studied by many researchers, including JEANNEL & RACOVIŢĂ (1929), SCHMIDT *et al.* (1968), BOTOSENEANU *et al.*, (1967), SENCU (1979), etc. The last author has analyzed the genesis of the cave establishing four genetic stages (*see* Fig. 5). During the first stage Ponicova was flowing directly into the Danube along the southwestern margin of the limestone area. In stage two, the river has been captured somewhere at the level of the Speleothems Passage. A relict saddle ("Poiana Popii") has been preserved at the altitude of 184 m. In the third stage, a second capture has occurred, this time in the right bank of the river, at the level of the Bats Passage (the upper entrance). Eventually, in the final stage, the river has adopted the actual level of the Streamway Passage. A small natural bridge located some 100 m upstream the main entrance suggests that the capture points in stages 3 and 4 were actually located further upstream and that part of the former cave passages were subsequently destroyed by collapses.

Ponicova is generally a well-ventilated cave, strongly influenced by the temperature variations at the surface, except for the deeper sectors of Speleothems Passage and The Muddy Passage. The temperature may vary, according to the seasons, between 9 °C and 22 °C in the well-ventilated passages (average humidity: 60–78%), while the deep parts of Speleothems Passage benefits of a fairly constant temperature of 11–11.5 °C and a high humidity (~95%).

Samples

BOTOSENEANU *et al.* (1967) made the first mention on cave bear (*U. spelaeus*) bones that have been found in Ponicova Cave. However, these bones were not collected, apparently due to their serious degradation, which would have prevented any diagnosis. During a reconnaissance trip in 1998, we discovered a skull fragment cemented into a hardened clayey matrix, into the ceiling, at the very dead-end of the Speleothems Passage (see Fig. 2 and Fig. 3). Several small fragments (samples PGP1) of this skull were collected at that time but most of it was carefully removed during a subsequent visit in 1999.

The fragments collected allowed the partial reconstruction of the skull at the Laboratory of Paleontology — "Emil Racoviţă" Institute of Speleology. This part consists of the left parietal, and the posterior orbital bone of a bear skull. Dimensionally it fits well within the variation range of a juvenile *Ursus spelaeus* or of a young adult of *U. deningeri.* Several remains of rodents have been also collected but they definitely belong to much younger (Holocene) specimens.

Four calcite samples were also collected. Sample PGP2 was the 'root' of a broken stalagmite and sample PGP3 was a 30 cm-tall stalagmite, both from Speleothems Passage. In longitudinal section, sample PGP3 show a fine lamination with an alternation of white opaque and dusty-gray laminae. This appearance may be considered as indicative for a predominantly evaporative regime of precipitation.

Samples PGP4 and 5 were fragments of flowstone taken from the base and the top of the Laders' Passage, respectively (*see* Fig. 2). PGP4 was part of a more massive, tufa-like deposit located some 1.5 m above the base of the passage; PGP5 has a more compact appearance and was deposited on the passage floor. The morphology of these samples differs very much from that of a regular cave flowstone (Fig. 4). Sample PGP4 shows a very porous structure, which resembles to that of a tufa; in case of sample PGP5, the pores are replaced by shrinkage cracks, suggesting that the calcite precipitation took place under freeze-thaw conditions.

Dating methods

Al samples have been dated by alpha-spectrometry at the U-series laboratory in Bergen University, Norway. For the calcite samples we used the standard procedure described,

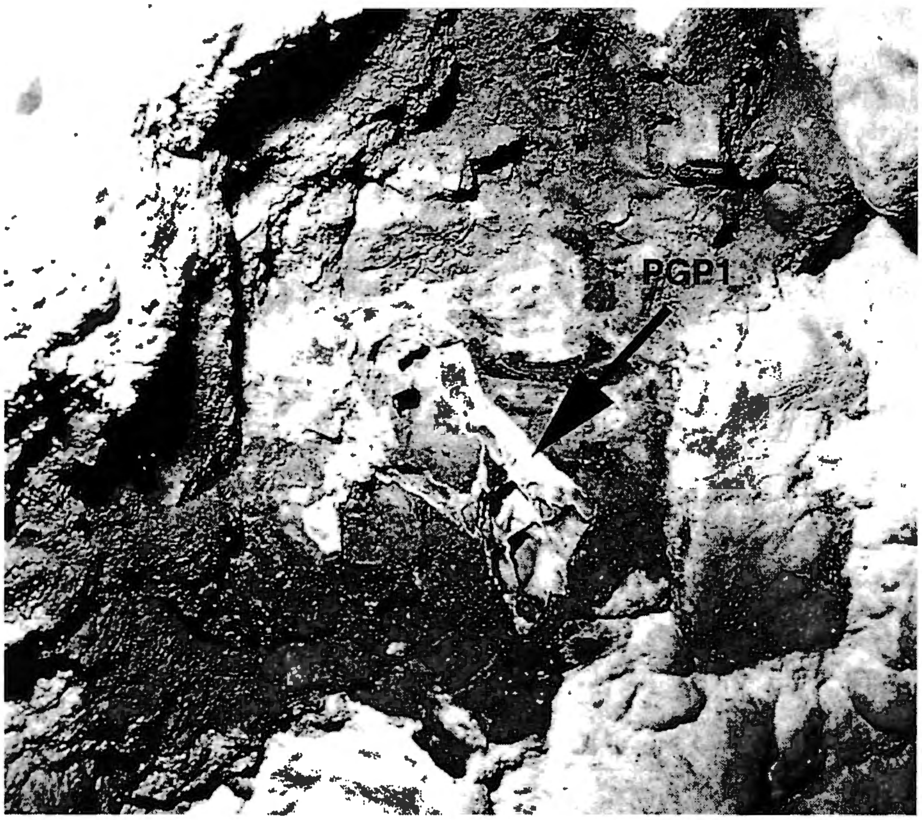

Fig. 3. The skull of *Ursus deningeri, in situ*. The surrounding matrix is a hardened, red, clay.

*Le crâne d'*Ursus deningeri *in situ englobé dans une matrice consolidée d'argile rouge.*

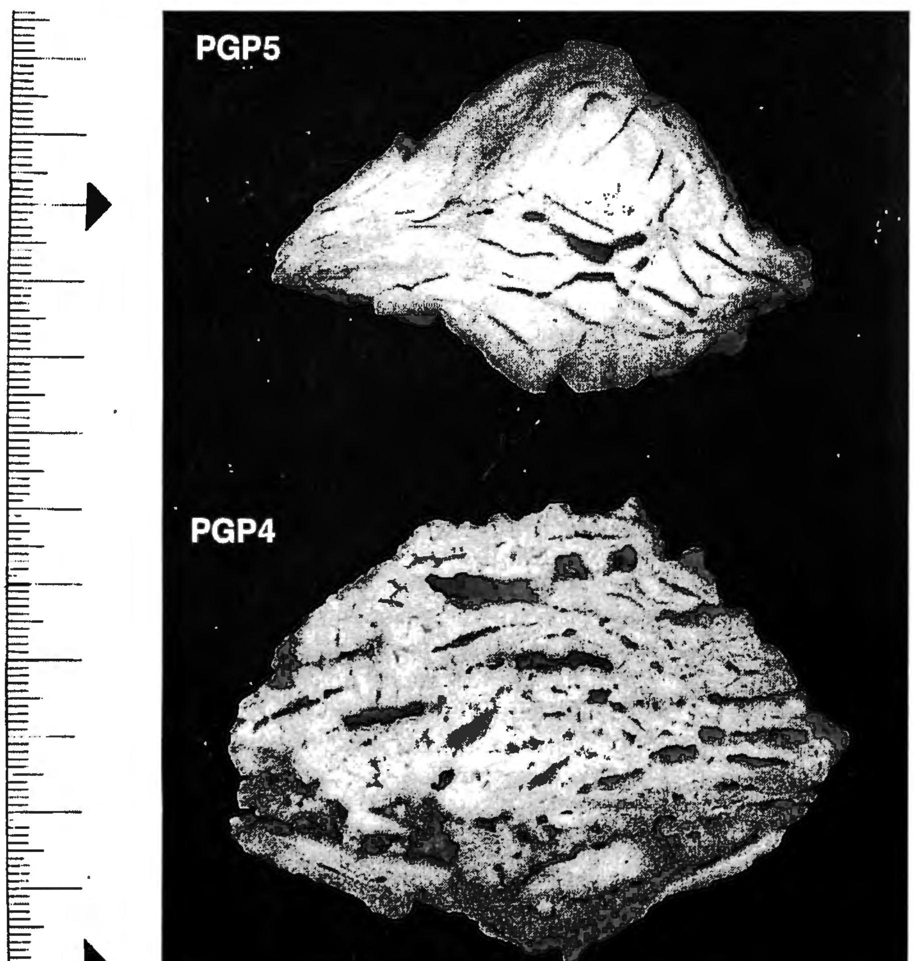

Fig. 4. Sections through the samples PGP4 (down) and PGP5 (up). Note the tufa-like structure of sample PGP4 and the 'shrinking' cracks of PGP5. See text for further comments.

Sections à travers les échantillons PGP4 (en bas) et PGP5 (en haut). A noter la structure tufière de l'échantillon PGP4 et les fissures de contraction du PGP5. Voir le texte pour détails supplémentaires.

for example, in Lauritzen & Onac (1999). One date was performed on each sample, except for PGP3 where we have attempted to date both base and top of the stalagmite. The samples (20–40 g) were digested in HNO_3, spiked with a commercial $^{228}Th/^{232}U$ tracer and the solution was equilibrated by H_2O_2 oxidation and repeated boiling. U and Th were preconcentrated by scavenger precipitation on $Fe(OH)_3$, then the iron was removed by ether extraction in 9M HCl. U and Th were separated by ion-exchange chromatography, then the fractions were purified and electroplated on steel discs.

The bone fragments require a modified chemical procedure in order to extract the U and Th from phosphate matrix. This procedure has been thoroughly discussed by Lauritzen *et al.* (1997) and it is based on the liquid-liquid extraction (LLE) of U and Th by tri-*n*-octyl-methyl-ammonium chloride and – nitrate (*n*-TOMA) (Aliquat 336, Fluka art. no. 91042) from hydrochloric and nitric acid solutions.

Since U content in bones is usually high, samples of only 2–3 g are sufficient. Two small fragments of the skull were carefully cleaned, then incinerated at 500 °C for *c.* 6 h. The samples were digested in 9M HCl; $FeCl_3$ carrier and $^{228}Th/^{232}U$ spike were added. After oxidation, the iron was removed by ether extraction and the concentration of the Fe-free solution was adjusted at 6M HCl. U and Th were separated by liquid-liquid extraction with *n*-TOMA. U was first extracted in the organic phase using a solution of 0.1M *n*-TOMA in xylene, then back-extracted ('stripped') into 0.1M HCl. The Th fraction, remining in 6M HCl, was evaporated to dryness and redissolved in 6M HNO_3, then extracted into 0.5M *n*-TOMA and, further on, back-extracted into 0.1M HCl. The purified U and Th fractions were oxidized and electroplated onto steel discs.

For both methods, the alpha particle activity was counted for 2–4 days using an Ortec Octéte unit with silicon surface barrier detectors. Finally, each spectrum was corrected for background and delay since separation and the ages were calculated using standard algorithms (Lauritzen, 1993). All errors reported in this paper are 1_σ.

Results

The results of speleothem and bone fragments datings are shown in Table 1. One of the calcite samples (top of stalagmite PGP3) has been rejected due to the very high detrital Th content ($^{230}Th/^{232}Th < 1$) and it is not presented here. The remaining four samples also show high detrital contamination, the $^{230}Th/^{232}Th$ ratio varying between 2.7 and 14.5. Consequently, the corrected ages of samples PGP2 and PGP3 should be considered with caution, and only viewed as *minimum* ages.

The flowstone samples PGP4 and PGP5 show a lower contamination with detrital Th and their corrected ages may be considered as reliable.

All samples showed low U-contents (between ~0.04 and 0.1 ppm), which in turn results in quite high statistical errors of ~10% for the non-corrected ages.

Dating of the two bone fragments was considerably more successful. Since U-series dating of bones is generally considered problematic (*see* Schwarcz & Blacwell, 1992 or Blacwell & Schwarcz, 1995) we made two dating attempts to test for reproducibility. The first sample (PGP1a) was a small fragment of porous bone, while the second (PGP1b) was a thinner and smoother fragment of the parietal bone. The measured activity ratios and the ages calculated accordingly for the two samples are in very good agreement within the range of 1_σ errors. The high U-content, good chemical yields, and the absence of detrital Th allowed the calculation of ages that are statistically identical. The only noticeable difference is the U content, which is slightly (<10%) higher for

Table 1. The results of the speleothem and bone datings by U-series alpha spectrometry. First four dates were performed on calcite samples, and last two dates on bone samples. Ages written in bold were used in this paper. All errors are 1_σ.

Résultats des datations en spectrométrie alpha des spéléothèmes et de l'os. Les quatre premières datations ont été effectuées sur des échantillons de calcite et les deux dernières sur des échantillons d'os. Les datations en caractères gras ont été utilisées dans ce travail. Dans tous les cas l'erreur est de 1_σ.

	Lab. No.	Description	U cont. (ppm)	$^{234}U/^{238}U$	$^{230}Th/^{234}U$	$^{230}Th/^{232}Th$	Age (ka)	+err −err	Corr. age (ka)	+err −err
PGP2	1872	Stalagmite 'root'	0.072 ±0.004	1.526 ±0.105	0.064 ±0.007	2.7	7.15	+0.75 −0.75	3.19	+1.16 −1.16
PGP3	1873	Base stalagmite	0.041 ±0.004	2.858 ±0.339	0.063 ±0.009	3.4	6.98	+1.06 −1.06	4.00	+1.52 −1.51
PGP4	1811	Flowstone Streamway Pass.	0.079 ±0.003	1.576 ±0.066	0.265 ±0.019	14.5	32.81	+2.75 −2.69	29.89	+2.97 −2.91
PGP5	1812	Flowstone Ladder Passage	0.096 ±0.003	1.185 ±0.057	0.087 ±0.008	10.3	9.79	+0.97 −0.97	8.42	+1.11 −1.10
PGP1a	2119	Bone fragment (porous)	19.814 ±0.447	1.5016 ±0.027	1.0175 ±0.0329	10000	282.03	+39.81 −30.42		
PGP1b	2120	Bone fragment (parietal)	17.403 ±0.275	1.4643 ±0.020	1.0083 ±0.025	10000	277.32	+28.28 −23.17		

the porous bone, suggesting that the U-uptake was favored by its structure.

Discussion

The results of the datings of samples from Ponicova Cave will be first discussed from a paleontological perspective; further on, we will discuss their relevance for the karst evolution within the Danube Gorge area.

Paleontologic aspects

As mentioned before, the paleontological analyses of the skull did not allow a determination of the bear species beyond any doubt. In the absence of any teeth remains, the morphologic and morphometric observations have only permitted the recognition of the genus.

It is generally admitted that *Ursus etruscus* of the Villafranchian is the ascendant of the cave bear. The specimens of *U. etruscus* from Val d'Arno and Olivola, considered as typical for the Villafranchian of Italy proved to be constantly encountered in Lower Quaternary deposits throughout Europe (Newton, 1913; Bernson, 1931; Schreuder, 1945; Samson & Rădulescu, 1963).

Some rare bear remains have been signaled as occupying an intermediate position between *U. etruscus* and *U. deningeri.* Among these, the ones described from Jockgrim and Eberbach (Heller, 1939) are debatable, being morphologically closer to *U. etruscus* than to *U. spelaeus.*

Sörgel (1926) and Koby (1952) have noticed some distinct archaic features of the remains of *U. deningeri* from Süssenborn, which was considered by Zapfe (1946) as a subspecies (*U. deningeri süssenbornensis*). Other intermediate bear remains, such as *U. sakdillingensis* Heller, 1956, show a morphology which is closer to *U. deningeri* than to *U. etruscus*.

A posterior skull fragment, together with some other bone remains was described by Bonifay (1971) from the cave of Lunel-Viel as *U.* cf. *deningeri*; its age is considered to belong to the Mindel-Riss interglacial. The transversal width of this skull is 148 mm, which is comparable to that of the skull discovered in Ponicova Cave as well as to the skull described from Masbach (150 mm in both cases).

Thus, by taking into account both the dimensional and structural features of the skull and the calculated age of the bone fragments at ~277.32 (+28.3; –23.2) ka, the uncertainty has considerably narrowed and the skull fragment was assigned to the species *Ursus deningeri* v. Reichenau. Any other alternatives (e.g. juvenile *U. speleus*) have been rejected.

The morpho-structural analysis of the skull suggests a mature individual; its small dimensions may be considered as a manifestation of the sexual dimorphism (Kurten, 1955; 1958) and are indicative for a young specimen.

In general, *U. deningeri* is considered as a transition species with a rapid evolution. To our knowledge, our datings constitute **the first absolute age determination of bone remains for this species.** According to the determined age, the specimen of *U. deningeri* discovered in Ponicova cave lived during the cold (glacial) period corresponding to the marine isotope stage (MIS) 8.

Paleogeographic interpretation

As a typical multi-level cave, Ponicova has attracted the attention of many researchers studying the evolution of the Danube within its gorge sector (e.g. Sencu, 1979; Schmidt *et al.*, 1968). Its well-defined passage levels, as well as the relict saddle of Poiana Popii may be correlated with correspondent terraces of the river (Table 2). However, this is the first attempt to establish an absolute chronology for the incision rate of Danube during the Quaternary.

Two out of the five calculated ages are relevant for reconstructing the regional geomorphic evolution: that of the *bear-skull* (PGP1a,b) which postdates the formation of Speleothems Passage, and the *PGP4 flowstone* — which postdates the formation of the Streamway Passage. The remaining three samples have lesser significance due to their young age and to the lower precision of age determinations. They only account for a massive calcite precipitation in SW Romania during the Holocene warming, which may be well traced in many caves and travertine deposits of the region (see Constantin & Lauritzen, 1999; Constantin *et al.*, 2001; also Constantin S. *unpublished data*).

The age obtained for the PGP4 flowstone (*c.* 30 ka) is more relevant since this sample is clearly a vadose deposit that was located only 1.5 m above the subterranean river, within the Streamway Passage. Thus, it enables the estimate of a minimum age for the creation of this large, canyon-shaped passage and, accordingly, a minimum age of the corresponding second terrace of Danube.

Table 2. Correlation between the different geomorphic and cave levels and Danube's terraces within the gorge sector.

Corrélation entre les différents niveaux de surface et souterrains, d'un part, et les terrasses du Danube dans le défilé, d'autre part.

Cave level	Elevation (m asl.)	Terrace (elevation m asl.)	Age (ka)
Poiana Popii saddle	184	V (150–160)	
Speleothems Passage	143–112	IV (120–130)	>277
Bats Passage	116	III (100–117)	
Streamway Passage	80–65	II (80)	>30

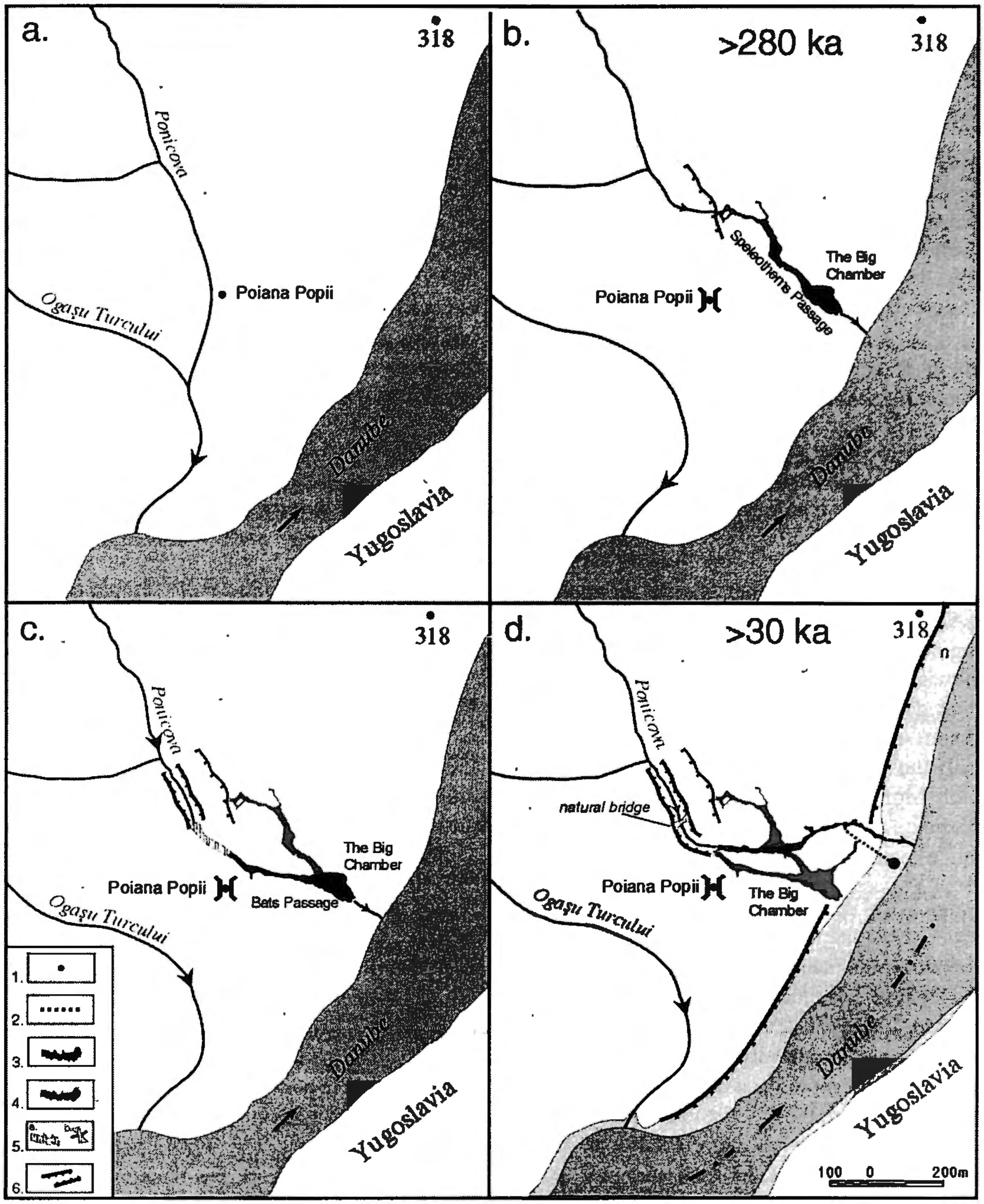

Fig. 5. Evolution of the Ponicova cave system (after SENCU, 1979, with modifications). Stages: (a) surface drainage over Poiana Popii; (b) underground capture through the Speleothems Passage (before 277 ka); (c) second capture at the level of Bats Passage (note that the passage extends upstream the current entrance); (d) modern phase: third capture at the Streamway level and direct drainage to the Danube. The natural bridge is a remnant of the former, collapsed, passages. The two shades of Danube designate the situation before and after the creation of artificial Iron Gates Lake. 1. Karstic spring; 2. Inferred underground drainage; 3. River (active) passages; 4. Dry (fossil) passages; 5. a. Inferred position of former cave passages; b. Natural bridge; 6. Gorge.

Evolution de la grotte de Ponicova (d'après SENCU, 1979, modifiée). Etapes (a) drainage de surface à travers la Poiana Popii; (b) capture souterraine à travers la Galerie des Concrétions (avant 277 ka); (c) seconde capture au niveau de la galerie des Chauves-Souris (à noter que la galerie se prolonge aussi bine en amont de l'entrée actuelle; (d) phase moderne: la troisième capture au niveau de la Galerie Active et drainage direct vers le Danube. Le pont naturel reste comme un témoin des galeries détruites d'amont. Les deux nuances de gris du Danube signifient le niveau de l'eau avant et après la formation du lac artificiel des Portes de Fer. 1. Source karstique; 2. Drainage souterrain supposé; 3. Galeries actives; 4. Galeries fossiles; 5. a. Position supposée des galeries actuellement détruites; b. Pont naturel; 6. Gorge.

Similarly, we may assume that the upper cave level (Speleothems Passage) is older than ~277 ka, which is the age of the *U. deningeri* skull. This figure may be thus taken as the lower limit for the formation of Danube's fourth terrace (120–130 m asl.).

The evolution of Ponicova cave system (Fig. 5) as inferred by the results of this work includes the initial underground capture of the river, through the Speleothems Passage, at some point in time well beyond ~ 277 000 years ago. It seems reasonable to assume this value as a minimum age of the IVth terrace of the Danube as well. Dating by means of cosmogenic isotopes of the relict pebbles found into the upper sector of this passage might extend this figure considerably, but this will be the subject of further research.

It will be hazardous to make any further assumptions concerning the timing of formation of the other cave levels. Nevertheless, it seems very clear that the lower (active) level shall be older than ~30 000 years, the age of PGP4 flowstone.

A tentative calculation of the subterranean river incision rate, based on the position of the sample at ~1.5 m above the stream will yield a *maximum* value of ~0.05 m/ka. This figure is one order of magnitude lower than the erosion rate value of 0.4–0.5 m/ka calculated for Crisul Repede river basin (Lauritzen & Onac, 1995) but this may be considered as normal taking into account only the large difference between the flow rates of the two rivers. Moreover, if we try to estimate Danube's incision rate based on the position of the second terrace (~20 m relative altitude), which may be considered as a base-level for the Streamway Passage, the maximum fluvial incision rate would be of ~0.67 m/ka, in accordance with the work cited.

The presence of small mammals remains in the terminal sector of Speleothems Passage is indicative for the existence of another cave entrance, located in the close vicinity, during the Holocene, since these species never live in the deep sectors of a cave. If we add to this: (i) the presence of anemolites, suggesting a strong air current and (ii) the observations on the structure of PGP3 stalagmite indicating evaporative conditions of precipitation, we may conclude that the total clogging of the Speleothems Passage took place only in the recent past, less than ~3 000 years ago. The stable meroclimate of this part of the cave is therefore only recent and the premises for further speleothem dating work in search for older specimens do not seem very promising.

Conclusions

The successful dating by U-series LLE method of two fragments of the same cave-bear skull from Ponicova cave yielded activity ratios and ages that are in very good agreement within the 1_σ errors range. The LLE method proved to be very useful in dealing with bone samples and the close replicates of the two coeval samples is encouraging. The ages obtained not only allowed the dating of the skull at ~277 (+28; –23) ka but were also crucial for the paleontological diagnosis. According to this, the skull belonged to a mature individual of *U. deningeri* v. Reichenau. This is also the first absolute dating of fossil remains for this species.

The determined age offers a first estimate on the antiquity of the Ponicova cave system and a minimum estimate for the age of the fourth terrace of the Danube, which is considered to represent its first base level.

U-series dating of PGP3 calcite sample allowed a second estimation for the minimum age of the lower cave level (the Streamway Passage) as of minimum 30 ka. This may be also considered as a minimal age for the second terrace of the Danube. Rough calculations yielded maximal incision rates of ~ 0.05 m/ka for the cave passage and of ~ 0.67 m/ka for the fluvial erosion rate of the Danube. These figures must be considered only as preliminary, and further work is required.

Finally, the morphology and structure of the speleothems from the topmost sector of the cave, together with the discovery of recent micro-mammals remains indicate that another cave entrance located in this zone may have been clogged not earlier than ~ 3 000 years ago.

Acknowledgements

All datings were performed in the U-series Laboratory, Bergen University. All paleontological work was done in the specialized laboratory of the "Emil Racovita" Institute of Speleology. Part of this work has benefited of the support for S. Constantin and A. Petculescu by the grant 5235 of Romanian Agency for Science, Technology and Innovation (ANSTI). We also thank Angela Teodorescu for help in the field and for drawing some of the figures. This is the 8th contribution to the Speleothem Pole-Equator-Pole (SPEP) III in Romania.

References

BERNSEN, J. J. A. (1931) Eine revision der fossilien Säugetierfauna und den Tonen von Tegelen. III. ***Naturhist. Maandblad*, 5.**

BLACKWELL, B. & SCHWARCZ, H. P. (1995) The Uranium series disequilibrium dating methods. In: *Dating methods for Quaternary deposits* (RUTTER, N. W., & CATTO, N. R., *Eds*.), Geological Ass. of Canada, St. John's, Newfoundland, pp. 167–208.

BONIFAY, M.-F. (1971) Carnivores quaternaries du Sud-Est de la France. *Mém. Mus. Nat. Hist. Nat.*, C, **XXI**, pp. 43–377.

BOTOSENEANU, L., NEGREA, A., & NEGREA, S. (1967) Grottes du Banat explorées de 1960 à 1962. In: *Recherches sur les grottes du Banat et d'Olténie (Roumanie, 1959–1962)*, Ed. CNRS, Paris, pp. 25–226.

CONSTANTIN, S., & LAURITZEN, S-E. (1999) Speleothem datings in SW Romania. Part 1: Evidence for a continuous speleothem growth in Pestera Cloşani during Oxygen Isotope stages 5–3 and its paleoclimatic significance. *Theor. Appl. Karstology*, **11-12**, pp. 35–46.

CONSTANTIN, S., ONAC, B. P., FLEITMAN, D., & TAMAS, T. (2001) Past vegetation changes in karst areas as revealed by a comparative isotopic study of two Holocene speleothems from Romania. *IGCP 448 Newsletter*, Karst Dynamics Lab., Guilin, China, pp. 67–73.

CVIJIC, J. (1908) *Entwicklungsgeschichte des Eisernes Tores*. Pettermans Geogr. Mitteilungen, Ergänzungsheft 160, Gotha.

FORD, D. (1997) Dating and paleo-environmental studies of speleothems. In: *Cave minerals of the world* (HILL, C. & FORTI, P. *Eds*.), NSS, Huntsville, pp. 271–284.

GRUBIC, A (1994) Geological features of Carpatho-Balkanides mountain system. In: *Ground waters in carbonate rocks of the Carpathian-Balkan mountain range.* (Stevanovic, Z. & Filipovic, B. *Eds*.), Carpathian-Balkan Geological Ass., Belgrade, pp. 9-34.

GRUBIC, A & BERZA, T. *Eds.* (1997) *Geology of Djerdap area.* Intl. Symp. "Geology in the Danube Gorges", 23–26.09.1997, Geoinstitut, Spec. Publ. 25, Belgrade, 306 p.

HELLER, D. P. (1939) Die Bärenzähne aus den Ablagerungen der ehemaligen Neckarsschlinge bei Eberbach im Odenwald. *Sitzungberichte der Heidelberger Akad. zu Wiss.math-naturw. Kl*,7.

HELLER, D. P. (1949) *Ursus (Plionarctos) stehlini* Kretzoi, der Kleine Bär aus den altdeluvialen Sanden von Mauer–Bammental und Mainz–Wiesbaden. *S. Ber. Heidelberg Akad. Wiss. Math-Naturw. Kl.*, **11**, pp. 1–60.

JEANNEL, R., & RACOVITA, E. (1929) Enumération des grottes visitées. *Arch. Zool. Exper. Gener.*, 68, pp. 293–608.

KURTÉN, B. (1955) Sex dimorphism and size trends in the cave bear *Ursus spelaeus* Rosenmüller & Heinroth. *Acta Zool. Fenn.*, **90**, pp. 1–48.

KURTÉN, B (1958) Life and death of the Pleistocene cave bear. *Acta Zool. Fenn.*, **95**, pp. 1–95.

LAURITZEN, S.-E. (1993) *"Age4U2U". Program for reading ADCAM energy spectra, integration, peak-correction and calculation of 230Th/234U ages*. Department of Geology, Bergen Univ., 5000 lines.

LAURITZEN, S.-E., & ONAC, B. P. (1995) Uranium-series dating of some speleothems from Romania. *Theor. Appl. Karstology*, **8**, pp. 25–36.

LAURITZEN, S.-E., & ONAC, B. P. (1999) Isotopic stratigraphy of a last interglacial stalagmite from Northwestern Romania: correlation with deep-sea record and northern latitude speleothem. *J. Caves Karst Studies*, **61**, *1*, pp. 22–30.

LAURITZEN, S.-E., HURUM, J. & ALSTAD, J. (1997) Simple liquid-liquid extraction of U and Th in tracer amounts from phosphate matrix for dating purposes. *Chemical Geology* incl. *Isotope Geoscience*, **137**, pp. 265–271.

KOBY, F. E. (1952) Note sur main de l'Ursidé de Süssenborn, *Eclogae Helvetiae*, 45, 2.

LOWE, J. J. & WALKER, M., J. (1997) *Reconstructing quaternary environments*. 2nd Ed., Longman Asia Ltd., Hong Kong, 446 p.

MEIN, (1976) Résultats du groupe de travail des vertebrés. Biozonation du Néogène meditéranneén à partir des Mammifères. In *Report on Activity of RCMNS Working Group* (SENES, J. *Ed.*), pp. 78–81.

MUTIHAC, V. (1990) *Structura geologica a teritoriului Romaniei.* Ed. Tehnica, Bucuresti, 420 p.

NEGREA, A., & NEGREA, S. (1979) Peşterile din Defileul Dunării şi fauna terestră. In : *Speologia.* Gr. Cerc. Compl. "Portile de Fier". Seria Monografica. (ORGHIDAN, T. & NEGREA, S. *Eds*.), Ed. Academiei RSR, Bucuresti, pp. 30–75.

NEWTON, E., T. (1913) On the remains of *Ursus etruscus* (=*Ursus arvernensis*) from the Pliocene deposits of Tegelen sur Meuse. *Verhandlingen van het geologischming bonwunding genoot shap.*, Woord Nederland en Kolonien. Geolog. Série, Deeb, 1.

POSEA, G., ILIE, I., GRIGORE, M., & POPESCU, N. (1969) Defileul dunărean al Porţilor de Fier. Caracterizarea reliefului – Diviziunile morfologice. In: *Geografia văii Dunării româneşti.* (NICULESCU, G. *et al., Eds.*), Ed. Academiei RSR, Bucuresti, pp. 271–277.

POSEA, G., GRIGORE, M. & POPESCU, N. (1976) Treptele morfogenetice din zona Defileului Dunarii. In: *Geografia.* Gr. Cerç. Compl. "Portile de Fier". Seria Monografica (IANCU, M. *Ed*.), Ed. Academiei RSR, Bucuresti, pp. 60–66.

SAMSON, P., M., & RĂDULESCU, C. (1963) Les faunes mammalogiques du Pléistocène inférieur et moyen de Roumanie. *C.R. Acad. Sci. Paris*, **257**, pp. 1122–1124.

SCHMIDT, N, POVARĂ, I., & PETCU, A. (1968) Aspecte ale reliefului calcaros din sectorul Cazanelor Mari. *Comunicări de Geografie, Soc. St. Geogr. R.S.R.*, **VI**, pp. 27–35.

SCHREUDER, A. (1945) The Tegelen fauna, with a description of new remains of its rare components. pp. 133–204.

SCHWARCZ, H. P., & BLACWELL, B. A. (1992) Archaeological applications. In: *Uranium-series disequilibrium: Applications to Earth, Marine and Environmental Sciences.* (IVANOVICH, M., & HARMON, R. S., *Eds*.), Clarendon Press, Oxford, pp. 513–552.

SENCU, V. (1979) Carstul din Defileul Dunarii. In : *Speologia.* Gr. Cerc. Compl. "Portile de Fier". Seria Monografica. (ORGHIDAN, T. & NEGREA, S. *Eds.*), Ed. Academiei RSR, Bucuresti, pp. 11–29.

SÖRGEL, W. (1926) Der Bär von Süssenborn. *N. Jahrbuch für Mineralogie*, Beilage Band, LIV B.

VÂLSAN, G. (1918) Asupra trecerii Dunării prin Porţile de Fier. Studiu de geografie critică. *Bul. S.R.G.*, XXXVII, pp. 133–152.

ZAPFE, H. (1946) Die altpleistozänen Bären von Hundsheim in Niederösterreich. *Jahrbuch der Geologischen Bundesanstalt*, XLI, *3–4*.

Theoretical and Applied Karstology, 13–14 (2000–2001), pp. 51–56

The Carbonate Island Karst Model applied to Guam

John Mylroie[1] * & John Jenson[2]

[1] *Department of Geosciences, Mississippi State University, Mississippi State, MS 39762, USA.*

[2] *Water & Environmental Research Institute of the Western Pacific, University of Guam, Mangilao, Guam 96923, USA.*

Abstract

The karst of tropical carbonate islands is unique because: 1) fresh water–salt water mixing occurs at the base and margin of the fresh-water lens; 2) glacioeustasy has moved the freshwater lens up and down through a vertical range of over 100 m; and 3) the karst is *eogenetic*, *i.e.*, it has developed in young carbonate rocks that have never been buried beyond the range of meteoric diagenesis. Carbonate islands can be divided into three categories based on basement-sea level relationships: simple carbonate islands (no non-carbonate rocks), carbonate cover islands (non-carbonate rocks beneath a carbonate veneer), and composite islands (carbonate and non-carbonate rocks exposed on the surface). These ideas form the Carbonate Island Karst Model (CIKM) which can be visualized in terms of a three-dimensional framework, with island size on the x-axis, sea-level change on the y-axis, and bedrock relationships on the z-axis. On Guam, tectonic uplift and glacio-eustatic sea level change have produced a complex history on this composite island. The aquifer is partitioned in the subsurface by the antecedent topography of the volcanic core of the island, and lens discharge is both diffuse and conduit controlled.

Keywords: carbonate island karst, karst model, Guam.

Le modèle karstique d'une île carbonatée appliqué au Guam

Résumé

Le karst des îles tropicales carbonatées est unique parce que: (1) une zone de mélange d'eaux douces et salines se trouve à la base et aux bords de la zone lenticulaire d'eau douce; (2) la glacio-eustasie a provoqué une migration verticale de la lentille d'eau douce avec un écart de plus de 100 m et (3) le karst est eo-génétique, c'est-à-dire développé dans des roches carbonatées jeunes, qui n'ont jamais été enterrées en dessous de la zone de diagénèse météorique. Les îles carbonatées peuvent être divisées en trois catégories par rapport aux relations entre le soubassement et le niveau de la mer: îles carbonatées simples (pas de roches non-carbonatées), îles à couverture carbonatée (il y a des roches non-carbonatées en dessous d'une couverture carbonatée superficielle) et îles composites (des roches carbonatées et non-carbonatées apparaissent en surface). Ces idées forment le Modèle Karstique d'Ile Carbonatée qui peut être visualisée dans un modèle tridimensionnel comprenant les dimensions de l'île sur l'axe x, les variations du niveau de la mer sur l'axe y et les relations avec le soubasement sur l'axe z. Dans le Guam, le soulèvement tectonique et la variation glacio-eustatique du niveau de la mer sont les causes d'une histoire complexe de cette île composite. L'aquifère est partagé en souterrain par la topographie du noyau volcanique de l'île et sa décharge se fait tant de manière diffuse que par des conduites.

Mots clés: modèle d'île carbonatée, modèle karstique, Guam.

* corresponding author. *E-mail address*: Mylroie@DeanAS.MsState.Edu

Karst in carbonate islands

Tropical carbonate islands are a unique karst environment that differs significantly from that found in temperate continental interiors, where most cave and karst research has been done. The differences center on three factors (MYLROIE & VACHER, 1999): 1) freshwater/saltwater mixing occurs within the island freshwater lens; 2) glacioeustasy has moved the freshwater lens up and down through a vertical range of over 100 m; and 3) the karst is *eogenetic* i.e., it has developed in carbonate rocks that are young and have never been buried beyond the range of meteoric diagenesis. The outcome of the first factor is that enhanced dissolution by the mixed waters at the base and margin of the lens augments the enhanced dissolution at the lens surface by mixing of vadose and phreatic waters to modify the shape of the lens over time. The consequent increase in hydraulic conductivity in the rock permeated by the lens eventually results in a thinner lens. The second factor, glacio-eustatic variation of the lens position—and variation in the time during which the lens occupies any given position in the section—results in a complex variation of porosity and hydraulic conductivity over the section of carbonate bedrock. If later carbonates are added above or adjacent to the original units, the lens will be thicker in the younger carbonates than in the older ones, creating a significant departure from an idealized lens shape (VACHER, 1988). Along the margin of the lens, flow velocity increases and the mixing zones at the top and bottom of the lens converge to form *flank margin caves*, typically the largest voids observed on small carbonate islands (MYLROIE & CAREW, 1995). Flank margin caves are not true conduits, but mixing chambers.

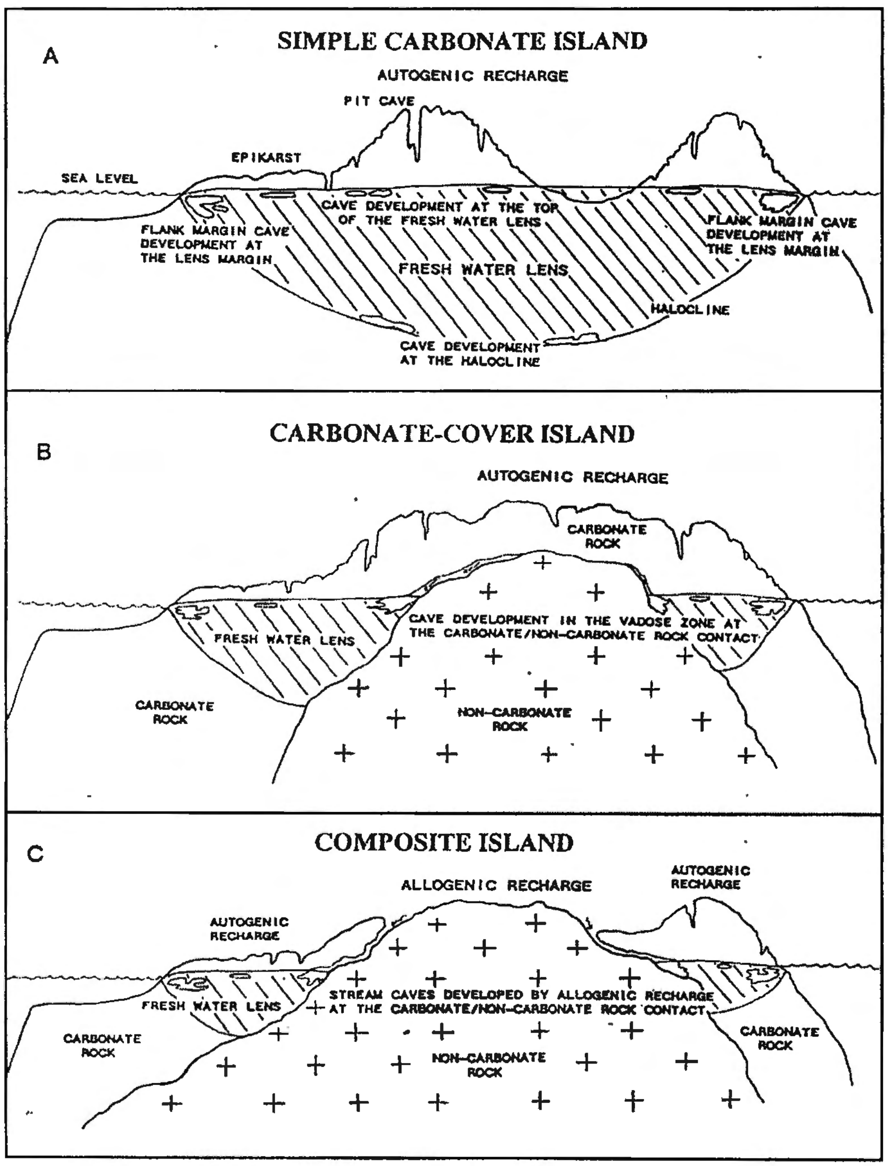

Fig. 1. Sea level and basement relationships for carbonate islands.
A. The *simple carbonate islands*, with no non-carbonate rock within the region of the fresh water lens.
B. The *carbonate-cover island*, where non-carbonate rock at depth can deflect vadose flow and distort the freshwater lens.
C. *Composite island*, where non-carbonate rock influences both surface and subsurface flow.

Relations entre le niveau de la mer et le fondement des îles carbonatés.
A. Ile simple carbonatée, *pas de roches non-carbonatées dans la zone de la lentille d'eau douce.*
B. Ile à couverture carbonatée; *les roches non-carbonatées du fondement peuvent dévier l'écoulement vadeux et déformer la lentille d'eau douce.*
C. Ile composite, *dont les roches non-carbonatées influencent tant l'écoulement de surface que l'écoulement souterrain.*

Their position with respect to the margin indicates former sea-level stillstands, and their size and spacing along the island margin are indicators of past flow conditions within the associated paleo-lens. The main consequence of the third factor *i.e.,* that the karst is eogenetic, is that progressive diagenesis everywhere throughout the young, highly porous carbonate results in a re-ordering of the host rock porosity. While the porosity remains constant or declines, it is rearranged into selected pathways that result in a much higher hydraulic conductivity (MYLROIE &VACHER, 1999). Karst development can also be influenced by the nature of the depositional environment of the carbonate rock, which can vary from eolian to lagoonal, shoal or reef. Variations in island size create differences in catchment and lens volume/island perimeter ratios that appear to inhibit conduit development in small carbonate islands but favor it in larger ones (MYLROIE & VACHER, 1999). As a result of these differences, plus the effects of salt water-fresh water mixing, sea level change, and eogenetic evolution of the karst, carbonate islands contain karst features and caves remarkably different from the typical fluvial karst formed in dense Paleozoic and Mesozoic carbonates of continental interiors.

Sea level-basement relationships

The three factors cited above are common to all carbonate islands, and produce karst features exhibited by all of them. Carbonate islands can be subdivided into three categories (Fig. 1) based on the relationship between the sea level and the carbonate-basement contact (MYLROIE & CAREW, 1997; 2000, MYLROIE & VACHER, 1999). The sea level-basement relationship has profound implications for the evolution of karst features. *Simple carbonate islands* have no non-carbonate rocks exposed at the surface or stratigraphically positioned within the range of glacioeustasy. *Carbonate cover islands* have non-carbonate rocks beneath a carbonate veneer, and the contact between them is within the position of the freshwater lens for all or part of a glacioeustatic cycle. *Composite islands* (VACHER, 1997) contain carbonate and non-carbonate rocks exposed on the surface. In carbonate cover islands, vadose waters infiltrating downward are shunted along the carbonate-basement contact, producing stream caves that carry water to the lens and/or sea level. In composite islands, this process is augmented by the development of sinks and insurgences at the surface expression of the carbonate-basement contact, which capture surface waters as well. In the phreatic zone of carbonate cover and composite islands, the lens can be subdivided into the *basal zone*, where the base of the freshwater forms the transition zone to the underlying marine water, and the *parabasal zone*, where the base of the fresh water rests on basement rock (MINK & VACHER, 1997). The parabasal zone is the zone of choice for groundwater development on carbonate islands because wells placed in the parabasal zone are relatively immune to lateral intrusion or upconing of marine waters.

Surface features

The surface of carbonate islands contains a characteristic epikarst, which differs from that in typical continental settings mostly as a result of the youthful age of the carbonates and the pervasive presence of salt spray, which collects on the rock surfaces and mixes with meteoric water to create a distinctive etching pattern. In the absence of allogenic catchments on adjacent non-carbonate terrain, sinking streams, blind valleys, and springs are rarely found. Closed depressions are common, but many represent constructional features produced by initial depositional variation, or subsequent tectonics. In such cases, the depressions, while internally drained by dissolution pathways, have not had the majority of their volume created by dissolutional excavation. Vadose flow along the contact between the carbonate and non-carbonate base on carbonate cover and composite islands, however, can undercut the overlying carbonate, producing large collapse voids that may prograde to the surface, as observed on Bermuda (MYLROIE *et al.*, 1995).

The Carbonate Island Karst Model

The variability of the initial carbonate depositional environment (e.g. reef, shoal, lagoon), the differential dissolution and diagenesis these rocks have undergone, and the relationship between carbonate and non-carbonate rocks thus combine to profoundly modify the classic Ghyben-Herzberg-Dupuit model of the freshwater lens of ideal islands. To provide an appropriate systematic geologic model, we seek to synthesize these characteristic features into a coherent framework, which we have labeled the Carbonate Island Karst Model (CIKM) (MYLROIE *et al.*, 2001). The model is summarized schematically in Figure 2. It provides the basis for accurate aquifer conceptual models for hydrologists working on water resource development, or for other engineering applications on carbonate islands. The initial research for the CIKM began in the Bahamas and Bermuda, simplistic carbonate and carbonate cover islands, respectively, in tectonically stable settings. Work progressed to Isla de Mona, Puerto Rico, a simple carbonate island that has been tectonically uplifted. The research has been extended to the island of Guam, a composite island in the western Pacific with a complex tectonic history. It is important to recognize that carbonate islands do not always fall into distinct categories, but may contain a range of characteristics that blend many island conditions, as shown below.

Guam and the Carbonate Island Karst Model

Guam was selected to apply insights gained in the Atlantic-Caribbean province to a Pacific location, while also incorporating the additional complexity of the island to extend and

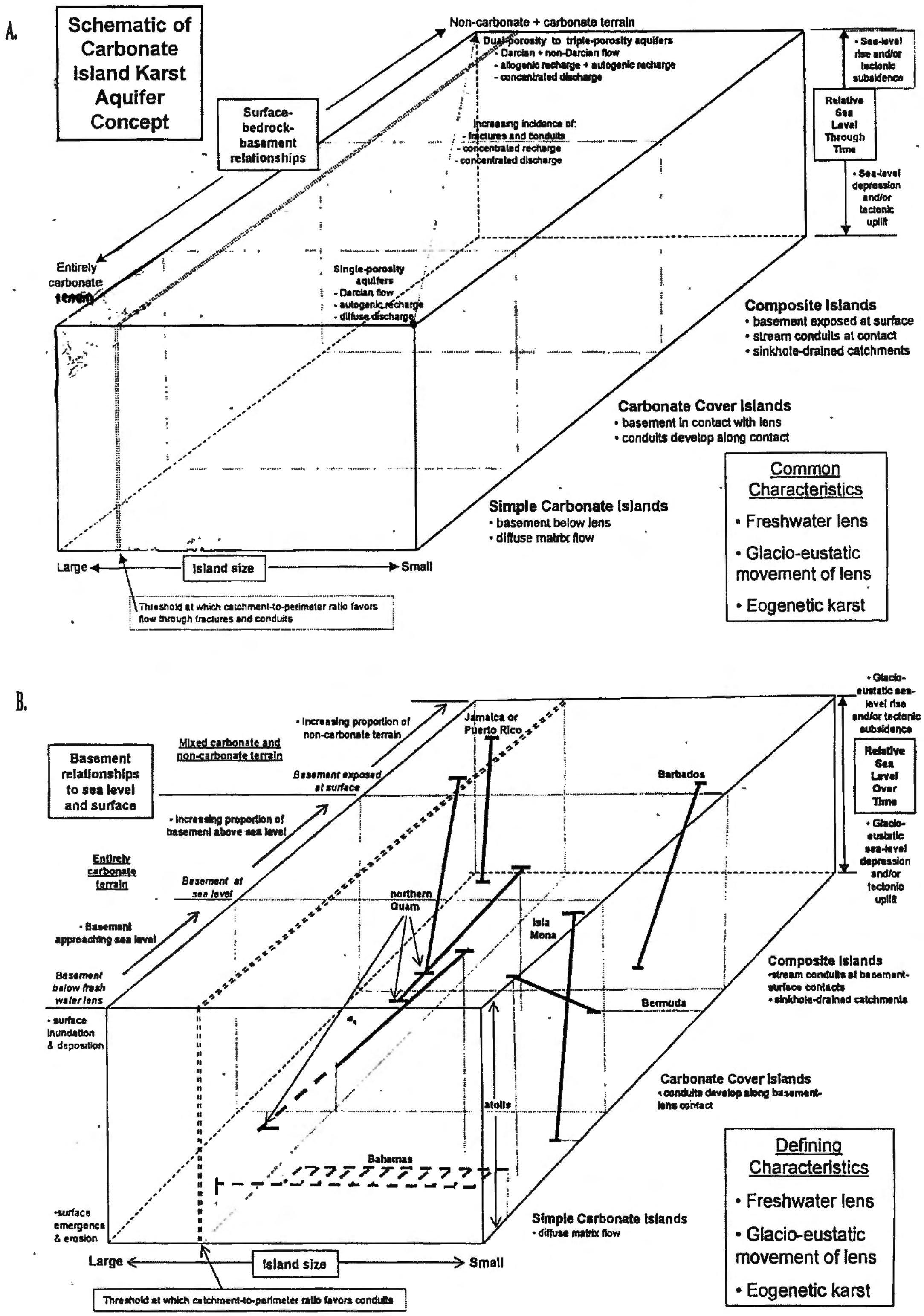

Fig. 2. A. Schematic diagram of the Carbonate Island Karst Model (CIKM). Any island karst should fall somewhere in the three-dimensional field presented here. See text for a discussion of terms and concepts shown in the schematic. B. Placement of sample islands within the field of the CIKM demonstrates how changes in island size, lens discharge, and island category occur when sea level varies.

A. Diagramme schématisé du Modèle Karstique d'une Ile Carbonatée (CIKM). Toute île karstique doit se retrouver dans la représentation tridimensionnelle présentée. Voir le texte pour une discussion sur les termes et les concepts présentés. B. Les positions des quelques îles dans le cadre du modèle CIKM démontrent les changements de la dimension de l'île, de la décharge de la lentille d'eau douce et de la catégorie de l'île par suite des oscillations du niveau de la mer.

refine the CIKM. Guam is a dual island—the southern half is volcanic with a few carbonate outliers, the northern half is carbonate with a few volcanic inliers. The carbonates are young, ranging in age from Miocene to Holocene. Tectonic uplift has been continuous in the Quaternary, overprinting the glacioeustatic sea level record and imposing a complex structural grain (joint and fault orientations) on the limestone units.

Guam displays features from each of the three subdivisions of carbonate islands described in the previous section. The northern half is mostly carbonate, with attributes of a simple carbonate island over about 80% of its surface area, where the limestone bedrock extends down to well below sea level. Beneath the other 20% of the surface, however, the volcanic basement lies well above sea level, as in the carbonate cover model. At two locations the basement extends to the surface, rising above the northern Plateau to give it attributes of a composite island. The southern half of Guam is uplifted volcanic terrain upon which lies remnants of once extensive reef-lagoonal limestones and occasional fragments of older shallow-water carbonate deposits that were incorporated into the younger volcanic units (Tracey *et al.*, 1964). In all cases except a few on the eastern coast, the base of the southern carbonate rocks is elevated above modern sea level. Such a position removes them from the direct influence of glacio-eustacy, and from the dissolution effects of fresh and marine water mixing. The karst of southern Guam is thus more analogous to larger islands such as Puerto Rico and Jamaica, where the interior carbonates produce caves and karst landforms similar to those in tropical continental settings. The diversity of karst environments on Guam has thus produced an especially wide variety of karst landforms and cave development, ranging from features characteristic of the simplest islands to features resembling continental landforms.

Lens discharge is mainly by diffuse flow, modified by porosity re-arrangement as diagenesis creates high-conductivity pathways in the rock occupied by the lens. Joints and faults appear important in developing these high-conductivity pathways (Jenson *et al.*, 1997). Given that glacio-eustatic lowstands have occurred several times during the Pleistocene and that the entire Pleistocene section has been raised above sea level on northern Guam, it is likely that a considerable span of the carbonate section now below sea level was in the vadose zone long enough for stream caves to have developed along the carbonate-basement contact. The hydrological implications of the vadose flow paths that formed during sea-level lowstands, and which now are partially embedded in the lens of the parabasal zone, are uncertain at this point. Several levels of terraces and horizontal grooves in the cliff faces indicate episodes of relative sea-level stillstands in the exposed subaereal section. In recent field work, we have observed that these horizons also exhibit widespread development of moderate-sized flank margin caves. The caves show clear evidence of re-invasion by chemically aggressive waters, another result of lens migration and overprinting following the interplay of tectonics and glacio-eustasy. Guam contains a bewildering variety of caves, karst features, and water flow pathways that defy existing simple island or continental models (Mylroie *et al.*, 2001). The CIKM, however, provides a common framework for uniting the geology and hydrology of this island into a single picture.

References

Jenson, J. W., Jocson, J. M. U., & Siegrist, H. G. (1997) Groundwater discharge styles from an uplifted Pleistocene island karst aquifer, Guam, Mariana Islands. In: *The Engineering Geology and Hydrology of Karst Terranes* (Beck, B. F., & Stephenson, J. B., *Eds.*), Balkema, Springfield, Missouri, pp. 15–19.

Mink, J. F., & Vacher, H. L. (1997) Hydrogeology of northern Guam. In: *Geology and Hydrogeology of Carbonate Islands. Developments in Sedimentology 54* (Vacher, H. L., & Quinn, T., *Eds.*), Elsevier Science, Amsterdam, pp. 743–761.

Mylroie, J. E., & Carew, J. L. (1995) Chapter 3: Karst development on carbonate islands. In: *Unconformities and Porosity in Carbonate Strata* (Budd, D. A., Harris, P. M., & Saller, A., *Eds.*), Vol. Mem. **63**, Am. Ass. of Petroleum Geologists, pp. 55–76.

Mylroie, J. E., & Carew, J. L. (1997) Land use and carbonate island karst. In: *The Engineering Geology and Hydrogeology of Karst Terranes* (Beck, B. F., & Stephenson, J. B., *Eds.*), Balkema, Rotterdam, pp. 3–12.

Mylroie, J. E., & Vacher, H. L. (1999) A conceptual view of carbonate island karst. In: *Karst Modeling Symposium: Charlottesville, VA* (Palmer, A. N., Palmer, M. V., & Sasowsky, I. D., *Eds.*) p. 48–58.

Mylroie, J. E., & Carew, J. L. (2000) Speleogenesis in young limestones in coastal and oceanic settings. In: *Speleogenesis: Evolution of Karst Aquifers* (Klimchouk, A. B., Ford, D. C., Palmer, A. N., & Dreybrodt, W., *Eds.*), NSS, Huntsville, AL, pp. 226–233.

Mylroie, J. E., Carew, J. L., & Vacher, H. L. (1995) Karst development in the Bahamas and Bermuda. In: *Terrestrial and Shallow Marine Geology of the Bahamas and Bermuda* (Curran, H. A., & White, B., *Eds.*) Vol. Geol. Soc. of America Special Paper **300**, pp. 251–267.

Mylroie, J. E., Jenson, J. W., Jocson, J. M. U., & Lander, M. (1999) Karst Geology and Hydrology of Guam: A Preliminary Report: Mangilao. *Water & Environmental Research Institute of the Western Pacific, University of Guam, Technical Report* No. **89**, 32 p.

Mylroie, J. E., Jenson, J. W., Taborosi, D., Jocson, J. M. U., Vann, D. T., & Wexel, C. (2001) Karst features in Guam in terms of a general model of carbonate island karst. *J. of Caves and Karst Studies*, **63**, *1*, pp. 9–22.

Tracey, J., I., Jr., Schlanger, S., O., Stark, J., T., Doan, D., B., & May, H., G. (1964) *General Geology of Guam*. U.S. Geological Survey Professional Paper 403-A, US Government Printing Office, Washington, D.C., 104 p.

Vacher, H. L. (1988) Dupuit-Ghyben-Herzberg analysis of strip-island lenses. *Geological Society of America Bulletin*, **100**, pp. 850–591.

Vacher, H. L. (1997) Introduction: Varieties of carbonate islands and a historical perspective. In: *Geology and hydrogeology of carbonate islands* (Vacher, H. L., & Quinn, T. M., *Eds*.), Volume Developments in Sedimentology 54, Elsevier, pp. 1–33.

Theoretical and Applied Karstology, 13–14 (2000–2001), pp. 57–65

Karst genetic model for the French Bay Breccia deposits, San Salvador, Bahamas

Lee Florea[1*], John Mylroie[2], & Jim Carew[3]

[1] *Kentucky Cabinet for Natural Resources, Frankfort, KY 40601, USA*
[2] *Department of Geosciences, Mississippi State University, Mississippi State, MS 39762, USA*
[3] *Department of Geology, University of Charleston, Charleston, SC 29424, USA*

Abstract

On the Island of San Salvador in the Bahama archipelago 30 breccia deposits can be found along the French Bay sea cliffs on the southeastern coast of the island. Breccia deposits of this type have not been observed on any other location on the island. These deposits have traditionally been interpreted as paleo-talus deposits from an eroding sea cliff formed on a transgressive eolianite deposited at the start of the oxygen isotope substage 5e sea-level highstand (ca. 125,000 years before present). New evidence supports a karst genesis. A survey of several deposits revealed a vertical restriction of +2 to +7 meters above sea level consistent with flank margin caves developed during the substage 5e still-stand. The morphologies of the features were found to be globular and contain distinct caliche boundaries, overhung lips, and smooth undulating bases. Petrographic results support a model in which voids are created and then infilled with a soil breccia. It can be concluded from these results that the deposits reflect qualities of a lithified soil breccia filling in breached flank margin caves.

Keywords: karst breccia, paleokarst, San Salvador.

Modèle génétique karstique des dépôts de French Bay Breccia, San Salvador, Bahamas

Résumé

Sur l'île de San Salvador (archipel de Bahamas) on a trouvé 30 dépôts de brèches situés le long de la côte de French Bay, dans la partie sud de l'île. Ces dépôts ont été traditionnellement interprétés comme des dépôts de paléo-talus d'une ancienne falaise marine, formés sur des éolianites transgressives qui ont été déposées au début du stage isotopique 5-e (haute mer). Les nouvelles données indiquent une genèse karstique. L'étude de quelques dépôts a révélé une disposition verticale restreinte de +2 jusqu'à +7 m au-dessus du niveau de la mer, correspondant aux grottes de flanc marginal développées durant le stage 5-e. La morphologie des formations est globulaire et inclut des horizons de caliches et des bases légèrement ondulées. L'analyse pétrographique suggère que les cavités ont été remplies d'une brèche terrigène. On conclut que ces dépôts représentent une brèche terrigène lithifiée qui a rempli des cavités de flanc marginal.

Mots-clés: brèche karstique, paléokarst, San Salvador.

Introduction

San Salvador Island is located in the eastern portion of the 1000 km Bahamian Archipelago (Fig. 1). The size of the island is relatively small: roughly 12 km wide by 19 km long (Fig. 2). All rocks exposed on San Salvador are Pleistocene and Holocene carbonates. The geologic record is dominated by subtidal facies at low elevations, and eolianites at higher elevations; the result of cyclic changes in the glacio-eustatic sea level. This produced cycles of carbonate deposition, during sea level high stands, and erosion, during sea level lowstands. Several of these sequences are apparent on the island, but only the sea level associated with the oxygen isotope substage 5e still-stand (125,000 BP) was high enough for marine facies to remain subareal in modern sea level conditions (Carew & Mylroie, 1994; 1997).

* corresponding author. *E-mail address*: mr_chaos@hotmail.com

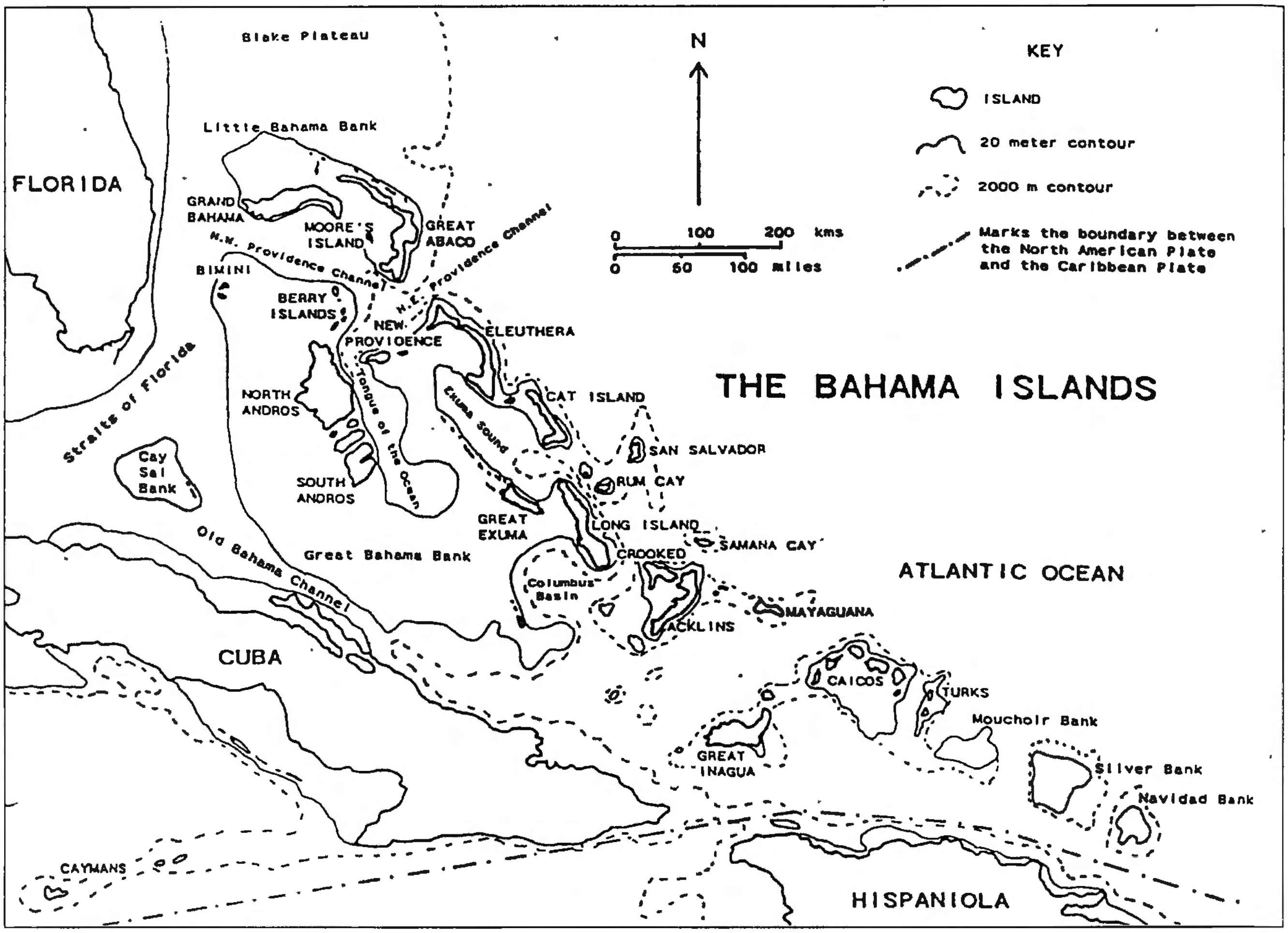

Fig. 1. The Bahama Islands (from CAREW & MYLROIE, 1994). *Les îles Bahamas (d'après CAREW & MYLROIE, 1994).*

The island is highly karstified with several morphologic manifestations of karst features. Inland pits, blue holes, karren of various forms, and caves are several types of karst features identified. Paleo-karst features are also present on the island in the form of infilled dissolution pockets, "palmetto stumps" (CAREW & MYLROIE, 1994), notches (MYLROIE & CAREW, 1991; REECE *et al.*, 2000), and breccia deposits (MARSHALL, *et al.*, 1984; FLOREA *et al.*, 2000).

On San Salvador, 30 breccia deposits can be found along more than 1km length of sea cliffs in French Bay (Fig. 2 and 3). Breccia deposits of this type have not been observed at any other location on the island. Similar breccia facies have been recognized within caves on other carbonate islands such as the Cayman Islands (JONES & SMITH, 1988), Isla de Mona (MYLROIE & CAREW 1995), and New Providence Island in the Bahamas (MYLROIE *et al.*, 1991). The deposits on San Salvador occur in Late Pleistocene carbonates of the French Bay Member of the Grotto Beach Formation.

The breccia deposits in French Bay consist of angular blocks of laminar-bedded oosparites ranging from 1 cm to more than 1 m in size within a red micritic matrix. This description indicates the deposits are soil breccias and distinguishes them from coastal breccias or back-beach rubble. Coastal breccia facies contain more rounded clasts as a result of continuous wave attack and contain a white sand matrix as opposed to a red (paleosol) matrix. The French Bay breccia deposits range from matrix to clast supported, and occur as promontories due to the more resistant nature of the paleosol matrix.

These deposits have traditionally been interpreted as paleotalus deposits from an eroding sea cliff of oxygen isotope substage 5e transgressive dune deposits ca. 125,000 years ago (French Bay Member of CAREW & MYLROIE, 1985). In this theory a substage 5e transgressive dune was eroded to produce sea cliffs during the substage 5e sea level maximum. When sea level fell at the end of the 5e substage, the sea cliff became an inland scarp; the resulting inland scarp underwent erosion and collapse producing cliff-base talus slope. Over time this talus lithified to produce a paleotalus associated with the surrounding solution pockets and paleosol. Recent rise in sea level has renewed coastal erosion on these paleotalus deposits producing the modern day distribution and location of this facies.

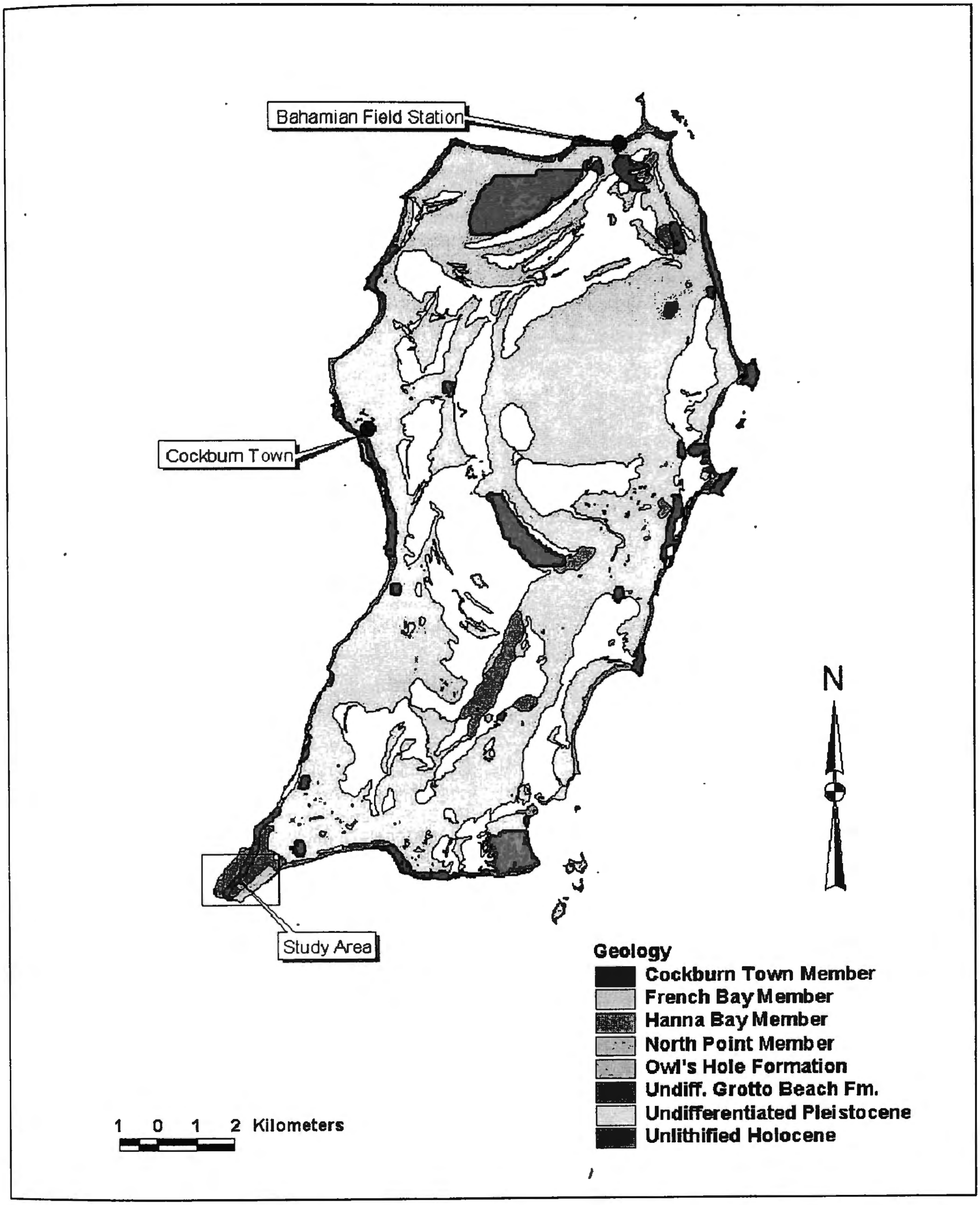

Fig. 2. Map of San Salvador with location of study area (data from ROBINSON & DAVIS, 1999).
Carte de San Salvador avec la situation de la zone étudiée (données extraites de ROBINSON & DAVIS, 1999).

Fig. 3. Breccia deposit on French Bay sea cliff.
Dépôts de brèche de la falaise de French Bay.

An alternative explanation for the development and distribution of the breccia deposits can be derived from the theory of flank margin cave development. Fresh water entering the groundwater system through precipitation floats on the saltwater as a lens thinnest near the discharge at the margins of the island and thickest where the recharge is maximum. Both the fresh and the saline water quickly become saturated with respect to calcite in a carbonate island environment. Mixing of fresh and saline water along the base of this lens produces a solution with renewed dissolution capabilities (PLUMMER, 1975). Thus, karst features tend to develop along this interface.

The thinning of the fresh-water lens near the discharge at the island margins increases the velocity of water due to a reduction in cross-sectional area. This increase in velocity combined with the intersection of the upper and lower mixing surfaces of the lens promote maximum dissolution potential (SANFORD & KONIKOW, 1989; MYLROIE & CAREW, 1988; 1990). In the Bahamas, the freshwater lens tends to be thickest in eolianite ridges and discharges along the flanks of these ridges. The caves associated with this dissolution process have been termed flank margin caves (MYLROIE & CAREW, 1990).

The morphology of flank margin caves reflects the manner in which they were formed. These caves are mixing chambers not conduits; therefore are formed independent of surface conditions, or hypogenic (PALMER, 1991). They contain large globular chambers with concave dissolution surfaces connected to others by narrow windows or not connected at all, have undulating ceilings and floors, and are vertically restricted. Because these voids form along the flanks of eolianite dunes, they tend to be clustered like "beads on a string" (VOGEL *et al.*, 1990).

If the French Bay breccia deposits were indeed the result of karst processes, several indicators would be present. The deposits would be distributed along a linear trend parallel to the paleocoastline. The deposit morphologies would reflect a void history by being globular with undulating bases and overhung lips. The deposits would appear as a sequence similar to "beads on a string." The boundary between the country rock and the breccia would be distinct and could include altered wall rock or stalagmitic material (flowstone).

The intent of this study was to characterize several of the deposits with field reconnaissance, accurate survey and morphology, photographic documentation, and petrographic analysis. From this, a conclusion of non-karstic or karstic genesis would be made. Finally, a new sequence of formation would be developed based on the results obtained.

Methods

A January 2000 survey was conducted of seven breccia deposits along the northeast section of the French Bay sea cliffs using fiberglass tape and *Suunto* compass and inclinometer (Fig. 3). Several survey transects were run across each of these seven breccia deposits and all seven deposits were linked by survey. On larger deposits, profile transects were taken to help in the characterization. Solution pockets and other features of interest proximal to the deposits were tied in to the survey to aid in mapping and the interpretation. A cartographic quality map of the surveyed deposits was generated and tied in to the 1984 MARSHALL *et al.* survey of the deposit locations (portion of map displayed in Figure 4). This map was georeferenced on ArcView and overlaid onto the topographic map of the island (provided by ROBINSON & DAVIS, 1999).

To support the breccia survey, a field investigation was conducted of various locations of geologic or hydrologic significance on San Salvador Island. Several karst features were visited and explored including several of the well-known flank margin caves (CAREW & MYLROIE, 1994; MYLROIE & CAREW; 1994). Stops were made at locations containing coastal and soil breccia facies. In addition, stops were made at sites of active cave collapse in the island interior and talus slope development.

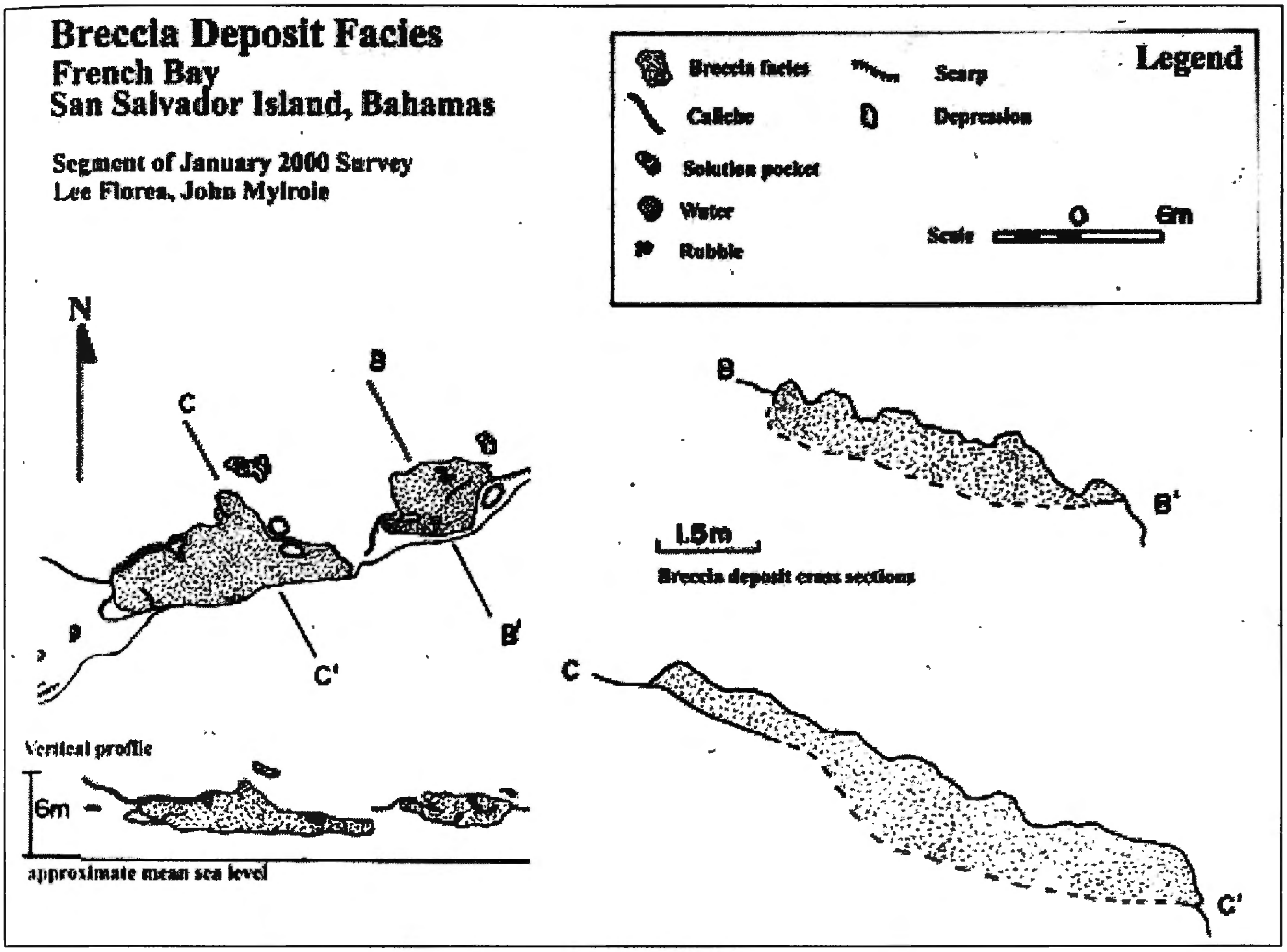

Fig. 4. Partial map of January 2000 breccia survey. *Carte partielle de la brèche relevée en Janvier 2000.*

Four samples were taken from one of the larger breccia deposits to use in petrographic analysis. These samples included: a sample from the country rock near the deposit, a sample from a clast contained within the deposit, a sample of the matrix, and a sample of the caliche boundary separating the deposit from the country rock. Thin sections were made from these samples at the University of Kentucky Department of Geology, and the analysis was performed using a petrographic microscope at the Kentucky Geological Survey.

Results

The survey of the breccia deposits revealed a vertical restriction in development of +2 to +7 meters above sea level (Fig. 4). Nearby solution features such as infilled solution pockets, "palmetto stumps" (Carew & Mylroie, 1994), and stalagmitic material (flowstone) in open phreatic pockets range from approximately +5 to +10 meters above sea level.

The deposit morphologies are globular, with undulating bases (Fig. 4). These boundaries are distinct and in some locations present a thick caliche layer separating them from the country rock and cross cutting structure (Fig. 5). The inland boundaries of the deposits have detectable overhung lips in locations. The distribution of the deposits themselves is random, yet do follow a "bead on a string" description typically associated with flank margin caves (Vogel *et al.*, 1990).

Petrographic analysis of the deposits revealed that the breccia clasts and the country rock are indistinguishable and are laminar-bedded oosparites, confirming previous results (Marshall *et al.*, 1984). Both country rock and clasts display evidence of dissolution activity such as partially dissolved ooids and vug development. Both also contain sparry cements of two generations: a first generation equant isopachous calcite and a calcite meniscus druse (Fig. 6).

Petrography of the matrix shows it to be unstructured and contain copious amounts of fine particulate detritus of Saharan origin (Muhs *et al.*, 1990) within a micritic calcite cement. The matrix also contains a large number of modified ooids weathered out of the original rock and occasional

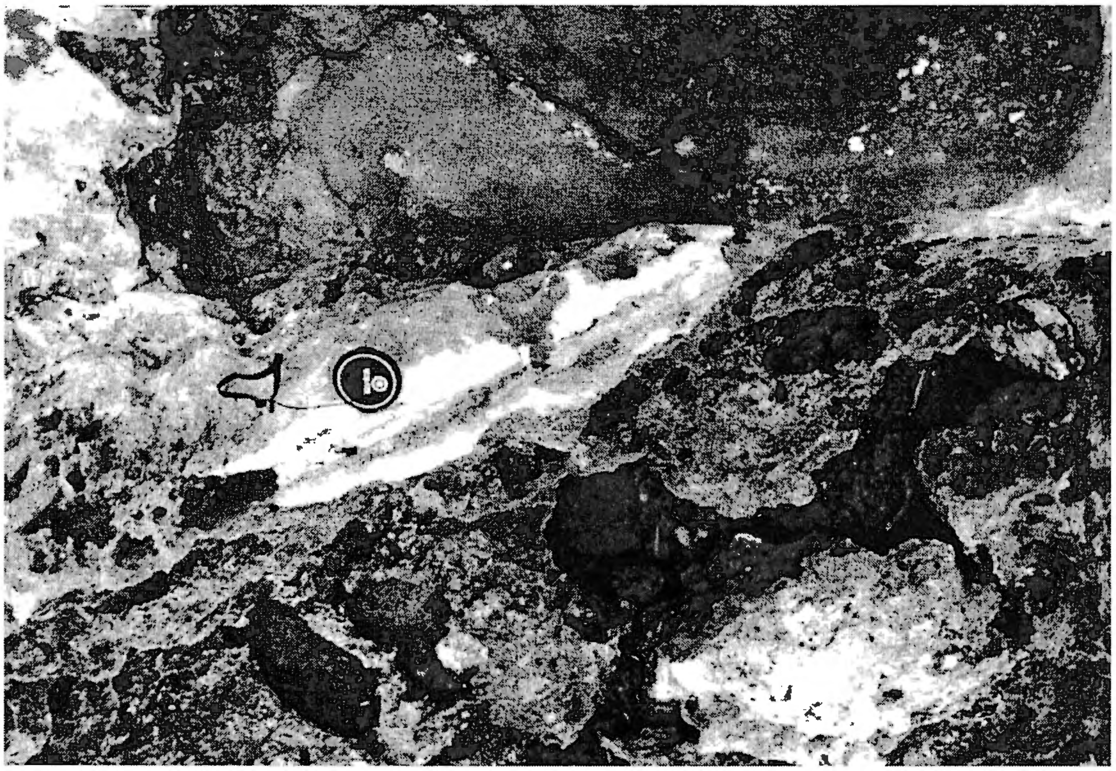

Fig. 5. Photograph of caliche boundary separating country rock (top) from breccia (bottom).
Limite de caliche séparant la roche calcaire en haut de la brèche en bas.

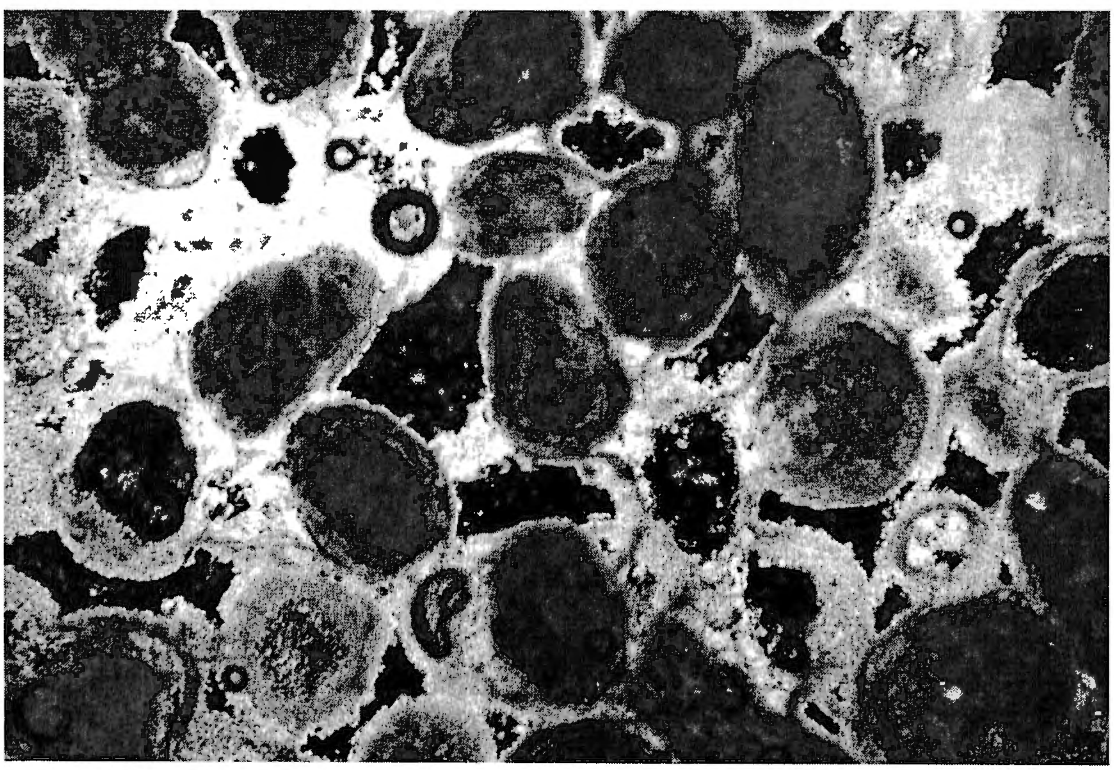

Fig. 6. Petrographic slide of clast material from breccia. Note dissolved ooids and two generations of calcite cement.
Photographie du matériel clastique de la brèche en lame mince. A noter les ooïdes dissous et les deux générations de ciment calcitique.

biolithic fragments. Voids within the matrix contain aragonite fibers. The caliche boundary is structured, displaying prominent layering and consisting primarily of layered micritic calcite with some fine particulate Saharan detritus (Fig. 7). Voids within the caliche contain a calcite meniscus druse of vadose origin and whisker calcite cement commonly found in Bahamian cave walls (VOGEL *et al.*, 1990).

Discussion

The vertical restriction of the deposits supports a karstic genesis. In the flank margin theory of cave development, the highest rates of dissolution are proximal to the shore at the intersection of the halocline and the water table. The elevations of the breccia deposits, +2 to +7 meters above sea level (Fig.4), are consistent with other flank margin caves on in the Bahamas that formed in response to the substage 5e sea level stillstand (MYLROIE & CAREW, 1990).

The presence of nearby paleosol features and stalagmitic material indicates dissolution activity at approximately the same time as the breccia formation. The elevations of these nearby solution features, +5 to +10 meters above sea level, indicate the presence of a paleo land surface at the breccia deposit elevation to a few meters above the breccia deposits (Fig. 4).

Petrography of the country rock and clasts show dissolution has occurred (Fig. 6). The first generation equant isopachous calcite is consistent with a fresh phreatic cementation zone (HARRIS *et al.*, 1985) that would have been deposited during void formation. The second-generation calcite meniscus druse would have been deposited in a vadose groundwater environment after sea level had fallen. The presence and structure of the caliche boundary layer supports a two-phase origin for the breccia deposits (Fig. 7): a void development phase in which the caliche is deposited as a secondary calcite deposit such as stalagmitic material or through biologically enhanced micritization (BATHURST, 1975), and a second collapse phase in which the void is filled with a proto-breccia.

What this evidence suggests is that the French Bay breccia deposits were formed through karstic processes. This does not eliminate talus from being a component of their formation. In fact, it is likely that talus generated from slope retreat processes is a portion of the material that filled these breached flank margin caves. This process can be observed today occurring on the other side of Sandy Point at Altar Cave (CAREW & MYLROIE, 1994).

Conclusions

The survey results as well as comparisons to morphologies of present day flank margin caves and sites of active talus formation show that the breccia deposits reflect qualities of a

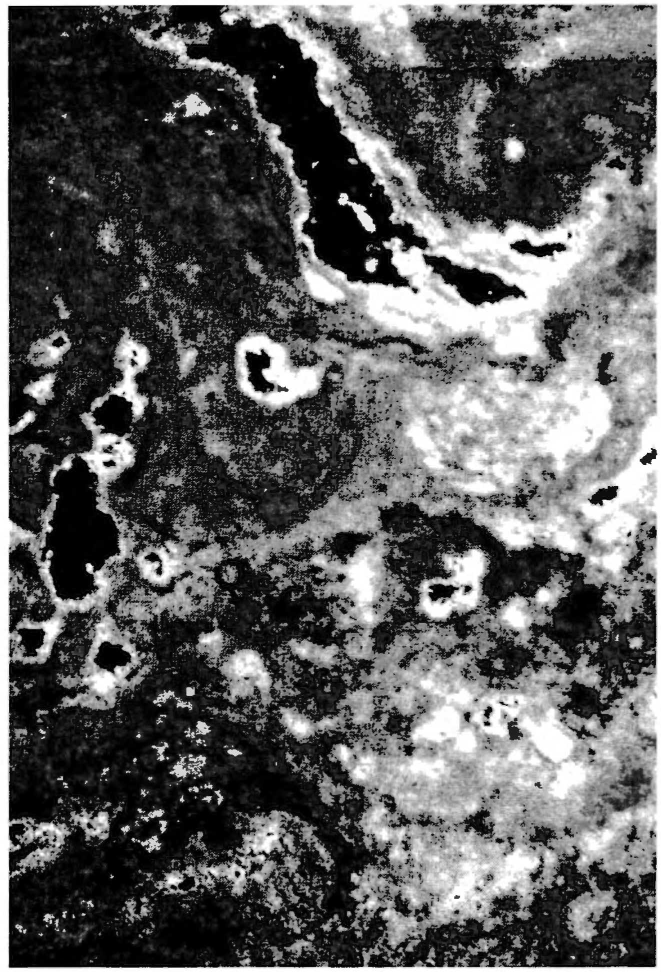

Fig. 7. Petrographic slide of caliche material (country rock direction is toward bottom). Note layered micritic calcite. *Photographie de la bordure de caliche en lame mince (la roche calcaire vers le bas). A noter la calcite micritique stratifiée.*

soil breccia filling in breached flank margin caves. These results combined with the petrography suggest the following sequence of events (Fig. 8):

1. A transgressive oolitic eolianite is deposited during the transgression of an oxygen isotope substage 5e highstand (CAREW & MYLROIE, 1985), approximately 130,000 years ago.
2. A raise in sea level during the substage 5e maximum cemented the eolianite and initiated dissolution along the halocline/water table interface, approximately 125,000 years ago.
3. Voids of significant size were produced in a short time span along the flank margin of this deposit (MYLROIE & CAREW, 1990).

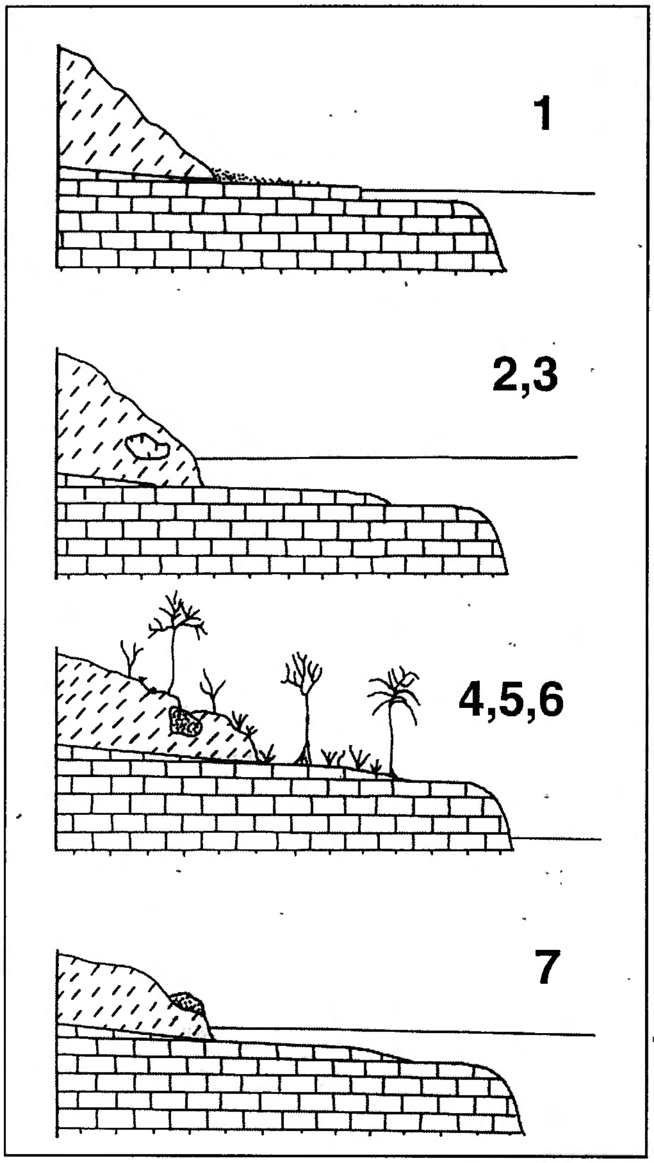

Fig. 8. Modified sequence of breccia development.
Phases de développement de la brèche.

4. After sea level withdraw at the end of substage 5e 120,000 years ago, these voids were exposed to vadose conditions and secondary modification occurred. Precipitation of calcite on the void wall developed a layer of stalagmitic material, and biologic activity enhanced micritization of the wall rock.

5. Denudation of the land surface eventually intersected the voids. Soil and ceiling collapse collected on the floor of the voids creating a thick layer of proto-breccia.

6. Vadose recharge lithified the proto-breccia into the present day deposit.

7. Continued erosion has stripped the remaining overlying country rock and has left the deposits standing in positive relief along the French Bay sea cliffs.

References

BATHURST, R. G. C. (1975) *Carbonate sediments and their diagenesis: Developments in sedimentology*, **12**, Elsevier, New York, 658 p.

CAREW, J. L., & MYLROIE, J. E. (1985) The Pleistocene and Holocene Stratigraphy of San Salvador Island, Bahamas, with Reference to Marine and Terrestrial Lithofacies at French Bay. In: *Pleistocene and Holocene carbonate environments on San Salvador Island, Bahamas* (CURRAN, H. A., *Ed.*), Guidebook for Geological Society of America, Orlando annual meeting field trip, pp. 11-61.

CAREW, J. L., & MYLROIE, J. E. (1994) *Geology and Karst of San Salvador Island, Bahamas: A Field Trip Guidebook*, Bahamian Field Station, 32 p.

FLOREA, L. J., MYLROIE, J. E., & CAREW, J. L. (2000) French Bay Breccia Deposits. San Salvador, Bahamas: Evidence for Karst Genesis In: *Karst Studies and Problems: 2000 and Beyond*, Proc. Joint meeting of Friends of Karst, Theor. & Applied Karstology, and IGCP 448, Presa Universitara Clujeană, pp. 44–48.

HARRIS, P. M., KENDALL, C. G. St. C., & LERCHE, I. (1985) Carbonate cementation – A brief review. In: *Carbonate cements* (SCHNEIDERMANN, N., & HARRIS, P. M., *Eds.*), Soc. of Economic Paleontologists and Mineraloligists Sp. Publ. **36**, 379 p.

JONES, B., & SMITH, D. S. (1988) Open and filled karst features on the Cayman Islands: Implications for the recognition of paleokarst. *Canadian Journal of Earth Sciences*, **25**, p. 1277–1291.

MARSHALL, P. E., RASOR, D., LAWSON, C., DECHENE, J. L., CAREW, G., SCHORR, C., & MYLROIE, J. (1984) Investigation of Breccia Facies, San Salvador, Bahamas (*abstract*), *Bull. of the South Carolina Academy of Science*, **46**, p. 109.

MUHS, D. R., BUSH, C. A., STEWART, K. C., ROWLAND, T. R., & CRITTENDEN, R. C. (1990) Geochemical evidence of Saharan dust parent material for soils developed on Quaternary limestones of Caribbean and western Atlantic islands. *Quaternary Research*, **33**, pp. 157–177.

MYLROIE, J. E., & CAREW, J. L. (1988) Solution Conduits as Indicators of Late Quaternary Sea Level Position. *Quaternary Science Reviews*, **7**, pp. 55–64.

MYLROIE, J. E., & CAREW, J. L. (1990) The Flank Margin Model for Dissolution Cave Development in Carbonate Platforms. *Earth Surface Processes and Landforms*, **15**, pp. 413–424.

MYLROIE, J. E., & CAREW, J. L. (1991) Erosional notches in Bahamian carbonates: Bioerosion or groundwater dissolution? In: Proc. Fifth Symposium on the Geology of the Bahamas (BAIN, R. J., *Ed.*), Port Charlotte, Florida, Bahamian Field Station, pp. 185–191.

MYLROIE, J. E., & CAREW, J. L. (1994) *A Field Trip GuideBook of Lighthouse Cave, San Salvador Island, Bahamas*. Bahamian Field Station, 10 p.

MYLROIE, J. E., & CAREW, J. L. (1995) Karst Development on Carbonate Islands in Unconformities and Porosity in Carbonate Strata. *AAPG Memoir*, **653**, pp. 55–76.

MYLROIE, J. E., & CAREW, J. L. (1997) Geology of the Bahamas. In: *Geology and hydrogeology of carbonate islands* (VACHER, H. L., & QUINN, T. M., *Eds*.), Elsevier, pp. 91–139.

MYLROIE, J. E., CAREW, J. L., SEALEY, N. E., & MYLROIE, J. R. (1991) Cave Development on New Providence Island and Long Island, Bahamas. *Cave Science*, **18**, *3*, pp. 139–151.

PALMER, A. N. (1991) Origin and Morphology of Limestone Caves. *GSA Bulletin*, *103*, pp. 1–25.

PLUMMER, L. N. (1975) Mixing of sea water with calcium carbonate ground water. In: *Quantitative studies in geological sciences* (WHITTEN, E., H., T., *Ed*.), *GSA Memoir*, **142**, p. 219–236.

REECE, M., MYLROIE, J. E., & JENSON, J. W. (2000) *Cave and Karst Development of Guam: Implications for aquifer history*. Program Guide, NSS Conv. 2000, Elkins, WV, p. A-15.

ROBINSON, M. C., & DAVIS, R. L. (1999) Preliminary Geographical Information System Analysis and Maps of Physical, Hydrological, Archaeological, and Biological Resources, San Salvador Island, Bahamas. In: *Proc. Ninth Symposium on the Geology of the Bahamas and Other Carbonate Regions* (CURRAN, H., A. & MYLROIE, J., E., *Eds*.), Bahamian Field Station, San Salvador, Bahamas, p. 101–109.

SANFORD, W. E., & KONIKOW, L. F. (1989) Porosity development in coastal carbonate aquifers. *Geology*, **49**, pp. 249–252.

VOGEL, P. N., MYLROIE, J. E., & CAREW, J. L. (1990) Limestone petrology and cave morphology on San Salvador Island, Bahamas. *Cave Science*, **17**, pp. 19–30.

Theoretical and Applied Karstology, **13–14** (2000–2001), pp. 67–73

Sur la présence de l'ardéalite dans la Grotte de Topolniţa (Plateau de Mehedinţi, Roumanie)

Gabriel Diaconu[1*] & Delia Dumitraş[2]

[1] *Institut de Spéologie "Emil Racoviţă", str. Frumoasă 11, 78114 Bucarest 12, Roumanie.*
[2] *Laboratoire des Resources Minerales, Institut Géologique, str. Caransebeş 1, 78344 Bucarest, Roumanie.*

Résumé

Il y à 70 années, dans la Grotte de Cioclovina (Monts Sebeş, Roumanie) un nouveau minéral — l'ardéalite — a été découvert en association avec le gypse et la broushite (HALLA, 1931; SCHADLER, 1932). Les auteurs ont identifié la même association minéralogique dans la Galerie Suspendue de la Grotte de Topolniţa (Plateau de Mehedinţi).
L'échantillon prélevé a été analysé en RX, IR, TDA et chimiquement. Les données obtenues, comparées avec les données standard, ont mis en évidence l'ardéalite, le gypse et la broushite. Le travail présente de même un point de vue original sur les conditions du milieu spéléique qui ont facilité la genèse de cette association minéralogique.

Mots-clés: minéralogie des grottes, ardéalite, phosphates, sulfates, Grotte de Topolniţa.

On the presence of the ardealite in Topolniţa Cave (Mehedinţi Plateau, Romania)

Abstract

Seventy years ago a new mineral — the ardealite — was discovered in Cioclovina Cave (Sebeş Mountains, Romania), associated with with gypsum and brushite (HALLA, 1931; SCHADLER, 1932). The authors found the same mineral association in Topolniţa Cave (Mehedinţi Plateau).
The sample taken was investigated by means of RX, IR, TDA and chemical analyses; ardealite, gypsum and brushite were identified by comparison with standard data. The genetic condition of the speleal environment that contributed to the formation of this mineral association are also discussed.

Key words: cave minerals, ardealite, phosphates, sulfates, Topolniţa Cave.

Conformément à RĂDULESCU & DIMITRESCU (1966), l'année 1931 est la date laquelle à F. Halla a réalisé un premier examen en RX d'un nouveau minéral prélevé de la Grotte de *Cioclovina* (Monts Sebeş), le hydrogèno-phosphato-sulfate de calcium tétra-hydraté, trouvé en paragenèse avec le gypse et la broushite.

Une année plus tard (1932) SCHADLER met au point la découverte du Halla, en présentant le nouveau minéral, l'ardéalite, avec tous les détails nécessaires pour être confirmé comme tel, y compris une analyse chimique complète grâce à laquelle il a établi la formule chimique structurale fondamentale: $[Ca_2(HPO_4)(SO_4) \cdot 4H_2O]$, ayant comme rapports $HPO_3 : SO_3 : CaO : H_2O = 1 : 0,863 : 1,834 : 3,980$.

Ultérieurement, ce nouveau minéral a été découvert dans dix autre pays, exclusivement dans le milieu spéléique (HILL & FORTI, 1997), sans qu'il eût été retrouvé (pendant tout cet intervalle de temps) dans une autre grotte de Roumanie.

L'identification de l'ardéalite dans la Galerie Suspendue de la Grotte de Topolniţa, toujours en association avec le gypse et la brushite, vient de compléter les données existantes sur la minéralogie du domaine spéléique national.

* corresponding author. *Fax*: +40-1-2113874.

La grotte de Topolniţa: données générales

Ayant une longueur totale (connue jusqu'à présent) de 20,5 km de galeries creusées dans le massif sur une dénivellation de 109 m (GORAN, 1981), *La Grotte de Topolniţa* est l'un des plus importants objectifs spéléologiques de Roumanie.

Les calcaires dans lesquels la cavité est creusée, affleurent au sud-ouest du Plateau de Mehedinţi, à environ 30 km nord de la ville de Drobeta -Turnu Severin, étant encadrée en grande ligne par le triangle des localités Cireşu – Jupâneşti – Marga.

L'âge des calcaires, appartenant à l'Autochtone Danubien, est attribué au point de vue chrono-stratigraphique à l'intervalle Tithonique – Aptien.

La barre des calcaires, orientée NNE–SSO, est délimitée à l'ouest par les schistes cristallins de la Nappe Gétique (Lambeau de Bahna) et à l'est par les roches sédimentaires en faciès de flysch de la Nappe de Severin.

La manière de développement des principales galeries de la grotte, ainsi que des observations sur la tectonique locale nous ont permis de supposer que, parallèlement aux failles d'encadrement de la barre calcaire il y a une faille supplémentaire (dans le voisinage de la Faille Ouest), toutes les trois étant affectées alternativement, du nord vers le sud, par des disjonctions transversales (probablement plus nouvelles), orientées OSO – ENE (Fig. 1).

En général, le système de galeries de la Grotte de Topolniţa est orienté d'une manière préférentielle sur ces deux directions (Fig. 2). L'échantillon soumis aux analyses minéralogiques a été prélevé du plancher de la Galerie Suspendue dont la longueur totale est de 226 m (Fig. 2A).

Dans la partie centrale de cette galerie il y a une grande salle avec des dimensions de 50 × 30 × 8 m. Dans une position excentrique, près de la parois gauche (le secteur est de la salle), se trouve un important dépôt de guano provenant d'une colonie de chauve-souris présente pendant la saison chaude à la voûte. Le dépôt, assez grand, est accumulé sous la forme d'un

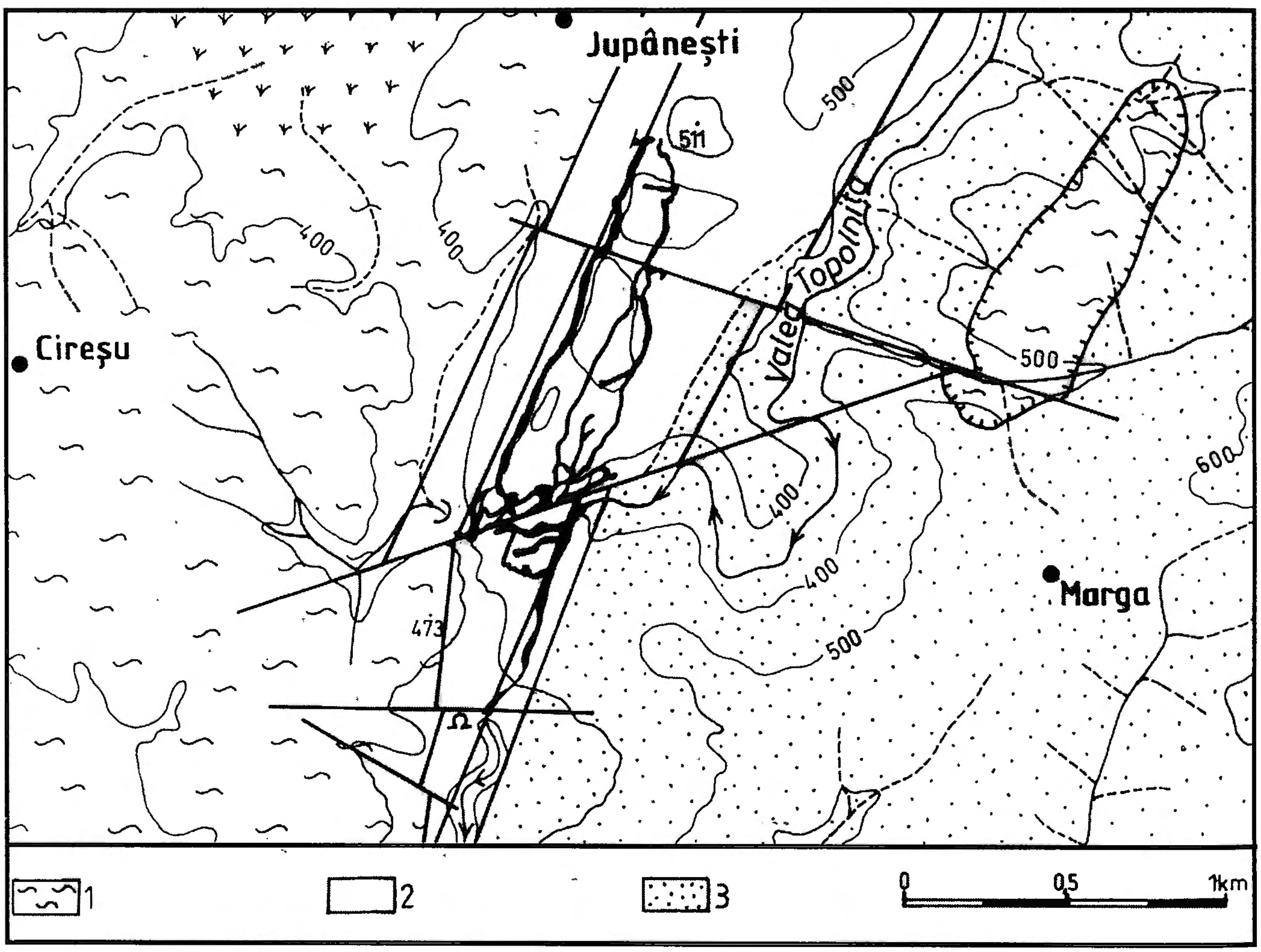

Fig. 1. Carte géologique de la zone d'emplacement de la Grotte de Topolniţa. 1: schistes cristallins; 2: calcaires; 3: depôts détritiques.
Geological map of the region of Topolniţa Cave. 1: crystalline schists; 2: limestones; 3: detrital deposits.

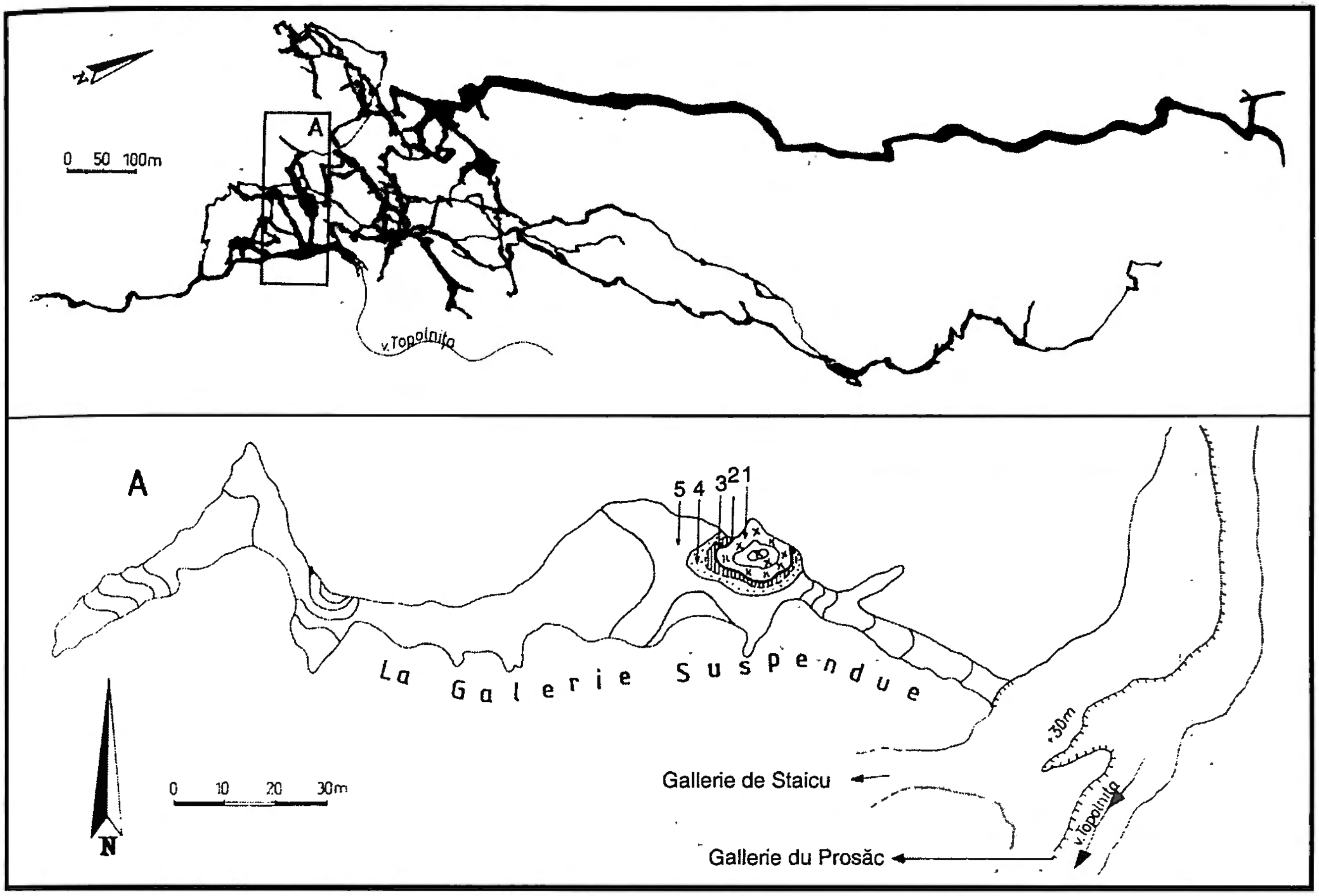

Fig. 2. Carte de la Grotte de Topolnița. En vignette (A) Plan de la Galerie Suspendue ; pour 1 à 5 voir les explications dans le texte. *Map of Topolnița Cave. Inset A: plan of Overhanged Passage. For mineral zones 1–5 see explanations in the text.*

dôme dépassant, dans sa partie centrale, 3 m d'épaisseur, témoin d'une présence continue de la colonie depuis bien longtemps.

Dans le secteur circonscrit à la zone d'influence de la solution éliminée de l'accumulation de guano, le plancher est recouvert d'une croûte minérale. Si à la limite extérieure la croûte est bien cimentée et évidemment calcitique, dans le voisinage du dépôt de guano elle devient très friable, étant pratiquement un agrégat microcristallin gris-jaunâtre, à aspect terreux.

L'échantillon prélevé de cette zone, analysé en RX, a mis en évidence une mixture composée (par ordre décroissante du poids) de *gypse*, d'*ardéalite* et de *broushite* (totalement subordonné on a identifié de la calcite).

Pour compléter les analyses en RX, des analyses en IR, thermiques différentielles et chimiques ont été également effectuées.

Interprétation des données analytiques

Des quatre minéraux identifiés à la suite de l'analyse en RX, nous détaillerons nos observations seulement sur les trois premiers (le gypse, l'ardéalite et la broushite). La

Tableau 1. Les valeurs standard du gypse comparées avec les valeurs obtenues sur le diffractograme. *Standard values of gypsum compared with those obtained for the sample.*

d : Gypse 74-1905	I	d : Gypse Topolnița
4.2783	999*	4.2780
3.1683	27	3.1590
3.0612	528	3.0660
2.8757	389	2.8770
2.7888	75	2.7920
2.4042	27	2.4080
2.2152	73	2.2150
2.0729	105	2.0740
2.0284	5	2.0370
1.8655	26	1.8670
1.8000	45	1.8030
1.7817	19	1.7830
1.6433	20	1.6430
1.4398	27	1.4380
1.4185	21	1.4190
1.3256	15	1.3250
1.2032	19	1.2040
1.1400	23	1.1410

Tableau 2. Les valeurs standard de l'ardéalite comparées avec les valeurs obtenues sur le diffractograme.
Standard values of the ardealite compared with those obtained for the sample.

d : Ardealite 83-1721	I	d : Ardealite Topolniţa
7.7480	999*	7.7630
4.5627	323	4.5620
3.9323	419	3.9320
3.8740	89	3.8770
3.3392	301	3.3400
2.9777	116	2.9970
2.8516	261	2.8510
2.7343	107	2.7320
2.5428	107	2.5440
2.5024	37	2.5040
2.4465	134	2.4470
1.9661	57	1.9610
1.8122	100	1.8120
1.6698	29	1.6680

Tableau 3. Les valeurs standard de la broushite comparées avec les valeurs obtenues sur le diffractograme.
Standard values of the brushite compared with those obtained for the sample.

d : Brushite 72-0713	I	d : Brushite Topolniţa
7.5900	999*	7.6130
3.7950	46	3.8050
2.7950	46	2.7920
2.6022	199	2.6020
2.0990	39	2.0930
1.9969	62	1.9950
1.8975	17	1.8980
1.8752	98	1.8740
1.5331	24	1.5330
1.4819	2	1.4820
1.4622	4	1.4610
1.3664	15	1.3670
1.3397	19	1.3390
1.1523	15	1.1520

Tableau 4. Les paramètres cristallographiques pour les trois minéraux de la Galerie Suspendue, la Grotte Topolniţa.
Crystallographic parameters of the three minerals from the Overhanged Passage, Topolniţa Cave.

Mineral	*a* (Å)	*b* (Å)	*c* (Å)	$\beta^{(o)}$	*V* (Å^3)	n(1)	N(2)
Gypse	5.682(7)	15.229(2)	6.494(1)	118.29(1)	495.014	6	36
Ardealite	5.722(1)	31.019(8)	6.238(2)	117.27(1)	984.155	9	47
Brushite	5.833(3)	15.170(6)	6.247(3)	116.65(3)	494.061	8	35

détermination a été fait en tenant compte des valeurs obtenues sur le diffractogramme comparées pour chaque espèce minérale avec les valeurs standard d'*International Center for Diffraction Data*, fiches 74–1905 (gypse), 83–1721 (ardéalite) et 72–0713 (broushite) (Tableaux 1, 2 et 3).

La concordance entre les valeurs obtenues et les valeurs standard, allant souvent jusqu'à l'identité, dénote un haut degré de cristallisation et une forte pureté des minéraux de l'échantillon. Il n'existe donc aucune incertitude sur le diagnostic, de sorte qu'on peut établir les paramètres cristallographiques pour les minéraux déterminés (Tableau 4). D'ailleurs, le diagnostic est confirmé par l'analyse en IR (Fig. 3).

La comparaison entre les valeurs enregistrées et celles présentées dans le catalogue de Moenke (1966) pour l'ardéalite (Tableau 5), nous montre :

- La présence des bandes d'absorption de 528 cm^{-1} et 860 cm^{-1} atteste tant l'existence de l'anion phosphate que sa vibration de liaison avec l'oxhydrile.
- L'anion sulfate est lui aussi très bien mis en évidence par les bandes d'absorption de 602 cm^{-1} et respectivement de 672 cm^{-1}.

Tableau 5. Les principales bandes d'absorption de l'ardéalite.
Main absorption bands of the ardealite.

Valeurs standard (cm^{-1})	Valeurs de Topolniţa (cm^{-1})
424	420
460	475
528	528
600	602
677	672
822	820
866	860
1013	1006
1109	1109
1145	1164
1675	1685
3370	3340

Les dernières bandes d'absorption (1685 cm^{-1} et 3340 cm^{-1}) confirment la présence de l'eau de cristallisation qui se trouve aussi dans la structure de l'ardéalite.

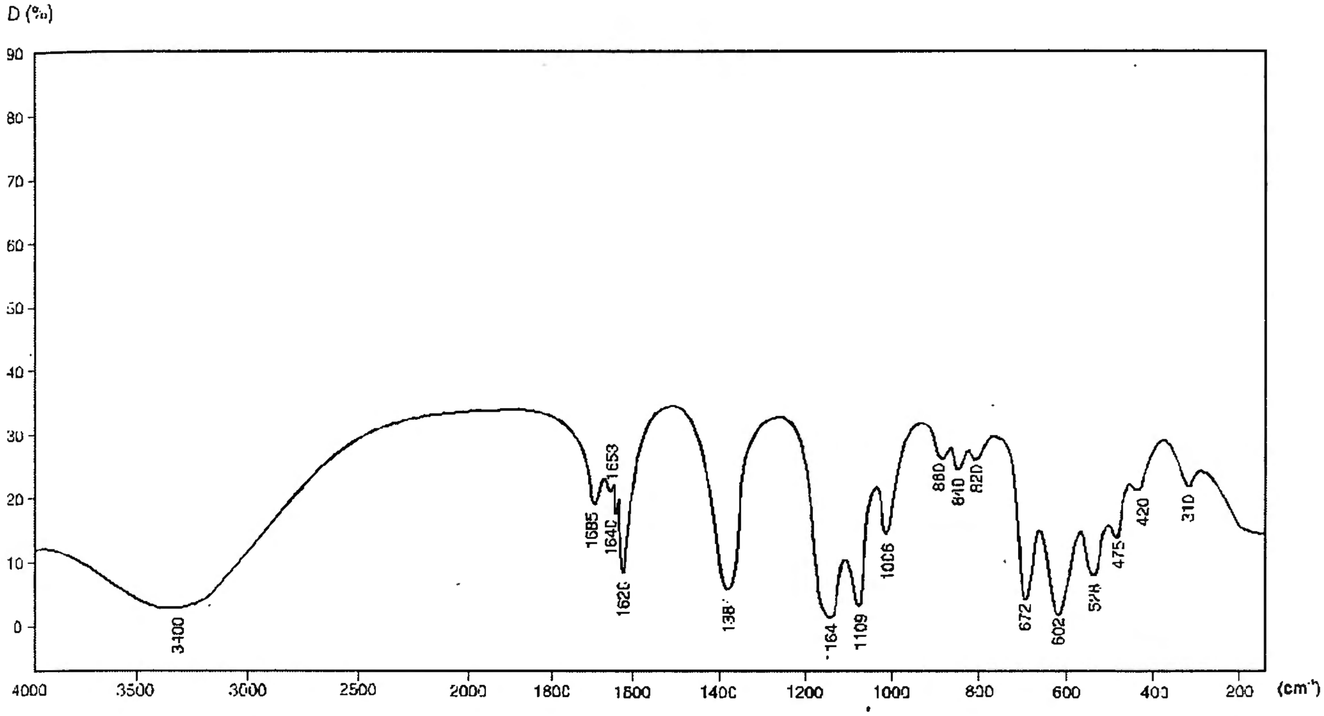

Fig. 3. Le spectre d'absorption en IR. *IR absorption spectra.*

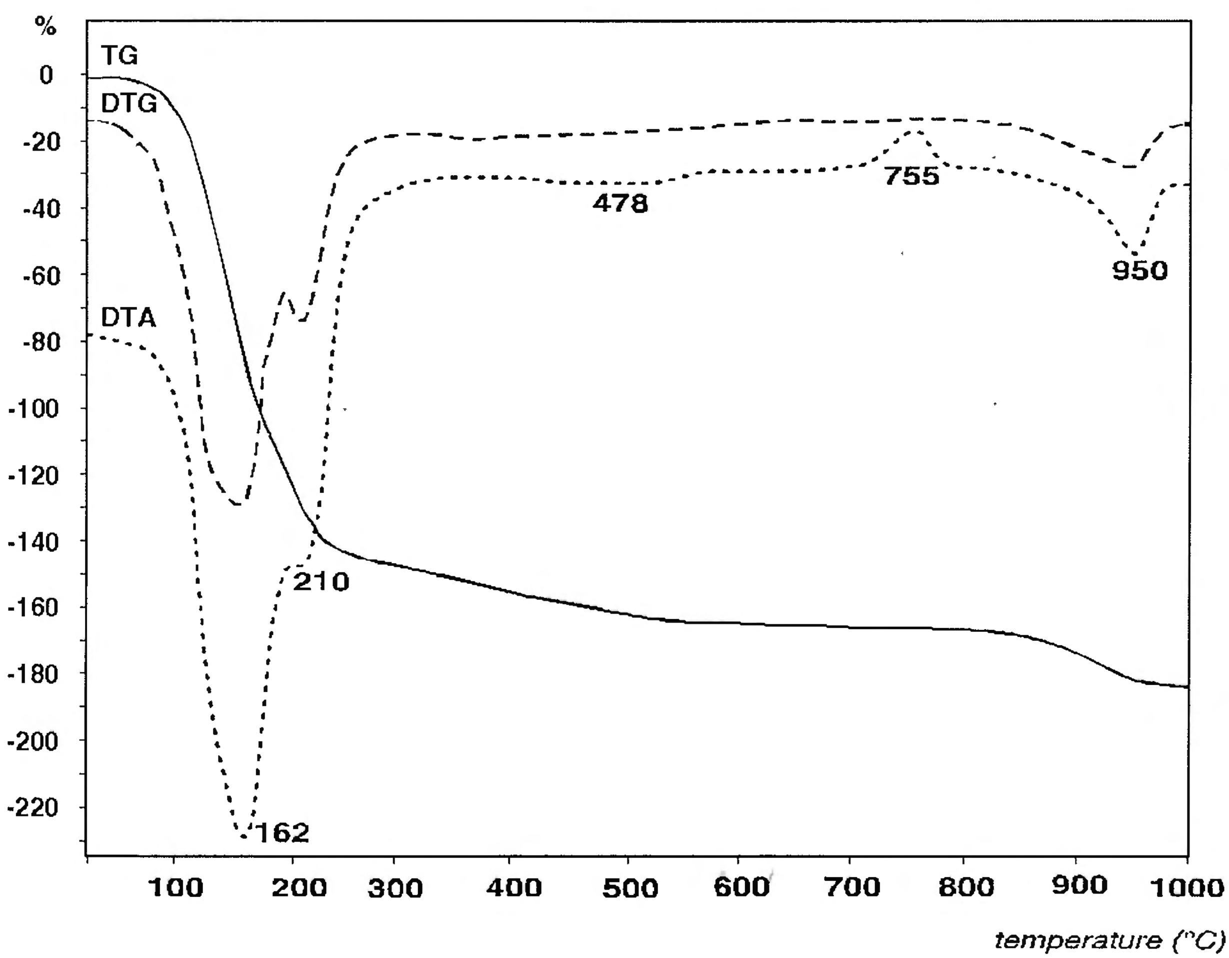

Fig. 4. L'analyse thermique diférentielle. *Differential thermal analysis spectra.*

L'analyse thermique différentielle de l'échantillon (marquée par les courbes DTA, DTG et TG raportées à T °C) (Fig. 4) met en évidence un premier processus de déshydratation déclenché à 100 °C qui finit autour de 300 °C, souligné par les pics endothermiques sur les courbes DTA et DTG à 142 °C et respectivement (plus faible), à 210 °C.

Le pic endothermique, très large, marqué autour de 478 °C est la conséquence d'une impureté avec carbonate de calcium (fait confirmé aussi par l'analyse en RX).

Le pic exothermique très bien surpris sur la courbe DTA autour de la valeur de 755 °C est, sans doute, déterminé par une modification structurale des anions de phosphate et de sulfate. Le processus de désintegration finale est en outre bien marqué sur les trois courbes par des pics endothermiques à 950 °C.

L'analyse chimique de l'échantillon par rapport aux données obtenues par SCHADLER (1932) est présentée dans le Tableau 6.

La présence de l'oxyde d'aluminium (Al_2O_3) dans l'échantillon de la Grotte de Topolniţa (2,44 %) associé avec un excédent de SO_3 (1,40 %), peut nous suggérer l'existence d'un sulfate d'aluminium, probablement la basaluminite – $Al_4(SO_4)(OH)_{10} \cdot 5H_2O$. Mais, aucune des analyses présentées antérieurement (en RX, IR ou DTA) n'ont confirmé cette supposition, aspect qui nous a fait présumer que l'échantillon a été contaminé avec argile provenue soit par voie éolienne, soit transportée par les eaux de percolation qui ont lavé la couverture de sol.

Tableau 6. Analyse chimique comparative entre l'échantillon prélevé de la Grotte Topolniţa et l'échantillon de la Grotte de Cioclovina (SCHADLER, 1932).
Comparative chemical composition of the sample taken from Topolniţa Cave and that analysed from Cioclovina Cave (SCHADLER, 1932).

Oxydes	Grotte Topolniţa (%)	Grotte Cioclovina (%)
CaO	30.39	31.61
SO_3	22.91	21.51
P_2O_5	19.46	21.85
Al_2O_3	2.44	—
Fe_2O_3	0.13	—
H_2O	22.90	25.14
Rez.	0.90	0.39
TOTAL	99.13	100.50

Les conditions de genèse de l'association minéralogique

L'association minéralogique constituée d'ardéalite, gypse et broushite est considérée comme une mixture spécifique pour le milieu spéléal classique (existant dans les cavités développées dans les roches calcaires). Sa genèse, dans la plupart des cas, est liée à la présence des dépôts de guano (HILL & FORTI, 1997).

Dans la Galerie Suspendue de la Grotte de Topolniţa cet aspect se confirme une fois de plus. Mais, ici, il y a une particularité que nous tenons à mettre en évidence.

Dans la Fig. 2A nous avons présenté la position occupée par le dépôt de guano dans l'espace de la galerie. Donc, il faut retenir que, dans le cas donné la solution génératrice de la paragenèse minéralogique a circulé d'une manière centrifuge, dans un plan *quasi*-horizontal, du côté du dépôt de guano vers l'extérieur et pas en profondeur. En conséquence, tout autour du dépôt de guano on peut départager, approximativement, quelques zones d'influence à disposition centroradiaire dans la succession suivante:

1. guano granulaire, relativement frais;
2. guano humide non-granulaire;
3. un premier "anneau" constitué d'une tâche humide que nous supposons broushitique;
4. un deuxième "anneau", relativement sèche, formé par un agrégat terreux microcristallin (les échantillons analysés ont été prélevés de cette zone). Sur d'autres diffractogrames en RX (non presentés dans ce travail), *le contenu en calcite augmentent fortement vers l'extérieur de l'anneau.*
5. la zone du plancher couverte d'une croûte calcitique.

Conclusions

Conformément à HILL & FORTI (1997), l'ardéalite représente le stade de début de la dégradation du calcaire au contact avec le dépôts de guano. Cette appréciation a été confirmée aussi dans le cas de la Grotte de Topolniţa mais, avec la spécification que le processus d'enrichissement en phosphate et sulfate du carbonate de calcium s'est produit grâce à une croûte de calcite pré-existante sur le plancher.

Le fait que le secteur de la galerie se trouve dans un méroclimat de transition, influencé par les variations climatiques de l'extérieur sous le contrôle de la morphologie locale, dont les températures positives durant la saison chaude ne dépassent jamais 12–13 °C, et dans la saison froide ne s'abaissent pas audessous de 6–7 °C, a favorisé la conservation de l'association

minéralogique à l'ardéalite. En outre, la position de la Galerie Suspendue à l'extrémité nord de la Galerie du Prosăc, satisfait la condition d'une baisse de l'humidité, au moins dans les saisons chaudes, qui est aussi nécessaire pour la formation de l'ardéalite.

Remerciements

Nous remercions vivement l'École des Mines de Saint-Etienne, France, pour l'aide à la réalisation des analyses en RX.

Bibliographie

GORAN, C. (1982) *Catalogul sistematic al peșterilor din România.* Ed. C.N.E.F.S., București, 496 p.

HALLA, F. (1931) Isomorphe Beizeihungen und Doppelsalzbildung zwischen Gips und Brushit. *Zeit. f. Kristallographie*, **80**, pp. 349–352.

HILL, C. A., & FORTI, P. *Eds.* (1997) *Cave Minerals of the world.* 2nd Ed., NSS, Huntsville, 464 p.

SCHADLER, J. (1932) Ardealit, ein neues Mineral. *Cbl. f. Miner.*, A, pp. 40–45.

RĂDULESCU, D. & DIMITRESCU, R. (1966) *Mineralogia topografică a României*. Ed. Academiei RSR, București, 376 p.

Theoretical and Applied Karstology, **13–14** (2000–2001), pp. 75–79

On the genetic conditions of black manganese deposits from two caves of Eastern Serbia

Vladimir Ljubojević[1*], Aleksandar Pačevski[1,2] & Jelena Ćalić-Ljubojević[1,3]

[1]*Student Speleologic and Alpinistic Club (ASAK), Studentski trg 16, 11000 Belgrade, Yugoslavia.*
[2]*Faculty of Mining and Geology, Dept. of Mineralogy and Crystallography, Studentski trg 16, 11000 Belgrade, Yugoslavia.*
[3]*"Jovan Cvijić" Geographic Institute, Serbian Academy of Sciences and Arts, Djure Jaksica 9, 11000 Belgrade, Yugoslavia*

Abstract

Portions of cave passages often have a black colour due to manganese deposits that occur as coatings on cave walls and ceilings, on clastic sediments, as well as on speleothems. On samples from the cave Buronov Ponor chemical analysis, infrared spectroscopy, X-ray diffraction and DTA analysis confirmed the presence of birnessite. In cave Cerjanska Pecina, the presence of manganese compounds in the black coating has been confirmed by chemical tests. In both caves it has been noted that cave passages with black coating have a distinct morphology. They are highly weathered showing an abundance of sharp protusions, potholes in the streambed and scallops. The paper studies these occurrences and the possible link between the manganese deposition, hydrology and morphology of the passages and petrologic composition. Although this link was not identified, some interesting questions regarding manganese deposition arose. It remains unclear why manganese deposition is limited only to a certain part of cave Cerjanska Pecina, and what caused the cyclicity in manganese deposition in the cave Buronov ponor.

Keywords: manganese deposits, chemical analysis, speleomorphology.

Sur la genèse des dépôts noir de manganèse dans deux grottes de la Serbie de l'Est

Résumé

Certains secteurs des galeries souterraines présentent souvent une couleur noire due aux pellicules de manganèse qui peuvent couvrir en égale mesure les parois, la voûte, les sédiments où les spéléothèmes. Les analyses chimiques, de spectroscopie en IR, de diffraction en RX et les analyses thermiques différentielles éffectuées sur des échantillons prélevés de la grotte de Buronov Ponor ont relevé la présence du birnessite. La présence du manganèse dans la pellicule noire de la grotte de Cerjanska Pecina a été aussi confirmée par l'analyse chimique. Dans les deux grottes on a observé une morphologie particulière des secteurs des galeries couverts par cette pellicule noire. Ils sont fortement érodés, présentant en abondance des arêtes vives, des vagues d'érosion et des trous dans le thalweg. Le travail traite de l'occurrence de ceux-ci et de la possible connexion entre la présence de la pellicule de manganèse, l'hydrologie et la morphologie des galeries et la pétrologie de la roche-mère. Même si cette connexion n'est pas certaine, l'étude a mis en évidence quelques questions intéressantes. C'est le cas de la présence du manganèse seulement dans quelques zones de la Cerjanska Pecina et du dépôt cyclique du manganèse dans le Buronov Ponor.

Mots clés: dépôts de manganèse, analyse chimique, morphologie spéléale.

Introduction

Black sediments composed of manganese oxides are a common occurrence in caves. They occur as crusts or coatings covering cave walls, stream clasts, and, sometimes, even speleothems. They originate from stream water, which contains manganese derived from surface organic material, probably precipitated due to bacterial activity (Hill & Forti, 1997, p.125). Manganese deposits are not a rare occurrence in caves in Serbia, but they have not been studied previously.

* corresponding author. *E-mail address*: fric@sezampro.yu

Manganese deposits in two caves — *Buronov Ponor* and *Cerjanska Pecina*, were the focus of our interest. In both caves, we noted that distinct parts of the cave differ from the rest, both in color (*i.e.* sediments on cave walls) and in morphology. The conspicuous parts of the caves are completely black. A thin layer of black coating covers not only the sediments on the floor, but also the walls, the ceiling and some of the speleothems. Besides that, the black parts of the cave differ from the rest of the cave also by their morphology: the passages are highly weathered, with abundant sharp rocky protrusions, potholes in streamded (SLABE, 1995, p.46), pendants, scallops etc.

Buronov Ponor and Cerjanska Pecina differ in geology and hydrological setting. Investigations in both caves have been performed to find out the nature of the black coatings, and if there is a link between their deposition and the morphology of the passages where they occur.

Buronov Ponor

Buronov Ponor is located on Mt. Miroc, in Eastern Serbia, in the "Iron Gates" Danube gorge. It is an intermittent ponor (swallet), with an entrance located at 287 m a.s.l., and the deepest part at 85 m a.s.l., only 15 m above Danube's current water level. Until late '60s, when the "Iron Gate" Dam was built, Danube's level was some 20 m lower, *i.e.* at 50 m a.s.l. The surveyed part of the cave is 2400 m long. Buronov Ponor is the last of the chain of swallets located along the western contact of Mt. Miroc karst, and supplied by short streams coming from Cretaceous shales. Buronov Ponor discharges directly into the Danube at Bele Vode springs (ZLOKOLICA *et al.*, 1996).

In the lowest part of the cave, there are 800 meters of presumably horizontal passages, inactive under normal circumstances, named Rio Negro and Mammoth Gallery. Their average cross-section is 5 × 5 meters. At three places they intercept narrow passages, located 15 meters below, occupied by a strong stream, with minimal flow of 0.5 m^3/s (in the dry season). All these passages in the lowest part of the cave are black – a black crust, up to 2 mm thick, covers the sediments (pebble), the walls and the speleothems. Only some of the speleothems, and some sediments (sand) are not covered by this coating. Unlike the rest of the cave, the cave rocky relief within these passages displays a high concentration of potholes in streambed, sharp protrusions, pendants and scallops.

Black coating has not been found only on the surface of the cave walls and sediments. Broken speleothems also show layers of black coating sandwiched between calcite layers.

Chemical analysis, infrared spectroscopy, X-ray diffraction and DTA of the samples of black coating were carried out. Chemical analysis proved the presence of Mn by 30%, and also the presence of iron (Fe). Infrared spectra (Fig. 2) shows prominent bands at 520 and 470 cm^{-1}, and correlate well with the birnessite spectra given by POTTER & ROSSMAN (1979, p. 1211). X-ray diffraction gave a curve similar to that of birnessite (MOORE, 1981, p. 644) although the identification is still uncertain due to the small number of diffraction peaks,

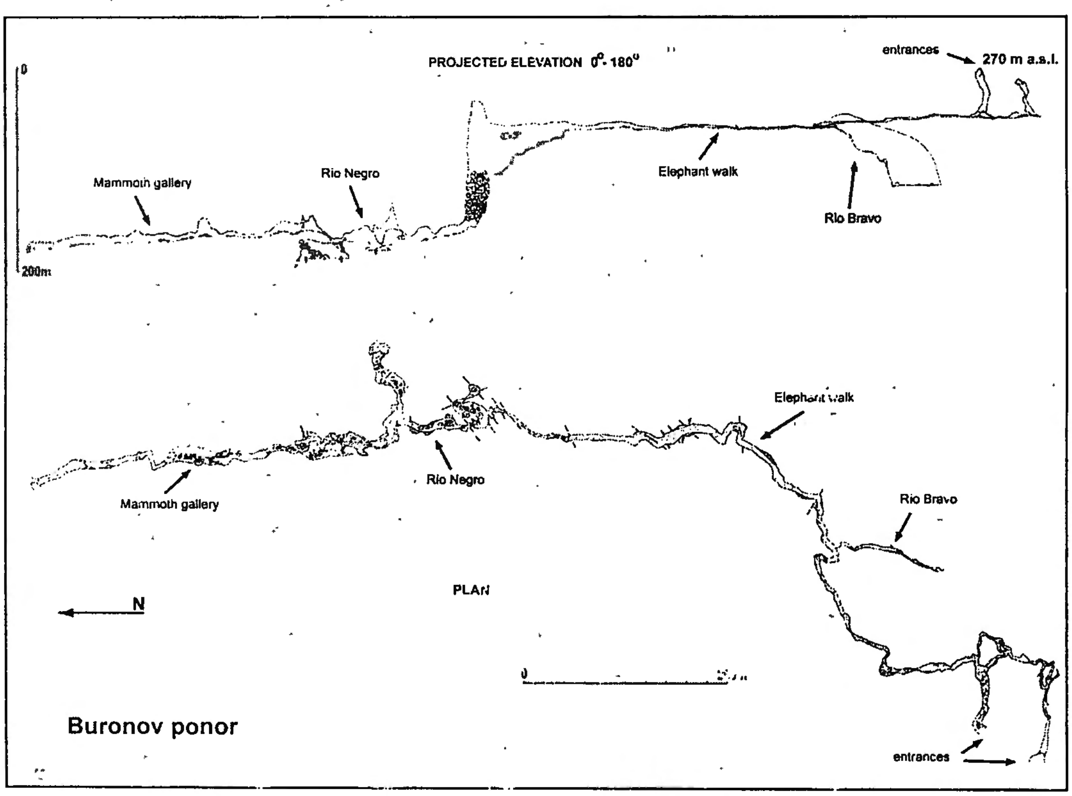

Fig. 1. Map of Buronov Ponor.
Plan du Buronov Ponor.

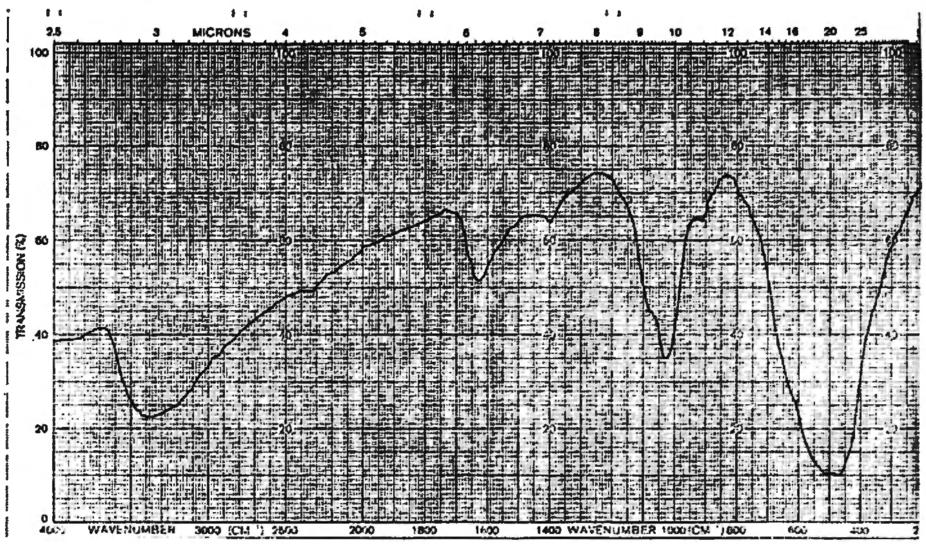

Fig. 2. Infrared spectrogram of the sample from Buronov Ponor.

Spectrogramme en IR de l'échantillon de Buronov Ponor.

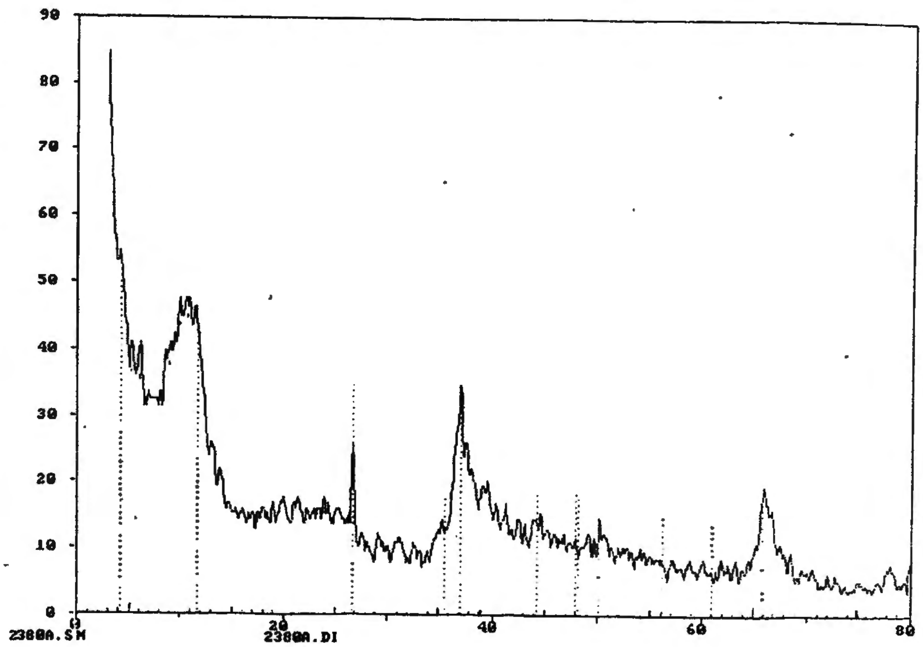

Fig. 3. X-ray diffractogram of the sample from Buronov Ponor.

Diffractogramme en RX de l'échantillon de Buronov Ponor.

caused by the amorphous structure of the material. DTA of the samples gave only two endothermic peaks, one due to expulsion of water, and the other due to dehydratation of the amorphous material.

Due to the amorphous structure of the coating, it was only possible to detect the presence of manganese in the form of birnessite. It is still impossible to tell whether any other minerals are present in the sample.

Petrographic analysis of samples from cave walls defined it as silty biomicritic limestone. The limestone is often fractured, with occasional brecciated zones.

Cerjanska Pecina

Cerjanska Pecina is a through cave, located in the hills 12 km north from town of Nis, in South-eastern Serbia. It is 6.025 meters long, and it ends with siphons that are less than 200 m away from the resurgence at spring Kravljansko Vrelo. Besides the stream entering the cave, coming from Permian sandstone, there are no significant tributaries in the cave. At some 3 km from the entrance, a narrow siphon is located. The cave stream sumps/in it, reappearing near the downstream end of the cave; still, the middle sector of the cave also shows traces of periodic waterflow (Ljubojević & Gerzina, 1997).

After the sump at the third kilometer, an abrupt change in passage morphology occurs. For the next 300 meters, the

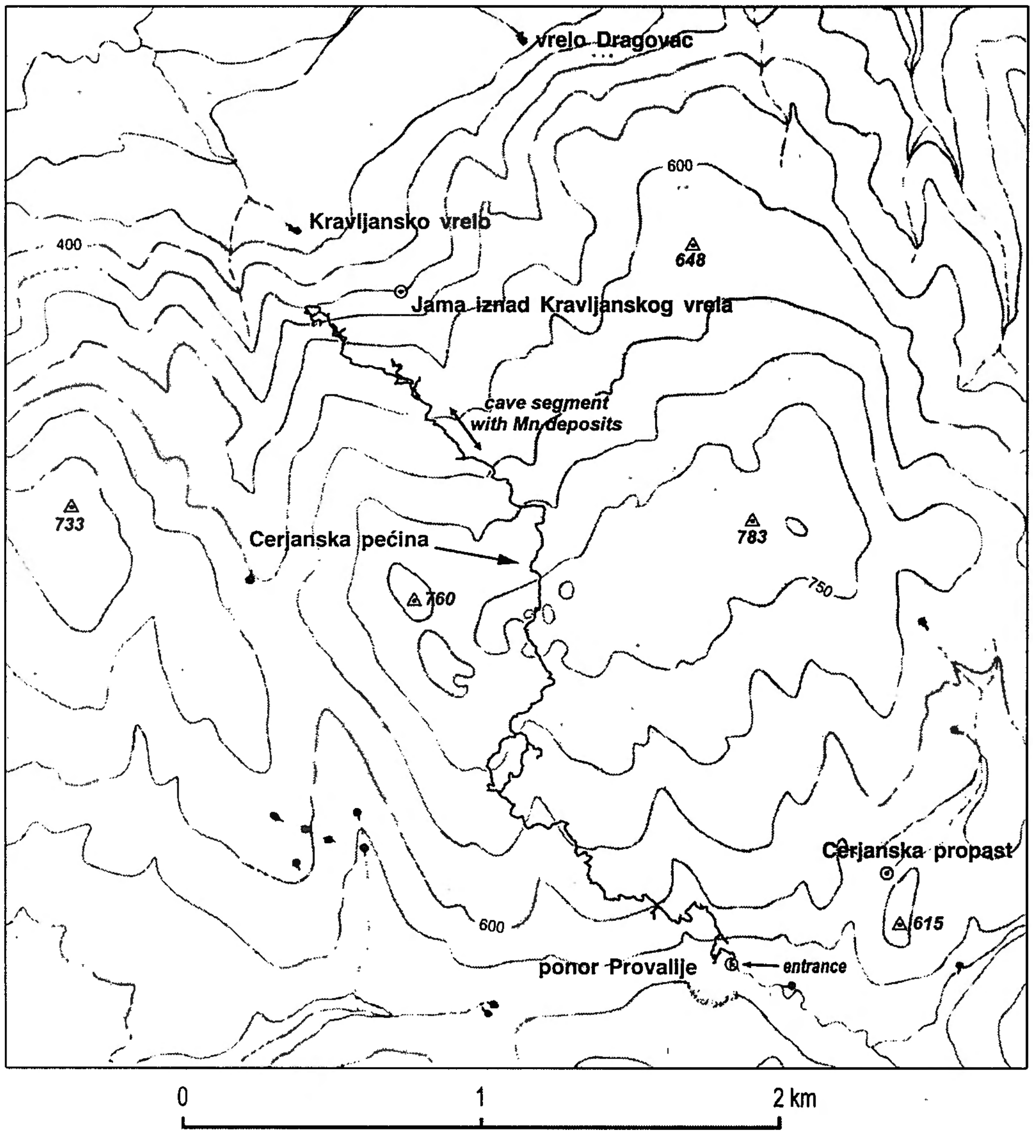

Fig. 4. Location and simplified map of Cerjanska Pecina.

Carte de situation et plan simplifié de la grotte de Cerjanska Pecina.

passage resembles in all details to the one in the lower part of Buronov Ponor, except that the speleothems are lacking. The walls are black, covered with the same type of coating as in Buronov Ponor, that is occasionally almost washed away.

Chemical tests (reaction with lead peroxide) proved the presence of Mn. Microscopic analyses of rock samples taken from Cerjanska Pecina show that most of the cave develops in limestones; however, within the above mentioned 300 m the host-rock is a silty sparitic dolostone showing equal content of calcite and dolomite.

Discussion

Since Mn deposition occurs at water-air interface (Onac *et al.*, 1997), it is reasonable to suppose that the passages in both caves have been periodically inundated. This is easy to presume in case of Buronov Ponor, where passages with Mn deposits lay just above the water table. In Cerjanska Pecina, there are traces of high waters and also of clastic infill of the cave, so periodic floodwaters could have been the source of Mn deposition there.

The authors expected that similar morphology in both caves to be caused by similar rock composition. However, that was not the case. The outstanding morphology of lower parts of Buronov Ponor may be attributed simply to strong turbulent flow. High susceptibility to erosion, can also be attributed to the increased porosity of the rock, which is caused by fractures and breccias in case of Buronov Ponor (Slabe, 1995). In case of Cerjanska Pecina, the difference in morphology might be attributed to greater susceptibility of porous dolostone to mechanical erosion.

The Mn deposition in lower parts of Buronov Ponor can also be attributed to periodical inundation, due to vicinity of water table. However, in Cerjanska Pecina is still unclear why

the Mn deposition occurred only in the 300 m long portion of the cave in dolomites. If Mn is precipitated from a stream, the same stream should have deposited Mn upstream and downstream from this part of the cave. Some of the possible causes of this anomaly in Mn deposition, that are yet to be studied in detail, include: higher susceptibility of the substrate (rock surface) for Mn deposition; presence of Mn-reducing bacteria limited to dolostone substrate; Mn precipitation from dripwater coming from the rock above the passage .

Buronov Ponor also rise questions related to Mn deposition. Layers of black coating sandwiched between calcite layers on broken speleothems point to periodic inundation of the passages. By precise dating of the speleothems, an approximate timing of the events that led to the deposition of manganese could be established. During those events, a passage of relatively great dimensions was, at least temporarily, completely filled with water – this suggests flow rates by few orders of magnitude greater than the ones currently flowing through the cave. Once the environment and timing for cyclic manganese deposition is defined, one should try to find out if it was caused by climatic events and/or variations of water table level (Danube River). This is one of the reasons we think it would be justified to study in detail the manganese deposits in cave Buronov Ponor.

Conclusion

This is the first research of manganese deposits performed on Serbian caves. Due to amorphous structure of the deposits, and lack of suitable laboratory facilities, incomplete results have been obtained. The link between passage morphology and manganese deposition has not been established. However, some interesting questions arose. In Cerjanska Pecina, it is still unclear why manganese deposition is bound only to a part of this single-conduit cave. In Buronov Ponor, cyclicity of manganese deposition implies a cyclicity of inundation of the lower parts of the cave, which could be correlated with climatic factors.

References

HILL, C., & FORTI, P. (1997) *Cave Minerals of the World*, Second Edition, NSS, Huntsville, AL., 464 p.

LJUBOJEVIĆ, V., & GERZINA, N. (1997) New speleomorphologic research of Cerjanska cave (Cerjanska pecina) *Proceedings of 3rd Symposium on karst protection,* Beograd, pp. 233–252.

MOORE, G. W. (1981) Manganese Deposition in Limestone Caves *Proc. 8th Intl. Congr. Speleol., Bowling Green*, I & II, pp. 642–644.

ONAC, B. P., TYSSELAND, M., BENGEANU. M., & HOFENPRADLI, A. (1997) Deposition of black manganese and iron-rich sediments in Vântului Cave (Romania). *Proc. 12th Inter. Congr. of Speleology, Switzerland*, **1**, pp. 235–238.

POTTER, R. M., & ROSSMAN, G. R. (1979) The tetravalent manganese oxides: identification, hydration, and structural relationships by infrared spectroscopy *American Mineralogist*, **64**, pp. 1199-1218.

SLABE, T. (1995) *Cave Rocky Relief and its Speleogenetical Significance*. ZRC SAZU, Ljubljana, 128 p.

ZLOKOLICA-MANDIĆ, M., & MANDIĆ, M. (1997) Buronov ponor. *Proc. 3rd Symposium on karst protection,* Beograd, pp. 245–253.

ZLOKOLICA M., MANDIĆ, M., LJUBOJEVIĆ, V. (1996) Some significant caves at the western rim of Miroc karst. *Theor. Appl. Karstology*, **9**, pp. 77–88.

Theoretical and Applied Karstology, 13–14 (2000–2001), pp. 81–85

Mineralogy and speleogenesis of the Ice-Cave from Poiana Vârtop (Bihor Mountains, Romania)

Nicoleta Feier[1], Gabriel Munteanu[1] & Bogdan P. Onac[2*]

[1]*Faculty of Biology and Geology, "Babeş-Bolyai" University, Kogalniceanu 1, and "Politehnica" Caving Club, O.P. 1, CP 449, 3400 Cluj-Napoca, Romania.*

[2]*Quaternary Research Group, Dept. of Mineralogy, "Babeş-Bolyai" University,Kogalniceanu 1, and "Emil Racoviţă" Institute of Speleology, Cluj Department, Clinicilor 5, 3400 Cluj-Napoca, Romania.*

Abstract

The cave of Poiana Vârtop in the NW Bihor Mountains hosts the fourth largest underground perennial glacier in Romania with a volume estimated to 12,000 m³. The ice accumulated within the cave as a result of trapping of subzero winter air through its single entrance near the top of the cave. The speleothem mineralogy is dominated by calcite, with minor amounts of included aragonite. Crusts of carbonate-hydroxylapatite (associated with bat guano) and goethite (associated with pyrite in the host limestone) are found at a few locations. Based on structural observations, dye traces, and cave galleries orientations, it is inferred that the cave is part of a much larger hydrologic karst system that also includes the nearby Humpleu-Poienita cave network.

Keywords: perennial ice block, speleothems, mineralogy, speleogenesis, Bihor Mts., Romania.

Minéralogie et spéléogenèse de la grotte de Poiana Vârtop (Monts du Bihor, Roumanie)

Résumé

La Grotte de Poiana Vârtop abrite un des plus grands dépôts de glace pérenne de Roumanie, dont le volume a été estimé à 12.000 m³. Après la localisation géographique, une présentation des éléments géologique et un brève description de la cavité, le travail traite de la minéralogie des spéléothèmes et des conditions qui ont favorisé l'accumulation de la glace. En se basant sur les observations effectuées, les auteurs concluent que la grotte fait partie du vaste système karstique qui inclut le réseau de Humpleu-Poieniţa.

Mots clés: bloc de glace pérenne, spéléothèmes, minéralogie, spéléogenèse, Monts du Bihor, Roumanie.

Geographic and geologic setting

The Ice-Cave from Poiana Vârtop (Vârtop Glade) (3415/3, in Goran, 1982) is located in the NW Bihor Mountains, within the plateau area that stretches between Ponorului Valley and Firei Valley (Lat. 46°39'96" N, Long. 22°46'85" E), at an elevation of 1340 m a.s.l. (Fig. 1).

The area has a temperate continental environment with precipitation evenly distributed throughout the year. The mean annual precipitation is approximately 1400 mm, whereas the mean annual temperature is 4 °C. January is the coldest month of the year (–7 °C), and July the warmest one (10 °C). From November to February most of the precipitation is snow; the snow cover preserves until late April. Normally, between mid-April and May, snow melts (Bleahu & Bordea, 1981).

According to Balintoni (1997) the study area belongs to the *Giurcuţa Lithozone* of *Someş Litho-group* that consists of schists, potassium feldspars-gneisses, amphibolites, and feldspar quartzites. Above these rocks, it lies the sedimentary unit of the *Bihor Autochthonous* (Alpine facies), that consists of an 800 m-thick sequence of mixed beds of sandstones, conglomerates, marls, and limestones (Mantea, 1985).

* corresponding author. *E-mail address*: bonac@bioge.ubbcluj.ro

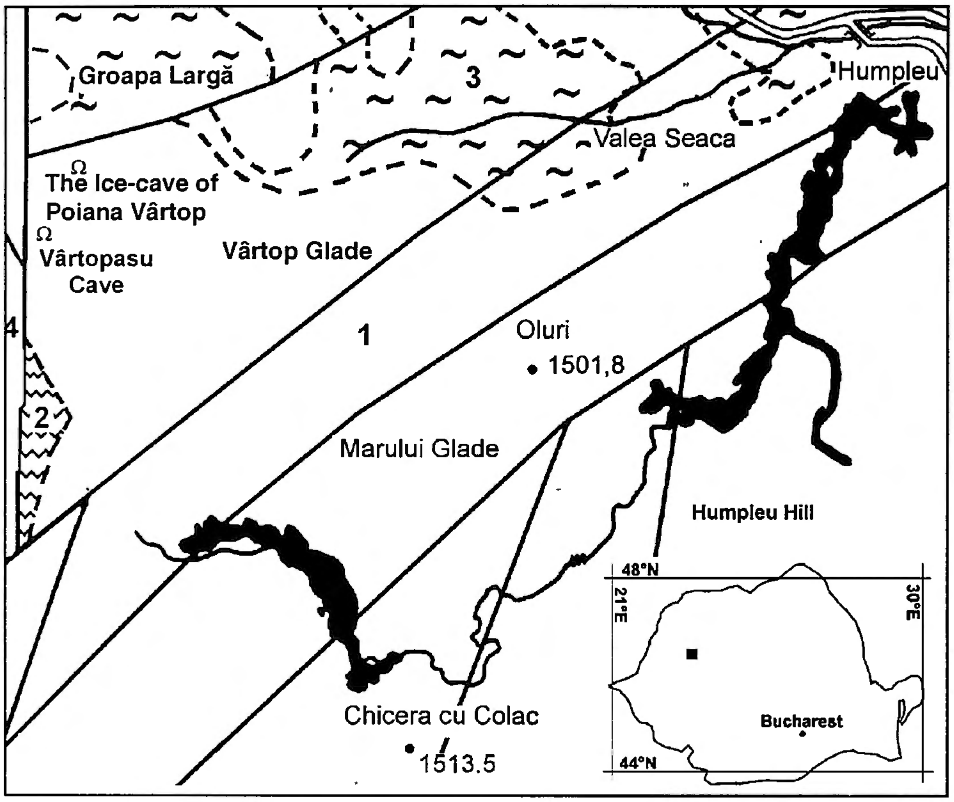

Fig. 1. Geological map of the investigated area with the location of the Ice-Cave from Poiana Vârtop and Humpleu-Poieniţa karst system. 1: Lower Cretaceous limestone; 2: Albioara limestone (Tithonian); 3: Gosau Formation (limestone with Hippurites, grey conglomerates and sandstones; 4: Quartzitic sandstone and conglomerates (Lower Liasic). *Carte géologique de la zone avec la situation de la grotte de Poiana Vârtop et du système de Humpleu-Poieniţa. 1: calcaires Crétacé inférieur; 2: calcaires d'Albioara (Tithonique); 3: Formation de Gosau (calcaires à Hippurites, conglomérats et grès); 4: Grès quartzifères et conglomérats (Liassique inférieur).*

Although the bedrock geology of this sector of Bihor Mountains is well known, little has been written about the karst geomorphology and caves of the area. The Ice-Cave from Poiana Vârtop lies entirely within the Lower Cretaceous limestone. At surface this rock is massive to medium-bedded, light blue-blackish limestone that weathers to a dark grey.

A set of microfacies analyses carried on three limestone samples collected from different part of the cave (Fig. 2a) enabled the following calcareous algae and foraminifera to be identified in thin sections: *Salpingoporella* sp and *Vercorsella scarselli* (De Casto). Their presence confirms the Barremian-Aptian age of the limestone (Bucur, *pers. comm.*). The limestone samples were X-rayed as being calcite or a mixture of calcite and dolomite.

The local structure is extremely complex due to the presence of the Someş Graben in the near vicinity. A number of high-angle normal faults that show parallel strikes were mapped over the entire region. The cave itself lies near the intersection of two faults whose direction is NE–SW and N–S respectively (Mantea, 1985).

The strike of the faults and their spatial extension, along with the dye tracing performed by Orăseanu (1996) provide the basis for a hydrogeological interpretation. The data suggest that the drainage pathways originated in organized or diffuse swallets around the Ice-Cave from Poiana Vârtop (including this cave) and are all directed towards the underground stream of Humpleu Cave (Fig. 3).

Description of the cave

The cave was discovered and first mapped by the Speleological Club "Z" Oradea in 1978. In 1985, members of the "Politehnica" Speleological Club discovered the lower part of this large chamber after descending through a narrow "window" opened due to the lowering of the ice block that forms 'the floor' of the Entrance Chamber.

The access to the cave is through a semicircular collapse sinkhole, on the northwestern side of the Vârtop Glade. After a short descent over slide rocks covered by a thin soil layer, the 22 × 5 m cave porch leads to a chamber that hosts a 12,000 m^3 perennial ice block. The *Entrance Chamber* has 60 m in length, a maximum of 25 m in width and about 5 m in height (Fig. 2a).

Along the southeastern wall, three narrow openings (1.5 × 0.5 m) give access to the lower part of the chamber through a 42 m long, steeply descending (40 °) ice slide (Fig. 2b). At the bottom of this chamber large quantities of frost debris are to be found. The lowest point of the cave is –38 m and it was reached in this sector, after descending another 5.5 m long and narrow passage (Fig. 2b).

Mineralogy of speleothems

Only conventional speleothems such as stalactites, flowstones and crusts were noticed in the Ice-Cave from Poiana Vârtop. Most of these speleothems are inactive and deeply corroded.

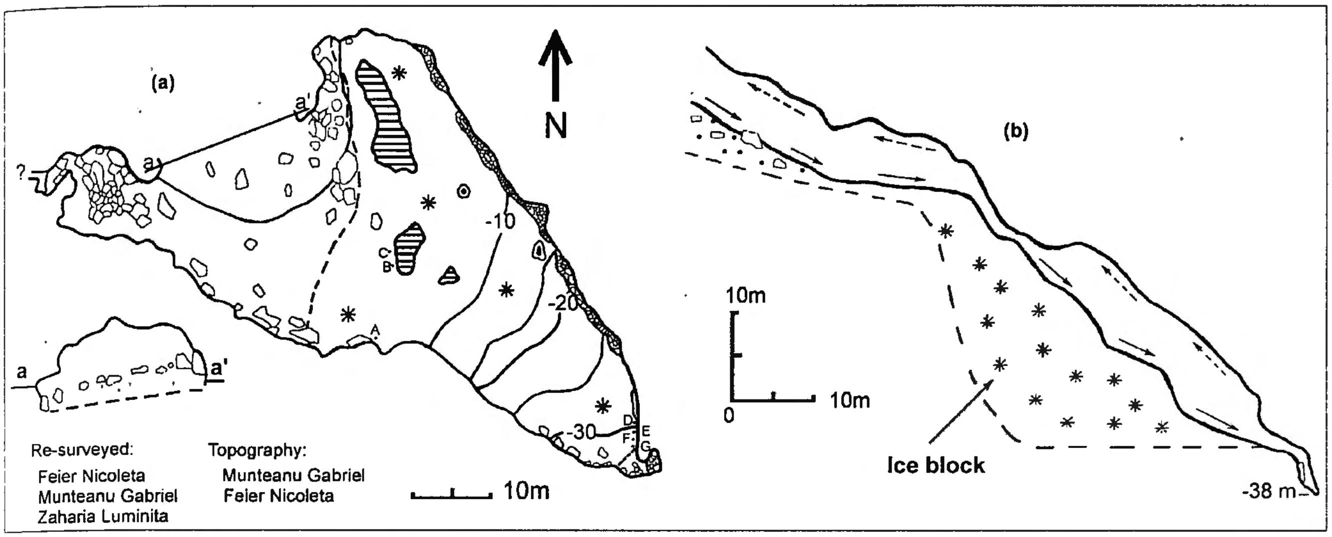

Fig. 2. (a) Map of the Ice-Cave from Poiana Vârtop. A – G = samples points; (b) Cross-section of the cave showing the ice block and the winter air circulation.
(a) Carte de la Grotte-glacière de Poiana Vârtop. A–G = points d'échanntillonage; (b) Section transversale avec la situation du bloc de glace et la circulation d'air en hiver.

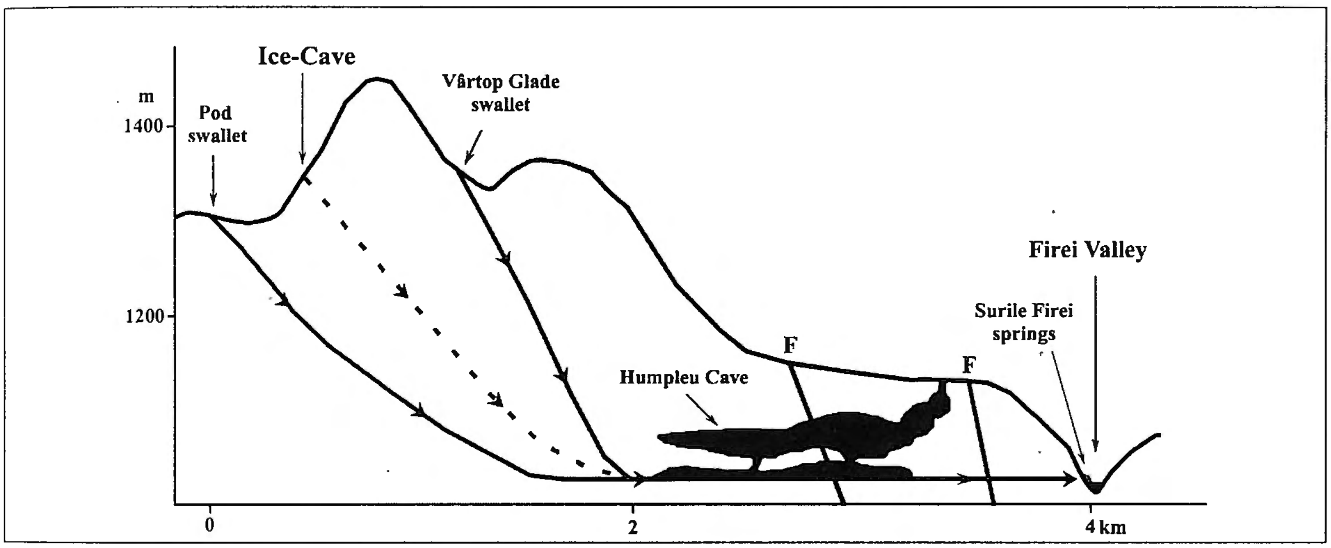

Fig. 3. Simplified hydrogeological transect showing the relationship between Şurile Firei Springs and the main swallets in the area of the Ice-Cave from Poiana Vârtop (Humpleu Cave profile is tentatively located within the cross-section). Note that the vertical scale is exaggerated.
Section hydrogéologique simplifiée montrant la relation entre la source de Şurile Firei et les principaux ponors de la zone de la Grotte-Glacière de Poiana Vârtop (la coupe de la Grotte de Humpleu est figurée de façon approximative). A noter que l'échelle verticale est exagérée.

Macroscopic and optical microscope observations, as well as X-ray diffraction analysis on seven crust samples revealed the presence of the following four minerals: calcite, aragonite, goethite and carbonate-hydroxylapatite. Calcite makes up the bulk of the flowstone, stalactite and corraloid deposits. Aragonite has only been observed in thin sections as layers of minute crystals with radially oriented c-axes that are sandwiched within layers composed of more coarse-grained calcite crystals. Goethite and carbonate-hydroxylapatite speleothems are restricted to very few places within the cave.

As expected, carbonate-hydroxyl-apatite was found as dark brown to black crusts in the near vicinity of an area that was earlier populated by bats. Therefore its origin was related to the reaction of phosphate solutions with limestone. The X-ray pattern shows a number of lines, most of them well marked and sharp. The strongest seven lines are listed in Table 1. The interplanar spacing and intensity values are very close to those recorded for carbonate-hydroxylapatite in the ICDD file 19-272.

Table 1. Comparison of X-ray diffraction lines for carbonate-hydroxylapatite collected in the Ice-Cave from Poiana Vârtop and those from ICDD file.
Comparaison entre les lignes de diffraction en rayons X de la carbonat-hydroxylapatite de la Grotte de Poiana Vârtop et celles des fichiers de l'ICDD.

ICDD 19-272		Sample #1357	
d(Å)	I	d(Å)	I
3.46	25	3.45	13
2.78	100	2.79	100
2.68	40	2,70	25
2.49	6	2.49	15
2.28	6	2.29	17
1.92	16	1.90	17
1.85	10	1.87	15

Goethite crusts form centimeter-size patches on the wall near the bottom of the cave. Oxidation of some pyrite from within the limestone seems to be the source for iron in these speleothems.

Speleogenesis

The cave is developed within an inclined lithologic contact, not far from the base of the aquifer. In vertical projection (Fig. 2b), the cave comprises an inclined passage that shows both phreatic features (pendants, scallops, corrosion pockets) and vadose (newly formed or corroded) speleothems.

Recent observations made within the cave showed that the cave has received substantial amounts of allogenic gravel and sand. This is a situation similar to that encountered in many caves in the neighborhood, including the major cave system of Humpleu-Poienița.

The morphology of the cave suggests that it could have been developed in two distinct phases:

(i) A shallow phreatic stage, when waters collected (diffuse or organized) from Groapa Largă and Vârtop Plateau were drained through the upper passages of Humpleu Cave, to feed small springs along Firei Valley (Fig. 3). This is the stage when gradual removal of the rock by dissolution allowed huge passages to be formed.

(ii) In the second stage, following the connection of the drainage conduit to a major outlet (i.e., Șurile Firei Springs) the cave begun its evolution under vadose conditions (Ford & Williams, 1989). Undercut by free-surface streams, the cave ceiling and wall became weakened fact that led to massive breakdown in the cave. Speleothem deposition is superimposed on the phreatic features. Frost wedging is also a late-stage process that was more effective near the cave entrance, but after accumulation of ice in the cave it became common throughout the cave.

We believe the current entrance has been created by slope processes that enabled mass movement of the limestone bedrock along joints with slippage along bedding planes.

The dye tracing experiments performed by Orăseanu (1996) indicated that the surface streams located at E, NE and N of the Ice-Cave from Poiana Vârtop sink through the swallets in the Groapa Largă area and Vârtop Plateau. Therefore we believe the investigated cave is part of much larger hydrologic karst system that also includes the Humpleu-Poienița cave network.

The entire system discharges at Șurile Firei Springs after crossing Humpleu Cave; the average flow rate measured reaches *c.* 80 l/s (Orăseanu, 1996).

Origin of the ice block

The Ice-Cave from Poiana Vârtop is a descending cavity that opens to the surface only on its upper part. For this reason it belongs to the category of cavities with bi-directional ventilation, in which the active phase is limited to the winter season (Racoviță, 1975). During the winter, cold and dense external air enters the cave and replaces an equivalent volume of relatively warmer underground air (Fig. 2b). In summer this exchange ceases somewhere at the surface of the ice block because the thermal ratio reverses and the cold cave air accumulated throughout the winter cannot rise to the surface. The long-term effect of such a thermo-circulation system is that the cave constantly accumulates cold air, and finally a glacial-type topoclimate is established within the cave. Therefore, one may conclude that cooling by accumulation of cold air represents the mechanism that is responsible for the perennial ice block formation in the Ice-Cave from Poiana Vârtop.

Like in the case of Scărișoara Ice-Cave, melting of snow and ice at the bottom of the cave entrance slope and the percolation water seems to be the source of water that subsequently accumulate in the form of ice layers in the Ice-Cave from Poiana Vârtop.

Unfortunately, the ice block structure is hidden behind a thin ice layer formed during summer when melting waters reach the underground environment with sub-zero temperatures.

The ice block lies in one large chamber occupying 2/3 of its volume. A rough estimation of the overall ice block volume is 12,000 m³, which means that the Ice-Cave from Poiana Vârtop hosts Romania's fourth largest underground glacier after Scărișoara, Focul Viu and Borțig.

Acknowledgements

We are indebted to Dr. Ioan Bucur (University of Cluj) for carrying out the microfacies analyses and to Ovidiu Pop, Jos and Geert Notenboom for their assistance in the field. Vlad Breazu is thanked for providing the GPS data. The fieldwork for this study was partly financed through the ANSTI grant B37/2000 to Tudor Tămaş.

References

Balintoni, I. (1997) *Geotectonica terenurilor metamorfice din Romania*. Ed. Carpatica, Cluj, 176 p.

Bleahu, M.,1 & Bordea, S. (1981) Munţii Bihor-Vladeasa. Ed. Sport-Turism, Bucuresti, 496 p.

Ford, D. C., & Williams, P. W. (1989) *Karst geomorphology and hydrology*. Unwin Hyman, London, 602 p.

Goran, C. (1982) *Catalogul sistematic al peşterilor din România*. ISER & FRTA-CCSS, Bucureşti, 496 p.

Mantea, G. (1985) Geological Studies in the Upper Basin of the Someşul Cald Valley and in the Valea Seacă Region (Bihor-Vladeasa Mountains). *An. IGG*, **68** pp. 1–91.

Orăseanu, I. (1996) Contributions to the hydrogeology of the karst areas of the Bihor-Vladeasa Mountains, Romania. *Theor. Appl. Karstology*, **9**, pp. 185–214.

Racoviţă, G. (1975) La classification topoclimatique des cavités souterraines. *Trav. Inst. Spéol. "E. Racovitza"*, **XIV**, pp. 197–216.

Theoretical and Applied Karstology, 13–14 (2000–2001), pp. 87–92

La genèse et l'évolution des grandes dolines (*obans*) de la zone karstique de Mangalia (Dobroudja du Sud, Roumanie)

Traian Constantinescu & Silviu Constantin*

Institut de Spéologie « Emil Racoviţă », str. Frumoasă 11, 78114 Bucarest 12, Roumanie.

Résumé

Pour expliquer la genèse et l'évolution des grandes dolines ou obanes de la zone karstique de Mangalia, Obanul Mare est le plus représentatif, du fait qu'ici ont été effectués de nombreux forages et qu'à son bord s'ouvre la célèbre Grotte de Movilé. Les sédiments accumulés dans l'oban sont des repères pertinents qui argumentent la genèse du celui-ci par effondrement karstique. Au cours de leur évolution, ces grandes dolines ont connu trois phases principales : de doline-lac, de doline-marécage et de doline-sèche.

Mots clés: oban, obans, doline-lac, doline-marécage, doline-sèche, Mangalia, Grotte de Movilé.

The genesis and evolution of the great sinkholes (obans) from the karst area of Mangalia (Southern Dobrogea, Romania)

Abstract

In order to explain the genesis and the evolution of the great sinkholes or 'obanes' from the Mangalia karstic area, the structure of "Obanul Mare" is discussed based on a series of boreholes and exploration pits and due to its proximity to the Movile Cave. The geological structure of the sediments accumulated in these sinkholes suggests their genesis through a karstic collapse mechanism. Subsequently, the great sinkholes underwent three main evolutionary phases: the "lake-sinkhole" phase, the "swamp-sinkhole" phase and the "dry-sinkhole" phase.

Key words: oban, obanes, lake-sinkhole, swamp-sinkhole, dry-sinkhole, Mangalia, Movile Cave.

La zone karstique de Mangalia se trouve à l'extrémité sud-est de la Roumanie, au bord de la Mer Noire (Fig. 1A). La région présente une horizontalité évidente. Les altitudes absolues sont comprises entre 0 et 40 m.

La morphologie générale montre deux larges vallées, Valea Mangaliei et Valea Obanelor, séparées par un interfluve (Constantinescu, 1989). Dans ces vallées affleurent des calcaires sarmatiens qui ont favorisé la formation d'un exokarst spécifique. Très représentatives sont les dépressions karstiques — grandes dolines dénommées en Dobroudja du Sud « oban »[1]. On peut reconnaître trois secteurs avec de telles dolines, représentant trois complexes exokarstiques dont celui de Movile est le plus important. Il comprend un groupe de trois dolines : *Obanul Mare*, *Obanul Mic* et *Obanul Blebea* (Constantinescu, 1995, Fig. 1).

Obanul Mare où se trouve la *Peştera de la Movile* (La Grotte de Movilé) est le plus représentatif pour la genèse et l'évolution de toutes ces grandes dolines. L'Institut d'Etudes et Projets d'Aménagements Fonciers (l'ISPIF) et l'Institut Géologique ont effectué en deux reprises, en 1986 et 1994, des forages et des puits qui ont apporté des données nouvelles sur sa structure de profondeur.

[1] oban (sing.) = grande doline ; on propose de maintenir le mot roumain ainsi : oban (sing.), obanes (pl.). En Roumain, le pluriel se prononce : « obánê ».

* corresponding author. *E-mail address*: Silviu.Constantin@geol.uib.no

La morphologie générale de Obanul Mare

Dans le cadre du complexe de Movilé, Obanul Mare s'impose d'emblée par la morphologie des deux composantes : *la bordure* et *la dépression proprement dite*.

1. **La bordure,** avec une largeur de 40–70 m, est composée essentiellement de calcaires sarmatiens et s'élargit progressivement vers le sud. Notons que la morphologie de la bordure sud a subi des changements importants après 1989, car plusieurs petites dolines ont été totalement colmatées par les déchets apportés de la ville Mangalia.

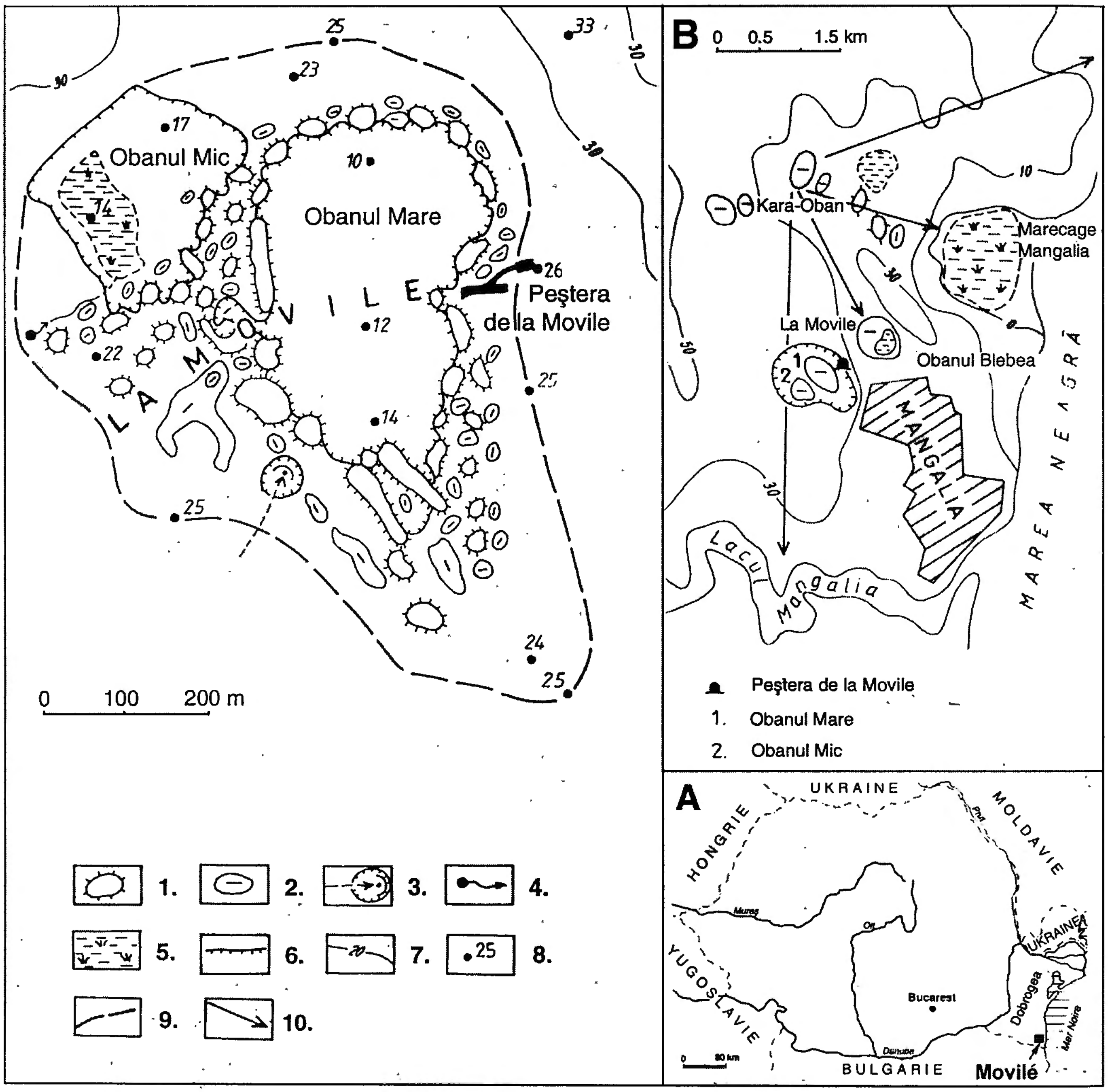

Fig. 1. Carte géomorphologique de la zone karstique d'Obane. Position de la zone de Movile en Roumanie (A) et dans la région de Mangalia (B). 1.« Movilé » (monticule calcaire conique) ; 2. Doline ; 3. Doline-ponor ; 4. Source permanente ; 5. Marécage ; 6. Abrupt ; 7. Courbe de niveau ; 8. Cote ; 9. Limite de l'ouvala de « La Movile » ; 10. Drainage souterrain démontré.
Geomorphic map of the karstic area of Obane. General location of the Movile area within Romania (A) and within the region of Mangalia (B). 1. "Movile" (conical limestone hillock); 2. Sinkhole; 3. Swallet-sinkhole; 4. Perennial spring; 5. Swamp; 6. Cliff; 7. Contour; 8. Elevation; 9. Limit of the "La Movile" ouvala; 10. Proved underground drainage.

La spécificité de la morphologie est donnée par l'ensemble « movilés » (= monticules)–dolines. L'altitude absolue la plus élevée, de 29,0 m, a été mesurée sur un monticule situé entre l'Obanul Mare et l'Obanul Mic. Les plus grandes dolines, par exemple celles qui se trouvent dans la partie sud, sont le résultat d'effondrements de la voûte des vides souterrains. Les autres sont l'effet de la présence de vides souterrains de dimensions plus petites (semblables à celles de la Grotte de Movilé), qui n'ont pas subi encore des effondrements karstiques.

2. **La dépression proprement dite** a une dénivellation générale de 10–14 m. La plus petite altitude absolue, de 9,5 m (c'est-à-dire la plus grande profondeur de l'oban) se trouve dans la partie nord-est. La dénivellation maximum dans le cadre de l'oban est donc de 19,5 m. Le fond de la dépression présente un petit soulèvement dans la partie centrale (13–14 m au centre et 10,0–10,5 m à la périphérie).

Résultats des forages de Obanul Mare

Initialement, l'oban a eu une profondeur plus grande qu'aujourd'hui, mais il a été colmaté avec des matériels lœssoïdes, transportés par le vent et des argiles lacustres. La présence des ces dépôts a été démontrée lors des forages effectués par l'ISPIF en 1986 (coordonateur Emanoil Constantinescu ; GEORGESCU *et al.*, 1987), qui ont permis de préciser que leur épaisseur dépasse 70 m (Fig. 2). L'analyse sommaire des dépôts a mis en évidence deux niveaux de sédiments, différenciés au point de vue minéralogique et de la texture, fait très important pour expliquer la genèse et l'évolution de l'oban.

Le niveau supérieur dont l'épaisseur est de 15–20 m, est constitué principalement de sols fossils développés sur des dépôts lœssoïdes. La présence des dépôts lœssoïdes solifiés indique l'existence d'une dépression qui a été colmatée avec les dépôts mentionnés. Les dépôts ont des couleurs diverses (variant du brune au jaunâtre). Les horizons de sols fossiles, correspondent aux diverses phases climatiques dans l'évolution de l'oban.

Il faut mentionner que dans la partie inférieure de ce niveau on a trouvé des blocs calcaires non altérés, qui peuvent représenter les dépôts d'effondrement karstique les plus récents.

Le niveau inférieur est constitué de dépôts argileux ayant une épaisseur de 25–30 m, composé de divers horizons d'argiles avec des intercalations des blocs calcaires. Théoriquement, ces dépôts peuvent se former, au moins partiellement, par la dissolution des calcaires sarmatiens mais leur structure, les couleurs et leur disposition spatiale (Fig. 2) suggèrent qu'ils peuvent être, en partie, allochtones.

A ce niveau tous les forages ont intercepté des blocs calcaires faiblement altérés ou même non-altérés ayant des épaisseurs qui varient entre 0,5 et 2 m.

La genèse et l'évolution d'Obanul Mare

On a anticipé que l'Obanul Mare est le résultat d'un effondrement karstique (CONSTANTINESCU,1989; LASCU, 1989). Nous nous bornons à mentionner maintenant deux arguments à l'appui de cette hypothèse:

- la présence des fragments (gros blocs) calcaires non-altérés dans les deux niveaux des dépôts;
- la présence de la Grotte de la Movilé — fragment d'un cavernement plus grand qui existait avant l'effondrement karstique, ainsi que la présence d'autres vides karstiques intersectés par les forages.

En conséquence, nous considérons que l'évolution d'Obanul Mare a connu trois phases principales.

Initialement, dans l'espace de l'oban actuel, il a eu un cavernement qui avait au moins deux niveaux. Le niveau inférieur était actif, c'est-à-dire traversé par des rivières souterraines. Bien que la Galerie Principale de la Grotte de Movilé ait une direction O–E et que, sur le même axe et au même niveau les forages F102 et F109 ont intercepté des vides souterrains (voir Fig. 2), on ne peut pas affirmer avec certitude que l'orientation principale du drainage souterrain était la même. Au contraire, les traçages effectués dans le Complexe de Kara-Oban par GASPAR & ORĂSEANU (1997) ont démontré une direction d'écoulement N–S, vers le Lac de Mangalia, à travers Obanul Mare (voir Fig. 1B). Il est donc raisonnable de supposer que le drain principal a été orienté selon cette direction et que la grotte de Movile ne représentait qu'un réseau secondaire dans l'ensemble du cavernement général.

a) **La Phase de Lac**. Après l'effondrement karstique, une dépression s'est formée (l'oban) et la continuité du cavernement a été interrompue. Le réseau des galeries a été détruit et les rivières souterraines ont été fragmentées en tronçons. En s'accumulant dans l'espace de l'oban, l'eau des ces rivières a formé un lac.

Certainement, une partie des eaux a continué à s'infiltrer dans le réseau souterrain ou directement dans les calcaires du fond de l'oban, mais le débit de ces infiltrations était plus faible que celui des rivières qui s'y déversaient. Le lac pouvaient être alimenté aussi par des sources mésothermales ascensionnelles comme, par exemple, la source interceptée par le forage F103 (voir Fig. 2). De telles sources puissantes sulfureuses, mésothermales et ascensionnelles sont présentes aujourd'hui encore dans l'Obanul Blebea, le Marécage de Mangalia et dans le Lac de Kara-Oban (LASCU *et al.*, 1995).

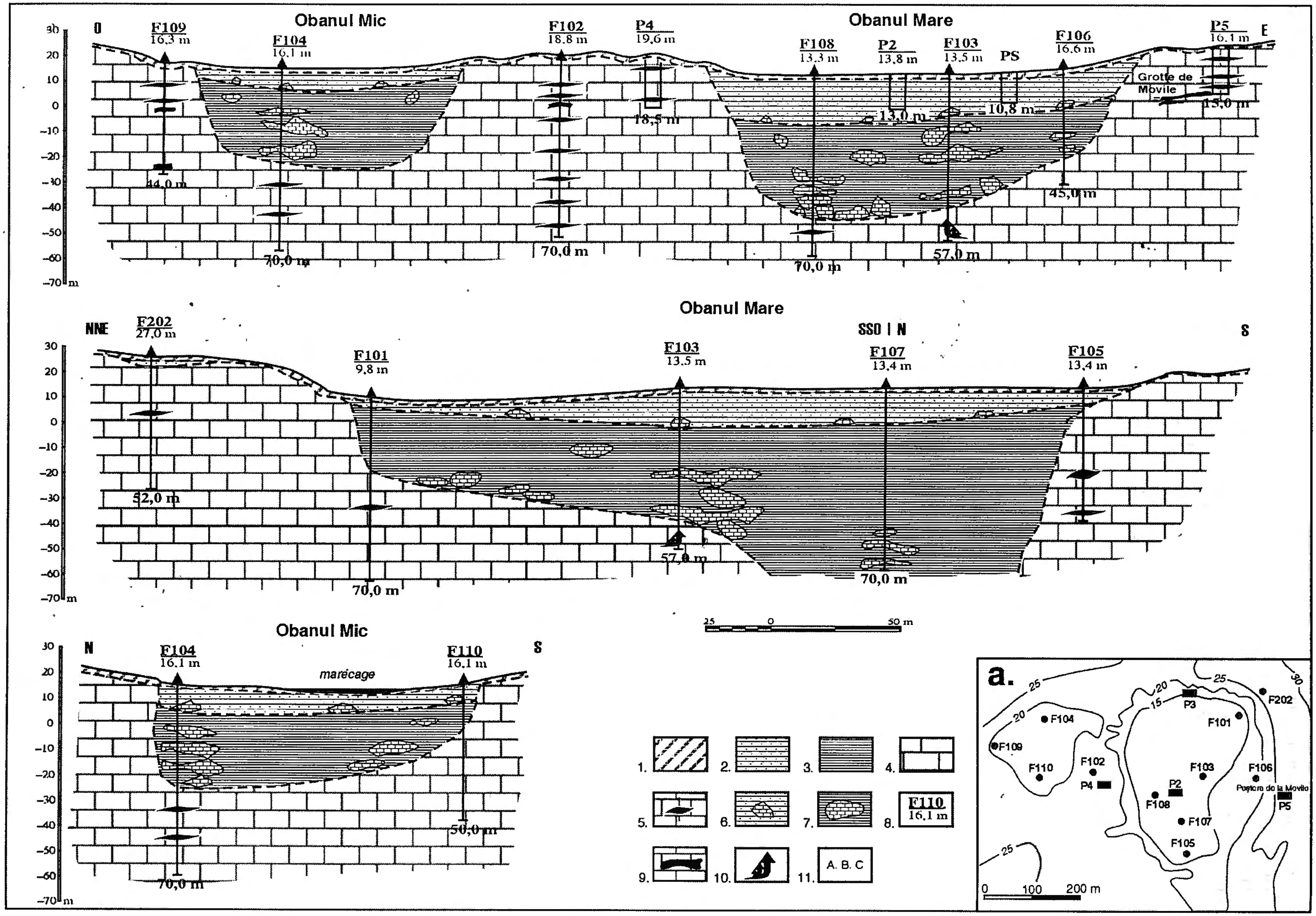
Obanul Mic
Obanul Mare
O
E
F109
16,3 m
F104
16,1 m
F102
18,8 m
P4
19,6 m
F108
13,3 m
P2
13,8 m
F103
13,5 m
PS
F106
16,6 m
P5
16,1 m
Grotte de Movile
44,0 m
70,0 m
70,0 m
18,5 m
13,0 m
10,8 m
15,0 m
45,0 m
57,0 m
70,0 m
Obanul Mare
NNE
F202
27,0 m
F101
9,8 m
F103
13,5 m
SSO | N
F107
13,4 m
F105
13,4 m
S
52,0 m
70,0 m
57,0 m
70,0 m
Obanul Mic
N
F104
16,1 m
marécage
F110
16,1 m
S
50,0 m
70,0 m
25
0
50 m
1.
2.
3.
4.
5.
6.
7.
8.
F110
16,1 m
9.
10.
11.
A. B. C
a.
25
20
15
30
P3
F202
F104
F101
F109
F110
F102
P4
F103
F106
P2
Peștera de la Movile
P5
F108
F107
F105
0
100
200 m

Fig. 2. Sections géologiques à travers les « obans » d'après les données de forages de l'ISPIF (interprétées par les auteurs). En vignette (a), plan de situation des forages et des puits. F=forage ; P=puits. Les chiffres placés en bas des forages indiquent la profondeur de ceux-ci. 1. Sols actuels; 2. Sols fossiles; 3. Dépôts argileux; 4. Calcaires du Sarmatien; 5. Intercalations argileuses; 6. Fragments calcaires non-altérés; 7. Blocs calcaires faiblement altérés ou non-altérés; 8. Altitude absolue des forages (puits); 9. Vides karstiques ; 10. Source mesothérmale ; 11. Horizons des sols.

Geologic profiles through the "obans" interpreted by the authors after the data of exploratory boreholes and wells of ISPIF. Inset (a) shows the situation of the boreholes and wells. F=borehole; P=well. The numbers at the bottom of the boreholes indicate their final depth. 1. Holocene soil; 2. Fossil soil; 3. Residual clayey deposits; 4. Sarmatian limestones; 5. Clayey intercalations; 6. Unaltered fragments of limestone; 7. Slightly altered or unaltered limestones; 8. Absolute altitude of the boreholes (wells); 9. Karstic voids; 10. Mesothermal source intercepted by the borehole; 11. Soil horizons.

La phase de lac a été, donc, la première dans l'évolution de l'oban. A ce temps là, la Grotte de Movilé se trouvait au-dessus du niveau de lac (le fond de l'oban) et communiquait probablement avec l'extérieur.

b) **La Phase de Marécage**. L'assèchement du lac a été déclenché par :

- l'accumulation des dépôts argileux et/ou lœssoïdes dans l'espace de l'oban qui a barré progressivement les sources ascensionnelles de l'aquifère mésothermale, sulfureux;
- une possible infiltration de l'eau du lac vers l'aquifère karstique, favorisée par la texture poreuse des calcaires lumachelliques du Sarmatien ;

En même temps, des dépôts lœssoïdes colmataient graduellement l'oban, de sorte que sa profondeur a été diminuée et le lac a été graduellement transformé en marécage. Dans cette phase, il est très probable que le fond de l'oban a été soulevé jusqu'au niveau de la grotte et même au-dessus de celui-ci, en interromprant ainsi sa communication avec l'extérieur mais, théoriquement, en phase de marécage l'interruption de la liaison avec l'extérieur pouvaient n'être que temporaire.

c) **La Phase d'Oban Sec**. En suivant la diminution du débit d'alimentation l'oban est resté à sec. Le colmatage avec des dépôts lœssoïdes a continué et le fond de l'oban a été soulevé au-dessus du niveau de la grotte, qui a été fermée, situation qui se maintient jusqu'à aujourd'hui.

Conclusions

On peut affirmer que dans son évolution, l'Obanul Mare a parcouru trois phases principales : oban-lac, oban-marécage, oban-sec.

En l'absence des preuves certaines en faveur de l'existence de ces phases, la présence dans la région d'autres « obans » se trouvant en différentes phases de colmatage, peut être considérée comme un argument pertinent. Par exemple, la phase d'oban-lac est représentée actuellement par le lac de Kara-Oban, la phase de marécage par la Mlaştina (=Marécage) de Mangalia et par Obanul Mic (Fig. 3) et la phase d'oban sec, par Obanul Mare (Fig. 4).

Le cavernement initial a été creusé par l'eau de l'aquifère mésothermal, ascensionnel de la Dobroudja du Sud. Ce cavernement

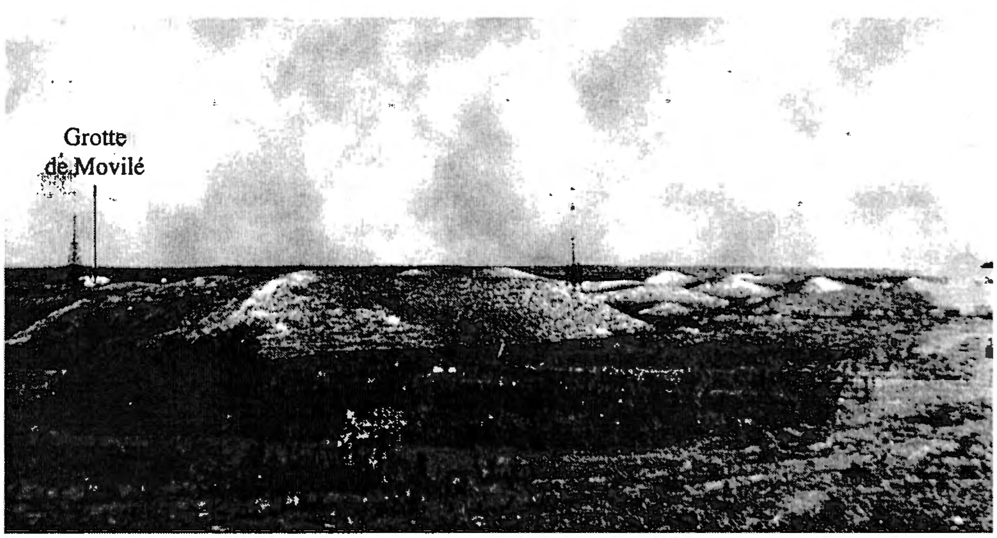

Fig. 3. Obanul Mic (phase de marécage) et la bordure sud d'Obanul Mare.

Obanul Mic (swamp phase) and the southern margin of the Obanul Mare.

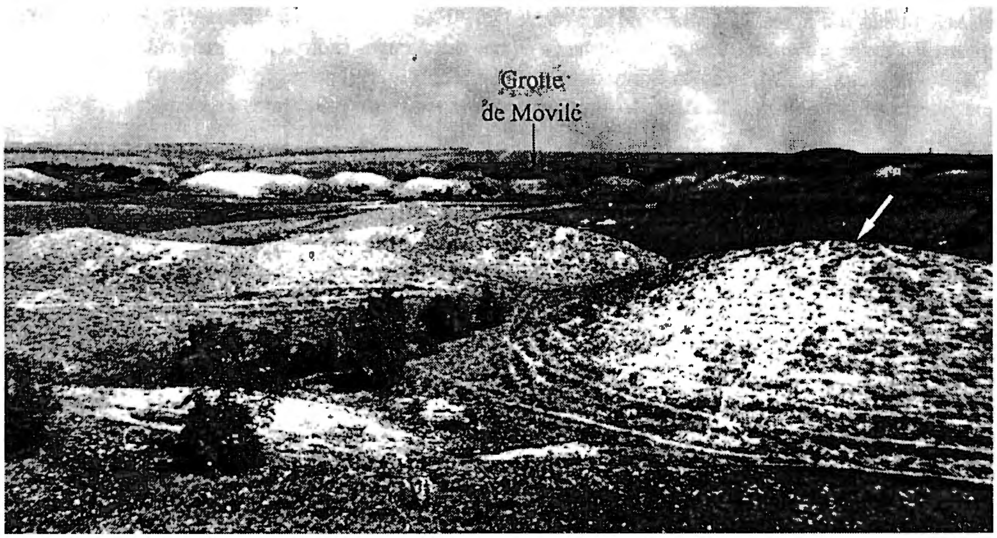

Fig. 4. Obanul Mare: la dépression proprement dite (phase d'oban-sec) et la bordure est. La flèche blanche indique le plus haut monticule (29,0 m) de la zone.

Obanul Mare : the depression (dry oban phase) and the eastern margin. The white arrow indicates the highest hillock of the area (29.0 m asl.)

a été détruit par effondrement karstique. La formation du niveau inférieur, des sédiments argileux, peut être partiellement attribuée à la dissolution des calcaires. A cet égard, on peut rappeler que tous les forages ont intercepté des intercalations argileuses lenticulaires dans les calcaires sarmatiens (Fig. 2). Mais la plupart des sédiments argileux, qui forment aujourd'hui un mélange avec des blocs calcaires ont été déposés dans des lacs formés dans l'espace des obanes. En dessous de ces dépôts, la karstification des calcaires sarmatiens a continué jusqu'à présent.

Compte tenu de l'épaisseur des dépôts identifiés dans les forages on peut affirmer que la profondeur maximale de l'Obanul Mare a été de plus de 70 m, dans sa partie sud (F107).

Par colmatage graduel, le lac s'est transformé en marécage et, ultérieurement, il a séché complètement; la partie supérieure des dolines a été remplie de dépôts lœssoïdes qui ont «coupé» aussi la communication avec l'extérieur de l'étage supérieur du cavernement, dont la grotte de Movilé en fait partie.

Bibliographie

Constantinescu, T. (1989) Considerations sur la zone karstique " La Movile" (Mangalia, Dobrogea de Sud, Roumanie), *Misc. Speol. Romanica*, **1**, pp.7–17.

Constantinescu, T. (1995) Le karst de type Movilé (Mangalia,Dobrogea de Sud, Roumanie). *Theor. Appl. Karstology*, **8**, pp.91–96.

Gaspar, E., & Orăseanu, I. (1987) Natural and artificial tracers in the study of hydrodynamics of karst. *Theor. Appl. Karstology*, **3**, pp. 31–107.

Georgescu, I., Trifan, L., Constantinescu, E., & Seletchi, E. (1987) Cercetarea complexă a unui amplasament în condiţii geologice speciale, în zona CET-Mangalia. *Lucrările ISPIF*, pp. 101–109.

Lascu, C. (1989) Paleogeographical and hydrogeological hypothesis regarding the originof a peculiar cave fauna. *Misc. Speol. Romanica*, **1**, pp 13–18.

Lascu, C., Popa, R., & Sârbu, S. (1995) Le karst de Movile (Dobrogea de Sud) (I). *Revue Roum. Géogr.*, **38**, pp.86–93.

Theoretical and Applied Karstology, 13–14 (2000–2001), pp. 93–99

24 h Tracer Tests on Diurnal Parameter Variability in a Subglacial Karst Conduit: Small River Valley, Canada

Jan-Henning Ross[1]*, Feride Serefiddin[2], Michael Hauns[3] & Chris C. Smart[4]

[1] *Göttelmann + Ross, Beratende Geowissenschaftler, Schulstrasse 4, D-78462 Konstanz, Germany.*
[2] *School of Geography and Geology, McMaster University, 1280 Main Street, West Hamilton ON L8S4M1, Canada.*
[3] *Institut für Hydrologie, Universität Freiburg, Fahnenbergplatz, D-79098 Freiburg, Germany.*
[4] *Department of Geography, University of Western Ontario, London Ontario NGA 5C2 Canada.*

Abstract

Repeated dye tracer tests were undertaken for two complete diurnal discharge cycles at Small River Glacier, British Columbia. The injection site is a well developed glacier moulin. Monitoring was done at a karst spring in a cave entrance 1530 m down valley. The spring is the major outlet of glacial meltwater and also drains karstified glacier forefields. High flow velocities and low dispersivities indicate a very well developed conduit flow system. Discharge and velocity show strong diurnal cycles and are controlled by the amount of meltwater. The relationship of increasing velocity with discharge is approximately linear. Dispersivity values do not show any significant variation under diurnal discharge cycles. These results show the importance of diurnal variation in a transient groundwater system.

Keywords: subglacial karst hydrogeology, diurnal discharge-velocity relationships, tracer tests.

Tests de traçage de 24 heures sur la variabilité des paramètres journaliers dans un conduit karstique sous-glaciaire: Small River Valley, Canada

Résumé

Des expériences de traçage au cours de deux cycles journaliers complets ont été entreprises sur la Small River Valley de British Columbia. Le point d'injection est un moulin glaciaire bien développé. Le traceur a été monitorisé 1530 m en aval, dans la source karstique d'une grotte. La source est une exutoire majeur de l'eau de fusion de la glace qui draine aussi des terrains karstifiés non-glaciaires. Les vitesses d'écoulement élevées et les dispersivités basses indiquent un système d'écoulement par conduits très bien développé. Les débits et les vitesses sont fortement variables au cours d'un cycle journalier et sont contrôlés par la quantité d'eau de fusion. La relation entre la vitesse d'écoulement et le débit est presque linéaire. La variation des valeurs de la dispersivité n'est pas significative au cours des cycles journaliers. Les résultats montrent l'importance de la variation diurne dans un système phréatique en régime transitoire.

Mots clés: hydrogéologie karstique sous-glaciaire, relation débit diurne-vitesse d'écoulement, tests de traçage.

Introduction

Glaciers are well known as highly dynamic hydrologic systems with strong seasonal and diurnal discharge variation. Cyclic changes in key climatic factors such as radiation and temperature cause a transient flow system. Seasonal development of a glacial flow system is e.g. described by Hock & Hooke (1993). Nienow *et al.* (1996) focused on diurnal cycles in a glacial system. Smart (1983, 1997) examined the influence of glacier hydrology on subglacial karst systems at Castleguard Cave and at Small River Glacier. Glacial meltwater is the main input source to these karst systems. Discharge variations of glacial meltwaters stimulate the flow regime in subglacial karst systems. Thus discharge of subglacial karst springs is linked to variations in the system feeding glacier discharge.

* corresponding author. *E-mail address*: ross@geowissenschaftler.de

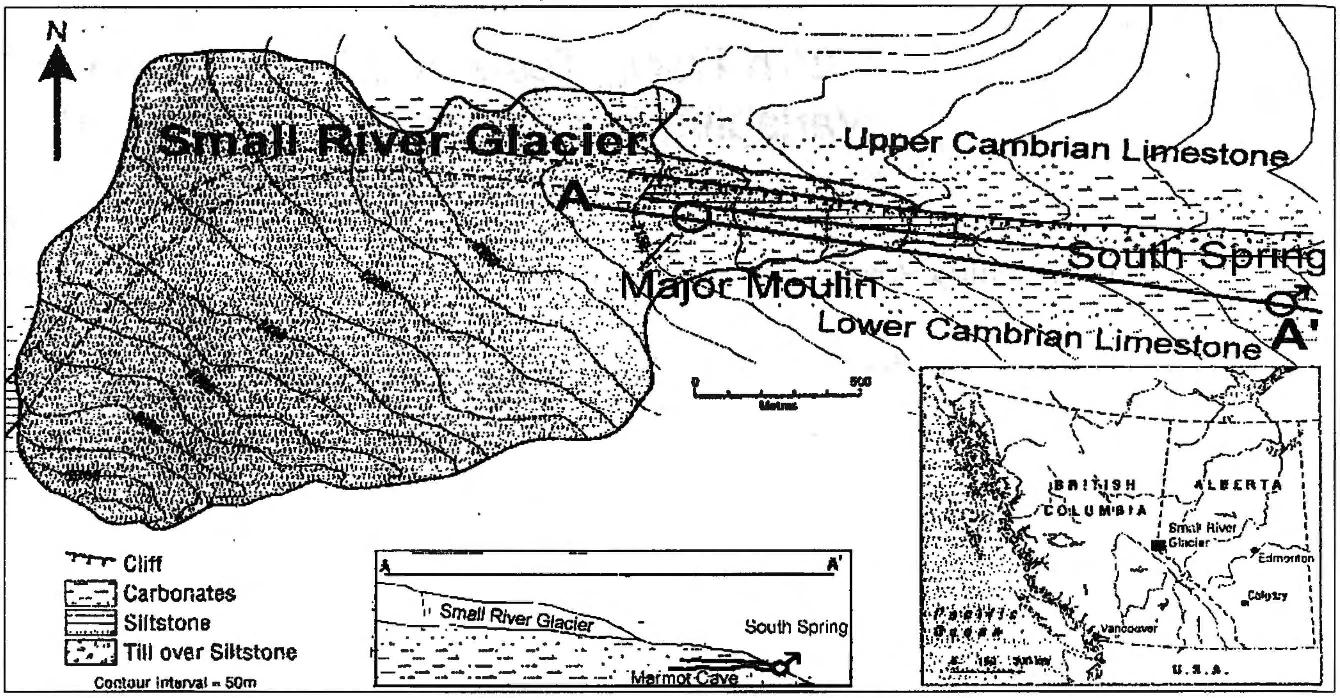

Fig. 1. Small River Glacier with underlying geology and cross-section from the tracer injection moulin to South Spring (based on SMART, 1996 and ORWIN, *pers. comm.*).
Situation géologique de la Small River Valley et section entre le moulin d'injection du traceur et le South Spring (d'aprés SMART, 1996 et ORWIN, comm. pers.*).*

Small River Glacier is a temperate glacier in the Western Canadian Rocky Mountains of British Columbia (Fig. 1). The glacier surface is 2.5 km^2 from 1900 m up to 2900 m a.s.l. The glacier is underlain by two northeastward dipping karstified carbonate units of the Cambrian Mural Formation. Most meltwater is drained by the karst system. About 1 km east from the glacier snout South Spring emerges at the entrance of the fault guided conduit system of Marmot Cave. South Spring is the major outlet of glacial meltwater from the main glacier area and drains some karstified glacier forefields as well. The catchment area of South Spring and its drainage properties of the glacier had been examined by previous investigations (LOWE, 1983; ZABO, 1995; SMART, 1997). Field work took place in the summer of 1999.

Objectives

Dynamic behaviour and the extremely high variability of karst hydrological systems and glaciers are well known. In most cases research is carried out for different events with not necessarily with the same border conditions each time. The scope of our experiments was to examine the diurnal variability of run-off processes within the short time range of entire 24 hour diurnal cycles. The objective was to observe parameter behaviour under transient flow conditions and within one hydrologic diurnal event. The primary methods of investigation were discharge gauging and short-term replicate tracer tests. The obtained data might provide an idea on the variability of hydrogeological parameters within the short-time range of an entire diurnal cycle.

Experiments

The first step was a check of the hydrologic drainage patterns from the glacier under low flow and flood conditions with several single tracer tests. These tracer tests proved that the previously investigated glacier-karst flow path (SMART, 1997; ZABO, 1995) was still existent and the possibility of replicate tracer injections of 2 hour intervals without interference of the previous tracer tests. The second step was the installation of a water level datalogger (Campbell CR 10) at South Spring. Stage/discharge relation was determined by tracer dilution gaugings from the final cave gallery to the spring (*c.* 150 m distance).

A large moulin in the middle of the main glacier lobe was selected as the injection site (cross-section in Fig 1). This glacier moulin drained the most important supraglacial stream. Major moulin is close to an englacial watershed (ZABO, 1995) and airborne photographs show a major faultzone in the bedrock of this area. Meltwater is likely to be drained after a short passage from the englacial conduit system towards the karst system.

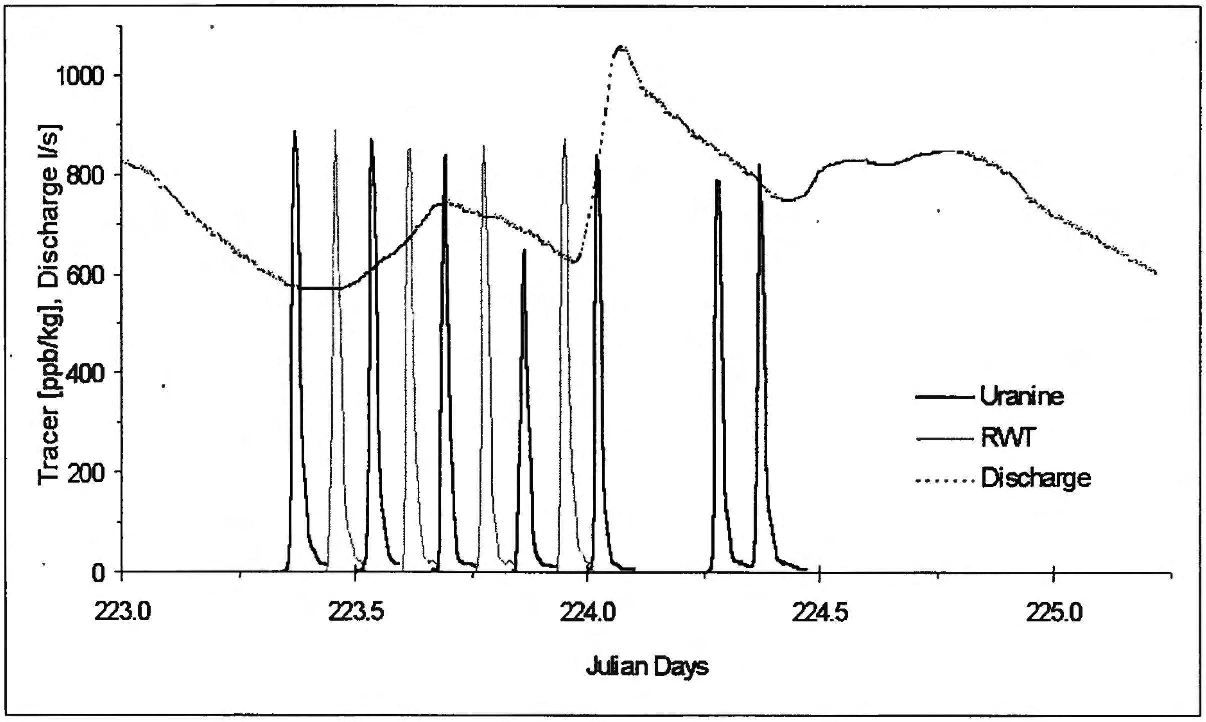

Fig. 2. Tracer breakthrough curves on 11/12 August and discharge. Rising discharge in the afternoon of Julian day 223 is a regular meltwater pattern. The bigger flood during the night to day 224 is due to a thunderstorm.

Courbes d'apparition du traceur durant la nuit de 11/12 Août et variation du débit. L'augmentation du débit l'après-midi du 223-e jour julien appartient au modèle normal de fusion. La crue enregistrée la nuit du 224-e jour a été provoquée par un orage.

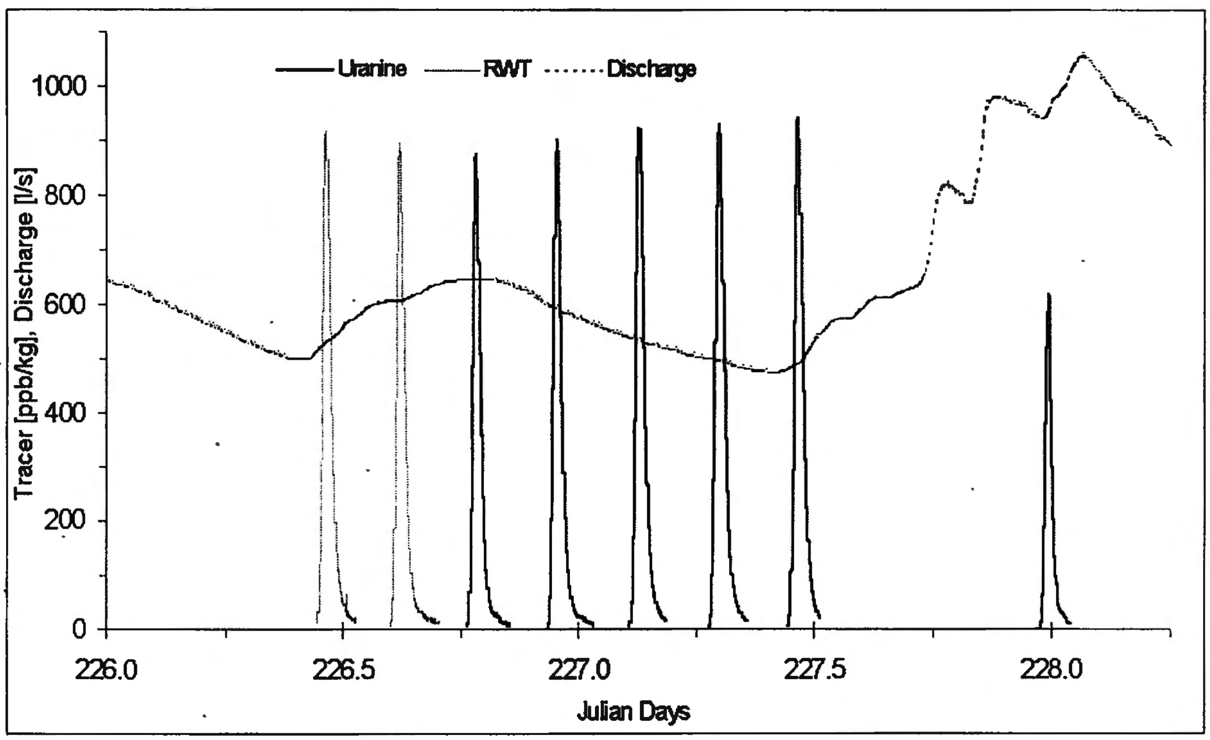

Fig. 3. Tracer breakthrough curves on 14/15 August and discharge. Rising discharge in the afternoon of Julian day 226 is a regular meltwater pattern. A storm flow event causes the next flood on day 227/228.

Courbes d'apparition du traceur durant la nuit de 14/15 Août et variation du débit. L'augmentation du débit l'après-midi du 226-e jour appartient au modèle normal de fusion. La crue enregistrée la nuit 227/228 a été provoquée par un forte pluie.

Tracer monitoring was done with a CGUN-FL02 flow-through field fluorometer (Schnegg & Doerflinger, 1997). Tracer concentrations were recorded with a time step of 4 minutes (test I) and 10 seconds (test II) with this device. Alternating applied tracers were the fluorescent dyes Rhodamine WT (RWT) and Uranine. 13 injections were made within 24 hours (including a 6 hour gap due to a thunderstorm) with 2 hour intervals from 11th to 12th of August 1999 (Fig. 2). A second diurnal cycle was traced on 14th and 15th August 1999 with 7 injections and 4 hour intervals (Fig. 3). A single test was added after storm flow on the evening of the 15th. During the replicate tracer injections discharge of the supraglacial stream was in the range of 50 l/s to 80 l/s with peak flow in the afternoon. Tracer injection mass varied from 0.08 kg to 0.18 kg. In Fig. 2 and 3 tracer concentrations are divided by injection mass in order to compare breakthrough curves of different tracer tests.

The following flow parameters were estimated by tracer breakthrough curves:

1. Time between dye injection and arrival time of the tracer peak at detection site.
2. Flow velocities (assuming a triangulated straight-line of 1530 m from moulin to spring, hence the true distance remains unknown).
3. Dispersion coefficient, which describes the dispersion of the tracer during the discharge process according to analytical solutions of Maloszewski & Zuber (1990), implemented in the model code TRACI (Werner, 1997) and by Sauty & Kinzelbach (1988) (implemented by Hauns & Jeannin, 2000).

Dispersivity is represented by the spreading of tracer within one flowpath. The dispersivity is equal to dispersion divided by mean velocity.

Results

Spring discharge

Discharge at South Spring shows regular diurnal changes from low flow in the morning to peak flow in the evening as a consequence of daily glacial ablation. During the 1999 monitoring period discharge varies from 450 l/s to 1050 l/s. In previous years recorded floods were up to 1500 l/s. Water temperature was very stable at ca. 1.6 °C. Electrical conductivity was about 40 µS/cm with slight anti-cyclic alterations. Water turbidity was about 3 NTU. This regular diurnal pattern is displaced by stormflow events leading to quick flood reactions at the karst spring. During those events there is a minor increase in electrical conductivity. A much more significant reaction to stormflow events is shown by turbidity, which increases by more then 10 NTU (Fig. 4).

Dye tracer tests

Injected tracer arrives very quickly at the spring after a flow time of 2–3 hours. Maximum flow velocities are in the range of 540 m/h and 746 m/h while corresponding peak flow velocities were between 472 m/h and 643 m/h. The peak of the breakthrough curve is very sharp and quick with a short, steep tailing. The breakthrough curve finishes after a short period, this means there is only a small retardation of dye within the conduit system. Calculated dispersion is in the range of 0.2 m^2/s to 0.5 m^2/s and dispersivity is about 2–3 m. These high flow velocities and low dispersivitiy values indicate a very well developed conduit system. Flow conditions are close to piston-flow (Fig. 2, 3, 4. and 6).

Flow velocities vary as a consequence of diurnal discharge variations, but without any extreme changes. There is a strong linear correlation between discharge and flow velocities at both events (Fig. 5). Peak flow velocities (V_{peak}) can be described with the following relation to discharge Q (correlation coefficient $r^2 = 0.98$):

$$V_{peak} = 0.36Q + 311$$

This correlation is valid, of course, only within the observed discharge range. Significant hysteresis effects, as described for diurnal variations of flow velocities in englacial conduits by Nienow *et al.* (1996) were not observed at South Spring. Diurnal hysteresis effects in englacial systems are caused by changes of the englacial flow patterns. Most of the South Spring conduit system is within the karstified limestone and only some 100 m of the passages are estimated to be within the ice.

No meaningful correlation for the variation of dispersivity values and diurnal discharge cycles was found. Differences between single values are not much larger than the results of replicate fitting approaches. All observed dispersivity values represent very well developed flow conditions (Fig. 6). Linear changes in flow velocities and stable dispersivity values indicate a stable conduit flow system without significant changes in flow paths. Hydraulic border conditions appear to be stable within the observed discharge ranges stable and a high percentage of the conduit system might be phreatic. This interpretation fits direct observations in Marmot Cave: South Spring emerges from a siphon in the cave entrance area, *c.* 50 m further on the cave river is accessible again, but soon disappears under another siphon. Hence the experiments were performed during medium discharge rates, extreme events might show different parameter behaviour.

Compared to other karst conduit systems South Spring flow velocities are very high and have extremely low dispersivities. The karst conduit system of the Rinquelle (Swiss Alps) has flow velocities in the magnitude of 111 m/h to 263 m/h and higher dipersivities (Rieg, 1994). This applies to most karst conduits of the Swabian Alb, Germany (Jakowski, 1995), too.

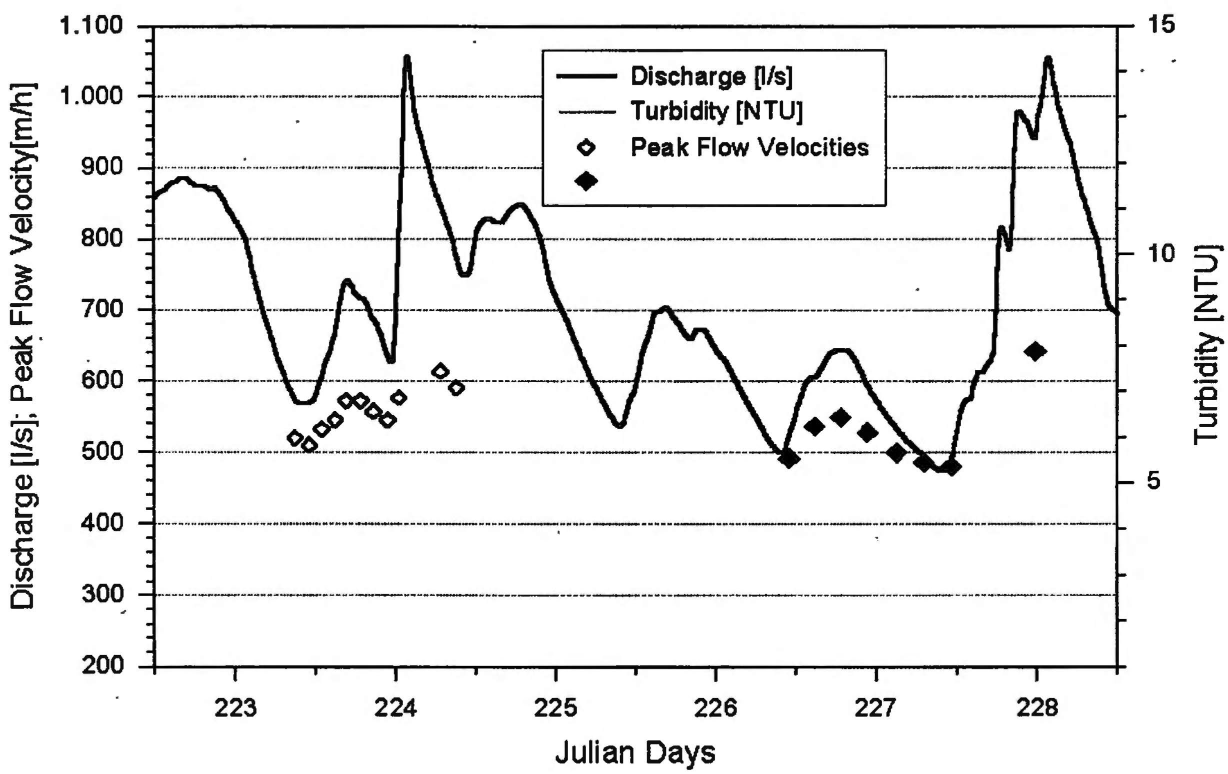

Fig. 4. Diurnal patterns of discharge, turbidity and flow velocities at South Spring.
Modèle des variations journalières du débit, de la turbidité et des vitesses d'écoulement de South Spring.

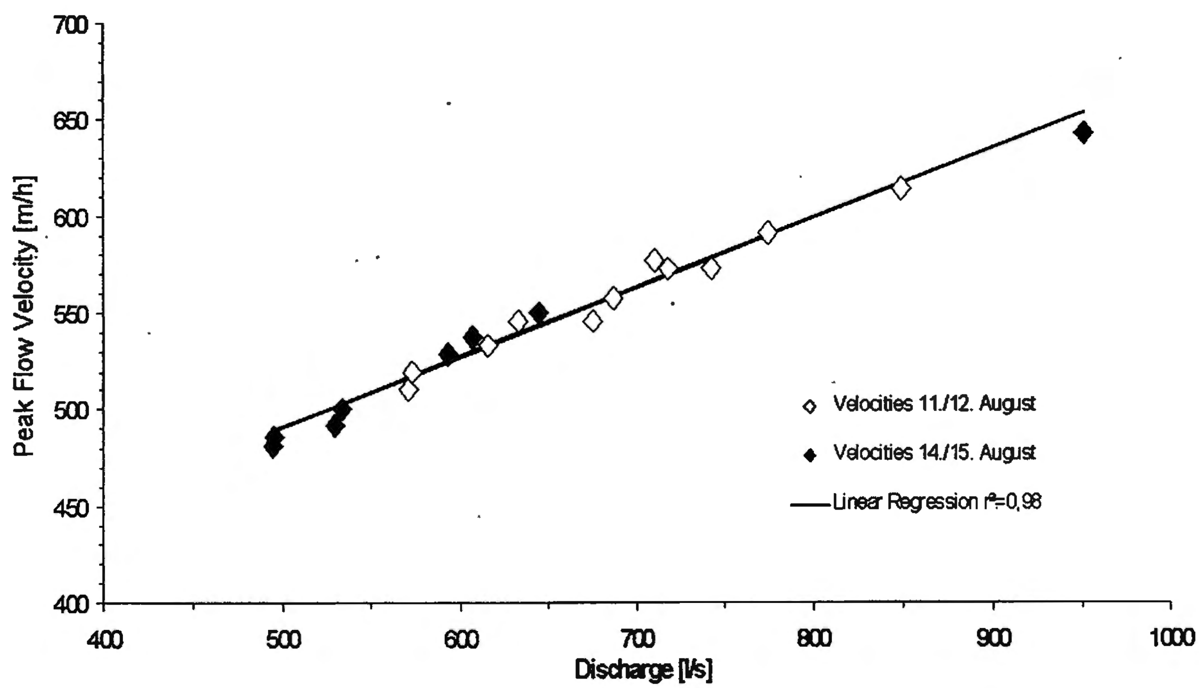

Fig. 5. Scatter-plot of peak flow velocities and discharge. Flow velocities vary significant as a consequence of discharge variations.
Diagramme de corrélation entre les vitesses d'écoulement maximales et le débit. Les vitesses d'écoulement sont fortement influencées par les variations du débit..

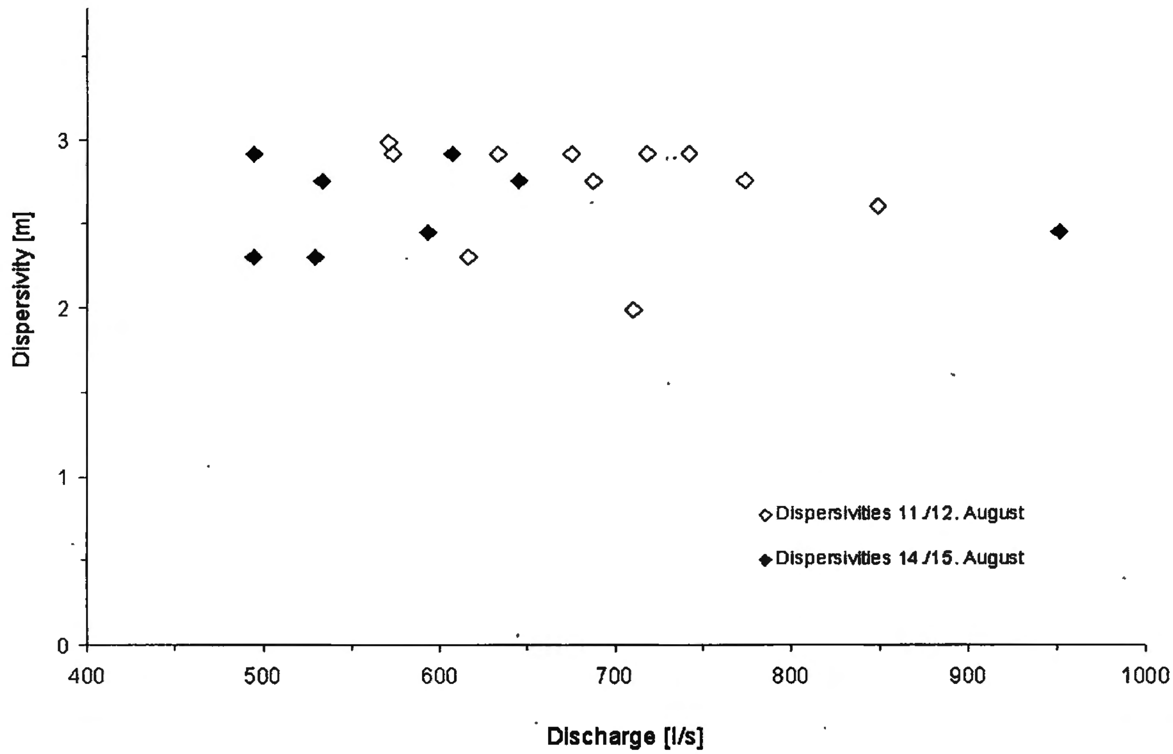

Fig. 6. Scatter-plot of dispersivities and discharge. Low and almost constant dispersivity values are indicating a well developed conduit system.
Diagramme de correlation entre les dispersivités et le débit. Les dispersivités basses et presque constantes indiquent un système de conduits bien développé.

Conclusions

Case study Small River Valley

The spatial scale of South Spring at Small River Glacier makes this site a suitable place for investigations on diurnal cycles of hydrological processes in a subglacial karst system. Short travel times of injected tracer and low dispersivity allow several injections a day without interference of single tracer tests (Fig. 2, 3).

Whereas flow velocities are strongly correlated to diurnal alternating discharge, dispersivity does not show significant changes. South Spring/Marmot Cave is a very well developed "high speed" conduit karst system with significant diurnal flow velocity changes. Analytical modeling results show geohydraulic conditions extremly close to piston-flow. The hydraulic system is partially under pressure flow conditions as interpretated by tracer tests and as directly observed in the cave.

- Within the investigated discharge range the flow system remains stable in one conduit system without changing flow paths. This conclusion is based on a linear discharge-velocity correlation and stable dispersivity values.
- The variation of storm flow induced events exceeds the variation of diurnal run-off cycles.

Subglacial Hydrology

- Online-fluorometers combined with dataloggers (Schnegg & Doerflinger, 1997; Smart & Zabo, 1997) are crucial tools to investigate on diurnal processes in alpine hydrology. Otherwise logistic problems in sampling and data processing would be tremendous.
- A single tracer tests gives only a random result within the diurnal parameter range of flow velocity without accurate information about parameter variabilitiy. Replicate tracer tests are necessary for estimating the geohydraulic parameter range of a flow system with diurnal cycling patterns.

Acknowledgements

Small River Research is supported by the Natural Sciences and Engineering Research Council of Canada and the University of Western Ontario. Thanks to John Orwin for datalogger support and Andy Calarco for surveying. Thanks to Shauna Flanagan and Kumari Karunaratne for assistance in the field. Reviewing by Jose M. Calaforra and Paul G. Marinos gave helpful suggestions and is gratefully acknowledged.

References

HAUNS, M., & JEANNIN, P.-Y. (2000) Tracer transport in karst conduits: a computational fluid dynamics-based modeling approach. In: *Karst Studies and Problems: 2000 and Beyond*. Proc. of the joint meeting of Friends of Karst, Theoretical and Applied Karstology/IGCP 448, July 2000 Cluj-Napoca, Romania pp. 56–62.

HOCK, R., & HOOKE, R. Le B. (1993) Evolution of the internal drainage system in the lower part of the ablation area of Storglaciären, Sweden. *Geol. Soc. Am. Bull.*, **105**, *4*, pp. 537–546.

JAKOWSKI, A. (1995) *Ermittlung der Dispersion und anderer geohydraulischer Parameter aus Markierungsversuchen in Karst- und Kluftgrundwasserleitern Baden-Württembergs*. Ph.D. Thesis. TH Darmstadt. 546 p.

LOWE, D. J. (1983) The Anglo-Canadian Rocky Mountain speleological expedition, 1983. *Trans. British Cave Research Ass.*, **10** pp. 213–244.

MALOSZEWSKI, P., & ZUBER, A. (1990) Mathematical Modelling of Tracer Experiments in Fissured Rocks. *Water Res. Res.*, **26**, *7*, pp. 1517–1528.

NIENOW, P., SHARP, M., & WILLIS, I. (1996) Velocity-discharge relationships derived from dye-tracer experiments in glacial meltwaters: implications for subglacial flow conditions. *Hydrological Processes*, **10**, pp. 1411–1426.

ORWIN, J. F. (*pers. comm.*) Geomorphological Map of Small River Glacier, British Columbia (*unpublished*).

RIEG, A. (1994) *Zur Hydrologie im Karstgebiet Churfirsten -Alvier*. Ph. D. Thesis. University of Freiburg.

SAUTY, J. P., & KINZELBACH, W. (1988) *CATTI (Computer Aided Tracer Test Interpretation)*. Delft, Indianapolis, 79 p.

SCHNEGG, P.-A., & DOERFLIGER, N. (1997) An inexpensive flow-through field fluorometer. *12th International Congress of Speleology, 1997 Switzerland*, **2**, pp. 47–50.

SMART, C. C. (1983) The Hydrology of the Castleguard Karst, Columbia Icefields, Alberta, Canada. *Arctic and Alpine Research*, **15**, *4*, pp. 471–487.

SMART, C. C. (1997) Hydrogeology of glacial and subglagiacal karst aquifers: Small River, British Columbia, Canada. *12th International Congress of Speleology, 1997 Switzerland*, **2**, pp. 315–318.

SMART, C. C., & ZABO, L. (1997) Experimental design, technique and protocol in fluorometric tracing of ground water. *12th International Congress of Speleology, 1997 Switzerland*, **2**, pp. 51–54.

WERNER, A. (1997) *Model Code TRACY*.

ZABO, L. (1995) *Fluorometric tracing of Subglacial Hydrology, Small River Glacier, British Columbia, Canada*. MSc Thesis, University of Western Ontario.

Theoretical and Applied Karstology, 13 (2000), pp. 101–111

Contaminant transport in karst aquifers

Dorothy J. Vesper, Caroline M. Loop & William B. White*

Department of Geosciences, and Materials Research Laboratory,
The Pennsylvania State University, University Park, PA 16802, USA.

Abstract

Contaminants are easily injected into karst aquifers through sinking streams, sinkholes, or through open fractures and shafts in the carbonate rock. Transport of the contaminants through the aquifer is by a variety of mechanisms depending on the physical and chemical properties of the contaminant. Contaminants consist of (1) water soluble compounds, both organic and inorganic, (2) slightly soluble organic compounds, less dense than water (LNAPLs), (3) slightly soluble organic compounds, more dense than water (DNAPLs), (4) pathogens, (5) metals, and (6) trash. Water soluble compounds (e.g. nitrates, cyanides, carboxylic acids, phenols) move with the water. But rather than forming a plume spreading from the input point, the contaminated water forms linear stringers migrating down the conduit system toward the discharge point. LNAPLs (e.g. petroleum hydrocarbons) float on the water table and can migrate down the water table gradient to cave streams where they tend to pond behind obstructions. DNAPLs (e.g. chlorinated hydrocarbons), in contrast, sink to the bottom of the aquifer. In the conduit system, DNAPLs pond in low spots at the bottom of the conduit and infiltrate sediment piles. Transport of both LNAPL and DNAPL is dependent on storm flow which can force LNAPL through the system as plug flow and can move DNAPLs by mobilizing the sediment piles. Pathogens (viruses, bacteria, parasites) are transported through the karstic drainage system because of the absence of filtration and retain their activity for long distances. Metals (e.g. chromium, nickel, cadmium, mercury, and lead) tend to precipitate as hydroxides and carbonates in the neutral pH, carbonate rich water of the karst aquifer. Metal transport is mainly as particulates and as metal adsorbed onto small particulates such as clays and colloids. Metal transport is also episodic. Metals migrate down the flow path under flow conditions that take small particulates into suspension. Trash is carried into karst aquifers through sinkholes and sinking streams. It is, in effect, a form of clastic sediment, and can be carried deep into the conduit system where it can act as a source term for other contaminants leached from the trash.

Keywords: LNAPL, DNAPL, metal contaminants, transport, aquifers.

Le transport des contaminants dans les aquifères karstiques

Résumé

Les contaminants sont facilement introduits dans les aquifères karstiques par l'intermédiaire des pertes, des dolines, des fractures ouvertes et des puits creusés dans la roche carbonatée. Le transport des contaminants dans l'aquifère dépend des propriétés physiques et chimiques du contaminant. Les contaminants peuvent être: (1) des composés solubles (organiques et minéraux), (2) des composés organiques peu solubles et moins denses que l'eau (les LNAPL), (3) des composés peu solubles et plus denses que l'eau (les DNAPL), (4) des pathogènes, (5) des métaux et (6) des ordures. Les composés solubles dans l'eau (par exemple les nitrates, les cyanates, les acides carboxyliques, les phénols) sont transportés avec l'eau en formant des filets linéaires orientés vers le bas du système de conduites, vers l'exutoire. Les LNAPL (par ex. les hydrocarbures du pétrole) flottent à la surface de l'eau et peuvent migrer dans les rivières souterraines et s'accumuler derrière des obstructions. Au contraire, les DNAPL (par ex. les hydrocarbures chlorés) ont la tendance à couler au fond de l'aquifère et à s'accumuler dans les points bas et à s'infiltrer dans les sédiments. Le transport des LNAPL comme des DNAPL peut être bien différent en conditions de crues qui peuvent pousser les LNAPL dans le système et aussi déplacer les DNAPL en mobilisant les remplissages sédimentaires. Les pathogènes (virus, bactéries, parasites) sont transportés tout le long du système karstique en l'absence de filtration et peuvent être actifs sur de longues distances. Les métaux (par ex. le chrome, le nickel, le cadmium, le mercure et le plomb) ont tendance à précipiter comme des hydroxydes et des carbonates dans les eaux karstiques carbonatées et à pH neutre. Le transport des métaux se fait sous forme particulaire et est facilité par l'absorption de ceux-ci à la surface des argiles et des colloïdes. Les métaux à la surface des particules en suspension migrent vers la base de l'aquifère en conditions d'écoulement normales. Enfin, les ordures sont déversées dans les aquifères karstiques dans des dolines et des pertes. Elles sont en fait une forme de sédiments clastiques et peuvent être transportées sur de longues distances dans le système de conduits où elles agissent comme une nouvelle source pour d'autres contaminants.

Mots clés: LNAPL, DNAPL, contaminants métalliques, transport, aquifères karstiques.

* corresponding author. *E-mail address*: wbw2@psu.edu.

Introduction

It is a truism that karst aquifers are more vulnerable to contamination than other types of aquifers. Sinking streams, sinkhole drains, and open fractures in the bedrock provide little or no filtration of incoming water. Large aperture solution openings provide easy pathways for the movement of contaminants. Localization of ground water flow in open conduits means that contaminants can be transported long distances with little dilution. All of these statements have been repeated many times. What has been given less attention is the great variability in both volume and velocity of water moving through conduit systems and the impact of this variability on contaminant transport. In those aquifers with well-developed conduits, peak flows may be 100 times the base flows. Velocities within the conduit system are much higher during storm flow than during base flow. A further variable is the characteristics of the contaminants themselves. All contaminants do not respond equally to the driving forces for transport through the karst aquifer.

The ability of the conduit system to store and release contaminants is dependent both on the nature of the contaminants and on the storm flow characteristics of the system. Although there is an extensive and rapidly growing literature on contaminants in porous media and fracture aquifers, the analysis of contaminant transport in karstic aquifers is just beginning (e.g. Hoke & Wicks, 1997). Our objective in the present paper is to describe the various types of contaminants and summarize some of the ways in which they are stored and transported in karst aquifers. The examples are drawn from our own research and from some previous thesis work at the Pennsylvania State University.

Sources and types of contaminants

Investigations of contaminant transport often classify the source terms into "point sources" and "diffuse sources" depending on whether the contaminant source is highly localized such as a pipeline break or spread out such as the runoff of agricultural chemicals from croplands. This distinction is less useful in karst where most contaminants tend to be input through sinkholes and sinking streams and thus are intrinsically point sources.

A more useful distinction is between "spills" and "leaks". A spill is an abrupt input of (usually) a large volume of contaminant. For example, a gasoline tanker truck wrecks on the highway. The gasoline flows into a nearby sinkhole. A leak is a continuous input of (usually) a relatively small volume of contaminant. The best examples are leaky underground storage tanks which continuously drip their contents into the underlying aquifer. The volume of contaminant is small at any given time although the quantity of contaminant may become quite large over long periods of time.

Contaminants can be classified depending on their physical and chemical properties. For liquids, the pertinent properties are their solubility in water, their density, and their vapor pressure (Fig. 1). Some liquids such as low molecular weight alcohols, are miscible with water in all proportions. Others have sufficient solubility that they are taken completely into solution at the concentrations that occur in ground water systems. Still others have low solubilities so that they separate from water to form immiscible phases separated from the water. The density of immiscible liquids is a key parameter. If the immiscible phase is less dense than water, it will float on the water surface. If it is more dense, it will sink. The third variable is the vapor pressure which separates organic liquids into a "volatile organic compound (VOC)" class and a "semivolatile organic compound (SVOC)" class. The boundary vapor pressure is set at an arbitrary 5 Torr (0.667 kPa). Although the boundaries in solubility and vapor pressure are set by arbitrary choices, it is important to remember that no compound is completely insoluble and no compound is completely non-volatile. This caveat is especially important in karst aquifers.

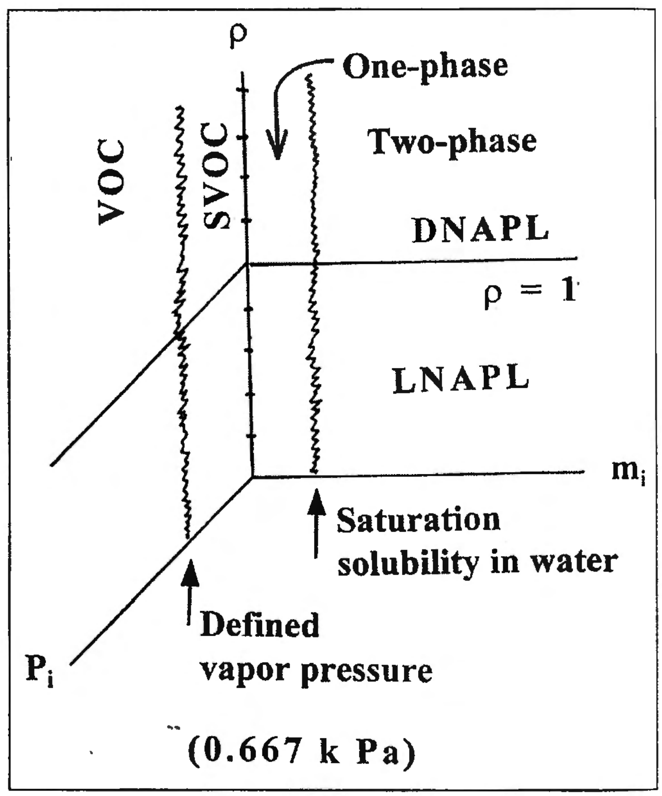

Fig. 1. Variables describing liquid and water-soluble contaminants.
Variables contrôlant les contaminants liquides et solubles.

With these and other aspects of contaminants in mind, it is possible to construct the following classification:

(1) **Water soluble compounds**. These are materials which would be taken completely into solution at all concentrations likely to be found. Water soluble inorganic compounds include ammonia and the nitrate ion, mostly derived from human and animal wastes and perhaps the most widespread of inorganic contaminants. Also water soluble are other inorganic ions such as chloride and sulfate as well as some highly toxic species such as cyanide ions derived from some industrial wastes. Some organic compounds are also water soluble such as alcohols, carboxyllic acids, phenols and some agricultural chemicals.

(2) **Light, slightly soluble organic compounds**. Light, non-aqueous phase liquids (LNAPLs) are those that will float on water. Gasoline, diesel fuel, home heating oil and related petroleum hydrocarbons are the most common examples. Gasoline is a complex mixture of low molecular weight, relatively volatile, saturated hydrocarbons. It is the presence of percentage quantities of aromatic hydrocarbons, benzene, toluene, ethyl benzene, and xylene (BTEX) that give gasoline its toxicity.

(3) **Heavy, slightly soluble organic compounds**. Dense, non-aqueous phase liquids (DNAPLs) will sink in water. Mostly these are chlorinated (or brominated) compounds. They include such low molecular weight, relatively volatile compounds as methylene chloride, CH_2Cl_2, trichloroethylene, C_2HCl_3 (TCE), and perchloroethylene, C_2Cl_4 (PCE) which are widely used as solvents, de-greasers, and dry cleaning agents. These materials are transported in tank car quantities and are often stored in underground tanks. Other DNAPLs include a family of compounds called polychlorinated biphenyls (PCBs). These materials are non-volatile, oily liquids which were once extensively used in electrical transformers and have been widely injected into karst and other aquifers by salvage operations intended to recover copper from scrap transformers. For some reason, old limestone quarries have frequently been the site of such operations.

(4) **Metals**. The term "metal", of course, is ambiguous. About two-thirds of the elements on the periodic table are metals. Most of these do not impose environmental problems because they are rare in nature and are rarely used in commercial products. We deal here only with a limited set of metallic elements, which, however, cover much of the range of behavior of the remaining elements. Two metals, iron and manganese, make up most of the natural background. These metals occur widely in sedimentary rocks and their oxides and hydrated oxides are common in cave deposits. Nickel and chromium appear in waste from chrome-plating and other non-ferrous metals industry and are typical representatives of the iron-group or transition-group elements. Both are toxic and both have been implicated as carcinogens. Zinc ores occur in carbonate rocks. Zinc and the chemically similar but more toxic cadmium occur widely as "galvanized" coatings on utensils, building materials, and other objects likely to end up in trash dumps.

(5) **Pathogens**. Viruses, bacteria, protozoa, and larger organisms are easily transported into karst aquifers because of the absence of filtering from the soil. Most wide spread of these are the fecal coliform group of organisms and the fecal streptococci bacteria. The presence of these organisms is the most common indicator of pollution from sewage or animal waste. Of most concern among protozoa is *"Giarida lamblia"* which is released in a cyst form in animal feces and is present in many surface waters. Sinking streams carry the stable cysts to the subsurface.

(6) **Trash**. Rural residents and even entire communities have from long tradition used sinkholes as waste disposal sites. Farmers routinely use sinkholes to dispose of dead animals and also empty containers of their agricultural chemicals. Unique among aquifers, sinking streams and sinkhole drains provide routes along which bulk trash can be carried for long distances inside the aquifer. The deposition of trash as "clastic sediment" provides a source term for leaching and release of contaminants for long periods of time.

Transport and Storage of Contaminants

The defining characteristics of karst aquifers are the rapid throughput times, localization of flow within essentially one-dimensional flow paths within the conduit system, and the presence of deposits of clastic sediments in most of the conduits. Each of these characteristics plays a role but a different role depending on the specific contaminant and on the detailed hydrogeology of the karst aquifer.

Water Soluble Contaminants

Soluble contaminants move with the water. In karst aquifers the water from diffuse infiltration through the soil, from sinkhole drains, and from sinking streams ultimately makes its way into the conduit system. The concentration of soluble contaminant should be determined by the concentration at the source adjusted for dilution by other water sources merging in the main conduit. By this model, the concentration of nitrates or other water soluble contaminants should decrease during storm flow because of dilution by the storm water. Although storm water dilution has been observed, what is observed in many cases, is a pulse of contaminant during storm

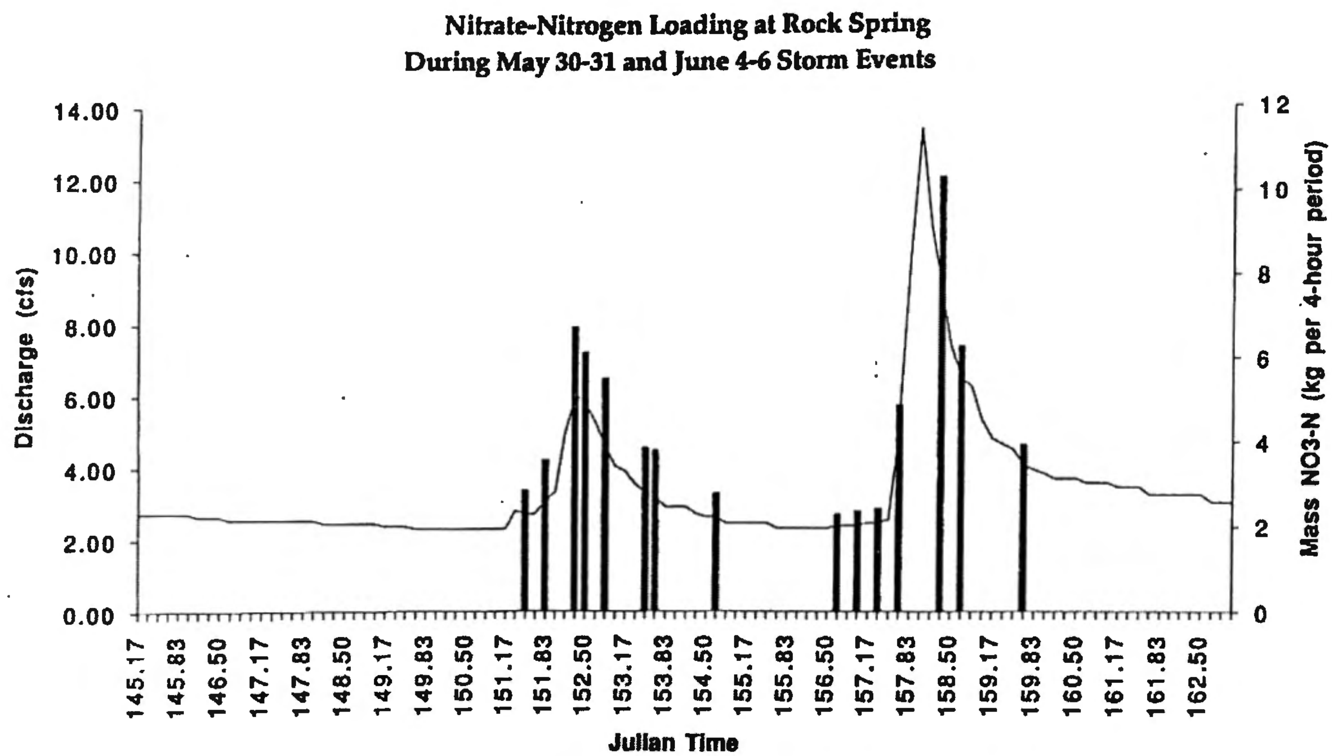

Fig. 2. Nitrate bursts during storm flow in Rock Spring Basin, Centre County, Pennsylvania. Data from UNDERWOOD (1994).
Pics de nitrates pendant les crues de Rock Spring Basin, Centre County, Pennsylvania. Données extraites de UNDERWOOD (1994).

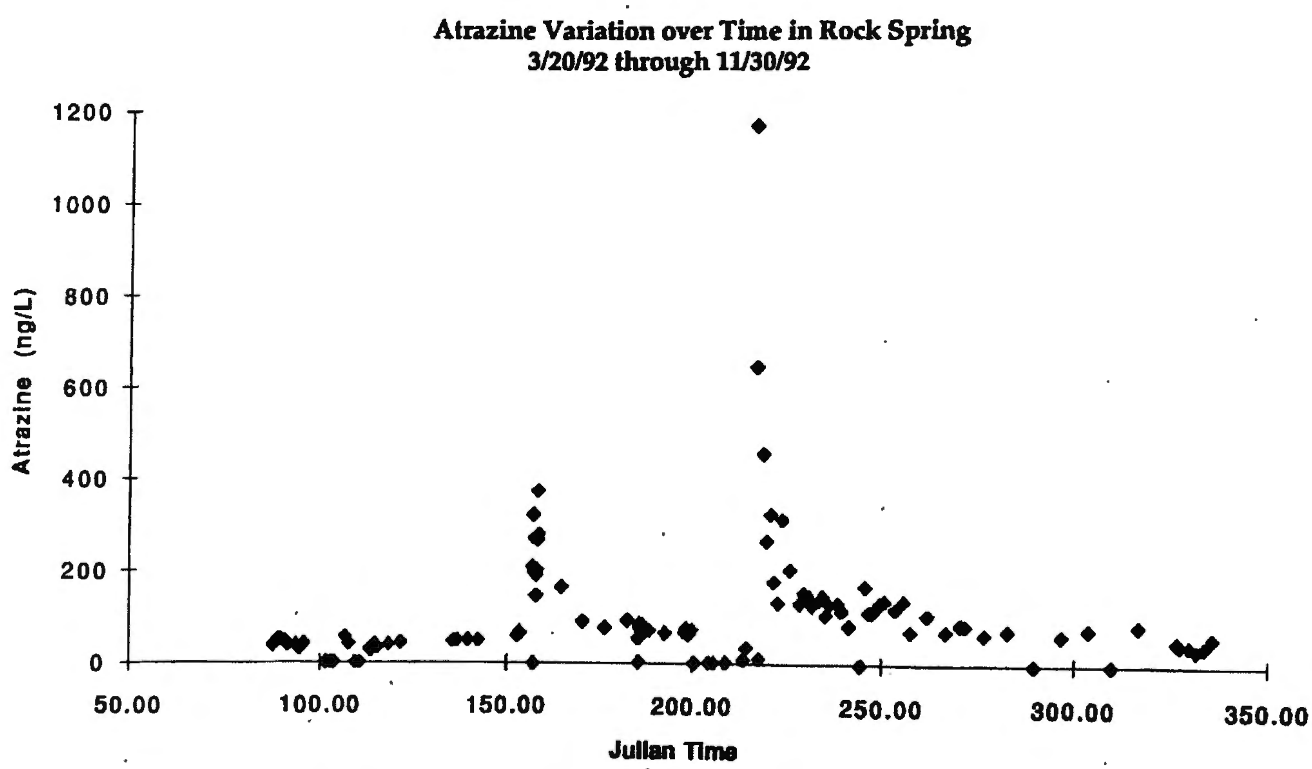

Fig. 3. Atrizine bursts during storm flow in Rock Spring Basin, Centre County, Pennsylvania. Data from Underwood (1994).
Pics d'atrazine pendant les crues de Rock Spring Basin, Centre County, Pennsylvania. Données extraites de UNDERWOOD (1994).

flow. The contaminant tends to ride the hydrograph, reaching a maximum concentration during peak flow (Fig. 2). The data in Figure 2 are from central Pennsylvania (UNDERWOOD, 1994). Similar results have been observed in Kentucky (CURRENS, 2000).

Nitrate levels in conduit fed springs tend to be highly variable because of the effects of dilution by storms whereas nitrate levels in fracture-fed springs tend to be relatively constant although the actual nitrate levels vary greatly from one spring to another (KASTRINOS & WHITE, 1986). The agricultural chemical atrazine also exhibits a storm pulse (Fig. 3). Since both flow and contaminant increase during storm flow, the actual flux of contaminant discharged from the aquifer is the convolution of the hydrograph and contaminant chemograph integrated over the storm pulse.

$$Flux = \int Q(t)C(t)dt \qquad (1)$$

Although the source of the spike in the contaminant is not known for certain, it seems possible that the role of storm flow is to leach contaminants stored in the overlying soil or in the epikarst.

Light Non-Aqueous Phase Liquids

LNAPLs will float on ground water. This has led to some remarkable contamination problems such as a lake of gasoline nearly two meters deep floating on the water table near Mechanicsburg, Pennsylvania (RHINDRESS, 1971). LNAPLs will float on underground streams and be carried along with the flowing water. The LNAPL will pond when the water ponds behind obstructions and becomes temporarily entrapped. Conduits generally create a trough in the water table so the LNAPL contamination in the conduit tributaries and in the fracture system tends to migrate toward the master conduit. During flood flow, the trough fills and conduits with free surface steams shift into a regime of pipe flow. Ponded LNAPL is lifted with the rising water and pressed against the ceiling. Any pockets in the ceiling will form traps for the LNAPL (EWERS *et al.*, 1991). If the ceiling is tight, the LNAPL is forced through the obstructions as piston flow. A burst of LNAPL then continues down the conduit. For this reason, spills of LNAPL do not necessarily appear at the karst springs immediately after the spill. Alternatively, if the ceiling is fractured, the piston flow drives the LNAPL upward where the vapors may rise into structures on the land surface. Fume problems in homes and other structures overlying conduit systems contaminated by LNAPLs may arise long after the initial spills (STROUD *et al.*, 1986).

Many common light hydrocarbon compounds have substantial solubilities and vapor pressures (Table 1). For accumulations of LNAPL ponded behind obstructions in conduits, the continuous sweep of fresh water beneath the pool will eventually dissolve and remove the pool. Likewise, the ponded LNAPL will gradually evaporate because of the vapor pressure of the compounds. In the process, of course, the air-filled cave passages become contaminated with hydrocarbon fumes. The turnover in cave air due to barometric changes will eventually flush out the contaminants but while they are present they are a substantial hazard to cave explorers, especially those who explore by carbide lamp. One of the most serious incidents occurred in Howard's Cave, Georgia in 1966 where a gasoline explosion set off by carbide lamps claimed three lives (BLACK, 1966).

Table 1. Solubilities of some light aromatic hydrocarbons (selected from FETTER, 1993).
Solubilités de quelques hydrocarbures aromatiques (d'après FETTER, 1993)

Compound	Solubility in water (mg/l)
Benzene	1780
Toluene	500
o-Xylene	170
Ethyl Benzene	150

Dense Non-Aqueous Phase Liquids

The pathways for heavy organic liquids migrating below the level of the epikarst will be fractures, shafts, and chimneys of various kinds. Possible storage sites in the aquifer include cavities and dry cave passages in the vadose zone, fractures in the phreatic zone, and the main conduit system where DNAPL can collect in pools beneath the water surface, and become incorporated into the clastic sediments that occupy the conduit. Because of the density difference, DNAPL compounds can occupy the pore spaces within the sediment pile where they can be sequestered for long periods of time.

The water table generally stands higher near the boundaries of karst ground water basins with hydraulic gradients that point toward the conduit system. DNAPLs reaching the water table do not necessarily follow the ground water down gradient toward the conduit but can continue to move vertically into any available storage spaces below local base level or can follow the dip of bedding planes in directions quite different from the hydraulic gradient.

The transport of DNAPL has both similarities and differences to the transport of LNAPLs. Processes in common include volitilization although this process is not as effective because in the case of DNAPL, the overlying water provides a protective blanket. Either type of contaminant can degrade in the carbonate water environment. The effectiveness of this process is strongly dependent on the specific DNAPL being considered. DNAPLs have a finite solubility (Table 2) and are also gradually stripped away by the continuing flow of fresh water in the conduit. DNAPL that forms distinct pools beneath flowing streams or in low places in water-filled con-

Table 2. Vapor pressures and solubilities of some chlorinated hydrocarbons (Fetter, 1993).
Tension de vapeur et solubilité de quelques hydrocarbures chlorés (Fetter, 1993).

Compound	Vapor Pressure (Torr, 20 °C)	Solubility in Water (mg/l)
Methylene Chloride	349	20,000
Carbon Tetrachloride	90	800
Vinyl Chloride	2660	1.1
Trichloroethylene (TCE)	60	1100
Tetrachloroethylene (PCE)	14	150

duits dissolves at rates given by the exposed area of the DNAPL pool and the specific dissolution kinetics of the particular compound. DNAPL pools can also be regarded as a sort of bedload and can be dragged downstream when flow velocities exceed a necessary threshold. Higher velocities may actually entrain the DNAPL pool so that it is flushed downstream in suspension. Unlike LNAPLs floating on the water surface and thus continuously in contact with the water, DNAPL that has sunk into the sediment pile on the floor of the conduit is protected. There will be a slow percolation of water through the sediment much like any other porous media flow but like other porous media flow, the flow velocities are very small, with only a slow turnover with the fast-moving water above. Thus, the stripping of DNAPL from the sediment pile will be much slower that the stripping of DNAPL constrained in distinct pools.

DNAPLs and other compounds are slowly degraded by chemical reaction with the water. The actual kinetics of this process have been measured by Knauss et al. (1999) for the specific example of trichloroethylene. The degradation reaction is:

$$2C_2HCl_3 + 3O_2 + 2H_2O \Leftrightarrow 4CO_2 + 6H^+ + 6Cl^-$$

The end products of the breakdown process are CO_2 and HCl. Because the reaction is with oxygenated water which is always in excess supply, the rate equation has the simple form:

$$\frac{dC}{dt} = -kC_0^n \quad (2)$$

By laboratory experiments, Knauss *et al.* (1999) found $n = 0.85$ and $k = 5.8 \times 10^{-7}$ sec^{-1} at 100 °C.

A process that applies to DNAPL but not as much to LNAPL is the movement of the sediment pile itself. Sediments in active conduits themselves form a continuous flux. New sediment is continuously injected into the conduit system and must be continuously flushed through and discharged at the spring. Otherwise, the conduit system would eventually clog completely. Unlike the flow of water, the flow of sediments is episodic. Flood flows must reach a certain threshold before the sediments can move as bedload and an even higher threshold before the sediment pile becomes completely entrained so that both sediment and any incorporated DNAPL are transported downstream.

A conceptual model for DNAPL transport in karst aquifers has been published by Wolfe *et al.* (1997). The rather complicated process of storage and DNAPL transport in karst aquifers has been reviewed by Loop & White (2001). Their conceptual model for DNAPL transport is given in Figure 4.

Metals

Metals in karst aquifers can be divided into three categories (a) alkaline earth metals derived from the carbonate rock — mainly calcium and magnesium with minor amounts of strontium and barium, (b) heavy metals occurring as part of the natural background—mainly aluminum, iron, and manganese with trace amounts of many other metals, and (c) contaminant metals introduced into the aquifer through human influences. The chemistry of the alkaline earth metals in karst ground waters is the subject of a huge literature on karst water geochemistry and is not of concern here. However, the concentrations and transport of other metals in karst systems has received much less attention.

In a recent study, Hodge *et al.* (1998) assessed trace metal concentrations in a carbonate spring as an indicator of the trace metal concentrations in the ancient marine environment. As expected, calcium and magnesium were present at much higher concentrations (10^{-3}– 10^{-4} mol/kg) than the potentially toxic meals arsenic, copper, chromium, and cobalt (10^{-7} – 10^{-9} mol/kg). Quinlan and Rowe (1977) found nickel and chromium in a Kentucky karst spring presumably derived from a metal plating plant in the upper reaches of the ground water basin.

To get a sense of the range of metals that might be expected, a composite sample was prepared from springs draining the Fort Campbell Army Base in western Tennessee/Kentucky. Water from the large regional Millstone Spring was mixed with sediment from the smaller Blue Spring. The clastic material was allowed to settle and the slightly turbid water was analyzed by inductively coupled plama-mass spectrometer. (Table 3). These data are indicative of the range of metallic elements that might be carried by karst ground waters.

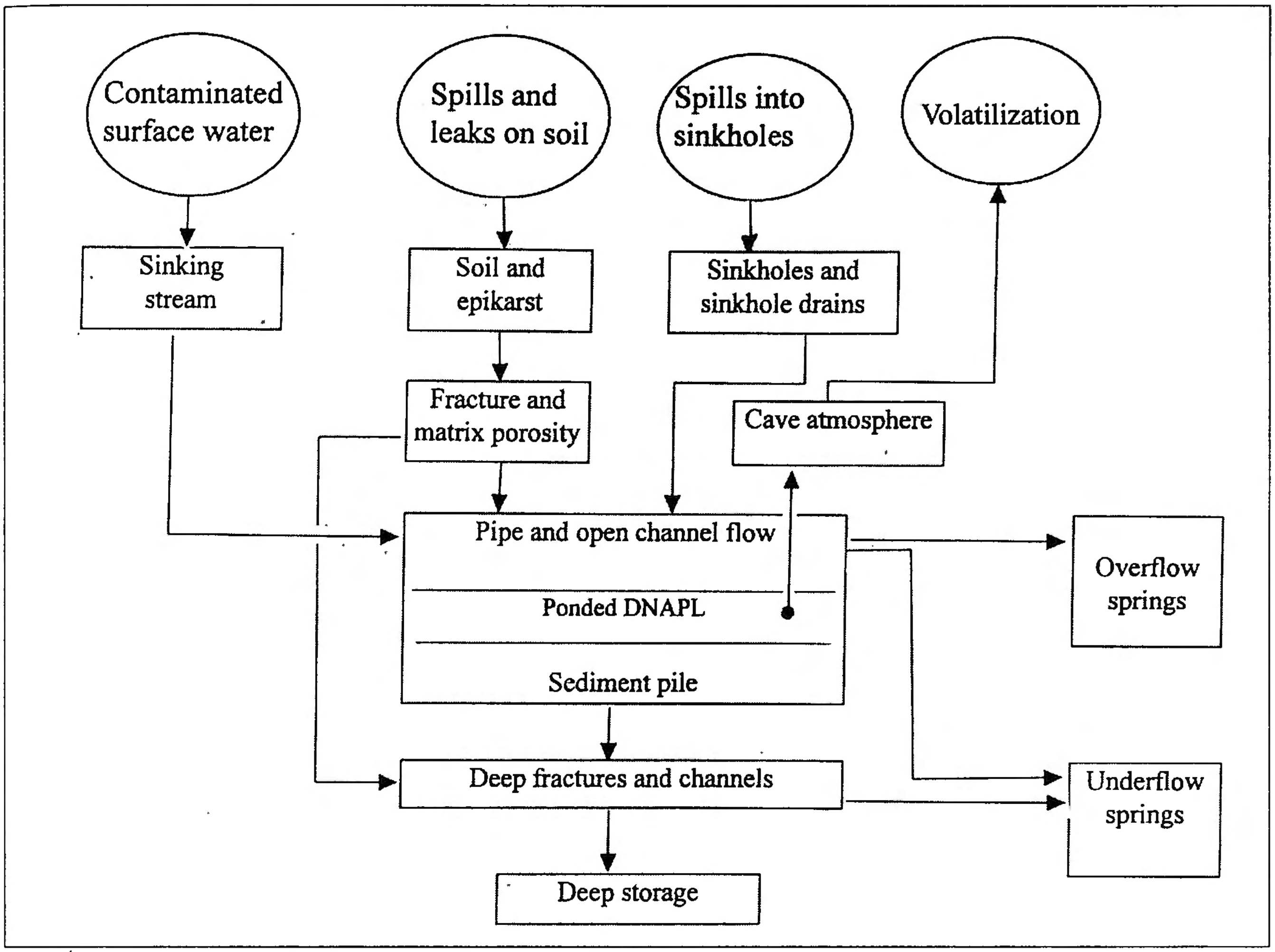

Fig. 4. Conceptual model for DNAPL storage and transport in karst aquifers. From Loop & White (2001).
Modèle conceptuel pour le stockage et le transport des DNAPLs. D'après Loop & White (2001).

Table 3. ICP-MS analyses of carbonate spring waters.
Analyses ICP-MS des sources carbonatées.

Element	Concentration (µg/L)
Al	16,300
As	17
Ba	157
Ca	51,000
Cd	0.93
Cr	26
Cu	13
Fe	11,000
K	4280
Mg	5800
Mn	1350
Na	5370
Ni	20
Pb	24
Zn	81

The aqueous chemistry of individual metal-water systems is, in general, well understood (Baes & Mesmer, 1976; Stumm & Morgan, 1996) and thermodynamic calculations can be made to determine the limiting solubilities. Figure 5 illustrates the case of the Ni–O–H system where nickel hydroxy complexes control the solubility. In karstic systems, the high carbon dioxide activities cause carbonates to be the limiting insoluble phase. Calculations for such systems as the Zn–O–H, Cd–O–H and Pb–O–H systems show that in all cases, precipitation of hydroxide or carbonate phases will limit the concentration of metal ions in karstic waters to low values. However, in all cases, at the pH and P_{CO_2} values of karst water, the equilibrium metal solubility would be well above drinking water standards.

The controlling factor in metal transport appears to be adsorption onto various substrates rather than equilibrium solubility. Metals can adsorb onto clays and other clastic particulates, onto organic material in the water, and onto iron or manganese oxides which often form coatings on cave streams.

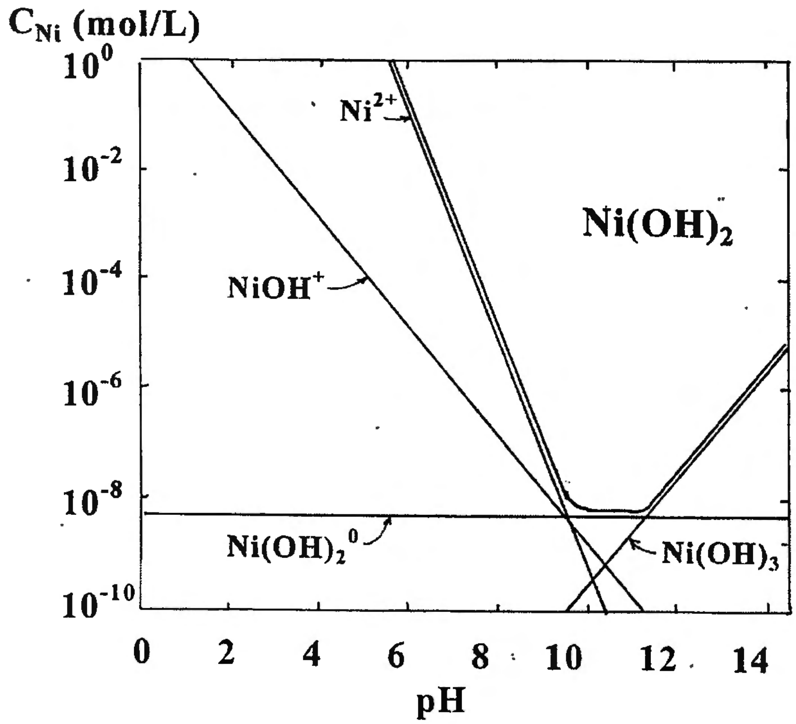

Fig. 5. Calculated speciation diagram for the system Ni–O–H. $Ni(OH)_2$ is crystalline nickel hydroxide.
Diagramme de spéciation du système Ni–O–H. Le $Ni(OH)_2$ est l'hydroxyde cristallisé de nickel.

Table 4. Chemical analyses of iron and manganese oxides from Rohrer's Cave, Pennsylvania. Data extracted from White *et al.* (1985).
Composition chimique des oxydes de fer et de manganèse de Rohrer's Cave, Pennsylvania. Données extraits de White *et al.* (1985).

Specimen	Fe (wt %)	Mn (wt %)	Co (wt %)	Ni (wt %)	Cu (wt %)	Zn (wt %)
Iron Oxide stalactite	43	0.01	<0.01	<0.01	0.01	0.01
Iron Oxide stalagmite	50	<0.01	<0.01	<0.01	0.01	0.01
Manganese Oxide Coating	3.5	12.4	1.60	1.57	0.45	1.52

Manganese oxides, precipitated onto stream sediments by the oxidation of the natural manganese background (White, 1997) act as extremely effective scavengers for heavy metals. Chemical analyses of manganese oxides from a selection of karst conduits revealed percentage quantities of such metals as copper, zinc, nickel and – in one case – cobalt (Table 4). These data also illustrate a "mutual exclusion." The hydrated iron oxide deposits contain negligible concentrations of other metals including manganese while the manganese oxide coatings are highly enriched in other transition metals but contain only relatively small amounts of iron.

McCarthy & Shevenell (1998) confirmed the link between metals and solids for ground water in the karst aquifer that underlies the Oak Ridge Reservation, Tennessee. They determined colloidal compositions via: (a) the chemical difference in total and filtered water samples, (b) direct soil measurements using X-ray diffraction, scanning electron microscopy, and energy dispersive X-ray spectroscopy, and (c) speciation modeling. In most wells, they found that aluminum, iron, manganese, and nickel were present primarily in the solid phase

Storm-associated changes in aquifer hydrology are known to impact ground water and karst spring chemistry. Recent research by Atteia & Kozel (1997) found that the abundance, size, and type of colloids discharged at a spring changed during storm events. The greatest abundance of large colloids was discharged coincident with the rising limb of the spring hydrograph. This has been interpreted as the re-suspension of colloids in the conduits due to increased ground water velocities. Colloids identified during the study included clays, granular minerals, and bacteria.

Although the study of metal transport in karst aquifers is far from complete, it is apparent that metals are stored in the aquifer primarily by adsorption onto various substrates. They move through the aquifer to the discharging spring when the particulates on which they are adsorbed are swept out of the aquifer by storm pulses.

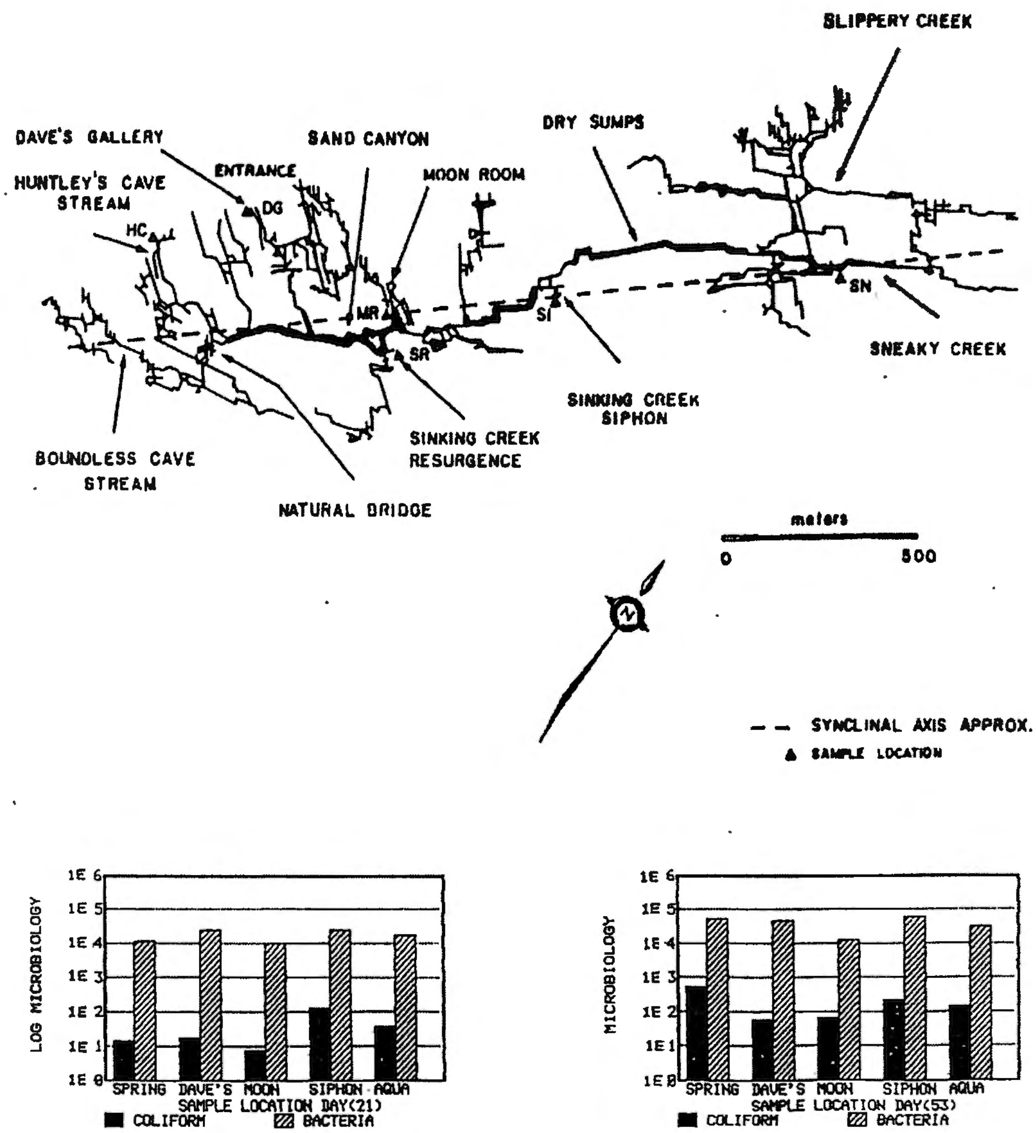

Fig. 6 Bacterial levels at various locations (shown on map) in the Butler Cave-Sinking Creek System, Bath County, Virginia, for day 21 (left plot) and day 56 (right plot) measured from August 1, the beginning of the water year. Data from CHESS (1987).
Niveaux bactériologiques dans divers endroits (indiqués sur la carte) dans Butler Cave-Sinking Creek System, Bath County, Virginia, pour le jour 21 (diagramme de gauche) et le jour 56 (diagramme de droite) mesurés à partir du 1er Août, début de l'année hydrologique. Données d'après CHESS (1987).

Pathogens

Although it has long been recognized that cave streams should not be used for drinking water, in reality, many cave streams and the springs to which they discharge are used as domestic and sometimes public water supplies. Because there is little filtering of recharge water from sinking streams or from storm runoff into sinkholes, it is quite obvious that microorganisms, including pathogenic ones, can be easily carried into the underground system. Typical sizes for microorganisms range from the submicrometer to hundreds of micrometers, in the range of fine-grained sediment. Organisms can be transported in suspension in the water and as attachments to particles of sediment or organic material.

Questions of the survival rate of microorganisms in karst aquifers is another matter. Recent investigations of cave microbiology (*see* e.g. SASOWSKY & PALMER, 1994) have revealed a rich diversity of organisms that seem to thrive very well deep within karst systems. On the other hand, those organisms that pose the greatest threats to humans might be expected to exhibit a high die-off rate. Hard data are sparse. An investigation of total bacteria and coliform bacteria in the Butler Cave – Sinking Creek System of Virginia (CHESS, 1987) showed

no evidence of die-off anywhere in the system. Roughly the same populations of organisms were found in streams deep within the system and at the discharging spring as occurred in the sinking surface streams (Fig. 6).

Trash

In many karst areas, sinking streams have cut small blind valleys into the land surface. These depressions, along with the ubiquitous sinkholes, have been used as trash receptors as long as there have been human populations. Sinkhole dumps are as much characteristic karst land features as the sinkholes themselves. Two aspects of sinkhole dumps relate to the general problem of ground water contamination in karst aquifers. Sinkholes act as funnels, collecting storm water runoff and channeling it into the sinkhole drain. The trash pile in a sinkhole behaves as an unlined landfill. Storm water leaches through the trash and what enters the karst drainage system below is essentially landfill leachate. Secondly, inwash during intense storms and soil piping failures of the sinkhole sediment combine to transport solid trash into the underlying conduit system. The trash becomes a form of clastic sediment and is moved down the flow field during intense storm flow in the same manner as any other clastic sediment. Trash carried deep within the conduit system becomes a source term for continuing contamination of the ground water and is located where clean-up is essentially impossible.

Trash injections into karst systems have not been systematically examined. Categories include domestic waste – a mix of materials not different from those usually deposited in engineered landfills, dead, often diseased farm animals, and – in more recent time – chemical waste. The latter takes the form of improperly cleaned containers for paint and agricultural chemicals which may be dumped in sinkholes as an alternative to proper recycling.

Conclusions

Contaminants to karst aquifers have been broadly classified into water-soluble organic and inorganic contaminants, slightly soluble organic contaminants, metals, pathogens, and trash. For each of these categories, there are multiple, complex, and interacting mechanisms for the transport, storage, and eventual release of the materials. Some of these are becoming understood. Others await detailed investigation.

The subject of contaminant transport in karst aquifers is perhaps the most important of the current generation of karst research subjects.

References

Atteia, O., & Kozel, R. (1997) Particle size distributions in water from a karstic aquifer: from particles to colloids. *J.of Hydrology*, **201**, pp. 102–119.

Baes, Jr. C. F., & Mesmer, R. E. (1976) *The Hydrolysis of Cations*. John Wiley, New York, 490 p.

Black, D. F. (1966) Howard's Cave disaster. *NSS News*, **24**, pp. 242–244.

Chess, D. L. (1987) *Comparisons of microbiology and selected anions for surface and subsurface stream waters for the Aqua Spring watershed of Burnsville Cove, Virginia*. M.S. Thesis, The Pennsylvania State University.

Currens, J. C. (2000) Ground-water quality in a karst aquifer following BMP implementation (*abstract*). *Proc. Natl. Speleol. Soc. Convention*, Elkins, WV, pp. A18–19.

Ewers, R. O., Duda, A. J., Estes, E. K., Idstein, P. J., & Johnson, K. M. (1991) The transmission of light hydrocarbon contaminants in limestone (karst) aquifers. In: *Proceeding of the Third Conference on Hydrogeology, Ecology, Monitoring, and Management of Ground Water in Karst Terranes*, Association of Ground Water Scientists and Engineers, pp. 287–306.

Fetter, C. W. (1993) *Contaminant Hydrogeology*. Prentice Hall, Upper Saddle River, NJ, 500 p.

Hodge, V. F., Stetzenbach, K. J., & Johanesson, K. H. (1998) Similarities in the chemical composition of carbonate groundwaters and seawater. *Environmental Science and Technology*, **32**, pp. 1481–1486.

Hoke, J. A., & Wicks, C. M. (1997) Contaminant transport in karst aquifers. In: *The Engineering Geology and Hydrogeology of Karst Terranes*, (Beck, B. F., & Stephenson, J. B., *Eds.)*, A.A. Balkema, Rotterdam, pp. 189–192.

Kastrinos, J. R., & White, W. B. (1986) Seasonal, hydrogeologic, and land-use controls on nitrate contamination of carbonate ground waters. In: *Proceedings of the Environmental Problems in Karst Terranes and Their Solutions Conference*, National Water Well Association, pp. 88–113.

Knauss, K. G., Dibley, M. J., Leif, R. N., Mew, D. A., & Aines, R. D. (1999) Aqueous oxidation of trichloroethene (TCE): A kinetic analysis. *Applied Geochemistry*, **14**, pp. 531–541.

Loop, C. M., & White, W. B. (2001) A conceptual model for DNAPL transport in karst. *Ground Water*, **39**, pp. 119–127.

McCarthy, J. F., & Shevenell, L. (1998) Processes controlling colloid composition in a fractured and karstic aquifer in eastern USA. *J. of Hydrology*, **206**, pp. 191–218.

Quinlan, J. F., & Rowe, D. R. (1977) Hydrology and water quality in the Central Kentucky Karst: Phase I. *University of Kentucky Water Resources Research Institute Research Report*, **No. 101**, 91 p.

RHINDRESS, R. C. (1971) Gasoline pollution of a karst aquifer. In: *Hydrogeology and Geochemistry of Folded and Faulted Rocks of the Central Appalachian Type and Related Land Use Problems* (PARIZEK, R. R., WHITE, W. B., & LANGMUIR, D., *Eds.*), Earth and Mineral Sciences Experiment Station, The Pennsylvania State University, **Circular 82**, pp. 171–175.

SASOWSKY, I. D., & PALMER, M. V. (1994) *Breakthroughs in Karst Geomicrobiology and Redox Geochemistry*. Karst Waters Institute Special Publication, **1**, 111 p.

STROUD, F. B., GILBERT, J., POWELL, G. W., CRAWFORD, N. C., RIGATTI, M. J., & JOHNSON, P. C. (1986) U.S. Environmental Protection Agency emergency response to toxic fumes and contaminated ground water in karst topography: Bowling Green, Kentucky. In *Proceedings of the Environmental Problems in Karst Terranes and Their Solutions Conference*, National Water Well Association, pp. 197–226.

STUMM, W., & MORGAN, J. J. (1996) *Aquatic Chemistry* (3rd Edition) John Wiley, New York, 1022 p.

UNDERWOOD, K. L. (1994) *Evaluation of pesticide and nitrate mobility in a conduit-flow dominated karst basin*. M.S. Thesis, The Pennsylvania State University, 204 p.

WHITE, W. B., SCHEETZ, B. E., ATKINSON, S. D., IBBERSON, D., & CHESS, C. A. (1985) Mineralogy of Rohrer's Cave, Lancaster County, Pennsylvania. *NSS Bulletin*, **47**, pp.17–27.

WHITE, W. B. (1997) Thermodynamic equilibrium, kinetics, activation barriers, and reaction mechanisms for chemical reactions in karst terrains. *Environmental Geology*, **30**, pp. 46–58.

WOLFE, W. J., HAUGH, C. J., WEBBERS, A., & DIEHL, T. H. (1997) Preliminary conceptual models of the occurrence, fate, and transport of chlorinated solvents in karst regions of Tennessee. *U.S. Geological Survey Water-Resources Investigations Report* **97-4097**, 80 p.

Theoretical and Applied Karstology, 13 (2000), pp. 113–117

Microtus (*Terricola*) *grafi miciaensis* (*Rodentia, Mammalia*), une nouvelle sous-espèce du site moustérien de Gaura Lupului (Crăciuneşti, Hunedoara, Roumanie)

Patrick Brunet-Lecomte[1] & Alexandra-Cristina Păunesco[2*]

[1] *UMR CNRS 5561 Biogéosciences, Laboratoire de Paléobiodivesité et Préhistoire de l'EPHE, Centre des Sciences de la Terre, 6, Bd. Gabriel, F-2100 Dijon, France.*

[2] *Laboratoire Départemental de Préhistoire du Lazaret, 33 bis, Bd. Franck Pilatte, 06300 Nice, France et l'Institut de Spéologie « Emil Racoviţă », str. Frumoasă 11, 78114 Bucarest 12, Roumanie.*

Résumé

Les particularités morphométriques de la population de *M. (Terricola) grafi* du site moustérien de Gaura Lupului (village de Crăciuneşti, département de Hunedoara, Roumanie), nous a incités à lui donner un rang sub-spécifique. Elle est décrite sous le nom de *Microtus (Terricola) grafi miciaensis*.

Mots clés: rongeurs, *Arvicolidae*, Pléistocène supérieur.

Microtus (Terricola) grafi miciaensis (Rodentia, Mammalia): a new subspecies from the Mousterian site of Gaura Lupului (Crăciuneşti, Hunedoara, Romania)

Abstract

The morphometric features of the population of M. (Terricola) grafi *from the Mousterian site of Gaura Lupului (Crăciuneşti village, Hunedoara county, Romania) entitled us to attribute it a specific rank. It is further on described under the name of* Microtus (Terricola) grafi miciaensis.

Key words: rodents, Arvicolidae, *Upper Pleistocene.*

Introduction

Le gisement moustérien de Gaura Lupului, dans l'ouest des Carpates a livré de nombreux restes de micromammifères parmi lesquels les six premières molaires inférieures (M_1) se rapportant à une espèce du sous-genre de campagnol *Microtus* (*Terricola*). Notre objectif est de préciser le statut spécifique de cette espèce, compte tenu d'une part de l'intérêt de ce groupe dans l'étude de la spéciation, et d'autre part de la situation biogéographique particulière de cette région.

Matériel

Le matériel étudié se compose des six premières molaires inférieures (M_1) de *Terricola* provenant du gisement moustérien de Gaura Lupului et de 14 M_1 actuelles de la localité de Nandru.

La grotte « Gaura Lupului » est située dans le secteur karstique Băiţa-Crăciuneşti, à une vingtaine de km au nord de la ville de Deva (département de Hunedoara), et à environ 1,5 km en direction NNO du village de Crăciuneşti. Elle est creusée dans le massif calcaire de « Măgura Peşterii », à une altitude relative de 527 m. Les fouilles ont été entreprises par Alexandru Păunescu, en 1999, et elles nous ont permis le recueil de nombreux restes de microfaune.

* corresponding author. *E-mail address*: acpaunescu@hotmail.com

Le matériel actuel provient des pelotes de rejection d'un rapace nocturne, ramassées à la base de son nid, sur le territoire du village de Nandru (département de Hunedoara).

Ce matériel a été comparé à : 15 populations actuelles (310 dents) de *M. (T.) subterraneus* de France, Suisse et Pologne, 3 populations actuelles (59 dents) de *M. (T.) tatricus* de Pologne (Tatras et Beskidy) et Slovaquie (Tatras) et 10 populations stratigraphiques de l'espèce fossile (164 dents) *M. (T.) grafi* du Pléistocène supérieur de Bacho Kiro, Bulgarie (BRUNET-LECOMTE *et al.*, 1992).

Méthode

Vingt-trois variables, notées V1 à V23 sont prises sur la surface occlusale de la M_1 (BRUNET-LECOMTE, 1988).

Onze indices odontométriques sont calculés : longueur relative de la partie antérieure de la M_1 LRPA=(V6–V3)/V6×100, inclinaison du rhombe pitymyen RP=V4–V3, fermeture de la boucle antérieure BA=(V20–V18)/V21×100, le rapport longueur/largeur de la M_1 V6V21=V6/V21 et 7 autres variables de la partie antérieure de la M_1 V10V9=(V10–V9)/V6×100, V11V9=(V11–V9)/V6×100, V12V10=(V12–V10)/V6×100, V12V11=(V12–V11)/V6×100, V18V17=(V18–V17)/V21×100, V19V17=(V19–V17)/V21×100 et V20V19=(V20–V19)/V21×100.

La morphologie générale de la M_1 est étudiée : (i) – par une analyse en composantes principales (ACP) faite entre les variables prises sur la surface occlusale de la dent entre les 20 dents des deux populations roumaines et (ii) – par une analyse canonique discriminante (ACD) faite entre les deux populations roumaines comparées aux 28 populations actuelles et fossiles de *M. (T.) subterraneus*, *M. (T.) tatricus* et *M. (T.) grafi*.

Les indices odontométriques ainsi que la longueur totale de la M_1 (variable V6) sont comparés entre les deux populations roumaines par un test *t*, complété par un test de Wilcoxon en raison des faibles effectifs des populations.

Le logiciel statistique est celui de SAS.

Résultats

Morphologie générale de la M1.

Les trois premiers facteurs de l'analyse en composantes principales expriment respectivement 59, 12 et 11% de la variance totale.

La description et la comparaison de la moyenne de ces facteurs entre les deux populations roumaines sont données dans le Tableau 1. Les moyennes ne sont pas différentes (p>0,10) pour le facteur 1 qui exprime un effet de taille, alors que les deux populations sont proches d'être différentes (p compris entre 0,05 et 0,10) ou différentes (p<0,05) pour les facteurs 2 et 3 respectivement qui expriment une variation de forme. La distribution des 20 dents dans le plan 2–3 des axes factoriels est donnée dans la figure 1: on observe une séparation partielle des deux populations, notamment dans le quart –/– du plan pour lequel 5 des 6 dents de Gaura Lupului sont présentes contre seulement 1 dent sur 14 pour la population de Nandru.

Les deux premiers facteurs de l'analyse canonique discriminante faite entre les 30 populations expliquent respectivement 39 et 18% de la variance inter-populationnelle. La distribution des centres de gravité des 30 populations dans le plan 1–2 (Fig. 2) montre que: l'axe 1 sépare les populations de *M. (T.) tatricus* de celles de *M. (T.) subterraneus* et de *M. (T.) grafi*, l'axe 2 sépare les populations de *M. (T.) subterraneus* de celles de *M. (T.) grafi*. Les deux populations roumaines occupent dans le plan 1–2 des positions sensiblement différentes : la population de Nandru occupe une position intermédiaire entre les populations de *M. (T.) subterraneus* et celles de *M. (T.) grafi*, alors que la population de Gaura Lupului occupe une position intermédiaire entre les populations de *M. (T.) tatricus* et celles de *M. (T.) grafi* sur l'axe 1 et une position en limite supérieure de celles de *M. (T.) grafi* sur l'axe 2 montrant ainsi une position relativement isolée dans le plan 1–2.

Tableau 1. Description et comparaison des facteurs 1, 2 et 3 de l'analyse en composantes principales obtenue à partir des mesures prises sur la surface occlusale de la dent entre les populations de Nandru et Gaura Lupului.

Description and comparison of the factors 1, 2 and 3 after the main components analysis based on measurements of the occlusal surface of the populations from Nandru and Gaura Lupului, respectively.

Variable	Population fossile (Grotte Gaura Lupului) N=6				Population actuelle (Nandru) N=14				Test t (p)	Test de Wilcoxon (p)
	Moyenne	Ecart type	Min	Max	Moyenne	Ecart type	Min	Max		
Axe 1	0,50	1,21	-1,44	1,68	-0,21	0,86	-2,65	0,7	p=0,152 NS	p=0,174 NS
Axe 2	-0,65	0,96	-2,15	0,76	0,28	0,91	-1,53	1,69	p=0,054 NS	p=0,091 NS
Axe 3	-0,90	0,40	-1,33	-0,38	0,39	0,93	-1,11	2,03	p=0,005S	p=0,004S

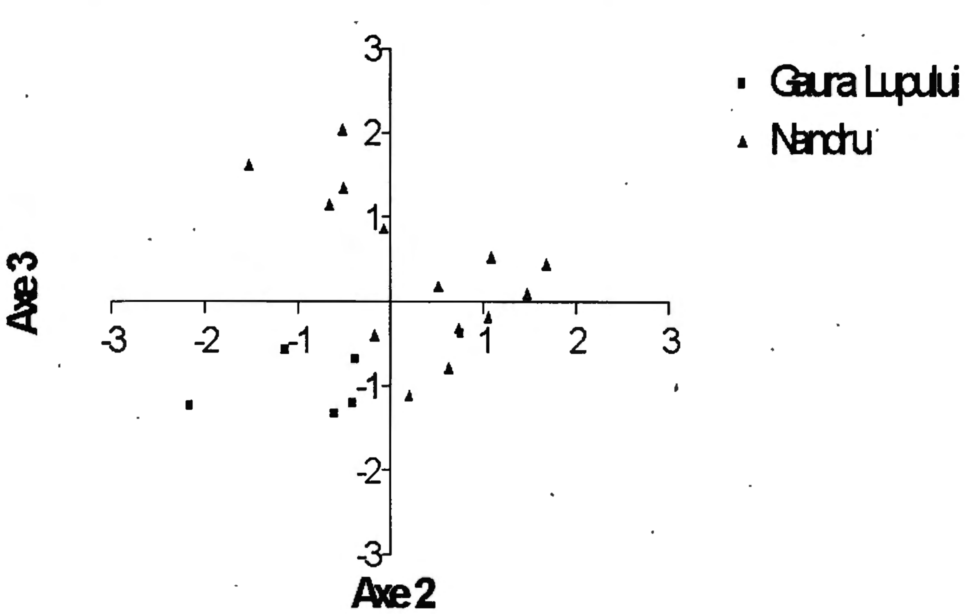

Fig. 1. Distribution des premières molaires inférieures des deux populations de Nandru et Gaura Lupului dans le plan 2-3 de l'analyse en composantes principales obtenue à partir des mesures prises sur la surface occlusale de la dent.

Distribution of the first lower molars of the two populations from Nandru and Gaura Lupului within the plan 2–3 of the main components analysis obtained by measurements on the occlusal surface of the teeth.

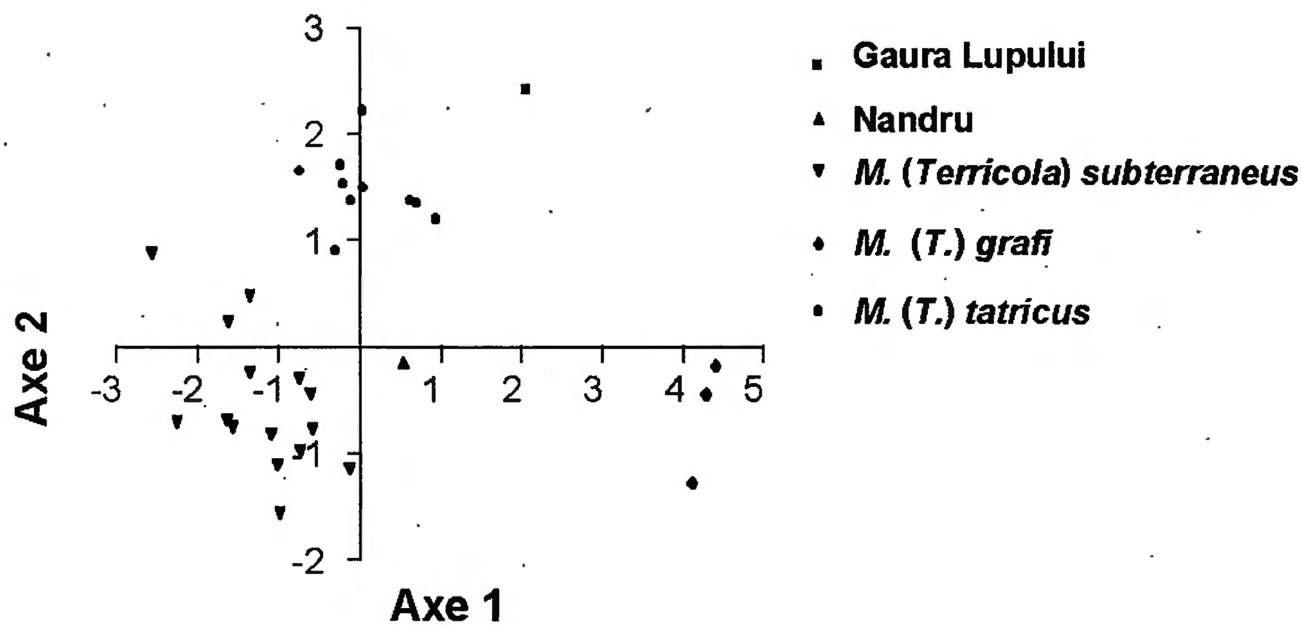

Fig. 2. Distribution des centres de gravité dans le plan 1–2 de l'analyse canonique discriminante faite entre les populations de Nandru, Gaura Lupului, de *M.* (*T.*) *subterraneus* (15 populations), *M.* (*T.*) *tatricus* (3 populations) et *M.* (*T.*) *grafi* (10 populations).

Distribution of gravity centers within the plan 1–2 of the canonic discriminant analysis performed between the populations of Nandru, Gaura Lupului, M. (T.) subterraneus (15 populations), M. (T.) tatricus (3 populations) and M. (T.) grafi (10 populations)

Analyse des indices odontométriques

La description et la comparaison de la longueur totale de la dent (V6) et des 11 indices odontométriques entre les deux populations roumaines sont données dans le Tableau 2. Deux indices, la longueur relative de la partie antérieure de la dent (LRPA) et l'inclinaison du rhombe pitymyen (RP), sont différents ($p < 0,05$) quel que soit le test utilisé et deux indices, V6V21 et V19V17, sont différents ($p < 0,05$) avec le test *t* et proches d'être différents ($0,05 < p < 0,10$) avec le test de Wilcoxon entre les deux populations. La population de Gaura Lupului se différencie ou est proche de se différencier de la population de Nandru par une longueur relative de la dent moins développée, un rhombe pitymyen moins incliné, une dent d'aspect plus étroit (V6V21) et l'indice V19V17 plus ouvert.

Tableau 2. Description et comparaison de la longueur totale de la première molaire inférieure (V6) et des 11 indices odontométriques calculés entre les populations de Nandru et Gaura Lupului.

Description and comparison of the total length of the first lower molar (V6) and the eleven odontometric indexes calculated between the populations of Nandru and Gaura Lupului.

Variable	Population fossile (Grotte Gaura Lupului) N=6				Population actuelle (Nandru) N=14				Test *t* (*p*)	Test de Wilcoxon (*p*)
	Moyenne	Ecart type	Min	Max	Moyenne	Ecart type	Min	Max		
V6 (mm)	2,672	0,224	2,290	2,900	2,581	0,173	2,070	2,740	*p*=0,340 NS	*p*=0,283 NS
LRPA (%)	50,7	1,6	48,2	52,9	52,7	1,7	49,8	55,5	*p*=0,023 S	*p*=0,035 S
RP (mm)	0,080	0,075	0,010	0,220	0,012	0,027	-0,040	0,050	*p*=0,007 S	*p*=0,018 S
BA (%)	20,7	10,6	6,7	30,7	15,4	3,4	7,5	20,4	*p*=0,102 NS	*p*=0,232 NS
V6V21 (sans unité)	2,83	0,19	2,62	3,10	2,67	0,13	2,51	3,01	*p*=0,034 S	*p*=0,076 NS
V10V9 (%)	15,1	1,0	14,0	16,3	15,5	1,7	12,0	19,4	*p*=0,600 NS	*p*=0,592 NS
V11V9 (%)	1,5	1,9	-0,4	4,7	0,6	1,0	-0,8	2,6	*p*=0,175 NS	*p*=0,430 NS
V12V10 (%)	3,2	1,1	2,2	4,7	2,1	1,8	-1,0	5,6	*p*=0,195 NS	*p*=0,201 NS
V12V11 (%)	16,7	1,9	14,1	19,6	16,9	1,5	14,9	19,2	*p*=0,766 NS	*p*=0,650 NS
V18V17 (%)	-4,1	6,9	-13,9	5,6	0,3	3,7	-7,8	7,4	*p*=0,077 NS	*p*=0,063 NS
V19V17 (%)	2,9	1,6	0,0	5,6	1,4	1,2	0,0	3,9	*p*=0,036 S	*p*=0,063 NS
V20V19 (%)	13,7	7,5	0,0	20,8	14,3	3,6	0,0	21,2	*p*=0,824 NS	*p*=0,710 NS

Discussion et conclusion

Le faible effectif des deux populations étudiées doit inciter à la prudence dans l'interprétation des résultats obtenus. Toutefois, l'analyse de la morphologie générale et l'analyse des indices odontométriques montrent que les deux populations roumaines sont assez différentes, et ne doivent pas être rangées dans le même taxon. La population actuelle de Nandru étant morphologiquement proche *de M. (T.) subterraneus*, peut être attribuée à la forme *M. (T.) subterraneus dacius* décrite de Roumanie.

La population du gisement de Gaura Lupului ne peut pas être attribuée à cette même sous-espèce de *M. (T.) subterraneus*.

Le plan 1–2 de l'anyse discriminante montre que l'espèce la plus proche de la population de Gaura Lupului est *M. (T.) grafi*, son centre de gravité étant situé à proximité de ceux des populations stratigraphiques de *M. (T.) grafi*, sans être inclus dans le nuage constitué par ceux-ci. C'est pourquoi nous proposons de décrire la population de Gaura Lupului comme une nouvelle sous-espèce de *M. (T.) grafi* (fig. 3.6 à 3.9).

Description de la nouvelle sous-espèce

Holotype: Spécimen 1 du niveau IV (sol 6) de la grotte Gaura Lupului.

Locus typicus: Grotte Gaura Lupului, village de Crăciuneşti, département de Hunedoara (Roumanie).

Stratum typicum: Niveau IV (sol 6) de la grotte Gaura Lupului dont l'âge estimé par le ^{14}C est de 34020 ± 500 B.P.

Derivatio nominis: D'après le nom de la localité romaine Micia, située à 15 km SE de Crăciuneşti (département de Hunedoara).

Diagnose: Caractéristiques de la M_1: rhombe pitymyen non incliné (V4–V3: 0,078) ; partie antérieure moyennement développée (V6–V3/V6×100: 50,63) ; rapport longueur/largeur (V6/V21: 2,828) plutôt grand.

Description: voir supra.

L'examen de nouvelles dents de cette région et d'âge semblable permettra de préciser le statut de cette nouvelle forme.

M. (Terricola) subterraneus de Nandru (de 1 à 5) et *M. (T.) grafi miciaensis* de Gaura Lupului (de 6 à 9).

M. (Terricola) subterraneus *from Nandru (1 to 5) and* M. (T.) grafi miciaensis *from Gaura Lupului (6 to 9).*

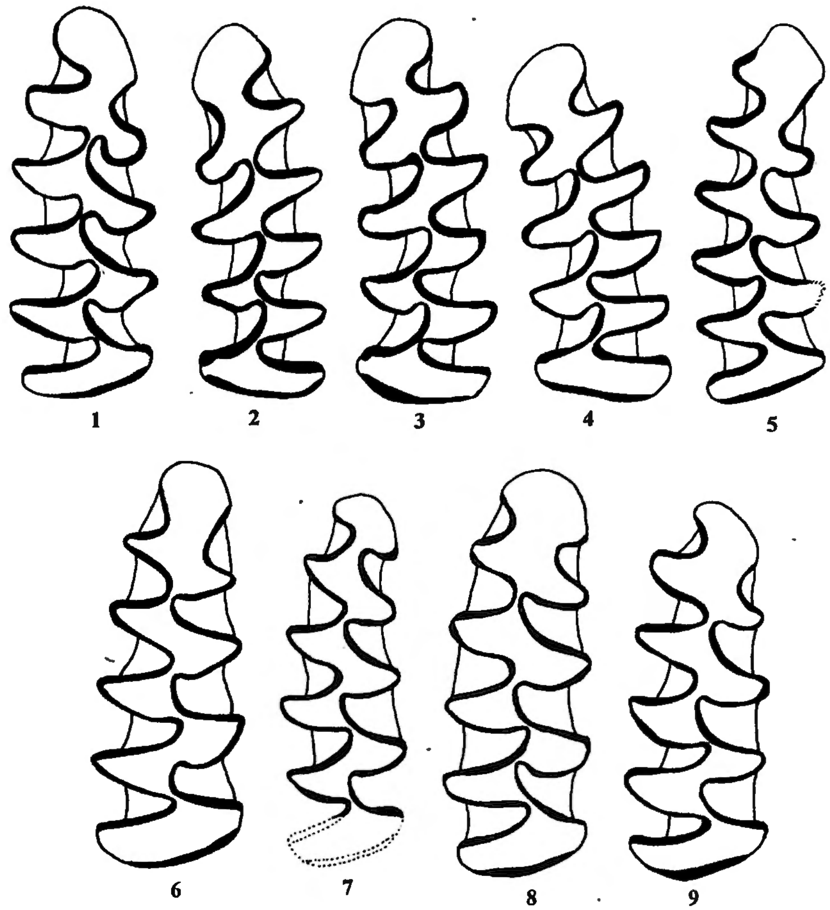

Bibliographie

Brunet-Lecomte, P. (1988) *Les campagnols souterrains (Terricola, Arvicolidae, Rodentia) actuels et fossiles d'Europe occidentale.* Thèse Doctorat de l'Université de Bourgogne, Dijon, 146 p.

Brunet-Lecomte, P., Nadachowski, A., & Chaline, J. (1992) *Microtus (Terricola) grafi nov. sp.* du Pléistocène supérieur de la grotte de Bacho Kiro (Bulgarie). *Geobios*, **25**, *4*, pp. 505–509.

Book Reviews

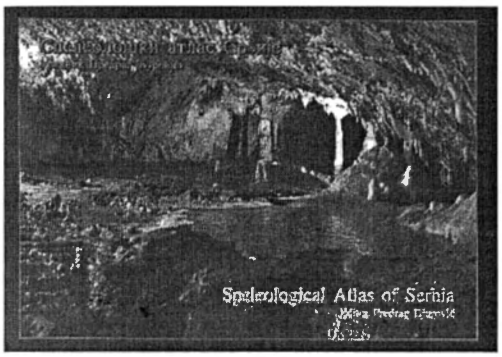

Speleological Atlas of Serbia

Predrag Djurovic, *Editor*

Ed. "Jovan Cvijic" Geographical Inst., Serbian Academy of Sciences & Arts, Special Issue 52, Belgrade, 1998.

290 p (+32 unnumbered pages), 14 color photographs, A3 format, hardcover, ISBN: 86-80029-15-7.

Bilingual (Serbian and English).

price: USD 50; on sale to the "Jovan Cvijic" Geographical Institute, Djure Jaksica 9, 11000 Belgrade, Yugoslavia. email: gijcsanu@eunet.yu

The official reference-year of this book is 1998, but it was only in March 1999 that it was actually printed. As much as I would try to keep this review far from politics, I still cannot disregard that this atlas appeared in the middle of a war! And, as a speleologist, a frequent visitor of the Serbian karst and a friend of Serbian cavers, I cannot stop wondering how the publishing of this book was still possible, given the circumstances...

The Speleological Atlas of Serbia is structured in two parts: the first, general section, is dedicated to several presentations of the Serbian karst as viewed from geological, hydrogeological and geomorphic perspectives. It also includes outlines of the present knowledge in some specialized speleological fields, such as: cave paleontology, biospeleology, prehistoric sites and cave use and management in Serbia. This synthesis is especially useful to the foreign reader since little has been published so far on the karst from Serbia, which was always eclipsed by its Dinaric counterpart.

In the second section 81 caves and potholes are presented according to a model that includes: a short description of the cavity and its important features, a general location map, a small topographic and another geological map that would give the reader an idea about the basic settings and, on the opposite page, the plan and/or the profile of the respective cave. If there is a criticism I have for this book it is at this point since, in my opinion, both the topographic and the geologic maps are sometimes hard to read because of too many contours and/or details. This is especially the case of the cavities located in deeply dissected relief or in complicated geological settings. However, due to the large-size format of the book, the cave maps are generally clear and easy to read.

The quality of the print is overall very good, except, perhaps for the 14, full-page, color photographs that introduce each chapter. Apart form this slight weakness, the book offers what we would expect any atlas to offer: many maps accompanied by concise and professional scientific information. Therefore, I can only congratulate the Editor and the authors for their hard work. The Speleological Atlas of Serbia is a very fine book, despite (or, maybe, especially due to!) the numerous economical and political problems that our Serbian colleagues had to face during the last ten years. And, I daresay that it is the kind of national speleological atlas that many countries (including mine!) would like to be able to offer to the international speleological community.

Silviu Constantin

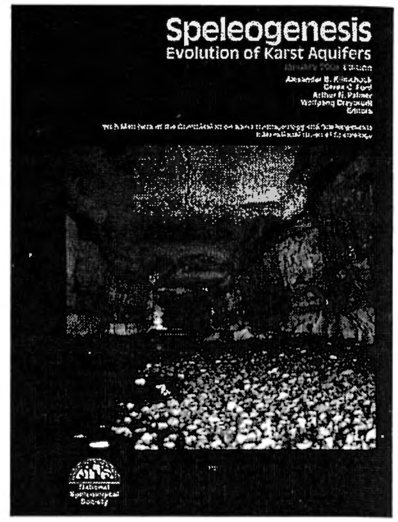

Speleogenesis. Evolution of Karst Aquifers.

Klimchouk, A. B., Ford, D. C., Palmer, A. N. & Dreybrodt, W., *Editors*

National Speleological Society, Huntsville, Alabama, 2000.

528 p, letter format (8 1/2×11"), hard cover, ISBN 1-879961-09-1.

standard price: USD 60; online orders at: http://www.caves.org

If one ever starts working on karst and in caves, then inevitably one of the first questions asked is how are caves formed under various geomorphologic and geologic settings? The simpler the question, the more complex the answer. This is why *44 authors* from *15 nations* have put their knowledge into one integrated volume that aims to present the advances made in recent decades in our understanding of the formation of dissolutional caves.

Speleogenesis. Evolution of Karst Aquifers is an extensive collection of papers covering the fields of karst groundwater flow, fundamentals of speleogenetic processes, development of cavities and cave systems in various settings, and the meso- and micromorphology of caves. Speleogenesis in noncarbonate lithologies and some practical aspects of speleogenetic studies such as porosity and permeability, the role of speleogenesis in the development of hydrocarbon and mineral deposits, etc. are also presented.

After the introduction, in which the Editors make a concise radiography of the book, a chapter is devoted to overviewing speleogenetic studies from a historical perspective.

Chapter 3 (*Geologic and Hydrogeologic Controls of Speleogenetic Development*), Chapter 4 (*Theoretical Fundamentals of Speleogenetic Processes*), and Chapter 5 (*Development of Cavities and Cave Systems in Various Settings*) are the heart of the book. These chapters present the results of new research and provide new perspectives on existing information by discussing case studies. Unfortunately, many well-known karst and cave sites are missing (Chinese subtropical karst, caves such as Frasassi, Lechuguilla, and large and deep shafts from the Alps, Mexico, Mulu, etc.). In addition, some of the case studies are of limited interest to the general reader. Furthermore, not all of the subchapters are equally readable. For example, the chemistry and dynamics of cave genesis might be difficult to comprehend for nonspecialists.

In many ways, it is these three chapters that make this book worth buying, because they provide a challenging and refreshing examination of the most important issues of speleogenesis.

With few exceptions all chapters are well written; some of them, although succinct, provide fascinating accounts with a distinctly global flavor. Furthermore, the editors have skillfully interspersed them with major contributions in most of the chapters.

The book represents a testimony of a continuous interest in the evolution of karst aquifers and an example of a true multidisciplinary study maintained over a long time span. It will appeal to a wide readership in karst and cave science, as well as to general hydrogeologists dealing with karst terrains.

The Editors of this book should be commended for their dedication to such a tremendous work, without which we would have had to search through endless lists of publications on these topics.

The book has been well edited, illustrated (occasional imperfections on diagrams or photos will be forgiven by readers), and produced by the National Speleological Society. It will definitely serve as a reference book, until, we can hope, it will be superseded by a future edition covering this topic in another 20 years or more.

Bogdan P. Onac

Précis de Karstologie

par **Jean-Noël Salomon**

Presses Universitaires de Bordeaux, Bordeaux, 2000.

250 p, format 15.5 x 24 cm, 75 fig, 9 tab, 22 photos, ISBN: 2-86781-262-3.

prix: 32 € (210 FF).

La littérature karstologique vient de s'enrichir avec une nouvelle publication, due a Jean-Noël Salomon, professeur de géographie physique à l'Université Michel de Montaigne de Bordeaux, directeur du Laboratoire de Géographie Physique Appliquée de la même université et président de l'Association Française de Karstologie. Tel que le titre le montre d'emblée, il s'agit plutôt d'un manuel que d'un véritable traité scientifique. Mais ceci n'empêche point que, spécialement pour la France, sa parution constitue une nécessaire et longtemps attendue mise au point sur les multiples problèmes liés au relief karstique et sur l'état actuel des connaissances acquises dans ce domaine. C'est ce qui se détache clairement de la préface signée par le Président d'honneur de l'Association Française de Karstologie, le professeur Jean Nicod.

L'ouvrage débute avec une brève récapitulation des propriétés que présentent les roches susceptibles de constituer le support lithologique des formes propres au karst, notamment la roches carbonatées, et des particularités de la corrosion en tant que mécanisme fondamental qui préside à leur constitution. Sont passées ensuite en revue les principales formes qui composent le relief exokarstique, à savoir les lapiés, les dépressions fermées et les vallées développées dans les régions calcaires. Mentionnons que, quoiqu'il admette que la limite entre les poljés classiques et les autres types de dépressions karstiques est parfois difficile à tracer, l'auteur n'utilise le terme de «poljé» que pour désigner les vastes dépressions à fond plat et dont la longueur est de l'ordre de plusieurs kilomètres.

Les deux chapitres suivants sont consacrés au facteurs qui interviennent dans le processus de karstification, en précisant le rôle que jouent, d'une part, la structure et la tectonique des roches calcaires, et d'autre part, le contexte hydrodynamique dans lequel se déroule ce processus et qui est dépendant en grande mesure du relief de surface. D'un intérêt particulier sont les pages qui traitent de l'organisation et du fonctionnement des aquifères karstiques, car l'auteur insiste sur le fait que ceux-ci sont intimement liés a la porosité secondaire des roches carbonatées, dans lesquelles la circulation des eaux se fait uniquement le long des fractures et des joints de stratification. Il s'ensuit que l'aquifère karstique se distingue nettement d'une nappe phréatique, ce qui fait que le qualificatif de «phréatique» attribué souvent aux galeries des grottes ou au régime d'écoulement souterrain n'est guère justifié.

Une importante partie de l'ouvrage est réservée à l'influence que le climat exerce sur le relief karstique, en imprimant la spécificité si évidente des formes développées dans chacune des grandes régions climatiques du globe terrestre, depuis les karsts tropicaux et jusqu'à ceux des zones de hautes altitudes et latitudes. Elle est suivie d'une analyse de la karstification en relation avec le facteur temporel, qui aboutit à la conclusion que le paysage karstique est «un cumul d'héritages», car il conserve généralement les anciennes formes de surface par suite de la disparition du réseau hydrographique sous-aérien.

Après un rapide examen des éléments dont l'étude fournit des informations utiles pour la reconstitution de la genèse et l'évolution du karst (drainages souterrains, morphologie des galeries, dépôts autochtones et allochtones), l'ouvrage prend fin avec une récapitulation des principales modalités par lesquelles sont mises en valeur les ressources du karst et des problèmes que soulève l'exploitation économique de celles-ci.

Ecrit dans un langage qui allie la rigueur scientifique à un exposé plutôt didactique des faits et des théories, le Précis que nous propose Jean-Noël Salomon s'adresse non seulement à ceux qui, par leur spécialité ou par leurs occupations, s'intéressent au phénomène karstique, mais aussi au large public. En effet, le lecteur y trouve nombre d'informations qui doivent occuper leur place légitime dans la culture générale et qui sont présentées de manière à pouvoir être aisément comprises et assimilées. Il n'y a donc aucun doute que le premier bénéficiaire de cette nouvelle publication sera la karstologie elle-même.

Gheorghe Racoviţă

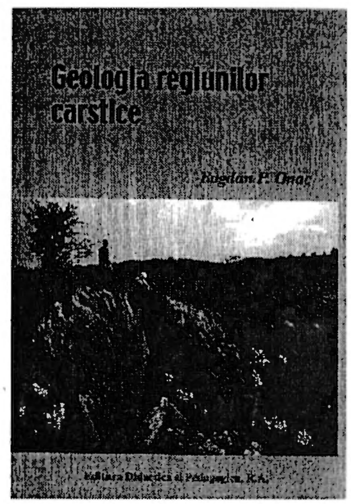

Geologia regiunilor carstice

by Bogdan P. Onac

Ed. Didactică şi Pedagogică R.A., Bucureşti, 2000.
400 p, format 16.5 x 24 cm, ISBN: 973-30-2266-7.
"Geology of Karst Regions", in Romanian; extended abstracts of each chapter in English.
price: USD 38 (postage included); on sale to the author: bonac@bioge.ubbcluj.ro.

The author of this book belongs to the young generation of Romanian karstologists but his expertise in this field of science is already vast. After a long stage as an amateur caver, he became a researcher at the "Emil Racoviţă" Institute of Speleology in Cluj-Napoca and graduated postdoctoral stages in Norway, Sweden and the USA. He also visited and explored many caves in Europe, Latin America and South Africa. This book appears as a necessity, a "summum" of his activity as a researcher and as a senior lecturer at the "Babeş-Bolyai" University.

Although the title of the book is "Geology of Karst Terrains", by content it is in fact a course of Karstology, in all meanings of this term: interdisciplinarity, complexity and systemic relations. The first chapters deal with geological issues: mineralogical and petrographical characteristics of karst rocks, physical and chemical principles of dissolution, elements of karst hydrogeology. The following section of the work addresses karst geomorphology: karst landforms, speleogenesis mechanisms and morphology of the underground. Other geological issues with specific relevance for karst landscapes are also addressed: the role of caves as a sedimentation environment (detrital, organic and chemical deposits), and a special topic on the crystallography and mineralogy of speleothems. The interpretation of Quaternary history based on cave deposits is another interesting part of the book; here, the new dating methods are thoroughly presented. After a short approach to cave climatology, including the specific problems of ice-caves, Bogdan Onac presents in a modern way the morphoclimatic systems and their associated karst landscape, the cyclic evolution of karst regions and the problem of paleokarst interpretation. The last section is dedicated to the management and protection of karst regions, including their economic issues.

The quality of the book is enhanced by a great number and variety of figures: maps, graphs, diagrams and photographs. All the chapters end with extended abstracts written in English and significant bibliographical lists.

"Geology of Karst Terrains" is a valuable synthesis of the newest information and trends in karstology and a book that will be welcomed by any specialist working in soluble rocks regions.

Sorin Roată

Scărişoara Glacier Cave. Monographic study

by

Gheorghe Racoviţă & Bogdan P. Onac

Ed. Carpatica, Cluj-Napoca, 2000.

140 p, format 17 x 24 cm, 52 fig, ISBN: 973-98752-1-1.

price: USD 15 (postage included); on sale to the authors: bonac@bioge.ubbcluj.ro.

Before the discovery of the Movile Cave in 1986, **Scărişoara Ice-Cave**, was undoubtedly the most studied cave in Romania. And even though today Movile seems to be, internationally, the most famous Romanian cave, for the Romanian public this first position is still occupied by Scărişoara.

The first researches in this cave were carried out by the great scientist Emil Racoviţă, as early as 1921. Systematic studies were launched by Racoviţă's successors approximately four decades ago and pursued within two stages, 1963–1968 and 1982–1992. More than 40 papers have been published, most of them being dedicated to the huge subterrannean ice-block and to its significances for the cave genesis and evolution.

The lines above are intended to emphasize the importance of this work, in fact *the first Romanian cave monograph of a high scientific level*. So far, the most important and/or beautiful caves of the country have been only presented in picture books.

The authors, reputed speleologists, have structured their work in logical and didactical sequence of nine chapters. From the very beginning (the Introduction) one can learn, among others, that Scărişoara is the biggest underground ice accumulation in Romania, with a volume of over 75,000 m^3. A short chapter dedicated to the cave exploration and research history, follows. The third chapter deals with the regional geographical, geological and hydrogeological settings. Scărişoara is here described as part of the extensive *Ocoale-Gheţar-Dobreşti* karst system of the Bihor Mountains.

Further on, a presentation of the cave (Chapter 4) is accompanied by a concise section dedicated to the speleogenesis of Ocoale-Gheţar-Dobreşti karst system (Chapter 5). More than half of the book is dedicated to the underground topoclimate and to the ice speleothems (Chapters 6 and 7). This is perfectly understandable if one takes into account that most of the systematic studies above-mentioned were specifically addressing those issues. The conclusions reached by our colleagues from Cluj after more than 15 years of extensive researches are of outstanding value. They systematically deal with the interpretation of specific parameters, such as: the ventilation system, the air movement and temperature, the meroclimatic structure of the cave, the ice temperature, the relative humidity, the evapocondensation, the morphology and structure of ice speleothems, dynamics of ice speleothems at the paleoclimate information stored in the ice block.

Apart from the study of those parameters, which intimately control the functioning of the underground system, an attempt to reconstruct the last 3,000 years paleoclimate based on the ice block structure is also presented. Calcite speleothem mineralogy and the results of U-series datings performed on samples from Scărişoara are only briefly discussed.

The last chapter is dedicated to the cave fauna, which was also intensively studied since, due to the peculiar topoclimate of this cave, it may be considered as living close to the borders of the ecological tolerance. Consequently, the underground biocenosis is dominated by a single troglobiont species, the *Pheleuon proserpinae glaciale*.

In the end, we shall stress once again the great value of this first monographic paper dedicated to a Romanian cave and our hope that it will be followed by further publications on other equally well-studied and important caves of the country.

Traian Constantinescu

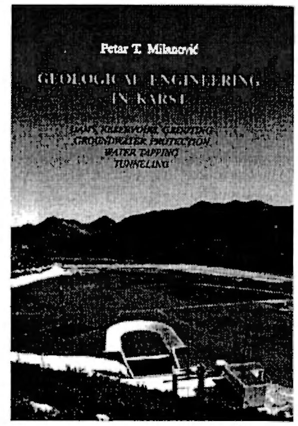

Geological engineering in karst

by **Petar T. Milanović**

Ed. Zebra, Belgrade, 2000.
347 p, format 16.5 x 24 cm, 190 fig, 11 color pages, hardcover,
ISBN: 86-7489-125-X.
price: USD 50 (postage included); on sale to the publisher: zebra@EUnet.yu.

Most of us dealing with activities ~~"related to karst" have~~ heard about Dr. Petar Milanović and his vast experience in engineering different projects in karst environment. It is worth mentioning the project implemented in classical karst area of the Trebisnica River that, in the early 70's, was the biggest in Europe. In fact this was only the beginning of a fruitful career including many other projects in Turkey, Iran or Greece. However, perhaps not many are aware of the existence of his latest book, entitled *Geological Engineering In Karst.*

Why is this book so important? First, because geological engineering in karst areas is a delicate matter both from the perspective of genuine environment preservation and from that of the reliability of the project itself. Secondly, because it is not a classical textbook considering only the theoretical aspects of the domain; it is rather the examples and the author's personal expertise that support the most important methods and technologies described.

The introductory chapters represent a comprehensive review of karst phenomena and groundwater in karst areas, viewed according to their possible impact on the engineering projects to be implemented in such areas.

The initial advantage of karst knowledge is highly exploited in the following chapters. Geological investigations, performed all over the world, for *dam sites*, *reservoirs*, *tunnels*, *grouting operations* as well as *water tapping* and *protection* have built up, through the years, authors' greatest expertise. That is why these major issues, supported by specific examples streamlining to major problems and their solutions are largely described and commented as Chapters 3 to 11. Methods and techniques for geological investigations aiming to increase the knowledge of the possible impact of karst features on projects are listed or presented in detail

There is no discrimination in showing either the success of the attempts or some failed projects in karst areas and the causes that led to failure. This is important since, in many cases learning from someone's mistakes may be possible... The most important chapter is *Grouting in karst*, a collection of more than 30 examples described over 112 pages, considering that grouting is an essential preliminary operation for any further construction of dams and reservoirs on karstified bedrock.

The final chapters, apparently less consistent than the previous ones are still clearly based on the author's (and his close collaborators) field experience and attempt to address several very specific issues that are still under debate, such as the *criteria for groundwater protection zoning* in karst regions, *groundwater tracing techniques* or *application of geophysical methods* in karst. The latest one is focused on high-tech procedures that can provide reliable information about underground extension and abundance (magnitude) of karst features.

The book will be of substantial benefit to any geologists, civil engineers and all types of professionals and experts, that can find an answer to their problems when dealing with karstified rocks.

Adrian Iurkiewicz

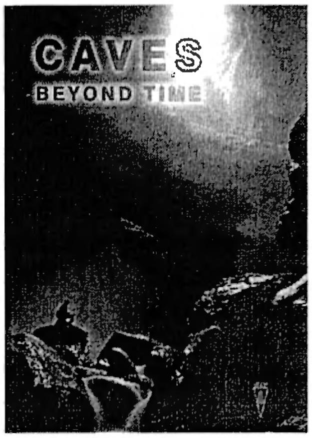

Caves Beyond Time

by **Cristian Lascu**

Edited by Group of Underwater and Speleological Exploration (GESS), Bucharest, 2001.

176 p, 155 color photographs, A4 format, hardcover,
ISBN: 973-85372-1-5.

English and Romanian versions available.

price: USD 35 (postage included); on sale to the editor: gess@dial.kappa.ro

A picture book is particularly hard to review. Since we are specifically dealing with artistic emotions, reviewers' comments can only be subjective. This latest album of the reputed speleologist and cave photographer *Cristian Lascu* makes no exception. For this reason, I will try to limit my comments only to the ingenious way the author has chosen in order to communicate his artistic and scientific message.

The 'catch' with this book comes when one is trying to fit it into a precise category. "Caves beyond time" is not what we would normally expect from an album dedicated to the Romanian caves. It lacks the customary geographic approach and some sort of rigidity that this approach would bring along. Of course, the book is abundantly illustrated and the photographs are taking us from the Black Sea coast to the high Carpathian ridges, from deep gorges to the tranquility of karst plateau meadows, from huge underground chambers through canyon-like passages, along rapids and waterfalls to the deepest Romanian sumps. But the order that links all these images into a coherent masterpiece is not the 'geographical' one. The pictorial succession seems to obey a combination of geological and philosophical principles and reflections regarding the Cave, which is seen both as an outcome and a witness of the immemorial Time.

It is at this point when one may feel the necessity of additional clarifications in order to fully understand the succession of the images within the book. And it is what the author has done by five short, but extremely suggestive, essays. The first one, "*The unknown geography*" attempts to explain why, despite the little extension of our karst, caves are so important for Romanians, and what can our karst offers to the world. A second essay, called "*The Stone House*" invites the reader to decipher the harmony and the simplicity of the underground architecture.

The third part, "*Water and time droplets*" is dedicated to the traditional 'stars' of almost any Romanian famous cave: the speleothems and the crystals. Here, again, the intimate combination of scientific information and philosophical reflections make up a highly unusual and innovative composition.

"*Caves, the first altars*" is, to my knowledge, one of the very few works addressing the historical links between the people living around the caves of the country and their rituals, myths, and religion. The journey starts from the prehistoric times, goes through pre-Christian periods and ends in our days, when orthodox monks are still using natural or artificial caves for meditation.

The finally chapter, "*The Cave Beyond Time*" is the only one that breaks the 'countrywide approach' since it is entirely dedicated to the world-famous Movile Cave.

In a foreword entitled "*A Foreign Visitor's View of Romanian Caves*", Robert Cronk wrote: "There is an old rethorical question: If a tree falls in the forest and there in no one to hear it, does it make a sound? There can be a similar question for the caves: If a cave remains undiscovered and in darkness, can it be beautiful?" As a Romanian speleologist, I think that Cristi Lascu's latest book may be indeed that trunk falling... and I am glad that I have been in the forest!

Silviu Constantin

Protection of karstic areas is a very hot subject nowadays and often a topic of headed discussions. Therefore, Raymond Tercafs' book appears to be a waited event. Senior Research Associate of the Belgian National Fund for Scientific Research in the Department of Animal Physiology of the University of Liège (Belgium), Raymond Tercafs has more than 30 years of experience in exploring and studying caves in Europe, North Africa, South America and Southeast Asia. With extensive knowledge on ecology, geology and computer application in cave management, his interest in cave protection is well known among the biospeleologists.

The protection of the subterranean environments. Conservation principles and management tools includes twelve chapters structured on several issues. The first chapters represent an introduction in karstology, biospeleology, and karst kinetics by explaining the basic principles governing the functioning of the very complex karstic systems. Such systems can be modeled and processes can be simulated, as is exemplified in one of these introductory chapters.

One of the most original parts for a book treating this subject is the psychological approach on the protection problems, explaining attitudes for and against environmental values.

The causes of deterioration of the subterranean habitats and their fauna are thoroughly and extensively treated, representing another important part of the book. Many examples of the author's personal experiences and taken from the bibliography are the foundation for the next chapters, which present the principles of management. Ordinary caves or show caves can be protected in a better manner with the help of the computer-elaborated models of management. Given the importance of the legislation concerning the cave protection an interesting chapter compares the laws form different North American and European countries.

Some ideas of Raymond Tercafs are gathered in the conclusion chapter leaving the readers to meditate over the differences between conservation and protection and over our abilities to elaborate really efficient management plans in the subterranean environment.

Always in the context of the general problematic of environment protection and using a rich and diverse bibliography, Raymond Tercafs has published *the first book* on the protection and management of underground habitats.

Oana Moldovan

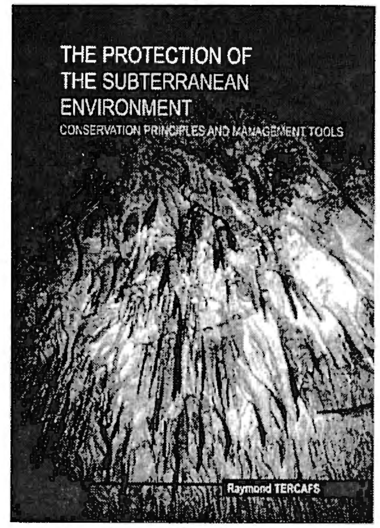

The Protection of the Subterranean Environment. Conservation Principles and Management Tools

by **Raymond Tercafs**

PSP Production Services Publishers, Luxembourg, 2001.
402 p, format 27.5 x 25 cm, 75 fig.
ISBN: 2-9599798-0-X.

In Memoriam

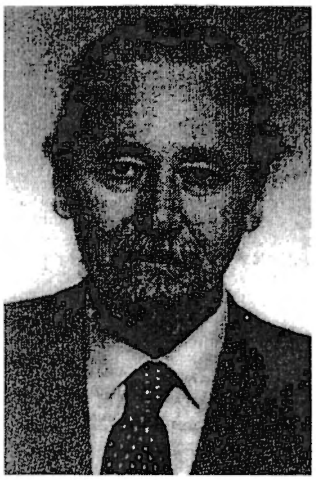

Petre-Mihai Samson

1930-2001

Le 22 avril, l'Institut de Spéléologie a perdu l'un de ses chercheurs d'excellence par la disparition du Dr. *Petre-Mihai Samson*. Sa carrière fut décisive dans la seconde moitié du siècle passé pour le développement de la paléobiologie des mammifères en Roumanie et, en général, pour les disciplines se rapportant à l'étude du Quaternaire.

Il était né le 7 février 1930 en France, à Toulouse où son père suivait des cours de spécialisation à l'Université Paul Sabatier. Avant qu'il commence ses études primaires, sa famille arrive en Roumanie et s'installe à Ploieşti, ville où il va accomplir son éducation au lycée Saints Pierre et Paul. Pendant son enfance et son adolescence son père lui avait appris l'amour et le respect de la nature dans de longues promenades aux alentours de sa ville d'adoption. Ainsi s'éveilla en lui sa vocation de naturaliste.

Il suit les cours de la Faculté de Biologie de l'Université de Bucarest où il est l'élève de Margareta Dumitrescu qui conduisait la chaire de Zoologie des vertébrés et qui orienta sa carrière vers l'étude des mammifères fossiles. Licencié en Biologie (1955), il commence ses études de paléontologie dans le cadre de l'Institut de Spéléologie "Emil Racovitza" à peine réorganisé sous la direction des professeurs Constantin Motaş, Traian Orghidan et Margareta Dumitrescu.

En 1956, il conduit les fouilles dans la grotte « La Adam » en Dobrogea centrale qui seront exécutées pendant plus de seize ans, la première découverte mettant au jour un ensemble mithriaque renfermant, entre autres objets de culte, deux bas-reliefs représentants le dieu Mithras. D'autres fouilles, dans la même région, sont emplacées dans la grotte de Casian et dans la Grotte des Chauves-souris à Gura Dobrogei qui fournissent de riches faunes de micromammifères du Pléistocène moyen, complétant ainsi les données sur le Pléistocène supérieur acquises dans la grotte « La Adam ».

A partir de 1962, il entreprend des investigations paléontologiques minutieuses dans la Dépression de Braşov en collaboration avec le Laboratoire de Géologie du Quaternaire conduit par Henriette Alimen et le Musée de Sfântu-Gheorghe représenté par Kovács Sandor.

En 1969, il présente au Congrès INQUA, tenu à Paris, la stratigraphie du Pléistocène supérieur en Roumanie, basée sur les résultats des fouilles entreprises dans le karst du centre de la Dobrogea et dans les dépôts fossilifères stratifiés de la Dépression de Braşov. Chercheur passionné, tenace et lucide, il s'engage à prospecter et explorer les gisements plio-pléistocènes du secteur médian de la vallée de l'Olteţ (1960–1963) où des riches faunes de mammifères sont découvertes à Tetoiu (Bugiuleşti) et Irimeşti.

Il continue en parallèle ses études sur les mammifères du Plio-Pléistocène et soutient (1975) sa thèse de doctorat en Biologie: Les Equidés fossiles de Roumanie (Pliocène moyen-Pléistocène supérieur) qui paraît un an plus tard dans la revue italienne Geologica Romana.

Ses recherches continuent avec la découverte d'associations de micromammifères datant du Pliocène supérieur et du Pléistocène inférieur dans la vallée de l'Olt à Slatina, Drăgăneşti-Olt et autres localités du secteur ouest du Bassin Dacique (1977–1983). Mentionnons aussi les fouilles entreprises dans le Pliocène inférieur et moyen de Drănic et Podari dans la vallée du Jiu, avec la collaboration d'une équipe française sous la direction du dr. Sevket Sen du Muséum national d'Histoire naturelle de Paris.

Esprit vif, animé d'une grande soif de connaître, il s'engage dans des contrats de recherches qui le détermine de tourner son attention vers les micromammmifères du Miocène moyen et supérieur du bassin de Crişul Alb (1978–1980). Quelques années plus tard, une collaboration établie avec les docteurs Jean-Louis Hartenberger et Jean Sudre du Laboratoire de Paléontologie des vertébrés du CNRS à Montpellier lui ouvre un nouveau domaine d'activité relatif aux mammifères multituberculés d'âge mésozoïque final du bassin de Haţeg.

J'ai eu le privilège d'être son ami et collaborateur pendant presque 50 ans, partageant avec lui aussi bien la fatigue des longues journées sur le terrain que la joie de chaque nouvelle découverte.

Esprit d'une grande finesse, le dr. Petre-Mihai Samson se distinguait par sa prodigieuse culture, son extrême exigence poussée jusqu'au scrupule et son sens aigu de la critique. Epris de peinture et dessinateur accompli, il exécutait lui-même l'illustrations de ses travaux. Il aimait aussi la littérature, la musique et la danse.

Sa personnalité d'exception, son intelligence pénétrante et son talent de brillant causeur resteront gravés dans la mémoire de tous ceux qui se sont honorés d'être ses amis et ses collaborateurs. Personnellement, je lui garderai un très fidèle souvenir tout le reste de ma vie.

Dr. Constantin Rădulescu
Membre correspondant de l'Academie Roumaine

Information for contributors to *Theoretical and Applied Karstology*

Contributions to TAK may be submitted for publication as **Articles** (usually up to 8000 words) or as **Short Notes** (usually up to 2000 words). Larger articles, such as **Reviews** may also be published but the subject and size of these should be discussed first with the Editors.

Manuscripts must be submitted in **English** or **French**, in electronic format accompanied by two hard (paper)-copies. The order of preference for electronic submission is: (1) e-mail attachment, (2) floppy-disk(s), (3) CD, (4) ZIP Disk (100 or 250 Mb). For fast submission of large files, FTP transfer may be arranged.

We currently use IBM- compatible PCs and can read most popular word-processor, spreadsheet and graphic file formats; if you are using OS/2 or AppleMac, please format your disk as a DOS disk. Also, please consult us if your graphic files were saved under an uncommon format (e.g. the *.fpw format of FigP , *.sta format of Statistica and alike) or if you used special character sets (such as East European, Turkish, etc.) for diacritical marks. In any case, the hard-copy is essential for reference as we may unknowingly lose parts of your text or formatting in the conversion process. Also note that after acceptance, all the corrections or revisions to your paper will be made only on hard-copies in order to reduce the possibility of error.

Papers should be headed by the **title** and the **author(s) full name(s)**. This will be followed by the **complete address(es)** of all the authors. If more than one author, please specify the name and address of the person to whom the correspondence and proof should be sent.

An **abstract** (up to 300 words) in paper's language should be placed directly after the title and author(s)' name(s), followed by the **keywords**. If possible, these will be followed by the translation of the title, abstract and key-words in the 'secondary' language of the paper (English if the paper's main language is French and vice-versa); else the translation will be made by the Editors at no charge for you.

References cited in the text (and only these) should be listed, in alphabetical order, on (a) separate sheet(s), after the heading **References/ Bibliographie**, taking for example an older issue of TAK. References should be cited in the text in parentheses, in small capitals using the "name and year" ('Harvard') system, e.g. "(Ahrens, 1962)" except when the author's name is part of the sentence, e.g. "Ahrens (1962) has shown that ...". When reference is made more than once to same author and year, a, b, c, etc. should be added to date in the text and reference list. If more than two authors it is in order to put "et al." behind the first name, e.g. "(Klein *et al.*, 1988)" within the text, but *all authors* should be listed in the Reference list. In general, one should follow the American Psychological Association (APA) Method of referencing. If in doubt, please consult us.

Mathematical equations should be numbered in consecutive order throughout the text, using Arabic numerals.

Figures (maps or line drawings in black Indian ink on transparent paper) should be prepared in anticipation of reduction; small symbols or fine details may reproduce poorly. If possible, the original figures shall not exceed 31 x 20 cm. The number of folded plates being limited, only one figure exceeding this size will be, as an exception, accepted. Only black-and-white **photographs** may be published, therefore, if you send color photographs make sure that the important details will be legible when converted to grayscale. Whenever possible, please send us the illustration in both electronic and hard-copy format, but, as a rule, the original will always be preferred over the electronic version.

Plates, figures and tables should be numbered consecutively, with Arabic numerals, in order of appearance. The top of the figure should be indicated whenever exists any possibility of ambiguity. Please indicate in the manuscript where the caption-figure or group of figures is to be inserted.

The **captions** and explanations of the figures and tables will be doubled-spaced typed on separate sheets, in both volume's languages, if possible.

Acknowledgements should be placed at the end of the text, after the heading Acknowledgements, before the References.

Upon acceptance, an edited proof of the contribution will be sent to the authors for final revision. Normally, the proof will be sent by email, as a PDF file. Authors are expected to print the file, make the final corrections (if necessary) sign the Agreement for Publishing and fax it, together with the revised proof, to the Editors. Authors bear sole responsibility for the content of their contribution; this includes obtaining any clearance for the use of copyrighted materials.

As a general rule, NO manuscripts will be returned, regardless if the paper was accepted or not.

Papers accepted by the Editorial Board and published into TAK will become the property of the Publisher. No article or any part thereof may be reproduced in whatever form without the written permission of the Publisher.

A total of 25 reprints of each paper will be supplied to the authors free of charge. Authors will benefit of discount prices for additional reprints if ordered before publication.

EDITURA ACADEMIEI ROMÂNE

In this issue: